SFEI | AQUATIC SCIENCE CENTER

NUMBER 737 JULY 2014

# Estimating Regional Pollutant Loads for San Francisco Bay Area Tributaries using the Regional Watershed Spreadsheet Model( RWSM):

## Year's 3 and 4 Progress Report

July 11, 2014

Prepared by:
Lester McKee, Alicia Gilbreath, Jing Wu,Marshall Kunze, and Jennifer Hunt - SFEI

For

Bay Area Stormwater Management Agencies Association (BASMAA)

RegionalMonitoring Program for Water Quality in San Francisco Bay (RMP)

Sources Pathways and LoadingsWorkgroup (SPLWG)

Small Tributaries Loading Strategy (STLS)

SAN FRANCISCO ESTUARY INSTITUTE and the AQUATIC SCIENCE CENTER
4911 Central Avenue, Richmond, CA 94804 • p: 510-746-7334 (SFEI) • f: 510-746-7300 • www.sfei.org

# Estimating Regional Pollutant Loads for San Francisco Bay Area Tributaries using the Regional Watershed Spreadsheet Model (RWSM):

# Year's 3 and 4 Progress Report

**Prepared by**

**Lester McKee, Alicia Gilbreath, Jing Wu, Marshall Kunze, and Jennifer Hunt**

**San Francisco Estuary Institute, Richmond, California**

**On**

**July 11th, 2014**

**For**

**Bay Area Stormwater Management Agencies Association (BASMAA)**

**And**

**Regional Monitoring Program for Water Quality in San Francisco Bay (RMP)**
**Sources Pathways and Loadings Workgroup (SPLWG)**
**Small Tributaries Loading Strategy (STLS)**

# ACKNOWLEDGEMENTS

We were glad for the support and guidance of the Sources, Pathways and Loadings Workgroup of the Regional Monitoring Program for Water Quality in San Francisco Bay. The detailed work plan behind this work was developed through the Small Tributaries Loading Strategy (STLS) during a series of meetings in the summer of 2011. Michelle Lent is acknowledged for her contributions to early drafts and her work on mathematical methods for parameter estimation. Local members on the STLS are Arleen Feng, Lucy Buchan, Khalil Abusaba and Chris Sommers (for BASMAA) and Richard Looker, Jan O'Hara, and Tom Mumley (for the Water Board). This project was completed with funding provided by the Bay Area Stormwater Management Agencies Association (BASMAA) and the Regional Monitoring Program for Water Quality in San Francisco Bay (RMP).

This progress report can be cited as:

McKee, L.J., Gilbreath, A.N., Wu, J., Kunze, M.S., Hunt, J.A., 2014. Estimating Regional Pollutant Loads for San Francisco Bay Area Tributaries using the Regional Watershed Spreadsheet Model (RWSM): Year's 3 and 4 Progress Report. A technical report prepared for the Regional Monitoring Program for Water Quality in San Francisco Bay (RMP), Sources, Pathways and Loadings Workgroup (SPLWG), Small Tributaries Loading Strategy (STLS). Contribution No. 737. San Francisco Estuary Institute, Richmond, California.

# TABLE OF CONTENTS

# INTRODUCTION

The RMP is providing direct support for answering specific Management Questions (MQs) through multi-year Strategies. The four key Management Questions of the RMP's Small Tributaries Loading Strategy (STLS) (SFEI, 2009) include:

1. Which Bay tributaries (including stormwater conveyances) contribute the most to Bay impairment from POCs;
2. What are the annual loads or concentrations of POCs from tributaries to the Bay;
3. What are the decadal-scale loading or concentration trends of POCs from small tributaries to the Bay; and
4. What are the projected impacts of management actions (including control measures) on tributaries and where should these management actions be implemented to have the greatest beneficial impact.

The Multi-Year Plan (MYP) (2011) was created and updated each year (BASMAA, 2011; BASMAA, 2012; BASMAA, 2013) to provide a more comprehensive description of the STLS-supported activities over the next 5-10 years, as well as detailing the rationale for the methods of addressing the four key MQs and providing the information required for compliance with the municipal regional stormwater permit (MRP; Water Board, 2009). Among the suite of activities recommended in the MYP was the development of the Regional Watershed Spreadsheet Model (RWSM) as a planning level tool for estimating total annual average loads from the small tributaries surrounding the San Francisco Bay at a regional scale (Figure 1). Given the regional nature, the simplistic parameterization, and calibration using watershed scale data, accuracy and precision at smaller scales will likely be questionable but gross comparisons of loadings per unit area between watersheds or areas within watersheds may provide useful supporting evidence for prioritizing management attention and focusing monitoring efforts where they are most needed.


**Figure 1. Small tributary area modeled by the regional watershed spreadsheet model (RWSM).**

During the RMP 2010 calendar year (year 1 of this project), version 1 of the hydrology component of the RWSM was developed. Two base hydrology model approaches were investigated: one using runoff coefficients based on land use and the other based on impervious cover. Initial versions of each model were calibrated to local hydrology data from 18 local watersheds with a wide variety of imperviousness, soil, and slope. Recommendations were made to address hydrology model weaknesses. The year 1 report also presented a review of land use and source areas in relation to PCBs, Hg, dioxins, Cu, and Se and provided recommendations for steps to develop event mean concentration (EMC) data to support the input side of the model. The report recommended the model structure for each pollutant, methods to fill data gaps, and priorities (Lent and McKee, 2011).

During RMP 2011 calendar year (year 2 of this project), version 2 of the GIS-based model was developed following Y1 recommendations. Several more calibration watersheds were added to increase the range of watershed characteristics including percent imperviousness character. In addition, gauge records with incongruent land use / impervious data were removed and land use categories were refined. For Year 3, a focus on the sediment and pollutant models was recommended (Lent et al., 2012).

This Progress Report details the various tasks completed in Year 3 and Year 4 of this work (Note the TRC and SC of the RMP have approved budget for Year 5). In Year 3 and 4, many aspects of the model were improved:

1) The model was migrated into the Python language platform, and a user-interface GUI was developed for easier manipulation by a moderately-able GIS user.
2) A pollutant module was developed and the first test case pollutant (copper) was modeled chosen because extensive data are available both from the Bay Area and in the world literature, and also because as a primarily dissolved constituent it serves to define the limitations of the hydrologic model alone and helps to set up realistic definitions for success for the other more difficult pollutants.
3) A previously developed sediment model (Lewicki and McKee, 2009) was migrated into the RWSM and improved through specific treatment of base geology in urban upland erosion processes. With these improvements, version two of the sediment model was run.
4) GIS information layers for source areas were developed through a collaboration between SFEI and EOA staff to support the Hg and PCB models. This was one of two major developments towards improving the Hg and PCB models prior to running version two of these models.
5) Land-use specific event mean concentrations (EMCs) for Hg and PCBs were estimated using inverse optimization mathematical methods and another 14 other methods based on literature review and a variety of estimation techniques previously generally conceived and recommended (Lent and McKee, 2011). This was the second major development towards improving the Hg and PCB models prior to version two of those models.
6) Version two of the Hg and PCB models was developed.
7) Pollutant profiles for polybrominated diphenyl ethers (PBDEs) and legacy pesticides were researched and written, each of which provides a conceptual model for developing RWSM modules for each of these pollutants.

In subsequent years, this Progress Report will be updated as necessary (approximately annually) to document additional work and improvements to the RWSM, while maintaining the content of all the information reported herein. However, for expanded detail about the first two years of the hydrology module development and initial forays into the sediment, Hg, and PCB models, please refer to the previous reports (Lent and McKee, 2011; Lent et al., 2012).

# WORK PLAN SUMMARY / FRAMEWORK

A comprehensive step by step work plan for developing a spreadsheet model for multiple analytes with a myriad of sources and/or land use relations was developed. This 9-step plan describes the general framework of modeling each analyte, however we anticipate slight modifications for each analyte and in subsequent years as lessons are learned or if proposed uses are expanded. The plan is briefly outlined below:

Step 1: Develop factsheet/methodology: The first step for each analyte is to review what is known locally or internationally about the sources or use characteristics and processes of release and transport of the constituent of interest. This information is then put together with what is known about available GIS layers on the proposed most important sources and a model structure and generalized work plan is recommended. In the case of the hydrology model, much work had already been done on this topic and a model structure was available to adapt for our uses. For suspended sediment, similarly, several modeling efforts have already been completed for the Bay Area largely negating the need for developing a factsheet as the technical basis for the model structure and methodology. The focus initially was on PBDEs and OC pesticides in relation to MRP provision C.14 (see report sections A9 and A10).

Step 2: Develop GIS layers: Once the model structure has been identified (Step 1), the next step is to collate the appropriate spatial data bases of source areas and land uses specific to the constituent to be modeled. In the case of our test case model (copper) or some of the other conventional urban pollutants such as PAHs, these may be the conventional land use classes (open space, agriculture, low density urban, high density urban, commercial, light industrial, heavy industrial and transportation), but even for these conventional classifications, pollutant specific decisions have to be made on how to group the several hundred land use categories that are typical in city and county land use data bases. In addition, since transportation land use is usually a mixture of lines and polygons in raw GIS data bases, pollutant specific decisions have to be made on the buffer width and on what to include with regards to transportation categories (roads, airports, etc.). In the case of PCBs and Hg, this step involved a considerable effort to collate and QA GIS information (see section A1).

Step 3: Collate input data and calibration data: In the case of the rainfall-runoff model, this included rainfall data, land use specific runoff coefficients, soils and slope data, and runoff data for 18+ calibration watersheds. In the case of the sediment model, since we are modifying an existing model to address known weaknesses, this will only need to include local geology, classification,

and relative erosion rates for each class or erosional province. Depending on the recommended model structure outlined in the fact sheet (Step 1) and the availability of spatial data sets (Step 2), for each of the pollutants, data on land use or source area specific event mean concentrations (EMCs) or soil concentrations would be collated along with available "bottom of the watershed" loadings information that has been collected in the past from Bay Area watersheds. In the case of sediment, PCBs and Hg, the development of input data was primarily achieved by manipulating the wealth of local data in various ways (see report section A2).

Step 4: Run version 1 of the model: Using the information and data developed in Steps 1, 2, and 3, the model will be run and compared to existing knowledge of loads from watersheds. This first run will be largely "proof of concept". Various forms of a sensitivity analysis can be run on v1 help to determine weaknesses in model structure, input and calibration data sets so that recommendations can be developed to guide future model versions.

Step 5: Improve model structure and/ or input data: Based on constituent specific recommendations from step 4, further spatial data base development could occur or exploration of other sources of coefficients or land use classifications. In addition, in this task more effort can be put into developing EMC data for model input including EMC back-calculations upon either water concentration or sediment concentration data or combinations of both data types either locally available or from elsewhere. For example, in the case of PCBs, we experimented, on three occasions, with the use of inverse optimization techniques to generate local estimates of event mean concentrations per each version of the model (see report section A2).

Step 6: Run version 2 of the model: Using the information and data developed in Steps 1, 2, 3, 4, and 5, the model will be run and compared to existing knowledge of loads from watersheds. This second run will necessarily incorporate a detailed sensitivity analysis and or/ Monte Carlo techniques to determine weaknesses in model structure, input and calibration data sets. Very specific recommendations will be developed to prepare for decisions on further GIS layer development or consolidation, back-calculation techniques, or a need for specific field data collections to support model improvements.

Step 7: Complete FINAL input data set: Based on constituent specific recommendations and decisions from step 6, further spatial data base development could occur or exploration of other sources of coefficients or land use classifications. In addition, more effort can be put into back-calculation techniques. Pollutant specific EMC data or reconnaissance bottom of the watershed data in combination with back-calculation techniques may be collected in the field or specific watersheds may be targeted for bottom of the watershed loads data to be used for model calibration.

Step 8: Run version 3 (likely FINAL) of the model: Using the information and data developed this in Steps 1, 2, 3, 4, 5, 6, and 7, the model will be run and compared to existing knowledge of loads from watersheds. This "FINAL" version will include documentation of model weaknesses for specific land uses or source areas. In addition, the model accuracy and precision will be

analyzed for each constituent at scales of specific watersheds, Bay margin segments, and the Bay as a whole.

Step 9: Complete model packaging and user manual: Model packaging and documentation will be completed to ensure complete transparency between the model development group (SFEI staff, STLS team) and information users, and that the model results are repeatable, the model is expandable as appropriate, and that the model is not used for purposes it is not designed for. Such an open source model will mean that those who are not the originators of the model can run the model, however an open source model will require that, from 2012 forward, appropriate model structure and suitable user documentation is considered at each step of model development.

Table 1 outlines the 9 steps and sub-steps for each of the constituents that the RWSM will, or is likely to, engage. Steps completed at the date of writing the plan (Spring, 2012), are highlighted in light gray in this table with the reference noted. Years when we anticipated completing tasks were noted, however, the timeline has slipped somewhat since then but generally the structure and proposed activities has not changed.

# POLLUTANT SPECIFIC MODEL STRUCTURES

Each pollutant to be modeled may have a unique model structure, or architecture, depending on what landscape characteristics best explain differences in pollutant concentration across the modeled area, as well as what types of data are available for use in the modeling. During Step 1 of the 9-step process described in the previous section, data and information available on each pollutant is synthesized to propose model architecture and identify major data gaps that would be a barrier to developing regional loads estimates using the RWSM.

The pollutant modules can be driven by either the hydrologic model (for pollutant concentrations in water) or the sediment model (for pollutant concentrations on fine sediment particles, arbitrarily <62.5 microns) (Figure 2). The sediment model, in turn, can be driven by the hydrologic model or can be a stand-alone empirical model (Figure 2). When suspended sediment concentrations are used, the resulting loads are dependent on runoff volumes (this was the case for a version 1 of our sediment model that was presented in a work group meeting and described by Lent and McKee, 2011). Alternatively, the sediment modeling approach can be independent of runoff volumes such as local sediment yield estimates or soil loss equations.

The pollutant model is essentially a “concentration map” overlaid onto either the hydrologic model or the sediment model. The pollutant model can be based on any relevant spatial data set, ranging from actual data (sampled stormwater runoff concentrations) to data sets that serve as a proxy, such as land use or source areas. The constraints on the pollutant model are that it should provide a full spatial coverage of the region of interest and that it not be of dramatically higher resolution than the hydrologic or sediment model (to avoid the results being limited by resolution of the hydrologic or

sediment model). Aside from these constraints, there is flexibility in how the pollutant model is set up. For example, the underlying data can be categorical or continuous. In addition, multiple model types can be combined, e.g., one could apply real sampling data where it exists and proxy data elsewhere.

The choice of modeling approach will be pollutant-specific and will depend on whether a pollutant is mainly sediment-associated and what type of concentration data is available. Runoff models (or sediment models) and pollutant models interact in different ways depending on their relative boundaries to generate loads (Figure 3). In the simplest version of the volume-concentration model, the pollutant concentrations are associated with the exact same areas as the runoff amounts are calculated for. When the runoff model and EMC model perfectly overlap, the runoff, concentration and area can simply be multiplied together to generate loads (Figure 3: Identical boundaries example).

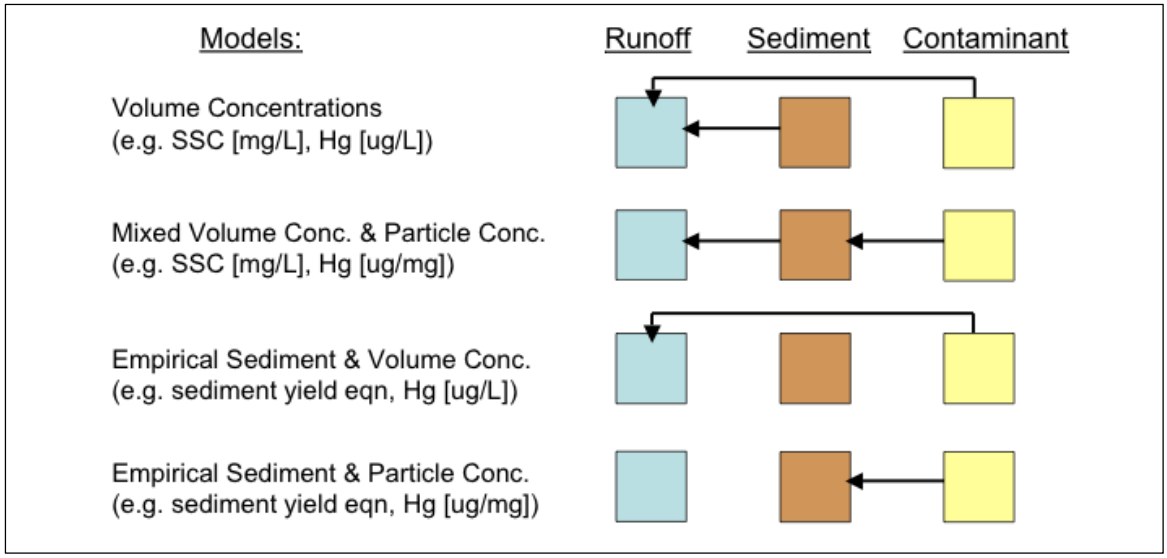


**Figure 2. Possible model interactions. Arrows indicate dependency on other model's output.**

However, when the runoff model and EMC model do not perfectly overlap, the loads calculation becomes a little more complicated since the areas have to be recalculated as the intersection of the runoff model and EMC model (Figure 3: Different boundaries examples). The first 'Different boundaries example' illustrates load calculation when using the ICM (30-m grid) with a land use- or source-based EMC model and the second 'Different boundaries example' shows load calculation using LUM runoff with a combined land use- and source-based EMC model. Thus, the hydrologic and sediment models should be developed to provide a suitable level of resolution and flexibility to support the loads generation objectives. A pollutant model based wholly or in part upon sediment transport will require land use or source area specific ratios between suspended sediment and pollutant concentrations. The preferred method is to determine the relative concentration of the particulate form of the target pollutant and sediment concentration in the water column. A ratio based on the sediment in the curb,

**Table 1. Regional watershed spreadsheet model (RWSM) planning matrix. The completed tasks are highlighted in gray and are marked with the reference. Years when the remaining tasks are anticipated are marked with the year anticipated; however these tasks are currently unfunded.**

| | | Loads calculation analytes | | | | | | | | | |
|---|---|---|---|---|---|---|---|---|---|---|---|
| Step | Description | Flow | SS | PCBs | Hg | Cu | Se | PBDE | OC pest | Dioxins | Nutrients |
| 1 | Develop fact sheet / methodology | ② | | | | | | | | | |
| 1a | Collate local data | ③ | ① | ③ | ③ | ③ | ③ | ⑤ | ⑤ | ③ | 2014? |
| 1b | Collate data from review of the world literature | ③ | ① | ③ | ③ | ③ | ③ | ⑤ | ⑤ | ③ | 2014? |
| 1c | Develep source area / land use categorization conceptual model | ③ | ① | ③ | ③ | ③ | ③ | ⑤ | ⑤ | ③ | 2014? |
| 2 | Develop GIS layers | ③ | ① | ③ | ③ | ⑥ | 2014? | 2014? | 2014? | 2014? | 2014? |
| 3 | Collate input data and calibration data | ③ | ① | ③④ | ③④ | ③ | 2014? | 2014? | 2014? | 2014? | 2014? |
| 4 | Run version 1 model and compare with calibration data | ③ | ①③ | WG presentation only | | ⑥ | 2014? | 2014? | 2014? | 2014? | 2014? |
| 5 | Improve input data and/ or model structure | | | | | | | | | | |
| 5a | Back-calculate RCs / EMCs / EFs from local or world data | ④ | ⑤ | ③ 2011 attempt not sucessful; ⑦ | ③ 2011 attempt not sucessful; ⑦ | | 2014? | | | | |
| 5b | Improve GIS layers | ④ | ⑤* | ⑥⑦ | ⑥⑦ | | 2014? | PCB/Hg level of effort may not be needed depending on the level of accuracy needed for the watershed specific and regional loading estimates | | | |
| 6 | Run version 2 model and compare with calibration data | ④ | ⑤ | ⑦ | ⑦ | Test case only; additional work not anticipated. | 2014? | | | | |
| 7 | Complete FINAL input data set | | | | | | | | | | |
| 7a | Further refine GIS layers if needed | 2013? | - | 2013? | 2013? | | 2014? | | | | 2015? |
| 7b | Further refine back-calculations if needed | - | - | 2013? | 2013? | | 2014? | | | | 2015? |
| 7c | Perform wet weather field sampling if needed | - | - | 2013? | 2013? | | 2013? | 2013? | 2013? | 2013? | 2015? |
| 8 | Run version 3 (FINAL) model and complete calibration / varification | 2014? | 2014? | 2014? | 2014? | | 2014? | 2014? | 2014? | 2014? | 2016? |
| 9 | Complete model packaging and user manual | 2013? | 2013? | 2013? | 2013? | | 2014? | 2014? | 2014? | 2014? | 2016? |
| | | | | | | | | | | | |
| | References | | | | | | | | | | |
| ① | Lewicki, M., and McKee, L.J, 2009. Watershed specific and regional scale suspended sediment loads for Bay Area small tributaries. A technical report for the Sources Pathways and Loading Workgroup of the Regional Monitoring Program for Water Quality: SFEI Contribution #566. San Francisco Estuary Institute, Oakland, CA. 28 pp + Appendices | | | | | | | | | | |
| ② | Ha, S.J., and Stenstrom, M.K., 2008. Predictive Modeling of storm-water runoff quantity and quality for a large urban watershed. Journal of Environmental Engineering 134, 703-711 | | | | | | | | | | |
| ③ | Lent, M.A. and McKee, L.J., 2011. Development of regional contaminant load estimates for San Francisco Bay Area tributaries based on annual scale rainfall-runoff and volume-concentration models: Year 1 results. A technical report for the Regional Monitoring Program for Water Quality. San Francisco Estuary Institute, Oakland, CA | | | | | | | | | | |
| ④ | Lent et al 2012 RWSM y2 documentation memo | | | | | | | | | | |
| ⑤ | This report. Funding from BASMAA via a contract with ACCWP | | | | | | | | | | |
| * | Note - the model resolution for sediment will vary from place to place given the need to use measured data where it exists and modeled data where it does not exist | | | | | | | | | | |
| ⑥ | This report. RMP funding ($20k/year) allocated to regional watershed spreadsheet model (RWSM) general development | | | | | | | | | | |
| ⑦ | This report. RMP funding ($80k/year) allocated to EMC development + depending on modeling outcomes perhaps a further $80-100k | | | | | | | | | | |

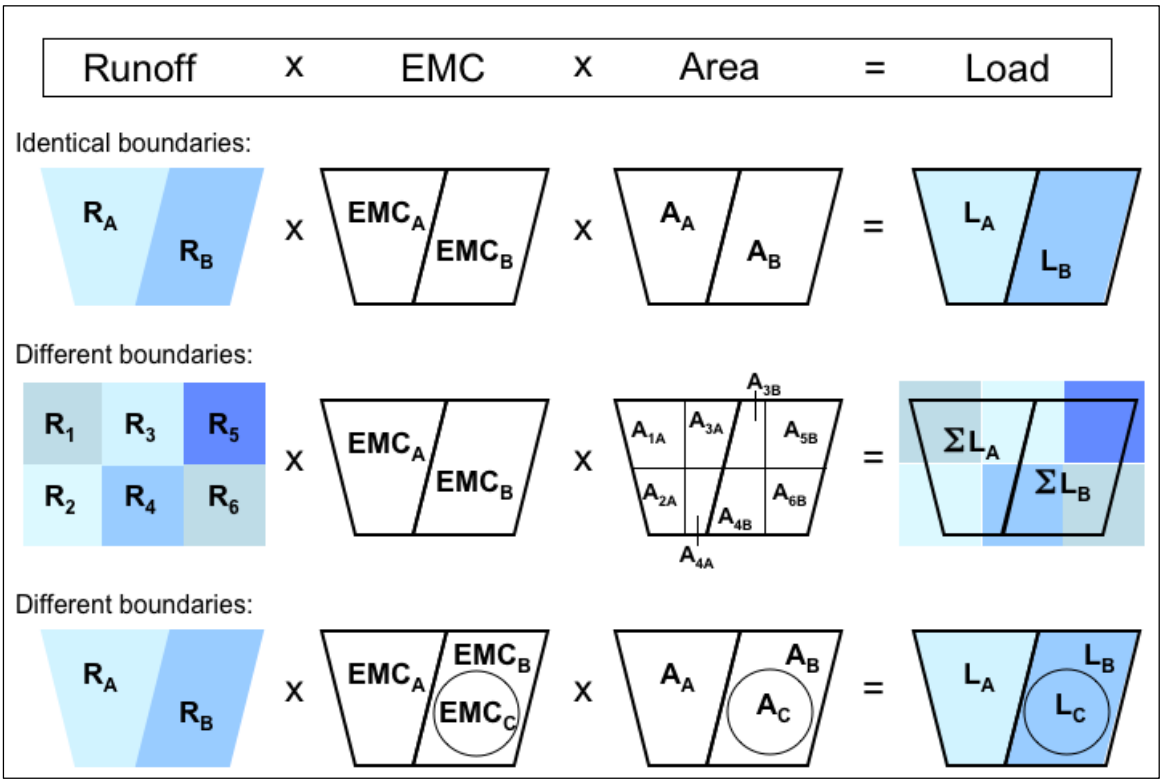


**Figure 3. Calculating loads for different model structures. A and B represent adjacent areas of different shape in the land use based model (LUM); The numbers 1-6 represent 30 m pixels in a continuous grid within the impervious cover layer of the impervious cover model (ICM).**

drop inlet or in soils in source areas will probably not be representative (McKee et al., 2003; Roger Bannerman, personal communication, December 2011).

An additional challenge presented by these model architectures is when the boundaries for the hydrologic model and the EMC overlay are not aligned; the resulting load estimates will take on different levels of model-output resolution (Figure 3). When the ICM is used with the land use or source based EMC model, the load aggregate (LA), will be the value $EMC_A$ times the aerially weighted average of the ICM grid values. So in the top aligned example (Figure 3), one ends up with two model output loads. In the bottom example, $EMC_B$ and $EMC_C$ are kept independent as opposed to being aerially averaged and the outcome is three model output loads instead of two. Given the difficulties in generating the EMC distribution, it may end up being problematic that the resolution of load output regulated by the resolution of EMC. There is an assumption (discussed more below) that the spatially constrained pollutant sources and the loads represented by the EMC's will be minimally affected by hydrologic variability because runoff variability is much less than the variability of contamination in the landscape.

# SUMMARY OF MODEL SIMULATIONS AND OUTCOMES

## GENERAL RWSM SUMMARY

Over the past four years, considerable effort has been undertaken to develop the Regional Watershed Spreadsheet Model (RWSM). The model was developed systematically starting with hydrology in parallel with a series of pollutant profiles (initially PCBs, Hg, Cu, dioxins, and Se with RMP funding and then subsequently sediment, PBDEs, and OC pesticides with BASMAA funding). Further work to improve the hydrologic basis was then completed before embarking upon a Cu model as a proof of concept, an improved sediment model as a basis for PCBs and Hg, and then the first full versions of the PCB and mercury models. The primary outcome from all this effort was a completed piece of draft model software (V1) that is ready for further development and application as appropriate data are developed to support improved model calibration or as management questions evolve.

### What can the RWSM be used for?

The RWSM is a planning level tool for estimating loads from the small tributaries surrounding the San Francisco Bay. It is being developed and calibrated at a regional scale using simple parameterization. It can be used for estimating regional scale annual average loads and should be useful for determining relative loading between sub-regions and more polluted versus less polluted watersheds. Accuracy and precision at smaller scales is challenged by the regional nature of the calibration process and the simplicity of the model. Gross comparisons of yields (loads per unit area) between watersheds or areas within watersheds may provide useful supporting evidence for prioritizing management attention but further field verification would be required.

Now that the expensive initial development phase is completed, there is great opportunity to further improve the model (2014 funding) and use it to start answering a variety of questions including improved estimates of regional and sub-regional scale loads, and relative loads between watersheds. Once calibration data has been collected that is inclusive of a broader range of source areas, improved regional loads estimates are expected (2015 funding). Loads estimates for smaller scale areas (e.g. small watersheds, sub-watersheds) may also begin to be possible with greater accuracy and precision.

## HYDROLOGY SUB-MODEL

The hydrology module development was the primary focus of the first two years of the RWSM (calendar years 2010 and 2011) and the proposed basis for Cu, dioxins, nitrogen species, and any other pollutant of interest whose transport process is at least 50% dissolved phase or strongly influenced by atmospheric deposition. Uncertainty remains about the use of hydrology model as the basis for PCBs and mercury and other more hydrophobic pollutants such as PBDE or DDT.

Initially during the first year of development, two base hydrology model approaches were investigated: one using runoff coefficients based on land use-soil-slope combinations and the other based on impervious cover. The impervious cover model appears to better relate to our conceptual model of landscape cover's effect on runoff and had the additional advantage of being decoupled from any land-use based pollutant model, however the pixel resolution of the input data made processing much slower. The land use model had the advantage of incorporating soil class and slope determination of the runoff coefficients and the processing time was much faster, but included the disadvantage of land use being a less precise runoff descriptor. The land use based model was chosen for further improvement in the second year; however, the option to return to the impervious cover model is possible if desired.

In the second year, the land use input dataset was upgraded to a higher resolution version, land use categories were refined to improve the treatment of runoff from the broadly aggregated categories, the calibration dataset was increased from 18 to 21 watersheds and improved to include watersheds with a broader range of imperviousness, and gauge records with incongruent land use / impervious data were removed. The overall outcome was an improvement in the logical nature of the flows in relation to our conceptual models of runoff generation and an acceptable calibration (median bias of +3% and overall accuracy of better than +/-75%). The current regional estimate of annual average flow to the Bay resulting from the model is 1,525 million $m^3$ (Table 2). Since the current model calibration was based on manually adjusting parameter coefficients using best professional judgment, the main weakness still to be addressed is fully incorporating the hydrologic model into the RWSM software using the auto calibration technique described in the sediment, PCBs, and mercury models below. In addition, the next version of the hydrology model should focus on the following improvements:

- Re-calibrate the model using the latest PRISM rainfall data layer release (2010 or later);
- To reduce the possibility of over-calibration, the calibration watershed data set should be split into two sets, one of which should be used to calibrate the model and the other to verify the calibration; this also could be done using a random set iterated 100x to generate error and range statistics for each coefficient that once applied in the model would generate mean and 95% confidence internal estimates for flows at watershed, sub-regional and regional scales;
- Incorporate runoff coefficients that have either a curvilinear function with imperviousness alone or runoff coefficients defined as a function of both land use, percent connected imperviousness and rainfall depth.

# COPPER MODEL

Due to the relative large knowledge about copper coefficients in relation to land uses and sources and the availability of a large calibration data set for the Bay Area, a copper model was developed as a test-case to learn about challenges associated with developing, for example, the PCB and mercury models. In the process of creating this model, we developed much of the basic structure that will be applied to other pollutants of more interest but which are more complex in source and transport processes.

Based on available local data and a review of international information, a basic land use structure was adopted as the base architecture for the copper model (industrial, commercial, residential, agriculture,

**Table 2. Preliminary sub-regional and regional scale runoff volume and loads for the Bay Area in relation to RMP Bay segments. Note, the number of significant figures does not reflect the accuracy of model outputs. Users should assume 2 significant figures when using these results in other contexts.**

| | Runoff ($Mm^3$) | Total Copper (kg) | Suspended Sediment (metric t)* | Total Mercury (kg)* | Total PCBs (kg)* |
|---|---|---|---|---|---|
| Lower South Bay | 246 | 6,517 | 416,226 | 87 | 19 |
| South Bay-East Side | 304 | 7,256 | 287,311 | 61 | 14 |
| South Bay-West Side | 64 | 1,675 | 132,061 | 39 | 12 |
| Central Bay-East | 29 | 831 | 68,290 | 13 | 8 |
| Central Bay-West | 39 | 928 | 76,853 | 15 | 3 |
| San Pablo Bay-East | 35 | 1,017 | 495,392 | 44 | 22 |
| San Pablo Bay-West | 552 | 22,734 | 435,175 | 98 | 8 |
| Suisun Bay | 257 | 8,657 | 694,686 | 131 | 31 |
| | | | | | |
| Total | 1,525 | 49,615 | 2,605,993* | 487* | 116* |

* Results will change with improved parameterization and re-calibration. There is considerable evidence (discussed briefly in the summaries below and in more detail in the attached appendices) that sediment loads are over estimated by about 30% (section A6), and PCB and Hg loads are over estimated by perhaps 3-fold (Section A8).

open space, transportation). The ABAG 2005 land use dataset was used as the geographical source of information, although there were challenges identified that could not be resolved with available budget. Coefficients for each land-use within the model architecture were developed from a review of local, arid west, and international literature. Issues related to regional variations and temporal variations were discussed and taken into account during the calibration procedure. Copper data collected in 15 watersheds in the Bay Area were used as the basis for model calibration using two configurations, one based on event mean concentrations (EMCs) and the other based on estimates of annual loads. A manual calibration procedure was used, adjusting parameters up-and-down and incorporating sensitivity analysis until the best model calibration was found. Although copper represents one of the richest datasets available, it was difficult to justify splitting the input concentrations between urban land uses because of the lack of more complex land use representation in the calibration watersheds; these issues are anticipated to PCBs and mercury in the future.

The regional load estimated using the best current calibrated model version (based on using the EMC calibrated input concentrations and assuming the agriculture input concentration = 64 ug/L) was 49,615 kg (Table 2). Based on the available calibration data sets, model calibration appeared to be better than +/-70%, and in this regard, similar to the hydrology model. Given the complexities of other pollutants relative to copper, an accuracy of +/- 70% may be the reasonable benchmark accuracy for other pollutants. A sensitivity analysis suggested that regional load estimates were most influenced by agriculture, transportation and open space land uses. After completion of the copper model, the key recommendations of greatest importance included:

- Quality check the hydrology model output to check for inconsistencies between imperviousness and land use classes considered highly impervious); possibly re-consider using impervious cover to underlie the hydrology model, or re-examine the general classification of the land uses.
- Adopt an automatic calibration routine for future sediment and pollutant model runs.
- When considering the locations for future field monitoring, consider monitoring land uses and source areas that are less represented in the currently available calibration watershed dataset.
- Consider the effects of time trends in stormwater concentrations and land use change in calibration watersheds in future pollutant model developments.
- Should further Hydrology Model development be undertaken, consider using a more comprehensive soils dataset and the latest PRISM rainfall data version.

# SUSPENDED SEDIMENT

Suspended sediment generation and transport was modelled as a function of geology, slope and current land-use while adjusting for watershed storage factors. Statistical analysis provided evidence that the most influential factor was geology with land use being the least influential factor. This helps to illustrate the weaknesses associated with using land-use based coefficients alone to generate sediment production and transport in unmonitored watersheds (Lewicki and McKee, 2009). The calibration of the sediment model was carried out through a constrained optimization method, a process that randomly samples loading coefficients within reasonable limits to search for an optimum combination that minimizes the difference between observed and simulated sediment loads. Attempts to develop a calibrated model without adjusting for watershed storage (reservoirs, hillslope and channel storage factors) failed; this seems logical but has the ramification that the subsequently developed PCB and mercury models will also need to include storage factors with the final step being “unadjustment”. Using the adjusted data, the difference between model simulated and observed loads at individual watersheds ranged from -98% to 1344% with 70% of the calibration watersheds within +/- 100% of observations; not unreasonable given the simplistic nature of the model. Model performance also didn’t appear to have any clear pattern in relation to quality of data, watershed size, or percent of imperviousness. However, other tests to determine model performance indicated that the sediment model was unable to converge to a stable solution and there were concerns that some of the parameters did not make logical sense. Based on the comparison with real available measurements, the current unstable model appears to be over predicting the loads in the 46 calibration watersheds by an average of 30%; by extension therefore, it was assumed that this would be true for the regional estimates ( 2.6 million metric t: Table 2) and about double loads previously reported (Lewicki and McKee, 2009). The sediment model remains unverified (all available data were used to calibrate the model with none separated for verification). Given that both PCB ( extreme case) and mercury concentrations have greater variability than sediment in the landscape, it is possible that the results from uncalibrated unstable sediment model could still be sufficient to support the development of the PCB and mercury models to estimate PCB and Hg loads.

Recommendations:

Listed below in order of priority, several improvements to the methodology were suggested during our experts’ workshop and in response to developing the first version of the model:

- Given rainfall and runoff are a major driver in sediment yield (and currently only implicitly in the model), investigate adding explicit factors representing different aridity between watersheds;
- Once a climatic factor is added in to the model parameterization, re-explore the choice of parameterization for geology-slope-land use combinations.
    - The default will be the existing 10 model parameter choices
    - If the default is found to be unstable, we could explore an expanded/reduced set of parameters. This may improve model performance given that other parameters such as Franciscan and Great Valley for some slope and land use categories are represented in more than 10 out of the 46 watersheds for at least 10% of the watershed area.
- Decide on a subset of the watersheds for model verification.
- Investigate the possibility of incorporating a proxy for sediment storage, such as sediment delivery ratio (SDR) or travel distance into the statistical analysis, as an optimization variable.
- Given the high variability in Tertiary and Franciscan erosiveness, investigate the possibility of splitting out more erosive sub-units from less erosive sub-units.
- Further improving model performance requires better ways to constrain loading coefficients than just a simple range. Future model structures could incorporate important sediment generation processes (e.g. buildup, washoff, and supply and transport limitation) into the modeling procedure.

# PCBS AND HG

Based on available local data and a review of international information, PCBs and mercury appear to be associated with a range of land uses and source areas where these substances were synthesized or refined and turned into products for society. Due mainly to lack of information on PCB and Hg event mean concentrations in water associated with land uses and source areas, PCB and Hg loads were modeled as a function of suspended sediment loads and particle ratios for specific land use or source areas (the concentration of the pollutant (mg) in relation to suspended sediment(kg)). Since many of the source areas of interest are not well mapped in standard land use mapping databases such as the National Land Cover (NLC) database or our local ABAG land use database, before modelling could occur, considerable effort was made by BASMAA and the RMP to further develop the GIS basis for the model. Given the availability of particle ratio data at the outlets of 22 watersheds and loadings data available in 11 watersheds (note both particle ratio and loadings data have variable quality), an auto-calibration procedure was used to optimize parameter coefficients for each land-use and source area used in the final model structures. Based on the development and outcomes to-date, regional loads estimates of 487 kg Hg and 116 kg PCBs were estimated and appear to be around 3-fold too high. Using the regional flow estimate (Table 2) and combining it with the PCB and Hg loads from the RWSM simulations, these loads equate to annual average regional concentrations of 76 and 319 ng/L for PCBs and Hg respectively which are high relative to our local observations to-date. Completing a similar thought experiment for sediment, regional average particle ratios of 0.092 and 0.38 mg/kg for PCB and Hg respectively were computed; again relatively high in relation to actual observations. The model has a number of weaknesses some of which can be immediately addressed and others will require further field data collection. These are summarized as follows:

- Weak structural basis for model
    - The sediment model is unstable and not calibrated well (see above and section A6)
    - Some of the important source areas are not represented well (low or absent)
- Uncertain parameter coefficients
    - Calibration data for any given watershed based on field studies are not accurate or precise; model therefore is being calibrated against data of variable quality
    - There is a lack of constraint on the relative order of the parameter coefficients in the auto-calibration process; leads to illogical outcomes on many calibration trials
- Calibration unstable & bias towards moderate pollution watersheds
    - Larger, less polluted watersheds tend to be over-simulated
    - Smaller, more polluted watersheds tend to be under-simulated
    - Many of the more polluted watersheds are only represented by a few parameter coefficients leading to unreliable relative loads comparisons
    - The calibration watersheds do not correspond to management priority watersheds
- Regional watershed loads are biased high
    - In the Bay Area, cleaner watersheds cover a large area (for example, the 10 largest watersheds cover more that 70% of the drainages area of small tributaries. Over predictions of these areas caused by high estimates of parameter coefficients for agriculture or open space leads to over-predicted regional loads

As a result, the loading estimates based on the current model runs (Table 2: 117 kg PCB and 487 kg Hg), appear to be 3-fold too high. At this time, partly due to a lack of a sensitivity analysis, it is difficult to know which of these issues are most responsible for modeling results appearing too high. Thus it was proposed to focus on known and easily fixable issues first before moving onto hard issues later. To increase model performance in relation to key management questions, recommendations included:

- Increase the quality assurance of the GIS basis of the model. BASMAA has been continuing to improve the source area GIS but there are issues that could be addressed through comparative review of specific weaknesses such as incorrect land use assignment of some Bay margin areas.
- Simplify parameterization and lower acceptance criteria for parameter inclusion or perhaps create a one or several global source area parameters. Explore adding data quality weighting factors based on:
    - The real proportions of land uses and source areas in the region
    - A focused part of the region (e.g. the urbanized area) to learn more about weaknesses.
- Complete field data collection of particle ratio data for additional calibration watersheds where source area categories of interest (that are under-represented in the current model calibrations) occur.
- Once such data are available (summer 2015), recalibrate the PCB and Hg models using more parameters (adding those of high interest and simplifying those of lesser interest), using a greater number of iterations to increase stability with the hope of increasing spatial accuracy.
- Compare the new results to existing local data; with additional calibration data, additional parameterization, and weighted calibration to focus model performance around key management questions, the likely outcome will be better relative loads between watersheds and better spatial resolution.

# APPENDICES

## APPENDIX 1. GEOGRAPHIC INFORMATION DEVELOPMENT TO SUPPORT MODELING

### A1.1 Improvements from previous version

Previous datasets that identified source areas for PCB/Hg like the "Prop13" point datasets were created nearly a decade ago (McKee et al., 2006), and existed in disparate shapefiles with differing attribute tables. These point datasets were previously the only source area data that were available to support the RWSM. The current update expands the source area categories, includes more data sources that have been updated since 2006, and merges data and fields of similar geometric types to reduce disparity. Further, all data are now grouped into land use categories that can be attributed with unique pollutant load coefficients. In addition, all new data now have robust metadata that documents its origins and methodology.

### A1.2 QA process, pitfalls, and solutions

As multiple datasets originating from databases with very different schema were combined to produce the new source area datasets, condensing all the relevant information into a few essential fields was a challenging task. Some datasets had SIC code attribution that made categorization easier, but others presented labeling challenges and required different categorizing methodologies. Similarly, many data points had latitude / longitude coordinates, whereas others were identified in space by street addresses. These locations were geocoded using ArcGIS 10.0 and combined with points plotted from X/Y coordinates. All plotted points with lat/long coordinates were assumed to be correct, and a random subset (25%) of geocoded points were spot-checked for accuracy against Google Maps. Of the subset, 70% of the geocoded points were correctly placed, and the others were mostly located on the same street but with a different street address. Through the QA process, many addresses comprised of solely zip codes were discovered and hand-plotted using Google Maps as a reference. Lastly, as many duplicates with names that differed slightly arose, QA record names and addresses were used to identify locations that might be identical.

### A1.3 Table of geospatial products

Source area data were developed for use in the PCB/Hg module for the RWSM. These data will serve as additional inputs to the PCB/Hg module to identify areas of estimated high pollutant concentration. These source areas will be calculated differently from other areas based on attributes that differ among categories. The data created covers three geometry types: points, lines, and polygons. All source datasets for each geometry type were merged together into one dataset with attributes detailing their category, which left three source data inputs. Polygon buffers of non-polygon data serve as inputs to the RSWM model.

Table 2 lists the data sources for each geometry type. The “Query Used” column refers to the specific attributes used to query records. The “Field Mappings” column refers to the native fields incorporated into the source area points concatenated “ID” field. The “Data Steward / Link” column highlights the entity that produced and houses the data and what methodology was used, or a link to a page where the data may be downloaded. Table 3 details the attribute schema used to place points in different category / subcategory assignments. As multiple disparate datasets were combined, the schema used may be less than ideal for some categories, but best professional judgment was used to minimize uncertainty. Appendix A lists all SIC codes referenced with their descriptions.

**Table 1. Currently available GIS layers to support pollutant load modeling using the regional watershed spreadsheet model (RWSM).**

| Source Dataset | Geometry Type | Query Used | Field Mappings | Data Steward / Link |
|---|---|---|---|---|
| Industrial Storm Water General Permit Notice of Intent Permit Data for San Francisco Bay Region[1] | Points | See Appendix 1 Attachment 1 | ID = WDID<br>TYPE = SIC<br>description | http://www.waterboards.ca.gov/water_issues/programs/stormwater/industrial.shtml |
| Envirostor Cleanup Sites database | | NAME or PAST_USES = 'AUTO', 'DRUM', 'METAL','SHIP' | ID = ENVIROSTAR ID<br>TYPE = PAST_USE | http://www.envirostor.dtsc.ca.gov/public/data_download.asp |
| EPA Superfund Sites | | site_name = 'AUTO', 'DRUM', 'METAL','SHIP'<br>rhs_name ~ 'MERCURY','PCB' | ID = EPA_ID | http://cumulis.epa.gov/supercpad/cursites/srchsites.cfm |
| Toxic Release Inventory, 2011[2] | | contaminant = 'MERCURY COMPOUNDS','MERCURY', 'PCB' | ID = TRI FACILITY ID | http://dtsc.ca.gov/database/index.cfm |
| California EPA Air Resources Board, 2008 | | CASid = 7439976 (mercury), 1336363 (PCB) | ID = FACID<br>TYPE = SIC<br>description | http://www.arb.ca.gov/app/emsinv/facinfo/facinfo.php |
| RMP Prop 13 Auto Disassembly | | kept non-redundant records | | SFEI - derived from SF Regional Water Quality Control Board records for active auto / truck dismantling facilities |
| RMP Prop 13 Hg/PCB Hotspots | | kept non-redundant records that were not spills | | SFEI - derived from multiple sources: Bay Spill Reports, DTSC CalSites, Superfund, PADS, PG&E, TRI |
| RMP Prop 13 Hg Emissions 2000-2007 | | derived from Air Resources Board | ID = FACID<br>TYPE = SIC<br>description | SFEI |
| Power Plants | | | | National Energy Technology Laboratory (NETL) - http://www.netl.doe.gov/technologies/carbon_seq/natcarb/download.html |
| Metal Recyclers Locations | | kept non-redundant records | | SFEI - derived from SF Regional Water Quality Control Board records for metal recycling facilities<br>EOA – performed a Google search for current day (2012) metal recyclers and kept all relevant and non-redundant records. |
| Railroad and Historic Rail Spurs | Lines | | | SFEI - derived (2006) from USGS modern rail lines and historic USGS topoquads (primarily 1959) |

| | | | | |
|---|---|---|---|---|
| Electrical Properties | Polygons | | | EOA – proposition 13 point data converted to polygon data via heads up digitizing; Additional properties were added based on OpenStreetMap data downloaded via Weo Geo (http://www.weogeo.com/) |
| Military Parcels | | | | EOA – selected polygons identified as military in ABAG land use data from 2005, and overlaid those polygons onto the latest parcel data from Alameda County, Contra Costa County, Santa Clara County, and Solano County. Military parcels that are open space are not included. |
| Ports | | | | EOA - selected polygons identified as port in ABAG land use data from 2005, and overlaid those polygons onto the latest parcel data from Alameda County, Contra Costa County, Santa Clara County, and Solano County. The data was edited to include only parcels that are associated with ports. |
| Industrial, 1968 | | | | EOA - derived from ABAG land use data from 2005 as well as parcel data from Alameda County, Contra Costa County, San Mateo County, Santa Clara County, and Solano County. Data was compared against aerials from 1968 downloaded from http://earthexplorer.usgs.gov/ |

1. Listed as “waterboard permits” in “Source” field, and broken into two subcategories. All records with XY values are labeled “lat/long”, and all others were geocoded using ArcGIS 10 and are labeled “geocode”.
2. all applicable records from TRI were redundant with others, and therefore no records in product were attributed “TRI” in “Source” field

**Table 2. Category and subcategory attribution schema for point data.**

| Category | Subcategory | Assignment Criteria |
|---|---|---|
| Recycling | Auto | -SIC 5015,7532<br>-SIC 5093 and 'auto' in name<br>-superfund or envirostor and 'auto' in name<br>-in Prop13 autodism database |
| | Drums | -SIC 2655<br>-if no SIC, 'drum' in past uses or name, or confirmed by Google search |
| | Waste | -SIC 4953,5093 |
| | Metals | -SIC 5093 and 'metal' in name<br>-if no SIC, must have "METAL RECLAMATION" or "RECYCLING – SCRAP METAL" in past uses<br>-all nonredundant metal recycleries from EOA dataset were also included |
| Manufacturing | | -SIC 3312,3315,3316,3317,3321,3324,3325,3341,3353,3356,3357,3363,3364,<br>3365,3369,3399,3411,3412,3423,3441,3442,3443,3444,3451,3462,3469,3471,3479,<br>3491,3494,3496,3498,3499<br>-if no SIC, must have "MANUFACTURING – METALS" in past uses, or if from RMP dataset, based on expert opinion |
| Cement | | -SIC 3241 |
| Cremation | | -SIC 7261 |
| Transport | Ship | -SIC 3731,3732,3812,4412,4449,4481,4482,4489,4491,4492,4493,4499<br>-if not in any other category, if "SHIP" in past uses |
| Power Plant | | All power plants in dataset were included. |

# Appendix 1 Attachment 1. SIC table for Industrial Storm Water General Permit Notice of Intent Permit Data for San Francisco Bay Region.

| SIC | Description |
|---|---|
| 2655 | Fiber Cans, Tubes, Drums, and Similar Products |
| 3241 | Cement, Hydraulic |
| 3271 | Concrete Block and Brick |
| 3272 | Concrete Products, Except Block and Brick |
| 3273 | Ready-Mixed Concrete |
| 3312 | Steel Works, Blast Furnaces (Including Coke Ovens), and Rolling Mills |
| 3313 | Electrometallurgical Products, Except Steel |
| 3315 | Steel Wiredrawing and Steel Nails and Spikes |
| 3316 | Cold-Rolled Steel Sheet, Strip, and Bars |
| 3317 | Steel Pipe and Tubes |
| 3321 | Gray and Ductile Iron Foundries |
| 3322 | Malleable Iron Foundries |
| 3324 | Steel Investment Foundries |
| 3325 | Steel Foundries, NEC |
| 3331 | Primary Smelting and Refining of Copper |
| 3334 | Primary Production of Aluminum |
| 3339 | Primary Smelting and Refining of Nonferrous Metals, Except Copper and Aluminum |
| 3341 | Secondary Smelting and Refining of Nonferrous Metals |
| 3351 | Rolling, Drawing, and Extruding of Copper |
| 3353 | Aluminum Sheet, Plate, and Foil |
| 3354 | Aluminum Extruded Products |
| 3355 | Aluminum Rolling and Drawing, NEC |
| 3356 | Rolling, Drawing, and Extruding of Nonferrous Metals, Except Copper and Aluminum |
| 3357 | Drawing and Insulating of Nonferrous Wire |
| 3363 | Aluminum Die-Castings |
| 3364 | Nonferrous Die-Castings, Except Aluminum |
| 3365 | Aluminum Foundries |
| 3366 | Copper Foundries |
| 3369 | Nonferrous Foundries, Except Aluminum and Copper |
| 3398 | Metal Heat Treating |
| 3399 | Primary Metal Products, NEC |
| 3411 | Metal Cans |
| 3412 | Metal Shipping Barrels, Drums, Kegs, and Pails |
| 3421 | Cutlery |
| 3423 | Hand and Edge Tools, Except Machine Tools and Handsaws |

| SIC | Description |
|---|---|
| 3425 | Saw Blades and Handsaws |
| 3429 | Hardware, NEC |
| 3431 | Enameled Iron and Metal Sanitary Ware |
| 3432 | Plumbing Fixture Fittings and Trim |
| 3433 | Heating Equipment, Except Electric and Warm Air Furnaces |
| 3441 | Fabricated Structural Metal |
| 3442 | Metal Doors, Sash, Frames, Molding, and Trim Manufacturing |
| 3443 | Fabricated Plate Work (Boiler Shops) |
| 3444 | Sheet Metal Work |
| 3446 | Architectural and Ornamental Metal Work |
| 3448 | Prefabricated Metal Buildings and Components |
| 3449 | Miscellaneous Structural Metal Work |
| 3451 | Screw Machine Products |
| 3452 | Bolts, Nuts, Screws, Rivets, and Washers |
| 3462 | Iron and Steel Forgings |
| 3463 | Nonferrous Forgings |
| 3465 | Automotive Stamping |
| 3466 | Crowns and Closures |
| 3469 | Metal Stamping, NEC |
| 3470 | Metal Services, nec |
| 3471 | Electroplating, Plating, Polishing, Anodizing, and Coloring |
| 3479 | Coating, Engraving, and Allied Services, NEC |
| 3482 | Small Arms Ammunition |
| 3483 | Ammunition, Except for Small Arms |
| 3484 | Small Arms |
| 3489 | Ordnance and Accessories, NEC |
| 3491 | Industrial Valves |
| 3492 | Fluid Power Valves and Hose Fittings |
| 3493 | Steel Springs, Except Wire |
| 3494 | Valves and Pipe Fittings, NEC |
| 3495 | Wire Springs |
| 3496 | Miscellaneous Fabricated Wire Products |
| 3497 | Metal Foil and Leaf |
| 3498 | Fabricated Pipe and Pipe Fittings |
| 3499 | Fabricated Metal Products, NEC |
| 3731 | Ship Building and Repairing |
| 3732 | Boat Building and Repairing |
| 3743 | Railroad Equipment |
| 3911 | Jewelry, Precious Metal |

| SIC | Description |
|---|---|
| 3914 | Silverware, Plated Ware, and Stainless Steel Ware |
| 3915 | Jewelers' Findings and Materials, and Lapidary Work |
| 4412 | Deep Sea Foreign Transportation of Freight |
| 4424 | Deep Sea Domestic Transportation of Freight |
| 4432 | Freight Transportation on the Great Lakes - St. Lawrence Seaway |
| 4449 | Water Transportation of Freight, NEC |
| 4481 | Deep Sea Transportation of Passengers, Except by Ferry |
| 4482 | Ferries |
| 4489 | Water Transportation of Passengers, NEC |
| 4491 | Marine Cargo Handling |
| 4492 | Towing and Tugboat Services |
| 4493 | Marinas |
| 4499 | Water Transportation Services, NEC |
| 4953 | Refuse Systems |
| 5012 | Automobiles and Other Motor Vehicles |
| 5013 | Motor Vehicle Supplies and New Parts |
| 5015 | Motor Vehicle Parts, Used |
| 5093 | Scrap and Waste Materials |
| 7261 | Funeral Services and Crematories |

# APPENDIX 2. EVENT MEAN CONCENTRATION DATA DEVELOPMENT

## A2.1 Mathematical methods of estimation

A series of simple and sophisticated mathematical estimation methods were employed to develop land-use specific event mean concentrations (EMCs) for analytes poorly characterized in the storm-runoff literature. We focused on Hg and PCBs initially since these are the highest priority pollutants in relation to provisions C.8.e., and C.11. and C.12. of the Municipal Regional Stormwater Permit (MRP) (Water Board, 2009), however, the same methods could be explored for suspended sediment concentrations (SSC), and if local data become sufficiently available, the same methods could be applied to other MRP analytes (e.g. Provision C.14. OC pesticides and PBDEs). Initially we focused on inverse optimization (see section A2 details) but we also used a series of simple algebraic and statistical methods some within GIS (see section A2 for details). The results of all this effort can be seen in the following summary tables for PCBs (Table 4) and for Hg (Table 5). What is seen is that:

There is very little data for either PCBs or Hg available in water (ng/L); most of the data are concentrations based on particles in the water column or sediment/soil concentrations (mg/kg),

The data for each land use or source area varies considerably across a row but generally the across row variability is lesser than the down column variability with as few exceptions in the case of PCBs; this give us some initial hope that the models may calibrate. These data provide the basic starting point for development of the PCB and mercury models. It is these data that we used as input to the auto calibration technique on the front end of each model (see section A8 on PCBs and mercury models for details).

### A2.1.a EMC estimates based on Bay Area data manipulation

As outlined in the first report of the RWSM (Lent and McKee, 2011), there are a number of simple algebraic methods that can be applied to post-calculate estimates of EMCs from data presented in previous reports (e.g. Mangarella et al., 2010), or existing Bay Area data bases (Yee and McKee, 2010). The results of these methods are presented in Table 4 (PCBs) and Table 5 (Hg). Each row in these tables represents the range of EMC estimates for each land-use or source area. Each method numbered one through 15 did not result in an estimated EMC for every row; rather together we used the 15 methods to populate as many rows as possible. The numbers in each row therefore represent a range based on the estimation methods. Since the model incorporates an auto-calibration procedure, it was not necessary to qualify each data point in these tables with a certainty factor, but it should be recognized that all these numbers carry some level is not a high level of uncertainty.

Method 1. The average annual PCB and Hg loads reported in Mangarella et al. (2010) that were derived from the mass balance reported by McKee et al., (2006) were divided by the flow volume for

**Table 4. Estimated PCB input "event mean concentrations" for the Regional Watershed Spreadsheet Model (RWSM). For details on the methods, see text in the rest of this report section. Refer to the text for an explanation of methods 1 to 15. Green indicates proposed base model and orange indicates additional parameterization to explore during the calibration process.**

| Land use or Source Area | GIS layers available in Calibration watersheds? | PCBs conceptual concentration (Lent and McKee, 2011) | Method | | | | | | | | | | | | | | | Variation (Max/Min) | Mean | Calibration boundaries | | | | | |
|---|---|---|---|---|---|---|---|---|---|---|---|---|---|---|---|---|---|---|---|---|---|---|---|---|---|
| | | | Water (ng/L) | | | | Sediment (mg/kg) | | | | | | | | | | | | | Proposed categories | Min | 10%ile | Median | 90%ile | Max |
| | | | 1 | 6 | 7 | 7 | 2 | 3 | 4 | 5 | 8 | 9 | 10 | 11 | 14 | 15 | | | | | | | | | |
| **All industrial** | **Yes** | | 96 | | | | | | | 0.13 | | | | | | | | 1 | 0.13 | | | | | | |
| Older industrial | **20** | M | | | | | | | | | | 2.80 | 1.80 | 0.60 | 0.48 | 0.07 | | 40 | 1.15 | Older Industrial | 0.010 | 0.029 | 0.60 | 4.2 | 36 |
| Newer industrial | **Yes** | M/L | | | | | | | | | | | | 0.093 | 0.23 | 0.03 | | 8 | 0.12 | | | | | | |
| Military | **1** | H | | | | | 1.92 | 0.49 | 0.80 | | | | | 4.2 | 0.67 | 0.72 | | 9 | 1.47 | | | | | | |
| Electrical transformer and capacitor (manufacture/repair/testing/storage/use) | **12** | VH | | | | | 10.71 | 0.46 | 1.33 | | | | | 36 | 0.01 | | | 3,600 | 9.70 | electricTransf | 0.010 | 0.191 | 1.33 | 26 | 36 |
| Electric power generation | | | | | | | 10.71 | 0.46 | 1.33 | | | | | 36 | 0.01 | | | 3,600 | 9.70 | | | | | | |
| Cement production | | | | | | | | | | | | | | | | | | | | | | | | | |
| Cremation | **4** | | | | | | | | | | | | | | | | | | | | | | | | |
| Oil refineries / petrochemicals | | M | | | | | 0.04 | 0.03 | 0.03 | | | | | 0.60 | 0.03 | 0.03 | | 21 | 0.13 | | | | | | |
| Manufacture (steel or metals) | **13** | M | | | | | 3.16 | 0.11 | 0.73 | | | | | 0.60 | 0.15 | 0.06 | | 53 | 0.80 | manufMetals | 0.060 | 0.086 | 0.38 | 1.9 | 3.2 |
| Recycling (drum) | **1** | H | | | | | 1.09 | 1.09 | 1.09 | | | | | 4.2 | 0.14 | 0.01 | | 420 | 1.27 | | | | | | |
| Metals recycling | **4** | M/L | | | | | 1.78 | 0.76 | 0.80 | | | | | 0.093 | 0.15 | 0.04 | | 44 | 0.60 | | | | | | |
| Marine repair and marine scrap yards | | | | | | | | | | | | | | 0.093 | | | | 1 | 0.09 | | | | | | |
| Auto recycling/ refurbishing | **8** | | | | | | 0.60 | 0.11 | 0.17 | | | | | 0.093 | 0.37 | 0.02 | | 30 | 0.23 | recycAuto | 0.020 | 0.057 | 0.14 | 0.5 | 0.6 |
| General waste recycling / disposal | **7** | | | | | | | | | | | | | 0.093 | 7.14 | 2.22 | | 77 | 3.15 | recycWaste | 0.093 | 0.52 | 2.22 | 6.2 | 7.1 |
| **All transportation** | **Yes** | | | | | | | | | | | | | | | | | | | | | | | | |
| Marina's | | | | | | | | | | | | | | | | | | | | | | | | | |
| Transport (ship) | | M | | | | | 2.97 | 1.13 | 1.29 | | | | | 0.60 | 0.45 | 0.26 | | 11 | 1.12 | | | | | | |
| Transport (rail) | **Yes** | | | | | | 1.27 | 0.17 | 0.41 | | | 1.50 | 0.00061 | 0.60 | | | | 2,459 | 0.66 | transpRail | 0.00061 | 0.084 | 0.50 | 1.4 | 1.5 |
| Transport (air) | **4** | | | | | | | | | | | | | | 0.06 | | | 1 | 0.06 | | | | | | |
| Freeways | **Yes** | | | | | | | | | | | | | | | | | | | | | | | | |
| Streets | **Yes** | | | | | | | | | | | | | | | | | | | | | | | | |
| **Urban (except industrial)** | **Yes** | L | 32 | | | | | | | 0.088 | | | | 0.011 | | | | 8 | 0.05 | Urban_other | 0.00017 | 0.003 | 0.22 | 1.3 | 3.0 |
| Commercial | **Yes** | | | | | | | | | | | | | | 0.95 | 0.16 | | 6 | 0.56 | | | | | | |
| Older urban | **Yes** | | | | | | | | | | | 0.15 | 0.15 | | | | | 1 | 0.15 | Older Urban | 0.0034 | 0.015 | 0.28 | 1.9 | 13 |
| High density residential | **Yes** | | | | | | | | | | | 0.0003 | 0.00017 | | 0.22 | 0.03 | | 1,294 | 0.06 | | | | | | |
| Low density residential | **Yes** | | | | | | | | | | | | | | | | | | | | | | | | |
| **All nonurban** | **Yes** | VL | 19 | 1.15 | 0.35 | 4.32 | | | | 0.0015 | 0.017 | 0.0140 | 0.00031 | 0.0009 | | | | 55 | 0.01 | Ag/Open | 0.00017 | 0.014 | 0.030 | 0.19 | 0.23 |
| Agriculture | **Yes** | | | | | | | | | | | | | | 0.03 | | | 1 | 0.03 | | | | | | |
| Open space | **Yes** | | | | | | | | | | | | | | 0.23 | 0.01 | | 23 | 0.12 | | | | | | |
| Marine sedimentary geology / soils | | | | | | | | | | | | | | | | | | | | | | | | | |
| | | | | | | | | | | | | | | | Variation (Max/Min) | | | 1,437 | | | | | | | |

**Table 5. Estimated Hg input "event mean concentrations" for the Regional Watershed Spreadsheet Model (RWSM). For details on the methods, see text in the rest of this report section. Refer to the text for an explanation of methods 1 to 15. Green indicates proposed base model and orange indicates additional parameterization to explore during the calibration process.**

| Land use or Source Area | GIS layers available in Calibration | Hg conceptual concentration (Lent and McKee, 2011) | Method | | | | | | | | | | | | | | | | | | Variation (Max/Min) | Mean | Calibration boundaries | | | | | | |
|---|---|---|---|---|---|---|---|---|---|---|---|---|---|---|---|---|---|---|---|---|---|---|---|---|---|---|---|---|---|
| | | | Water (ng/L) | | | | | | | | Sediment (mg/kg) | | | | | | | | | | | | Proposed categories | Min | 10%ile | Median | 90%ile | Max |
| | | | 1 | 6 | 7 | 7 | 12 | 12 | 12 | 13 | 2 | 3 | 4 | 5 | 8 | 9 | 10 | 11 | 14 | 15 | | | | | | | | | |
| **All industrial** | **Yes** | H | 182 | | | | 5 | 692 | 49 | 130 | | | | 0.34 | | | | 3.0 | | | 9 | 1.67 | | | | | | | |
| Older industrial | **20** | H | | | | | | | | | | | | | | 0.63 | 0.62 | 3.0 | 0.20 | 0.13 | 23 | 0.92 | Older Industrial | 0.13 | 0.22 | 0.68 | 5.6 | 9.0 |
| Newer industrial | **Yes** | | | | | | | | | | | | | | | | | 3.0 | 0.30 | 0.18 | 17 | 1.16 | | | | | | | |
| Military | **1** | | | | | | | | | | 0.462 | 0.14 | 0.224 | | | | | | 0.50 | 0.42 | 4 | 0.35 | | | | | | | |
| Electrical transformer and capacitor (manufacture/repair/testing/storage/use) | **12** | MH | | | | | | | | | 5.46 | 0.28 | 0.672 | | | | | 1.0 | 1.22 | 0.31 | 20 | 1.49 | electricTransf | 0.28 | 0.30 | 0.84 | 3.34 | 5.5 |
| Electric power generation | | | | | | | | | | | | | | | | | | 1.0 | 1.22 | 0.31 | 4 | 0.84 | | | | | | | |
| Cement production | | | | | | | | | | | | | | | | | | 1.0 | | | 1 | 1.00 | | | | | | | |
| Cremation | **4** | | | | | | | | | | | | | | | | | 1.0 | 0.18 | 0.14 | 7 | 0.44 | crematoria | 0.14 | 0.15 | 0.18 | 0.84 | 1.0 |
| Oil refineries / petrochemicals | | | | | | | | | | | 1.204 | 0.938 | 0.798 | | | | | 1.0 | 0.98 | 0.98 | 2 | 0.98 | | | | | | | |
| Manufacture (steel or metals) | **13** | | | | | | | | | | 1.946 | 0.294 | 0.434 | | | | | 1.0 | 0.52 | 0.31 | 7 | 0.75 | manufMetals | 0.29 | 0.30 | 0.48 | 1.47 | 1.9 |
| Recycling (drum) | **1** | VH | | | | | | | | | 2.408 | 1.26 | 1.26 | | | | | 9.0 | 0.68 | 0.67 | 13 | 2.55 | | | | | | | |
| Metals recycling | **4** | | | | | | | | | | 6.79 | 0.616 | 0.938 | | | | | 9.0 | 0.53 | 0.32 | 28 | 3.03 | | | | | | | |
| Marine repair and marine scrap yards | | | | | | | | | | | | | | | | | | 9.0 | | | 1 | 9.00 | | | | | | | |
| Auto recycling/ refurbishing | **8** | | | | | | | | | | 4.564 | 0.308 | 0.546 | | | | | 9.0 | 0.35 | 0.17 | 53 | 2.49 | recycAuto | 0.17 | 0.24 | 0.45 | 6.78 | 9.0 |
| General waste recycling / disposal | **7** | | | | | | | | | | 1.708 | 0.42 | 0.742 | | | | | 9.0 | 0.66 | 0.31 | 29 | 2.14 | recycWaste | 0.31 | 0.37 | 0.70 | 5.35 | 9.0 |
| **All transportation** | **Yes** | | | | | | 7.5 | 35 | 16 | 18 | | | | | | | | | | | | | | | | | | | |
| Marina's | | | | | | | | | | | | | | | | | | | | | | | | | | | | | |
| Transport (ship) | | M | | | | | | | | | 4.256 | 0.686 | 1.008 | | | | | 0.32 | 0.51 | 0.35 | 13 | 1.19 | | | | | | | |
| Transport (rail) | **Yes** | | | | | | | | | | 0.756 | 0.322 | 0.392 | | | | | 0.32 | | | 2 | 0.45 | transpRail | 0.32 | 0.32 | 0.36 | 0.65 | 0.8 |
| Transport (air) | **4** | ? | | | | | | | | | | | | | | | | | 0.14 | 0.11 | 1 | 0.13 | | | | | | | |
| Freeways | **Yes** | L | | | | | | | | | | | | | | | | 0.13 | | | 1 | 0.13 | | | | | | | |
| Streets | **Yes** | | | | | | | | | | | | | | | | | 0.13 | | | 1 | 0.13 | | | | | | | |
| **Urban (except industrial)** | **Yes** | | 122 | | | | 1.7 | 66 | 24 | 26 | | | | 0.28 | | | | 0.13 | | | 2 | 0.21 | Urban_other | 0.11 | 0.13 | 0.32 | 0.89 | 4.3 |
| Commercial | **Yes** | | | | | | | | | | | | | | | | | | 0.47 | 0.30 | 2 | 0.39 | | | | | | | |
| Older urban | **Yes** | | | | | | | | | | | | | | | 0.16 | 0.16 | | | | 1 | 0.16 | Older Urban | 0.12 | 0.18 | 0.50 | 3.2 | 6.6 |
| High density residential | **Yes** | | | | | | | | | | | | | | | | | | 0.95 | 0.31 | 3 | 0.63 | | | | | | | |
| Low density residential | **Yes** | | | | | | | | | | | | | | | | | | 0.18 | 0.18 | 1 | 0.18 | | | | | | | |
| **All nonurban** | **Yes** | VL | 82 | 38.9 | 8.31 | 252 | | | | | | | | 0.056 | 0.21 | 0.14 | 0.0061 | 0.041 | | | 34 | 0.09 | Ag/Open | 0.070 | 0.079 | 0.12 | 0.26 | 0.32 |
| Agriculture | **Yes** | | | | | | 1.8 | 6.6 | 3.9 | 6 | | | | | | | | | 0.13 | 0.07 | 2 | 0.10 | | | | | | | |
| Open space | **Yes** | | | | | | 2.3 | 48 | 6.1 | 13 | | | | | | | | | 0.32 | 0.10 | 3 | 0.21 | | | | | | | |
| Marine sedimentary geology / soils | | | | | | | | | | | | | | | | | | | | | | | | | | | | | |
| | | | | | | | | | | | | | | | | | | | Variation (Max/Min) | | 99 | | | | | | | |

each land use estimated by Davis et al. (2000). This resulted in an estimate of EMC for three basic land use classes for both PCBs (Table 4) and Hg (Table 5).

Method 2. The maximum concentrations in San Francisco Bay Area "industrial areas" reported in Lent and McKee (2011) in Table A3-3 (PCBs) and Table A4-3 (Hg) based on data reported by Yee and McKee (2010) were multiplied by an enrichment ratio of 1.4 to take into account the preferential resuspension of fine material (<250 micron) that is in suspension during peak flow when the majority of transport is occurring (e.g. Gilbreath et al., 2012). This method resulted in particle-based EMCs for a variety of land uses and source areas for both PCBs (Table 4) and mercury (Table 5).

Method 3. These estimates were computed using the same method described in method 2 but based on median concentrations.

Method 4. These estimates were computed using the same method described in method 2 but based on mean concentrations.

Method 5. The median sediment concentrations derived from BASMAA bed sediment studies (KLI, 2001; Salop et al., 2002) as summarized and reported in McKee et al. (2006) (Table 6-1) (Industrial: Hg: 0.24 mg/kg; PCBs: 0.094 mg/kg; urban except industrial: 0.2 mg/kg; PCBs: 0.063 mg/kg; All non-urban (Open): 0.04 mg/kg; PCBs: 0.0011 mg/kg) were multiplied by an enrichment ratio of 1.4 to take into account the preferential resuspension of fine material (<250 micron) that is in suspension during peak flow when the majority of transport is occurring (e.g. Gilbreath et al., 2012). This method resulted in particle-based EMCs for 10 source areas of both PCBs (Table 4) and Hg (Table 5).

Methods 6. The flow weighted mean concentration (FWMC) was computed for Marsh Creek near Brentwood based on samples gathered during WY 2012 (a relatively dry year) (McKee et al., 2013). This resulted in an estimate of EMC for water for nonurban land use both PCBs (Table 4) and Hg (Table 5).

Method 7. These estimates were computed using the same method described in method 6, only reporting minimum and maximum concentrations rather than the flow weighted mean.

Method 8. These estimates of particle-based EMCs were based on falling stage samples taken from Coyote Creek at Hwy 237 (McKee et al., 2009). Data were generated from both PCBs (Table 4) and Hg (Table 5).

Method 9. These estimates are the mean results of initial "back-calculation" techniques (see section A2 for details). Hg: Table 7: Hg optimization: Optimized concentration statistics (3 land uses). PCBs: Table 11: PCBs optimization without Santa Fe: Optimized concentration statistics (5 land uses).

Method 10. These estimates were computed using the same method described in method 9, only reporting median concentrations rather than the mean.

Method 11. These EMC particle ration estimates are the range of particle concentrations observed in the Bay Area reported by Yee and McKee (2010) using only non-zero data divided into six categories for PCBs (VH, H, M, M/L, L, VL) and for Hg (VH, H, M/H, M, L, VL). We used a log-normal distribution to calculate the mean statistic for each category which was then adjusted assuming an enrichment ratio of 1.4. This method resulted in particle-based EMCs for 16 PCBs source areas (Table 4) and 20 Hg source areas (Table 5).

Method 12. These estimates of EMC in water are the minimum, maximum and median concentrations derived from a review of world literature previously completed and reported in Table A4-5 of Lent and McKee (2011). This method resulted in concentrations for Hg only (Table 5).

Method 13. These estimates were computed using the same method described in method 12, only reporting mean concentrations.

Method 14. These estimates of particle-based EMCs are the mean concentrations derived from analyzing GIS source area spatial data with PCB and Hg soils / street/drop inlet sediment data reported by Yee and McKee (2010). We programed the GIS analysis to assign all PCB and Hg sediment data to the source area types or land uses within a 20 m buffer. The analysis of the data allowed a PCB or Hg data point to be assigned multiple source areas or land uses. Roads and highways were removed prior to this analysis because these broad common linear features in our landscape would have captured all the points there therefore the mean would then be just the mean of the majority of the data and be meaningless. The mean for each category was calculated and then the maximum mean category for each pollutant is identified. All points with multiple intersections that include highest mean source area/land use were compared to the max source area/land use mean for that pollutant. If pollutant concentration was higher than max source area/land use mean, that point was assigned to that source area/land use. If the pollutant concentration was lower than the highest category mean, then the concentration was compared to next highest mean in the list. If the concentration was greater than the average of the two means, then it was assigned to max category mean. If lower, the concentration remained unassigned and added to the next looping iteration of this analysis until each data point is assigned one source areas/land-use designation.

Method 15. These estimates were computed using the same method described in method 14, only reporting median concentrations instead of means.

### A2.1.b Parameter estimation using inverse optimization

Parameter estimation (also known as inverse optimization) methods were used to derive source or land-use specific concentrations from downstream concentration data (Figure 4). This approach of back-calculating multiple source concentrations from downstream storm runoff concentrations has been successfully used before (Silverman et al., 1988; Ha and Stenstrom, 2008). The methodology employed for this work was in part based on Ha and Stenstrom (2008) and builds upon worked presented

previously in SPLWG meetings (Lent, 2011). The objective here was to support the development of the next versions of the PCB and Hg model modules by:

a) Further developing the inverse optimization methodology (further prove the concept), and
b) Using the techniques to estimate land use/source area EMC input data for many land uses/source areas as possible.

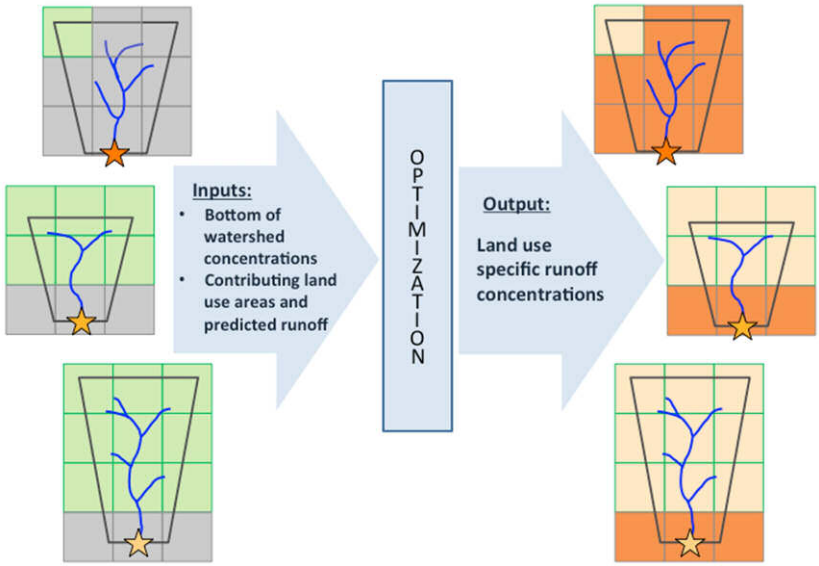


**Figure 4. Overview of deriving land use specific concentrations from downstream concentrations. The underlying grid represents land use types, which are assumed to have a consistent runoff concentration (Note: while shown here as a spatial grid for visualization purposes, land use within the model is not spatially explicit, rather it is simply a fraction of a watershed's area). Brightness of the stars represents the concentration measured at the bottom of the watershed. The optimization computes what runoff concentration each land use type would have in order to generate the concentration observed at the bottom of the watershed.**

## *A2.1.b.i Methods*

### Overall Approach

The overall approach entailed running the optimization within a Monte Carlo loop that fed the optimization a set of randomly chosen observed (actual) concentration data points, one from each calibration watershed (Figure 5). The optimization then searched the parameter space of land-use specific concentrations, and computed "simulated" downstream concentrations from these parameters, using a simple model that incorporated categorized land use and runoff. An underlying hydrological model used runoff coefficients and area to compute proportions of runoff from each land use category.

The goal of the optimization was to minimize the difference between observed concentrations and the simulated concentrations for each watershed while keeping the land-use specific concentrations consistent across watersheds. The optimization was performed in R and the land-use analysis was performed in ArcGIS.

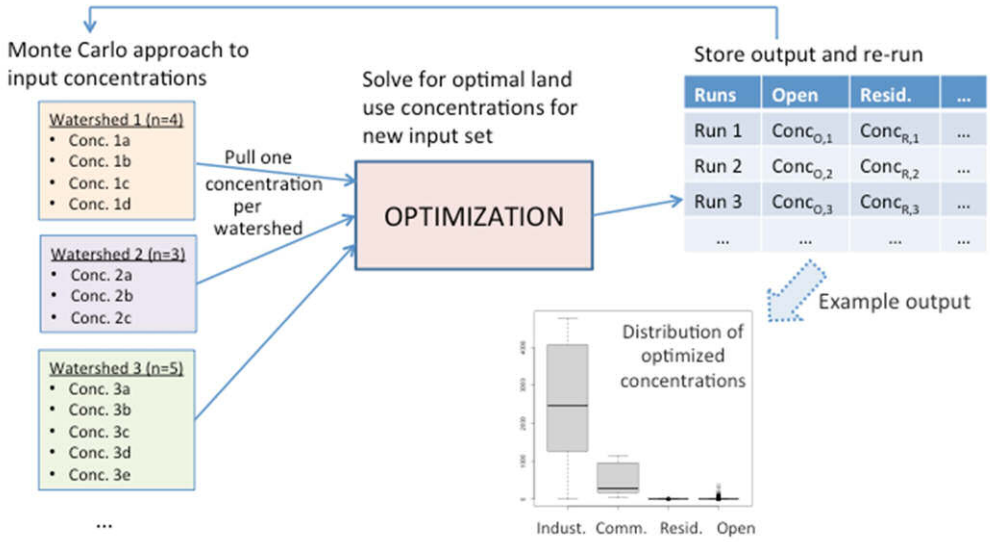


**Figure 5. Overall structure of mathematical estimation approach.**

### Input concentration and land-use data

Downstream sampling wet weather particle concentration data sets were compiled for 21 local watersheds for Hg and PCBs (Figure 6). Particle concentration was estimated as the ratio of concentration of the pollutant in water to the concentration of suspended sediment in that same water sample. This is not strictly a particle concentration since some dissolved phase occurs even using wet season runoff but is served as a useful approximation and a way of removing the influence of variable sediment erosion on water concentrations from the input data set. Watersheds considered outliers for a particular pollutant were not included (e.g., Guadalupe watershed for Hg). The data sets were split with 12 watersheds in the calibration set and 8 or 9 watersheds in the validation set. The watersheds were carefully assigned to the calibration and validation sets to ensure each contained a range of concentrations and land-use characteristics. Additionally, watersheds likely to be used for RSWM Hg or PCBs model calibration were withheld from the calibration sets (to avoid calibrating both the input parameters and the model itself with the same data set).

Spatial data (GIS layers) were compiled for the land-use categories of interest. The initial land-use categories were selected based on earlier work showing that watershed concentrations of Hg and PCBs positively correlated with presence of older (defined here as developed before 1954) urban areas, in particular industrial areas (Greenfield et al., 2010). The land-use proportions were computed for each

watershed to serve as input into the optimization. In order for the optimization to be successful, the land-use categories chosen must be adequately represented in the calibration watersheds; underrepresented categories will act as free parameters and generate meaningless EMCs. A category would be considered underrepresented if the signal-to-noise ratio is too low for the category to be statistically different from others. The "signal" would be a function of the data set size (e.g., number of watersheds with representative land use) and data set strength (e.g., proportion of representative land use in monitored watersheds), as well as the actual variance of concentrations running off of land within that category.

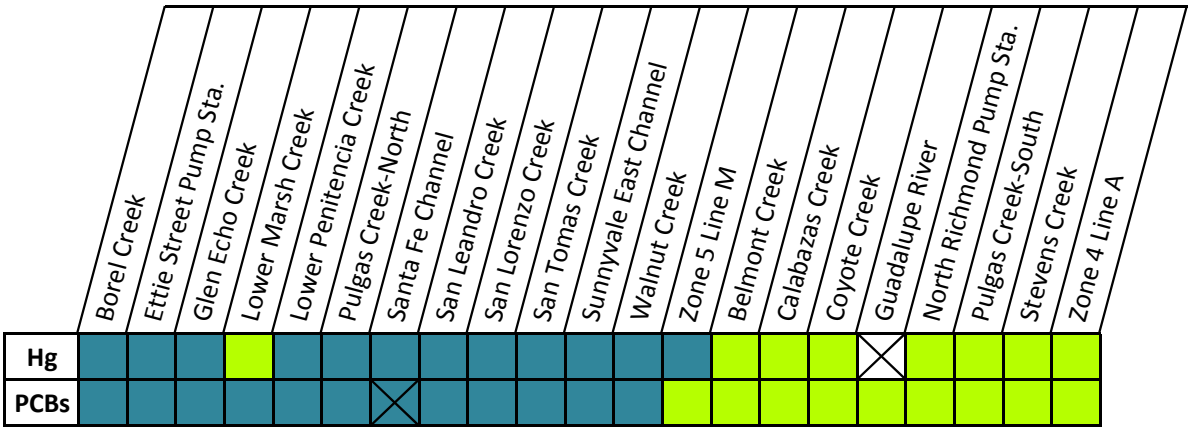


**Figure 6. Calibration and validation watersheds for mercury and PCBs. Blue represents a watershed used for calibration and green represents used for validation.**

### Underlying concentration-hydrology model

The underlying model provided the connection between the observed data and the parameters being optimized, i.e., the land-use specific concentrations. A simple linear model was used to relate the concentrations being optimized to the downstream concentrations. Simulated downstream concentrations were approximated as weighted sums of contributing land-use (LU) specific concentrations, where the weights were the proportion of runoff (a function of area and hydrology):

$$Conc_{i,Sim} = \sum_{j=1}^{n} f_{i,LU_j} * Conc_{i,LU_j} \quad \text{where} \quad f_{i,LU_j} = \frac{RC_j * Area_{i,j}}{\sum_{j=1}^{n}(RC_j * Area_{i,j})}$$

$$for\ watershed\ i\ and\ land\ use\ j$$

The hydrologic behavior of different land-use types was approximated with runoff coefficients (RC). The initial RC values were taken from the RSWM's calibrated land-use based hydrology model. A simplification in this approach is the lack of pollutant storage in the system; all pollutants suspended in runoff are assumed to be transported downstream. The same simplification was used in the current

structure of the RWSM pollutant model. In reality, in-stream pollutant transport is a complicated process of advection, partitioning, deposition, and re-suspension, and so sources further upstream from the measurement location may exhibit a fainter signal than sources close by. However, given "bottom of the watershed" sampling and standard Bay Area development patterns with developed lowlands and less developed headwaters, the attenuation of more distant sources (i.e., open and agricultural areas) may be implicitly captured in the data, and thus in the optimization. As a result, the concentration developed for distant areas should not be thought of as direct runoff concentration, but instead the portion of that concentration expected to travel downstream.

### Optimization structure

One of the most important components of optimizations is the objective function, an equation that evaluates the state of the optimization. An optimization has arrived at an optimal solution when the objective function is at its global maxima or minima for the search space. The objective function developed for this work is as follows:

$$Minimize\ \ Z = w_{i,r}\sum_{i=1}^{m}\left(Conc_{i,Obs} - \ Conc_{i,Sim}\right)^2 + \lambda\sum_{j=1}^{n}\sum_{i=1}^{m}\left(Conc_{i,LU_j} - \frac{\sum_{i=1}^{m} Conc_{i,LU_j}}{m}\right)^2$$

$$where\ Z\ is\ the\ objective\ function\ value, m\ is\ the\ number\ of\ modeled\ watersheds,$$

$$and\ n\ is\ the\ number\ of\ different\ land\ use\ categories\ represented\ in\ the\ model.$$

The first term in the objective function serves to minimize the difference between observed concentrations and the simulated concentrations at the sampled outlet of the watershed, and the second term forces convergence of concentration values for each land-use type. The parameters being optimized (i.e., decision variables) are the land-use specific concentrations ($Conc_{LU}$). The simulated concentrations ($Conc_{Sim}$) are computed from the current set of land-use specific concentrations at each iteration of the optimization. The weights on the first term, $w_{i,r}$, can be set to represent confidence in observed data points (e.g., a questionable data point, r, can be given a low weight, reducing its impact on the optimization). The weight on the second term, λ, sets the relative importance of the two objective function terms, controlling the level of convergence required of the land-use concentrations. These weights were selected using professional judgment and were tested during the sensitivity analysis.

No underlying distribution was assumed for the optimized concentrations, unlike in a maximum likelihood approach. Rather, the distributions of the land-use specific concentrations were built up "blindly" via the Monte Carlo approach, allowing the data to suggest the shape of the underlying distribution.

The optimization solver used was a limited-memory modification of the Boyd-Fletcher-Goldfarb-Shanno (BFGS) method with box constraints. The BFGS method is a quasi-Newton approach; it uses function values and gradients to build up a picture of the surface to be optimized (while it is tricky to picture this for many a parameter problem, if there were only two parameters to be optimized, they would be represented along x- and y-axes, while the z-axis would represent the objective function value and the

optimization surface would be formed by the objective function value for each pair of parameter values within the solution space). The major benefit of this approach was its compatibility with constraints; putting well-informed bounds on parameters being optimized reduces the searched parameter space (and thus computation time) and increases the likelihood of convergence to a stable solution. Here, bounds were used to focus the search space, not to serve as active constraints. Accordingly, when an optimization ran up against a bound, the bound was increased to the point where the bound was no longer constraining the solution.

### Monte Carlo discussion

The optimization was set up within a Monte Carlo loop to allow incorporation of actual variability present in watershed sampling data. The Monte Carlo loop was set up to pull one data point from each calibration watershed's data set (n=3 to 7), so each iteration of the optimization was run on randomly sampled data set. To check for convergence, increasing numbers of runs were tested and various percentiles of results were tracked (Figure 7). The number of iterations needed to converge depended on the pollutant and number of land-use/source area concentrations being optimized.

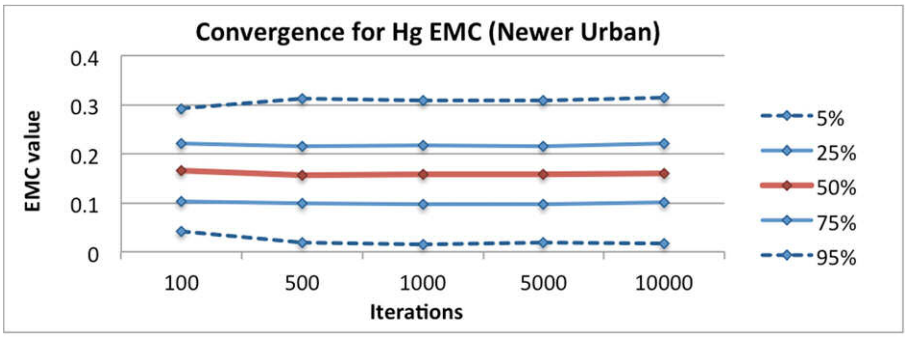


**Figure 7. Example Monte Carlo convergence with increased iterations. Event mean concentrations (EMCs) plotted for a suite of percentiles.**

## *A2.1.b.ii Results analysis and presentation*

The results were presented graphically using box and whisker plots. The conventional distribution of the box and whisker was used, i.e. the box represents the first and third quartiles, the midline represents the second quartile (median), the whiskers represent the 1.5 interquartile range, and circular markers represent outlier points. In addition, the results were also summarized in tabular form to facilitate comparison of our results to the small amounts of information developed previously and reported in peer-reviewed literature. For comparing watersheds' observed and simulated concentrations, the median values were used. The statistical significance of watershed results was checked using the Wilcoxon rank-sum test (also know as Mann-Whitney test). The Wilcoxon rank-sum test is a nonparametric test for the difference in two means and is appropriate when the assumption of normality does not necessarily hold for the two distributions being compared.

### Mercury

The first set of land-use categories used to optimize runoff concentrations of mercury was mainly based on development level and age. (At the time of this study, no mercury-specific source area GIS data sets were available for immediate use, so only "conventional" land-use categories were tested. As mercury-specific GIS data sets come available, they should be tested within this framework.) The initial land-use breakdown was 1) old (pre-1954) industrial land, 2) old non-industrial urban area, 3) newer urban areas, and 4) undeveloped land. The initial results showed that the older industrial land-use category exhibited a very large spread in runoff concentrations that spanned the other land-use categories' concentrations, suggesting that, for the calibration data set, there was no consistent mercury signal from older industrial land (Figure 8a). (A quick check showed this was indeed true for this data set: the watersheds with significant old industrial areas were Pulgas Creek-North (32%) and Ettie Street catchment (13%), and the one with the larger old industrial area exhibited lower mercury concentrations.) The results of the other categories were consistent with expected behavior, so the optimization was re-run with old industrial land folded back into the old urban land-use category. The results of the revised optimization are shown with concentration ranges of representative watersheds from the validation set (Figure 8b). The optimized concentrations for older urban land were within the range measured for Pulgas Creek-South, a 98% older urban catchment. Likewise, the optimized concentrations for newer urban land were in line with the concentration data collected from Calabazas Creek watershed, which contains 79% newer development. The concentrations optimized for undeveloped (open and agricultural) areas were compared against two mostly undeveloped watersheds: Coyote Creek (62% undeveloped) and Lower Marsh Creek (76% undeveloped) Both of these watersheds have historic Hg mining influence although the Mount Diablo Mine in Marsh Creek is considered higher risk for Hg transport than the Silver Creek Mine in the Coyote Creek watershed (Abu-Saba, 2003). The optimized concentrations for undeveloped land use were similar to the two mostly undeveloped watersheds, but with many outliers at the high end. These results may be a consequence of limited watershed data for undeveloped areas or, alternatively, there may be sources of mercury within some of these undeveloped areas (e.g., legacy mining sources).

The Wilcoxon rank-sum test on the distributions found that the land-use concentrations were all significantly different from one another (Table 6). Both urban land-use types exhibit relatively normal distributions with low spread, while the undeveloped land-use exhibits a thick-tailed log-normal distribution (histograms not shown). These distributions suggest that, within the calibration set, the older and newer urban areas are each emitting a fairly consistent mercury signal. The results of the optimization were used to calculate simulated downstream concentrations for both the calibration data set and the validation data set. The performance of the optimization can be judged in part on its results ability to generate downstream values similar to the observed concentrations. In particular, the validation data set, which was not used in the optimization, provides an unbiased evaluation of the optimization.

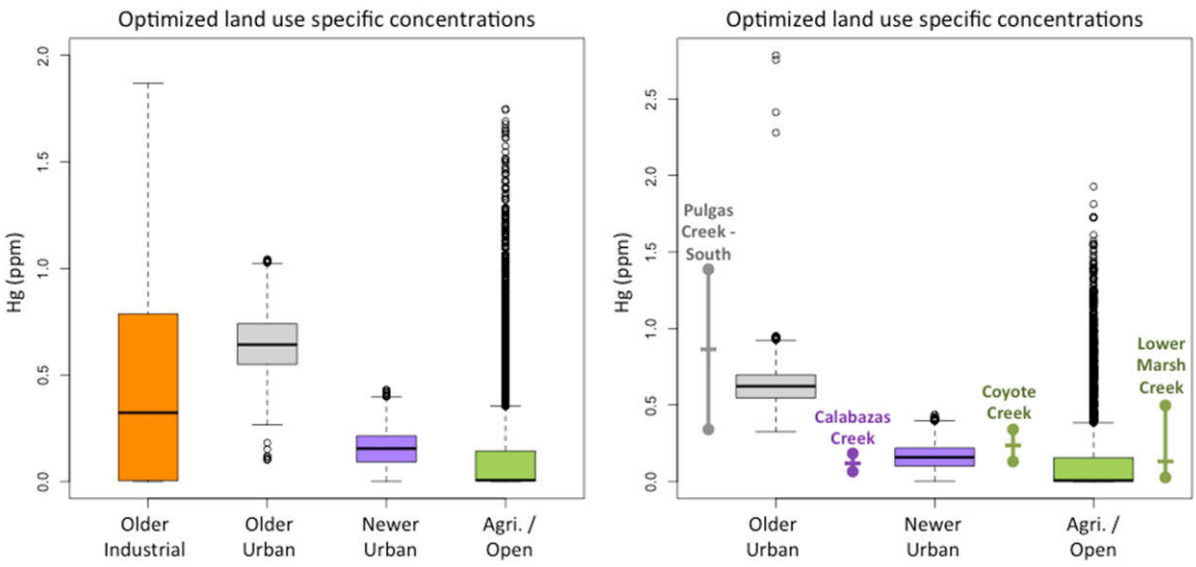


**Figure 8.a) Optimized Hg concentrations for four general land-use categories (5000 iterations), and b) Optimized Hg concentrations for three general land-use categories (5000 iterations). Hg concentration ranges shown for representative watersheds (horizontal line = median).**

**Table 6. Hg optimization: Optimized concentration statistics (3 land uses).**

| p-Hg (ppm) | Old urban | Newer urban | Agri./Open |
|---|---|---|---|
| Mean | 0.63 | 0.16 | 0.14 |
| Median | 0.62 | 0.16 | 0.0061 |
| St. Dev. | 0.12 | 0.086 | 0.26 |

Overall the simulated downstream (i.e., bottom of watershed) concentrations tracked fairly well with the observed concentrations for the calibration watersheds (Figure 9). However, there clearly are Hg signals that are not being captured by the three land-use categories. For example, San Leandro watershed has a notably higher Hg concentration than the optimization was able to predict, suggesting that there is a source area that is not adequately described by the land-use categories. Additionally, there are three older development watersheds (Ettie St. Pump Station, Glen Echo Creek, and Pulgas Creek-North), which are identical from the optimization's viewpoint (all 100% old urban) and so produce the same simulated mercury concentration. However, in reality, they emit different concentrations, but without distinguishing features (land uses or source areas), the optimization cannot capture these differences. If the distinguishing feature that causes Ettie St. Pump Station to have a higher Hg concentration than Glen Echo Creek and Pulgas Creek-North can be identified and incorporated into the optimization, the old urban concentration would likely decrease as the Hg contribution would be partially reallocated to the new category. This could be done in a future back-calculation effort or potentially resolved by implementing field monitoring if specific sources in these watersheds.

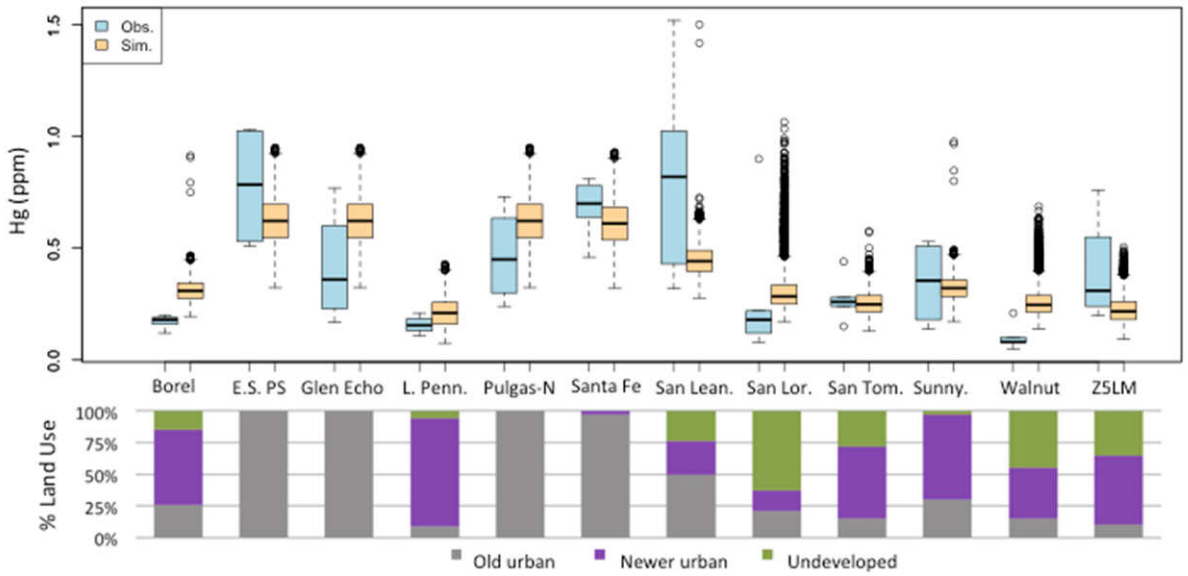


**Figure 9. Calibration watersheds: Observed versus simulated p-Hg concentration and land-use distributions.**

The simulated downstream concentrations were fairly similar to the observed concentrations for the validation watersheds, with the difference between the observed and simulated median value ranging from -44% to 79% (Figure 10 and Table 7). Given the calibrated hydrology model has a similar magnitude of uncertainty (Lent and McKee, 2011, Lent et al., 2012), these may be reasonable, but at this time, the question of how good is good enough (the success definition), has not been defined. In addition, there still are watersheds that the optimization was unable to adequately simulate. Belmont Creek has a substantially lower observed concentration and North Richmond Pump Station has a much higher concentration than would be predicted by the land-use distribution. As with the calibration results, these results suggest that there are unaccounted land uses or source areas, here artificially inflating Belmont Creek's simulated Hg concentration and underrepresenting Hg sources in North Richmond Pump Station.

### PCBs

The first set of land-use categories used for PCBs was: 1) old (pre-1954) industrial land, 2) old non-industrial urban area, 3) newer urban areas, and 4) undeveloped land. Additionally, a specialized PCBs-associated land-use layer, railroads, was available, so it was incorporated next. (Railroads are associated with PCBs because PCB-laden oils were used for dust suppression along railways, in electrical equipment, in the heavy equipment transmission and hydraulic oils, and because railway lines serviced heavy industrial land use during the peak of PCB use (SFEI, 2010).)

The initial results for the four general land uses are compared against representative watersheds from the validation set (Figure 11a). Unfortunately, there was no representative watershed for old industrial land use (Pulgas Creek-South had the highest percentage out of the validation set). The optimized PCBs concentrations for older urban land were within the range measured for Pulgas Creek-South, a 98% older urban catchment (22% industrial and 76% non-industrial). Meanwhile the optimized

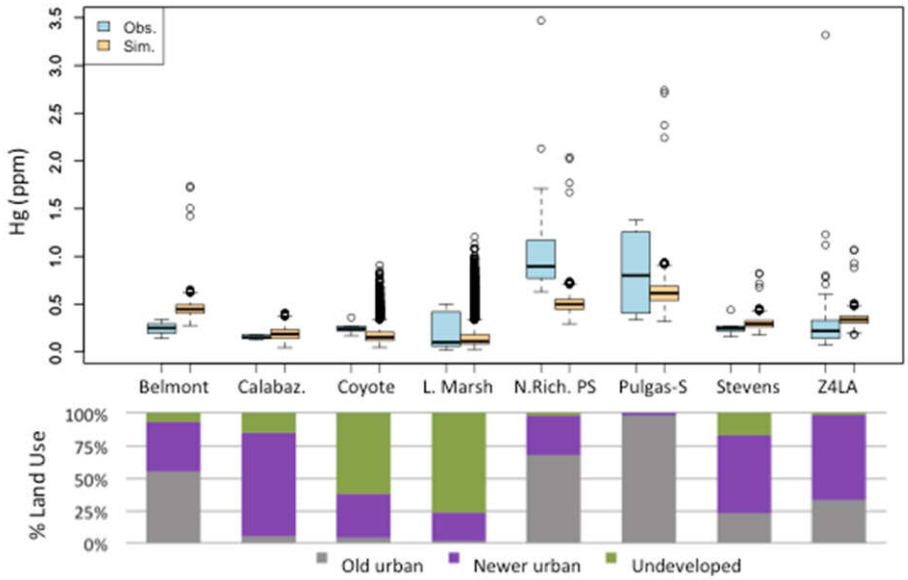


**Figure 10. Validation watersheds: Observed versus simulated p-Hg concentration and land-use distributions.**

**Table 7. Hg optimization: Validation set performance.**

| p-Hg (ppm) | Belmont | Calabaz. | Coyote | L. Marsh | N. Rich PS | Pulgas-S | Stevens | Z4LA |
|---|---|---|---|---|---|---|---|---|
| Observed (n) | 0.25 (4) | 0.15 (5) | 0.24 (6) | 0.10 (6) | 0.90 (16) | 0.80 (4) | 0.25 (6) | 0.22 (89) |
| Simulated | 0.45 | 0.19 | 0.15 | 0.11 | 0.50 | 0.61 | 0.29 | 0.34 |
| Difference | 79% | 24% | -36% | 10% | -44% | -23% | 20% | 54% |
| p-value | 7E-4 | 0.2 | 0.01 | 0.7 | 8E-12 | 0.9 | 0.06 | 2E-14 |
| Statistically different? | Yes | No | Yes | No | Yes | No | No | Yes |

concentrations for newer urban land were significantly lower than the concentration data collected from Calabazas Creek watershed, which contains 79% newer urban land. The concentrations optimized for undeveloped (open and agricultural) areas were compared against Coyote Creek (62% undeveloped). While the tail of the agriculture/open land-use concentrations overlapped with Coyote Creek concentrations, the bulk of the optimized concentrations were a fair amount lower. However, Coyote Creek might not be a representative example of PCBs concentrations emitted from undeveloped land since it received runoff from some of the heavy industrial area of San Jose that included a former electrical transformer manufacturing plant. When the railroad category was added, the optimized concentrations for the other land uses generally decreased somewhat (except agricultural/open, which essentially remained the same).

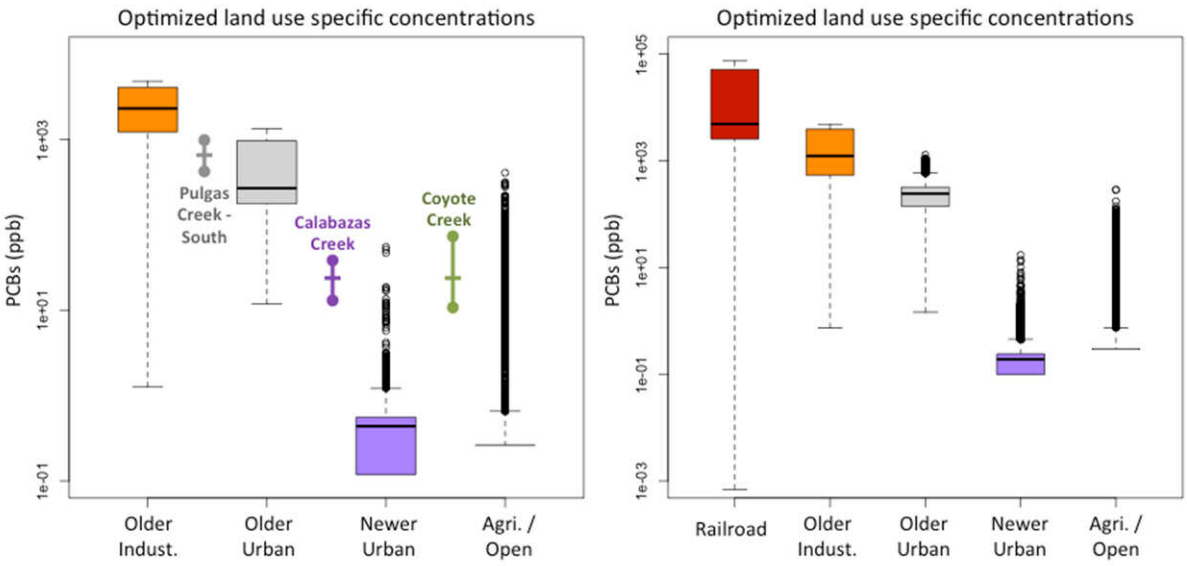


**Figure 11. a) Optimized p-PCBs concentrations for four general land-use categories (10,000 iterations), and b) Optimized PCBs concentrations for five land-use categories (10,000 iterations). p-PCBs concentration ranges shown for representative watersheds (horizontal line = median).**

The optimized concentrations for the railroad land use exhibited a huge spread (Figure 11b), suggesting that either there is not a consistent PCBs emission signal from railroads or the calibration set did not adequately represent the railroad category. It seems that spatial scales of PCB-concentration variability were not captured within railroad areas used in this study. This might either be resolved through improved input data and rerunning the back-calculation techniques or may require a field monitoring program for resolution.

Although there is plenty of scatter associated with outliers (the circular markers beyond the whiskers), the trends shown seem to make sense (Figure 11). For example, an argument could be made logically that railroad land-uses could reasonably exhibit higher concentrations than the old industrial category that includes a mosaic of land use and cover. It seems reasonable also that newer urban areas that are likely only receiving atmospheric deposition (low PCB loading) should have very low PCB concentrations whereas the ag/open space land-use category has 80 years of atmospheric loading and greater soil erosion to transport the PCBs off the land surface.

Table 8 and 9 summarize the basic statistics for the optimization of PCBs concentration across four and five land-use types (10,000 iterations each). It was not surprising that more iterations were needed for PCBs concentration optimization convergence than for mercury because PCBs span a much larger concentration range. For both optimizations, the Wilcoxon rank-sum test on the distributions found that the land-use concentrations were all significantly different from one another. The concentration distribution for both railroads and old industrial area was multi-modal with a very large spread while the distribution for old urban was bimodal with a moderate spread (histograms not shown). The distributions for newer urban and undeveloped land use both exhibit a thick-tailed log-normal

distribution (histograms not shown). These distributions suggest that the chosen land-use categories likely do not generate constant PCBs runoff concentrations, which is consistent with PCBs being a highly localized pollutant. However, the optimized concentrations may still be useful if they are able to adequately simulate downstream concentrations on a regional scale.

**Table 8. PCBs optimization: Optimized concentration statistics (4 land uses).**

| p-PCBs (ppb) | Old indust. | Old urban | Newer urban | Agri./Open |
|---|---|---|---|---|
| Mean | 2,200 | 510 | 0.42 | 5.8 |
| Median | 1,900 | 270 | 0.47 | 0 |
| St. Dev. | 1,600 | 390 | 1.1 | 20 |

**Table 9. PCBs optimization: Optimized concentration statistics (5 land uses).**

| p-PCBs (ppb) | Railroad | Old indust. | Old urban | Newer urban | Agri./Open |
|---|---|---|---|---|---|
| Mean | 23,000 | 1,800 | 240 | 0.24 | 5.9 |
| Median | 4,900 | 1,200 | 240 | 0.19 | 0 |
| St. Dev. | 25,000 | 1,600 | 150 | 0.40 | 17 |

The calibration watersheds' PCB concentrations are all being simulated as excessively high, except for Santa Fe (Figure 12). The land-use or source area that is driving Santa Fe Channel's notably high PCBs concentration is not adequately represented in the optimization. As a result it is likely that Santa Fe is driving old urban PCBs concentrations up, causing oversimulation of PCBs concentrations for most watersheds with significant old urban area (Borel Creek, Glen Echo Creek, San Leandro Creek, Sunnyvale Channel, plus others in validation set). Indeed, removing Santa Fe from the calibration set reduces the old urban PCBs concentration by nearly 40% (Table 10 and Table 11) and improves the fit of concentrations for the watersheds with significant old urban area (results not shown).

To investigate the potential bias introduced by Santa Fe channel's high PCBs concentrations (that is, without accounting for appropriate source area), the validation analysis was run with the original optimized concentrations (Table 8 and Table 9) and re-optimized concentrations without Santa Fe channel (Table 10 and Table 11). (Again the land-use concentrations were all significantly different from one another.) Figure 13 shows the median p-PCBs results for the validation set generated from a series of optimizations. The first simulation used the results of the four land-use categories optimization with Santa Fe Channel in the calibration set (Figure 11a; Table 8). This simulation showed how the validation watersheds' PCBs concentration was biased by Santa Fe's impact on old urban concentration (the simulated concentration's fit to observed values is decent only when old urban is a small percentage of watershed land use, otherwise, PCBs concentrations are oversimulated, i.e., simulated as being excessively high). The next simulation used the re-optimization of four land-use categories without Santa Fe Channel and the improved fit is clear (Figure 12 and Table 10). Likewise, the next two

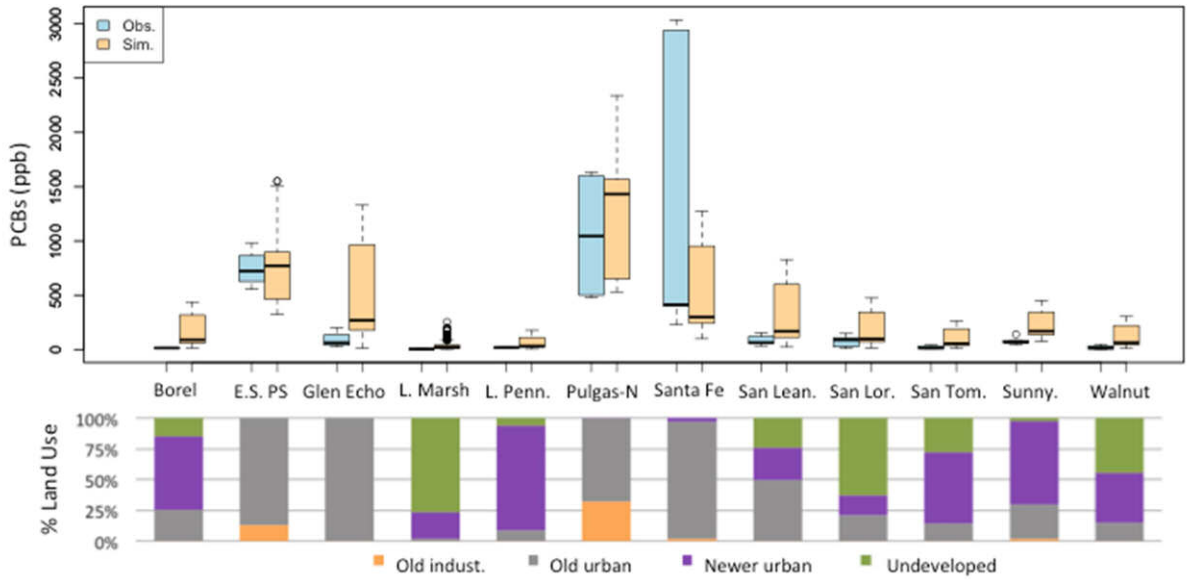


**Figure 12. Calibration watersheds: Observed versus simulated p-PCBs concentration and land-use distributions.**

**Table 10. PCBs optimization without Santa Fe: Optimized concentration statistics (4 land uses).**

| p-PCBs (ppb) | Old indust. | Old urban | Newer urban | Agri./Open |
|---|---|---|---|---|
| Mean | 2,800 | 150 | 0.87 | 20 |
| Median | 2,100 | 150 | 0.24 | 0.44 |
| St. Dev. | 1,400 | 81 | 2.6 | 31 |

**Table 11. PCBs optimization without Santa Fe: Optimized concentration statistics (5 land uses).**

| p-PCBs (ppb) | Railroad | Old indust. | Old urban | Newer urban | Agri./Open |
|---|---|---|---|---|---|
| Mean | 1,500 | 2,800 | 150 | 0.30 | 14 |
| Median | 0.61 | 1,800 | 150 | 0.17 | 0.31 |
| St. Dev. | 1,800 | 1,400 | 85 | 0.50 | 25 |

simulations are five land-use categories (now incorporating railroads) optimized with and without Santa Fe Channel (Table 10 and Table 11), and again the performance improved without Santa Fe Channel (two watersheds' results were upgraded to being statistically similar to observed data). Incorporating the railroad category does not generally improve fit of simulated to observed concentrations (Figure 13 and Table 12). While railroads are associated with PCBs to some degree, the PCBs signal seems to be inconsistent (at least in local watershed data set). However, part of the problem may arise from only some of the watersheds containing railroads, and in rather small proportions (only three calibration watersheds exceed 1% RR area with a maximum of 3.6%).

### Sensitivity Analysis

A number of model and objective function parameter values were chosen or calibrated based on professional judgment. Since these parameters could have taken on different values, it is important to test how sensitive the results are to them. The sensitivity analysis parameters were the runoff coefficients in the underlying model and the various weighting factors in the objective function. These parameters were tested one by one using the baseline Hg optimization.

The runoff coefficients (RC) used for the Hg optimization were 0.5 for older urban, 0.4 for new urban, and 0.2 for agricultural and open areas. These values were taken from the calibrated hydrology model. To test the sensitivity of the results to the choice of RC, the Hg optimization was run with 0.6 for older urban, 0.4 for new urban, and 0.1 for agricultural and open areas. The modified RCs had some impact on the optimized land-use specific concentrations and the resulting fit to observed data (Tables 13 and 14), so the choice of RCs should be made carefully (and should be consistent with the RCs that they will be used with later, e.g., in the RSWM).

The objective term weight (λ), which controls the relative importance of downstream concentration fit and concentration convergence, was set at 10. This value was arrived at by calibration; starting at 1, the objective term weight was increased over a series of test runs until the convergence term was weighted highly enough to force a reasonable level of consistency of land-use specific concentrations across watersheds. For sensitivity analysis, the objective term weight was set at 20. The results did not change much with the doubling of the objective term weight (Tables 13 and 14).

The observed data weights (w) were set to 1.0 except for one questionable concentration measurement from the San Lorenzo data set, which was set to 0.25 to reflect uncertainty over its validity. (The outlier was a measurement of 0.9 ng/mg, while the other five data points ranged from 0.08 to 0.2 ng/mg, values more consistent with a largely undeveloped watershed.) By weighting the outlier lower than the rest of the measurements, the optimization is less influenced by the outlier. The optimization was re-run with the outlier set to 1.0 (i.e., all data points treated equally regardless of confidence in validity of measurement). Allowing the outlier to be fully counted had a large impact on the optimization; the average concentration value of the agricultural / open land use went up over 50% and the standard deviations in all categories increased (Table 14). Given the sensitivity of the results to data weighting, it should be further tested.

## *A2.1.b.iii Preliminary Discussion & Recommendations*

Based on these initial results, the optimization approach was found to be quite promising for developing land-use specific estimated EMC data for RSWM input. Initial results for mercury showed consistent land-use associations, making it highly amenable to this approach. Meanwhile, initial results for PCBs showed that they exhibit less consistent land-use associations (likely due to its tendency to be highly localized). Finding appropriate land-use categories may require a fair amount more effort including development of source area based GIS layers (in progress) and the potential need to gather field data in watersheds where these source areas are represented). A further improvement is likely if field data could be found or generated that include more replication within categories to reflect within-category variability over multiple spatial scales. However, while the PCBs optimization results might never achieve

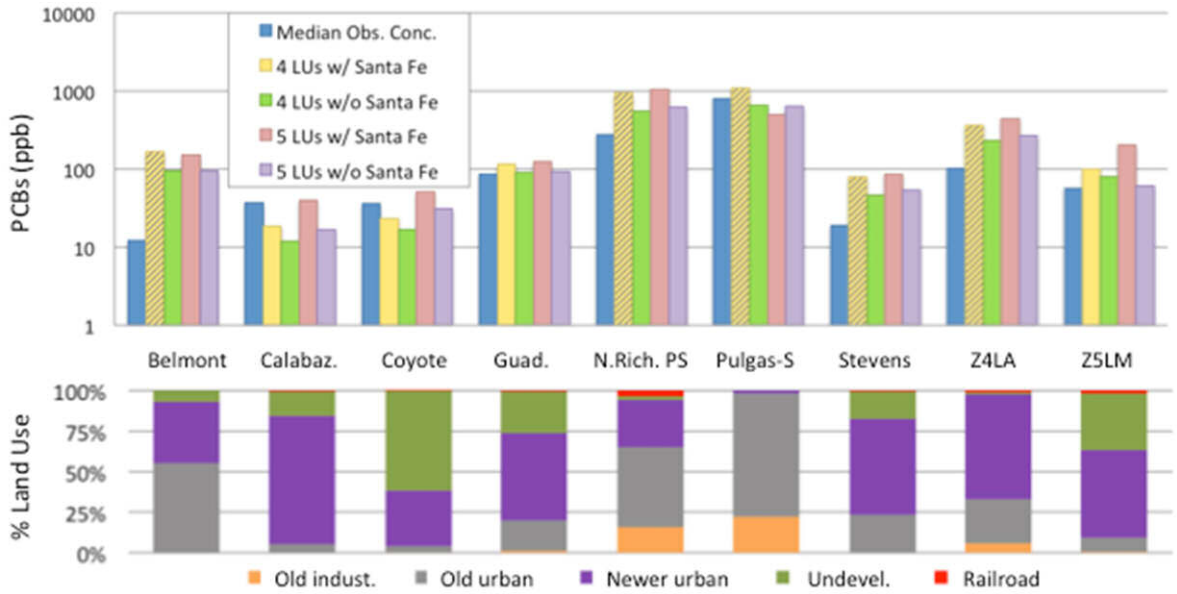


**Figure 13. Validation watersheds: Observed versus simulated p-PCBs concentration and land-use distributions. The watersheds with >20% old urban are noted with grey striping for the first simulation to highlight bias due to Santa Fe channel in calibration set.**

**Table 12. Observed and Simulated median p-PCBs (ppb) concentrations for validation watersheds**

| | Belmont | Calabaz. | Coyote | Guad. | N. Rich PS | Pulgas-S | Stevens | Z4LA | Z5LM | Summary |
|---|---|---|---|---|---|---|---|---|---|---|
| **Obs.** | 12 | 37 | 36 | 86 | 280 | 810 | 19 | 100 | 57 | - |
| **(n)** | (3) | (5) | (6) | (72) | (17) | (4) | (6) | (70) | (4) | |
| **4 LUs w/** | 170 | 18 | 23 | 120 | 950 | 1100 | 80 | 360 | 99 | - |
| **Santa Fe** | 1270% | -51% | -36% | 34% | 240% | 35% | 320% | 250% | 73% | **237% avg** |
| p-value | 0.002 | 0.3 | 0.8 | 5E-10 | 2E-10 | 0.9 | 0.002 | 2E-16 | 0.02 | - |
| Stat. diff.? | Yes | No | No | Yes | Yes | No | Yes | Yes | No | **4 same** |
| **4 LUs w/o** | 96 | 12 | 17 | 91 | 550 | 650 | 47 | 230 | 81 | - |
| **Santa Fe** | 690% | -67% | -53% | 6.3% | 100% | -19% | 150% | 120% | 41% | **108% avg** |
| p-value | 0.005 | 1E-4 | 0.07 | 0.5 | 6E-8 | 0.4 | 0.1 | 2E-16 | 0.2 | - |
| Stat. diff.? | Yes | Yes | No | No | Yes | No | No | Yes | No | **5 same** |
| **5 LUs w/** | 151 | 40.3 | 50.8 | 124 | 1040 | 496 | 87.3 | 436 | 203 | - |
| **Santa Fe** | 1100% | 8% | 40% | 44% | 280% | -39% | 360% | 320% | 250% | **263% avg** |
| p-value | 0.004 | 0.5 | 0.07 | 4E-15 | 2E-10 | 0.08 | 9E-4 | 2E-16 | 0.004 | - |
| Stat. diff.? | Yes | No | No | Yes | Yes | No | Yes | Yes | Yes | **3 same** |
| **5 LUs w/o** | 95 | 17 | 31 | 92 | 620 | 640 | 54 | 270 | 61 | - |
| **Santa Fe** | 680% | -53% | -16% | 7.8% | 130% | -21% | 190% | 160% | 6.8% | **121% avg** |
| p-value | 0.009 | 0.005 | 0.9 | 0.3 | 2E-7 | 0.4 | 0.05 | 2E-16 | 0.4 | - |
| Stat. diff.? | Yes | Yes | No | No | Yes | No | No | Yes | No | **5 same** |

**Table 13. Median p-Hg (ppm) concentrations for various runs.**

| | Old urban | | | Newer urban | | | Agri./Open | | |
|---|---|---|---|---|---|---|---|---|---|
| | mean | median | stdev | mean | median | stdev | mean | median | stdev |
| Baseline MC run | 0.63 | 0.62 | 0.12 | 0.16 | 0.16 | 0.086 | 0.14 | 0.0061 | 0.26 |
| Runoff coefficients | 0.61 | 0.61 | 0.10 | 0.13 | 0.12 | 0.084 | 0.12 | 0.0019 | 0.35 |
| Obj. term weight | 0.62 | 0.62 | 0.12 | 0.16 | 0.16 | 0.085 | 0.14 | 0.0029 | 0.27 |
| Data weights | 0.63 | 0.62 | 0.16 | 0.15 | 0.15 | 0.93 | 0.23 | 0.0032 | 0.42 |

**Table 14. Percent difference between validation watersheds' observed and simulated p-Hg results for various runs.**

| | Belmont | Calabaz. | Coyote | L. Marsh | N. Rich PS | Pulgas-S | Stevens | Z4LA |
|---|---|---|---|---|---|---|---|---|
| Baseline MC run | 79% | 24% | -36% | 10% | -44% | -23% | 20% | 54% |
| Runoff coefficients | 71% | -0.21% | -54% | -26% | -46% | -25% | 7% | 40% |
| Obj. term weight | 79% | 25% | -37% | 10% | -44% | -23% | 19% | 53% |
| Data weights | 78% | 20% | -35% | 12% | -45% | -23% | 19% | 49% |

perfect fit at the catchment scale, the results will likely produce reasonable results at more aggregated scales as long as the calibration data set is representative of the area.

To fully assess the potential of this approach, further development of input data sets, both spatial data sets (GIS layers) and calibration/validation data sets, is recommended. The next steps will entail looking for land uses and source areas with a consistent enough emission signal that inclusion in the optimization improves the fit. However, these land uses or source areas have to be well enough represented in the calibration data set to overcome the signal-to-noise issue, so more field sampling (specifically targeted to representative catchments) may be needed. If this does not resolve the variability in the output of the back-calculation methods, a field program might be required to develop local data.

To further this work, the following recommendations are made:

- Develop and test more pollutant-specific land-use categories (as supported by calibration data set),
- Test data weighting based on statistical confidence in data point (e.g., based on distance from mean observation or distribution variance),
- Test maximum-likelihood estimator approach assuming underlying log-normal concentration distribution, and
- Should it be required, a field program should be initiated in WY 2014 to address data gaps.

# APPENDIX 3. LAND USE/SOURCE AREA SPECIFIC FIELD OBSERVATIONS

The development of a regional watershed spreadsheet model (RWSM) for PCBs and Hg and other potential future focus pollutants requires a detailed understanding of concentrations in relation to land uses and source areas. The concentration information can be in the form of particulate pollutant concentrations (mg/kg) or the ratio of particulate concentration of pollutant to suspended sediment concentration (mg/kg) or in the form of water concentrations (ng/L). Depending upon the availability of data, each pollutant specific RWSM could either be based on annual average flow of water (million $m^3$/year) or annual average sediment load (metric tonnes) or perhaps some combination if data or a conceptual model of pollutant transport supports such a hybrid. Since the modeling time step is annual average, it follows that the input data needs to be annual average. The term event mean concentration (EMC) is used to describe the average concentration of suspended sediment or a pollutant for a single event derived from the total mass passing through a cross-section divided by the total flow passing through that same cross section (Lent and McKee, 2011). In the case of PCBs and Hg, there is insufficient EMC data available from existing peer-reviewed literature to form a detailed understanding of concentrations in relation to land uses and source areas (Lent and McKee, 2011).

The sampling required to generate accurate EMCs is usually not possible therefore EMC for a storm is approximated by either time- or flow-paced composite sampling that may or may not cover the entire hydrograph of a storm. Since for a given location, EMCs can vary up to 250 times between storms (Lent and McKee 2011), determining an annual average EMC requires monitoring many storms. The number of storms required should be lesser for less contaminated land use areas and greatest for adequately describing more highly polluted source areas; as few as seven storms and as many as 30 storms appear to have been used in the past (Lent and McKee 2011). There is also variability between sites for a given land use or source area category, necessitating fieldwork in a number of representative locations in order to obtain a “regionally representative average“. Another challenge is adequately describing and positioning a sampling location in relation to land uses or source areas. This is made difficult in the Bay Area for PCBs since many source areas are close to the Bay margin where flow may be tidally influenced, or on private property with no downstream public right-of-way. For these reasons, to-date, EMC development has focused on the use of existing data and various methods of mathematical back calculation (see section A2), rather than on empirical field observation. Once model weaknesses are determined through a sensitivity analysis on initial runs, a greater effort may be made on filling data gaps with field work during wet weather conditions in relation to high priority land uses and source areas.

# APPENDIX 4. MODELING

## A4.1 Use of geoprocessing tools for scientific research

When performing an analysis that involves spatial variables, from simple X-Y coordinates to complex surface modeling or vector overlays, it is often useful to preserve a geoprocessing workflow for iterative operations or to disseminate methodologies. The conventional method of workflow preservation is to create a geoprocessing tool with user parameters. As the operations needed to arrive at the estimated runoff concentrations or sediment loads are many, the development of a geoprocessing tool allows for multiple iterations using a variety of parameters with minimal user error. All tools in this study were developed in Python using the Arcpy framework in ArcGIS, the most commonly used GIS software by both public and private institutions.

### A4.1.a Model structure

Each part of the model is referred to as a "module". Base data for all pollutant modules is output from either the Hydrology or Sediment modules. As the inputs for each are very similar, a tool called "Baseline" was developed that has options for both. The main differences are that Hydrology uses soils and precipitation data as inputs, while Sediment substitutes soils for geology and does not accept precipitation.

The inputs for Baseline are shapefiles of watersheds, land use, and soils or geology data; rasters of precipitation and/or slope; and lookup tables for land use codes and runoff or sediment coefficients. Slope values are binned according to user input, land use values are binned via the lookup table, and categories for soils and geology are hardcoded. Watershed shapes are intersected with land use and soils / geology, and each resulting unique shape is then given an average precipitation and/or slope value. After the slope values are binned, a code that represents the unique combination of slope bin – land use bin – soils / geology is assigned to each shape. Runoff / sediment values are then pulled from the lookup table via code value and assigned as well.

The outputs for Baseline are tables and spatial data. One table reports the percentage of total watershed area for each data category (slope bin – land use bin – soils / geology) per watershed, the other table reports the percentage of total watershed area for each descriptive land use type per watershed, and two geodatabases (.gdb) include all spatial data: one ("results.gdb") includes all intersected watersheds attributed with codes and other relevant data, and the other ("temp.gdb") houses all interim data used in processing.

Further, Baseline has three modes: the first does all geoprocessing from scratch and outputs the .gdbs, the second takes results.gdb as input and recalculates a new code field based on new input parameters, and the third solely outputs tables from existing fields.

All pollutant modules accept "results.gdb" as an input parameter and add new fields into watershed intersects. Pollutant modules also reference lookup tables to arrive at load coefficients, and some

modules may include source area polygons as inputs that can change coefficient values depending on their proximity to other features.

### A4.1.b Integration into ArcGIS as ArcToolbox

Certainly, the development of the interactive GUI in ArcGIS was important to ensure better userability of the model. The tools are accessible through the ArcMap or ArcCatalog, and are found within an ArcToolbox currently called “RWSM_Tools.pyt”. This file is a “Python toolbox”, a toolbox development option available in ArcGIS 10.1. This new toolbox option allows for increased under-the-hood coding flexibility to modify Graphical User Interface (GUI) behavior, and conveniently keeps the code for all tools in one file. For the user, activating the tool is as simple as pointing and clicking, then inputting all the necessary parameters and pressing OK (Figure 14). The model internally handles the two different baseline calculations dependent on the user selection, the slope bins are similarly parsed internally from the input text and applied to raster queries, and many other processes are run behind the scenes. For the developer, making edits and upgrades is easier with a Python Toolbox for the reasons explained above, and therefore reworking the tool into this new format was a fruitful next step.

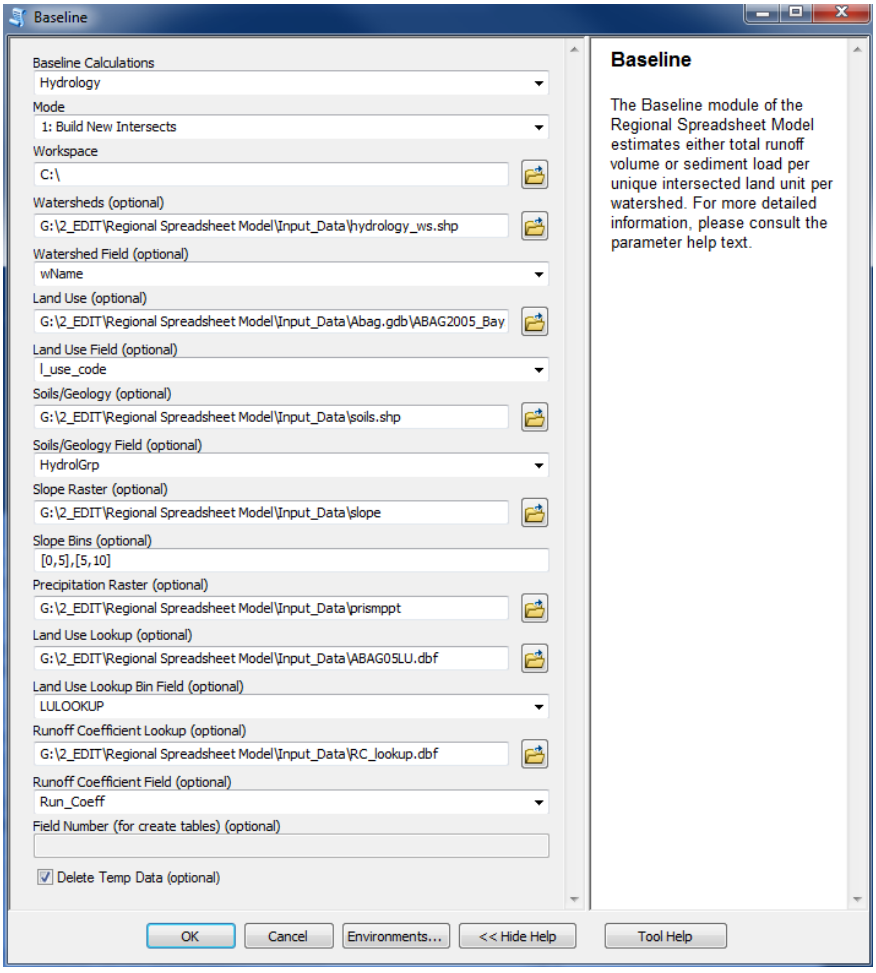


**Figure 14. Snapshot of ArcGIS Graphic User Interface for Baseline model.**

# APPENDIX 5. HYDROLOGY MODULE

The hydrology module development was the primary focus of the first two years of the RWSM (calendar years 2010 and 2011). As described in the "Pollutant specific model structures" section, along with the sediment model, the hydrology model is a primary driver of the pollutant models and so it was important to focus on bringing this model along prior to delving into the pollutant models. Initially during the first year of development, two base hydrology model approaches were investigated: one using runoff coefficients based on land use-soil-slope combinations and the other based on impervious cover (Figure 15). Each of these models had advantages and disadvantages relative to the other. The impervious cover model better related to our conceptual model of landscape cover's effect on runoff and had the additional advantage of being decoupled from any land-use based pollutant model, however the pixel resolution of the input data made processing run much slower. The land use model had the advantage of incorporating soil class and slope determination of the runoff coefficients and the processing time was much faster, but the disadvantage of land use being a less precise descriptor of runoff.

Initial versions of each model were calibrated to hydrology data from 18 local watersheds with a wide variety of imperviousness, soil, and slope. Both versions produced relatively similar calibration results, with the land-use based model slightly outperforming the impervious cover model (Table 15). The land use based model was chosen to move forward with improving in subsequent years; however the option remains open to return to the impervious cover model in future years if desired.

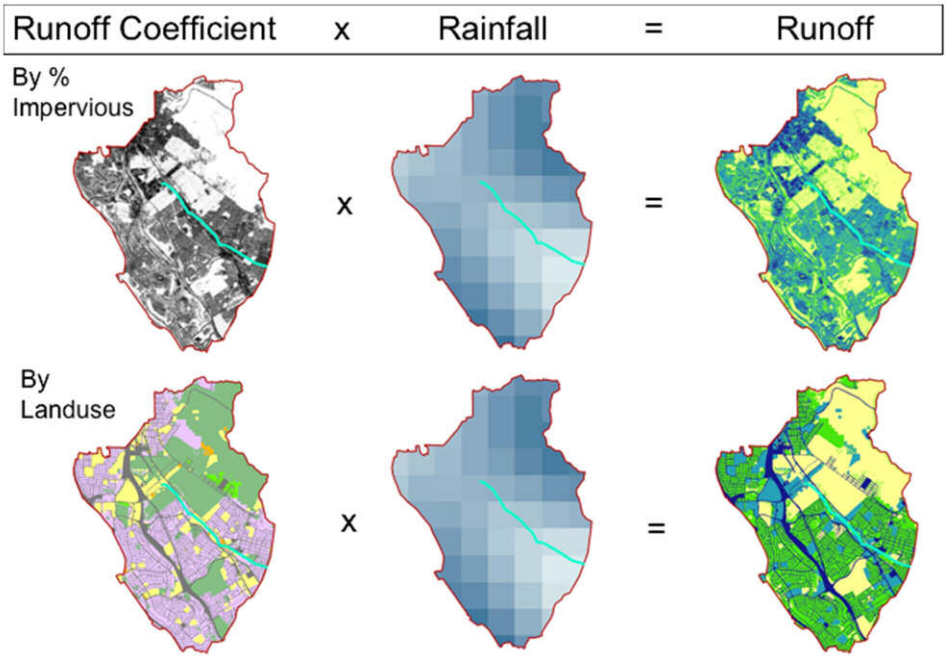


**Figure 15. Simplified visualization of the two rainfall-runoff models. To generate runoff volume, runoff was multiplied by its source area for each unit of land.**

**Table 15. Summary of model performances.**

| Model version | Mean | Median | Range |
|---|---|---|---|
| Land use based (Calibrated Browne) | +2% | +3% | -42% to +46% |
| Impervious Cover Model (0.45, 0.25) | 0% | +2% | -48% to +66% |

Following the 9-step process framework for modeling each constituent (see "Work Plan Summary" section near the beginning of this report), year two focused on addressing model weaknesses discovered in year one and running a second version of the hydrology model (steps 5 and 6 of the 9-step process). Specifically, the land use input dataset was upgraded to a newer version, which included several improvements in resolution over the older version. Land use categories were also refined to improve the treatment of runoff from the broadly aggregated categories, for example by separating the "Open" category into two subcategories "Open – infiltrative" and "Open – compacted". The calibration dataset was also improved in V2. Several more calibration watersheds were added to increase the range of watershed characteristics including percent imperviousness character. Also, gauge records with incongruent land use / impervious data were removed. Although the summary statistics of V2 suggest poorer model performance (Table 16), the improvements made in year two helped to strengthen the model by increasing the range of land use characteristics within the calibration dataset as well as by bringing the model into better alignment with what we know conceptually about runoff behavior in relation to land use characteristics.

**Table 16. Summary of model performance for version 2 of the hydrology model.**

| Model | Mean | Median | Minimum | Maximum |
|---|---|---|---|---|
| **Uncalibrated ABAG 2005** | +13% | +17% | -78% | +79% |
| **Calibrated ABAG 2005 (rev. cat.)** | +1% | +3% | -75% | +70% |

The governing equation of the resulting model was:

$$V_j = RC_j * I * A_j \qquad \text{Equation (1)}$$

where V = annual stormwater volume for unit of land j, RC = runoff coefficient for land unit j, I = average rainfall, A = area of land unit j. The RC was based on land use, slope and soil characteristics (See Lent and McKee (2011) for details). Further potential refinements to the hydrology model identified during year 2 and beyond include:

1) Re-calibrate the model using the updated 2010 release of the PRISM rainfall data layer;
2) To reduce the possibility of over-calibration, the calibration watershed data set should be split into two sets and calibrate to one set and then verify the calibration on the other;
3) Incorporate runoff coefficients that have either a curvilinear function with imperiousness alone or runoff coefficients defined as a function of both land use and percent connected imperviousness and rainfall depth.

Despite these recommendations, at the end of year 2, no further hydrologic model refinement was recommended as a priority in year 3; instead recommendations focused on shifting toward the sediment and pollutant models. It was expected that the development and calibration of the sediment, Hg and PCB water quality models in years 3 and 4 may highlight additional weaknesses in the hydrology model that may need to be addressed in subsequent years.

# APPENDIX 6. SUSPENDED SEDIMENT MODULE

## A6.1 Introduction

San Francisco Bay is impaired by mercury and PCBs (SFRWRCB 2006; SFRWRCB, 2008) and urban runoff from local watersheds has been identified as a significant pathway for these and many pollutants of concern (POC) (Municipal Regional Stormwater Permit (MRP); SFRWRCB, 2009). The permit contains provisions that require management actions and studies to address information gaps for mercury, PCBs, legacy pesticides, PBDEs, and selenium (provisions C.8., C.11., C.12., and C.14.). Fine suspended sediments (functionally defined as <0.0625mm), eroded from industrial areas and other components of the urban environment, are known to be enriched with these hydrophobic pollutants (Lent and McKee, 2011). Therefore, there may be considerable advantage to base estimates of hydrophobic pollutant loads on estimates of suspended sediment loads or a combination of flow and suspended sediment. Consistent with this premise, MRP Provision C.8.e(vi) requires permittees to design a robust sediment delivery estimate/sediment budget for local tributaries and urban drainages.

The objective of this report section is to briefly describe preliminary results from recent efforts to improve our understanding of sediment sources and transport processes in the urbanized Bay Area landscape at a regional scale. This section is largely a presentation of data and precedes a more detailed exposition (section A6 Attachment 1 and 2) that will include a thorough discussion of methods, further exploration of the results, model weaknesses, and recommendations for remaining opportunities for improvement.

## A6.2 Overview of methods

The suspended sediment data utilized are from 54 gauge stations compiled from three sources: USGS, Balance Hydrologics, and SFEI/RMP/STLS/BASMAA studies. The USGS has collected discharge and suspended sediment for at least three years at 39 stations in the Bay Area since 1956. Balance Hydrologics Inc. has collected suspended sediment data at 12 additional stations, plus additional data for an existing USGS station (Wildcat Creek). Data from three SFEI/RMP/STLS/BASMAA studies was also included: North Richmond Pump Station, Ettie Street Pump Station, and Zone 4 Line A. North Richmond and Ettie Street only had one year of data for each, while Zone 4 Line A had four years of data (Gilbreath et al 2012; Hunt et al 2012; McKee et al 2012). The interpretation of the data was supported by the following initial steps:

- Based on a review of the data in relation to completeness, representativeness of climatic conditions, and combining data from two gauge locations (where either meta-data or data suggested that was appropriate) 46 station locations were retained for analysis.
- The data were climatically weighted using regression based rating curves between peak annual flow and annual sediment load (c.f. Lewicki and McKee, 2009) to derive an average annual estimated load for each site and to improve comparability between sites. In California, a minimum of 20 years is ideal for climatic averaging (Inman and Jenkins, 1999), and given data availability, a 20-year period was chosen (water years 1992-2011).

- Data quality analysis was completed on the climatically weighted means. If the mean was derived from data that did not cover adequate climatic variability it was given a lower quality rating.
- A GIS boundary layer was generated for each of the watersheds/sub watersheds using the best available topographic information (Figure 1). A comparison between the existing boundary layer and the boundary as defined by the USGS was completed for 39 watersheds and revealed that most were within 1% of each other, with only a few watersheds with differences as large as 5% (primarily reflecting storm drain portions of watersheds in urban areas).
- The area upstream from reservoirs in each of the watersheds was also delineated using data provided by the Department of Water Resources Division of Safety of Dams (DSOD) database (http://www.water.ca.gov/damsafety/) that have an upstream contributing area greater than 3 $km^2$, for a total of 30 reservoirs (Figure 2).
- The loads from each of the 46 watersheds were normalized and adjusted in a variety of ways to increase the comparability of data across different watersheds for areas downstream from reservoirs including:
  - adding a factor to account for delivery ratio (NRCS, 1983) based on nonurban watershed area
  - adding a factor to account for reservoir trapping efficiency (Brown, 1944)
- Geological information for each watershed was generated. The generalized geologic mapping by Graymer et al (2006) was gathered as KML files, and transformed into a seamless shapefile for use in GIS. Bedrock geology was simplified into five classes: Franciscan, Great Valley, Quaternary, Salinian, and Tertiary. However, given that Salinian geology is only present west of the San Andreas fault, functionally only four geologic classes were present in our model area.
- Land-use information for each watershed was generated. Land use mapping by ABAG (2005) was used for both the hydrology component of the Spreadsheet Model and this Sediment Model. Two detail levels of land-use information were explored; a five category level (agriculture, urban high density, urban low density, industrial, open) and three category level (agriculture, urban, and open).
- Slope information for each watershed was generated. The slope layer was calculated using the USGS 10m digital elevation model (DEM), calculating average slope of each pixel, and outputting a slope map showing the pixel values and then summarized into the three broad slope categories. Three slope categories were chosen (<10%, 10-30%, and >30%)Categories were based on best professional judgment about sediment production in the Bay Area in relation to slope and natural breaks in the statistical distribution within the 46 watersheds with sediment data.
- The data layers were input in to ARC GIS for spatial analysis; for each of the 46 watersheds, a union was performed to output a number of polygons for each one of the unique combinations of physical attributes. A total of 60 unique combinations were possible; 3 slope classes, 5 geology classes (four lithologies plus a “water” category), and 6 land use classes (in addition to the five categories, the input data also had a “water” category). Each unique combination was given a three digit code.

For further details see Appendix 6 Attachment 1.

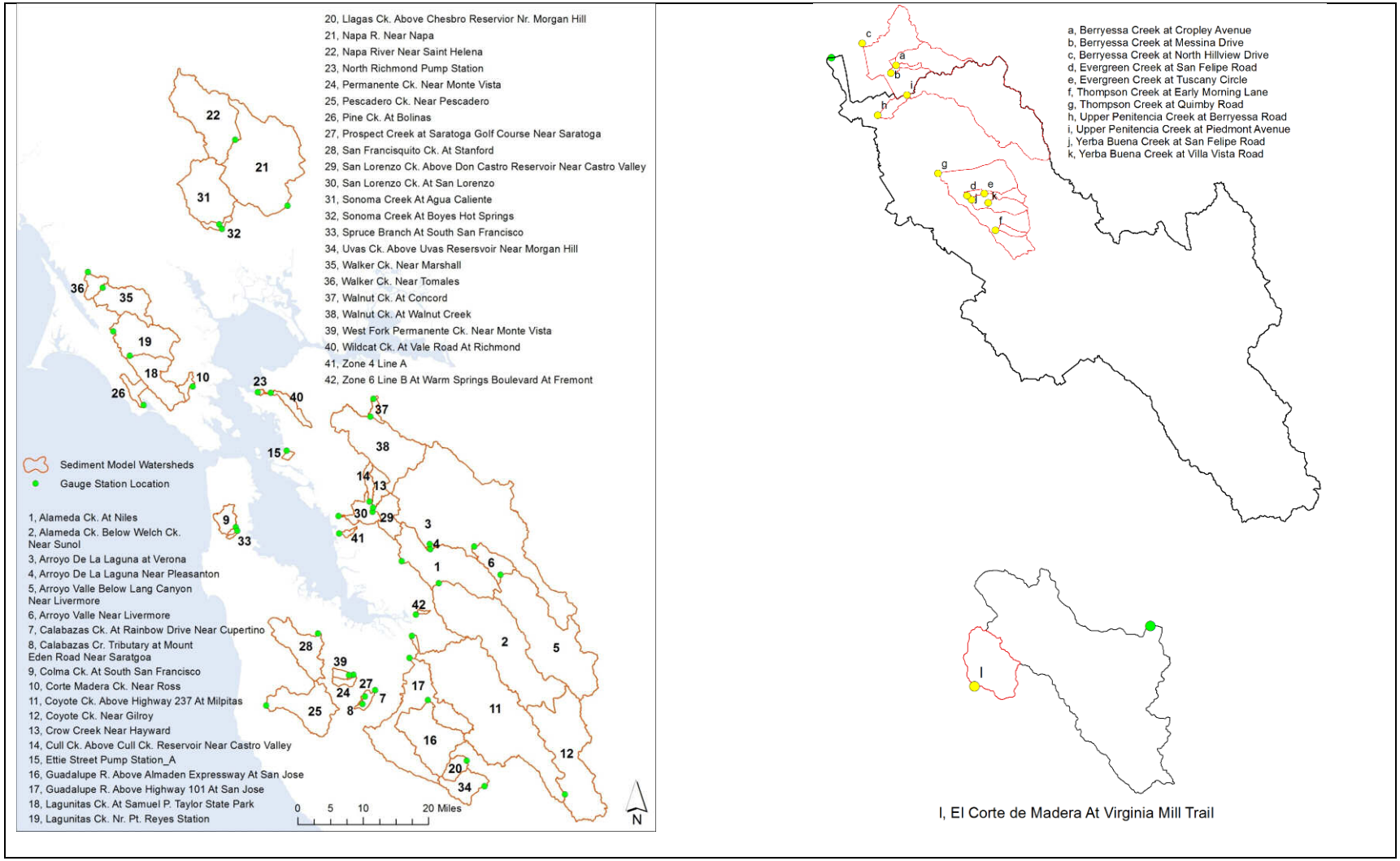


**Figure 1. Watersheds with available suspended sediment data in the Bay Area based on data collected by USGS (n=39), Balance Hydrologics Inc. (n=12) and SFEI/RMP/STLS/BASMAA studies (n=3). The right hand panel shows a zoom in to show the details of monitoring stations within Coyote Creek and San Francisquito Creek.**

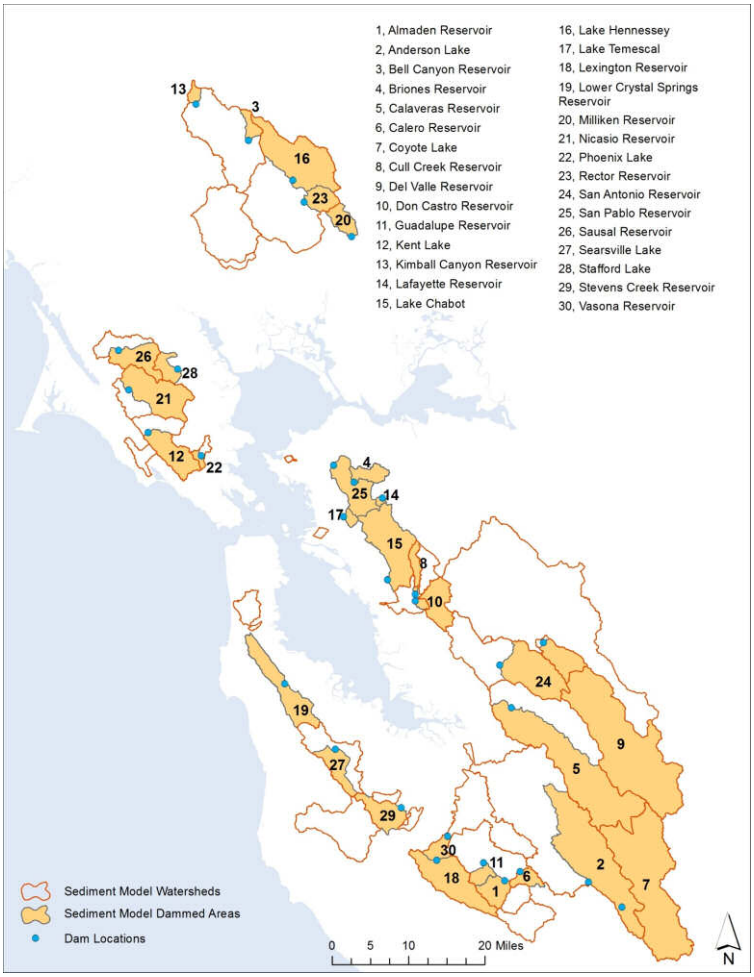


**Figure 2. Reservoirs in watersheds of the Bay Area that have an upstream contributing area greater than 3 km$^2$. Note that areas upstream of dams were removed from the analysis. Data source: Department of Water Resources Division of Safety of Dams.**

- After the union was performed, the area of the multiple polygons with each code was summed, producing a total area for each code for each watershed.

- Local sediment coefficients for each unique code were back-calculated using inverse optimization methods combining downstream mean annual suspended sediment loads and the 60 unique attributes using methods described by Silverman et al. (1988) and Ha and Stenstrom (2008). The data were systematically explored using two steps; an initial single parameter analysis to determine the influence of geology, slope, and land use on sediment loads and a multi-parameter analysis that explored the combinations together to derive "local coefficients" (For details see Appendix 6 Attachment 2 and note, the results presented in the attachment were based on a proof of concept optimization using 100 iterations).

- An experts' advisory group (Barry Hecht, Jeff Haltiner, Leonard Sklar) was convened on May 29th, 2013 to review the coefficients generated by the back-calculation methods and get any recommendations for improvements.

- The selected parameters and the range of loading coefficients for each parameter were then used as the basis for calibrating the sediment model. The calibration was carried out through a constrained optimization method ("Complex Method", Box 1965). Functionally, this was done by randomly sampling loading coefficients from a range of 5th percentile to 95th percentile as specified from Inverse Optimization procedure (Table 1), and running an auto-calibration procedure to search for the optimum combination of loading coefficients that minimizes the difference between observed and simulated sediment loads for all 46 watersheds simultaneously. A weighting factor (3= high quality; 2=medium quality; 1= low quality) was assigned to each watershed to reflect the quality of the observed data. The model calibration was done for both unadjusted and adjusted data.

- After initial calibration, a range of testing scenarios were explored to help understand the limitation of the current model structure and calibration procedure, with the intent to provide recommendations for future improvements. The testing scenarios included using non-adjusted and adjusted calibration data for all 46 watersheds, removing 14 nested watersheds and using the remaining reduced set of 32 non-nested watersheds, and trying different parameter choices (10, 8, and 6 parameters). In addition, we also tested how well the model performs by calibrating to well-simulated watersheds (+/-75% absolute error; same magnitude as the hydrology calibration (Lent et al., 2012)), under-simulated watersheds and over-simulated watersheds, respectively.

# A6.3 Results and Discussion

## A6.3.a Inverse optimization for developing local coefficients

Based on GIS analysis, each slope category was represented by a minimum of 29% across the combined area of the 46 watersheds used in the analysis (See Appendix 6 Attachment 2 for more details). Based on a single parameter analysis, sediment production for each of the three slope categories was significantly different, with the greatest sediment production from the moderate slope class (10-30%). Land with moderate slope is represented by at least 13% of the land area of every calibration watershed with the exception of three small urban watersheds (Zone 4 Line A, North Richmond Pump Station, Ettie Street Pump Station). Sediment production from the four geologic categories was also significantly different from each other with the sediment production from Tertiary volcanics estimated as being the greatest. The geologic class "Tertiary" covered at least 1% and up to 100% of all calibration watersheds with the exception of nine watersheds including our three 100% urban examples. Therefore inclusion of three slope categories and four geologic categories was carried forth into the multi-parameter analysis.

In contrast, the percentage of industrial and high-density urban land use area are not adequately represented in the currently available 46 watershed data set. An attempt was made to merge high density urban and industrial into one category, but predictive performance did not improve. Therefore a

simple set of land use classes were carried forth into the multi-parameter analysis (agriculture, urban, and open space). At least 1% urban land use occurred in each of the 46 watersheds with the exception of five (Prospect Creek at Saratoga Golf Course Near Saratoga; Alameda Creek Below Welch Creek Near Sunol; Walker Creek Near Marshall; Arroyo Valle Below Lang Canyon Near Livermore; Coyote Creek Near Gilroy) (See Appendix 6 Attachment 2 for more details).

The single parameter analysis indicated that geology was the strongest driver on sediment production in the 46 watersheds followed by slope, and lastly land use. However, the reader should be aware that the single parameter analyses do not remove the effects of the other physical characteristics and, as such, these single parameter analyses are indicators of trends, not absolute. For example, Tertiary volcanic geology tends to occur on moderate to steeper slopes and urban land use tends to occur on flatter slopes. Accepting these limitations, the single parameter analysis provides support for the basis of the work plan for this current work which was that the simple land use model applied by Lewicki and McKee (2009) is not suitable for the complex geology and slope conditions found in the Bay Area and that "local coefficients" should provide a better basis for prediction of sediment loads in unmonitored watersheds. A total of 36 combinations (3 slopes x 4 geologies x 3 land uses) were carried forth into the multi-parameter reverse optimization procedure estimating local coefficients (See Appendix 6 Attachment 2 for more details). Based on the inverse optimization procedure run to generate a starting point for the selection of parameters and coefficients, most single-factor categories tested seemed adequately represented in the data set and produced robust results. The sediment coefficient results were considered robust when the distribution of optimized coefficients were reasonably tight, i.e., did not span an excessive range nor have excessive outliers. The exceptions were industrial and high-density urban land use. Sediment coefficients for industrial land use ranged from close to zero to over 5000 metric tons/square km. Meanwhile, the distribution of results for high-density urban land use had many outliers. Thus urban land uses were grouped together. This is not ideal given one of the objectives of developing the sediment model is to support and provide a basis for the PCB and mercury models.

A multi-parameter inverse optimization was then carried out and the data manipulated in two ways:

1. Local coefficients derived from the raw unadjusted data would rely on the assumption that sediment storage is consistent across watersheds of differing size and land use - in effect generating local coefficients of net supply to the watershed outlet. Although there is clear evidence that this assumption is flawed in the Bay Area as a whole, this may be a reasonable assumption for the majority of our smaller urbanized watersheds on the Bay margin, the primary focus of this modeling effort.
2. Local coefficients derived from sediment data for the 46 watersheds adjusted for delivery ratio and reservoir trapping efficiency would have estimates of sediment storage built into the inverse optimization analysis - in effect generating local coefficients of net sediment erosion rather than net supply to the bottom of the watershed. However, a model generated with these local input parameters would require an additional step but have the disadvantage of forcing.

Based on the correlation between the physical characteristics and the results of single-parameter optimizations, the first multi-parameter analysis was performed using geology classes plus land use split

out for Tertiary and Quaternary classes. The predictive power of this classification scheme was slightly better than geology alone. The wide range of sediment yields exhibited by Tertiary agriculture and urban suggested that splitting the Tertiary class by slope, instead of land use, would improve performance further. This was trialed next but with no improvement in predictive power. It appeared from this analysis that the Tertiary/moderate slope class needed to be split further. Doing this yielded the potential final set of "local coefficients" (Table 1). The resulting parameters showed no trend in relation to any of the slope categories, any of the geological categories, or in relation to the percentage of a watershed in agricultural land use. We interpreted this as indicating no inherent bias in the resulting set of parameter coefficients. Both sets of "local coefficients" in this table, one based on unadjusted annual average sediment data for the 46 watersheds, and the other based on data adjusted for delivery ratio and reservoir trapping were carried forth into the calibration procedure of the RWSM with the intent of exploring which set of coefficients generated the most reliable model for the urbanized smaller watersheds on the Bay margin (See Appendix 6 Attachment 2 for more details).

**Table 1. Estimates of local sediment coefficients based on the results from reverse optimization analysis (500 iterations) on raw annual average sediment loads from 46 watersheds in the Bay Area and those same loads adjusted for delivery ratio and reservoir trapping efficiency.**

| Physical Characteristic | Franciscan | Great Valley | Quaternary | | | Tertiary | | | | |
|---|---|---|---|---|---|---|---|---|---|---|
| | – | – | – | – | – | <10% | 10-30% | | | >30% |
| | | | Agriculture | Urban | Open | | Agriculture | Urban | Open | |
| **Unadjusted (raw) data** | | | | | | | | | | |
| Mean | 289 | 144 | 23 | 46 | 31 | 668 | 2,381 | 2,178 | 392 | 691 |
| Standard Deviation | 282 | 221 | 92 | 157 | 122 | 623 | 2,616 | 2,100 | 589 | 579 |
| 5% | 2 | 0 | 0 | 0 | 0 | 0 | 0 | 70 | 0 | 8 |
| 25% | 78 | 1 | 0 | 1 | 0 | 183 | 277 | 485 | 1 | 212 |
| Median | 211 | 3 | 0 | 3 | 0 | 514 | 1,218 | 1,146 | 14 | 662 |
| 75% | 425 | 274 | 1 | 21 | 1 | 1,007 | 4,017 | 3,722 | 699 | 1,038 |
| 95% | 870 | 626 | 156 | 216 | 217 | 1,859 | 7,329 | 6,100 | 1,671 | 1,481 |
| **Adjusted data** | | | | | | | | | | |
| Mean | 1,795 | 1,167 | 1,329 | 192 | 193 | 3,612 | 9,353 | 8,146 | 1,727 | 3,905 |
| Standard Deviation | 1,168 | 1,461 | 2,214 | 548 | 692 | 2,339 | 8,646 | 7,030 | 2,784 | 2,826 |
| 5% | 61 | 1 | 0 | 1 | 0 | 508 | 2 | 418 | 1 | 53 |
| 25% | 1,042 | 4 | 1 | 4 | 1 | 1,957 | 2,459 | 2,522 | 3 | 1,892 |
| Median | 1,610 | 171 | 35 | 10 | 2 | 3,249 | 7,136 | 6,038 | 28 | 3,681 |
| 75% | 2,369 | 2,471 | 2,032 | 133 | 12 | 4,882 | 14,734 | 12,594 | 2,661 | 5,478 |
| 95% | 4,005 | 3,961 | 5,993 | 976 | 1,308 | 7,760 | 26,037 | 21,370 | 8,028 | 8,734 |

## A6.3.b Calibration of the sediment model

The baseline calibration involved running 5000 iterations to minimize the difference between models simulated and observed sediment loads at all 46 watersheds simultaneously. With unadjusted data, the calibration process pushed 9 of 10 parameters to the lower limit within hundreds of iterations, making further improvement on model calibration impossible. This indicated that the range of loading coefficients as listed in Table 1 was too high for the observed data and further calibration with this data set would not have yielded meaningful results. Therefore, the results for unadjusted data are not presented here. For adjusted data, the range of loading coefficients used in calibration appeared more compatible with the observed data. Table 2 shows the model calibration results, along with weight and percentage of imperviousness for each location. The difference between model simulated and observed loads at individual watersheds could range from -98% to 1344%, with 4 locations within 10% of difference, 9 with a range of 10-50%, 14 in the 50-100% range, and 11 greater than 100%. Model performance doesn't appear to have any clear pattern in relation to quality of data, watershed size, or percent of imperviousness.

**Table 2. Baseline model calibration results for adjusted data.**

| Watershed | Weight | Urban (%) | obseved loads (tons/yr) | simulated loads (tons/yr) | difference (%) |
|---|---|---|---|---|---|
| AlamedaCkAtNiles | 3 | 25.5 | 3585625.1 | 2938447.9 | -18.0 |
| AlamedaCkBelowWelchCkNearSunol | 3 | 0.7 | 556009.3 | 452748.3 | -18.6 |
| ArroyoDeLaLagunaatVerona | 1 | 31.7 | 1064689.4 | 2219109.3 | 108.4 |
| ArroyoValleBelowLangCanyonNearLivermore | 1 | 0.2 | 369449.8 | 1022275.8 | 176.7 |
| ArroyoValleNearLivermore | 1 | 9.0 | 527662.9 | 10269.8 | -98.1 |
| BerryessaCreekatCropleyAvenue | 1 | 7.0 | 26078.4 | 66025.2 | 153.2 |
| BerryessaCreekatMessinaDrive | 1 | 14.4 | 33658.9 | 66959.8 | 98.9 |
| BerryessaCreekatNorthHillviewDrive | 1 | 47.7 | 33966.5 | 122854.3 | 261.7 |
| CalabazasCkAtRainbowDriveNearCupertino | 1 | 54.7 | 25262.0 | 43812.0 | 73.4 |
| CalabazasCrTributaryatMountEdenRoadNearSaratgoa | 1 | 17.9 | 915.2 | 3907.4 | 326.9 |
| ColmaCkAtSouthSanFrancisco | 1 | 83.7 | 65401.4 | 51812.8 | -20.8 |
| CorteMaderaCkNearRoss | 3 | 44.6 | 63236.1 | 91766.5 | 45.1 |
| CoyoteCkAboveHighway237AtMilpitas | 2 | 49.6 | 352530.4 | 533130.9 | 51.2 |
| CoyoteCkNearGilroy | 1 | 0.1 | 604113.9 | 689284.3 | 14.1 |
| CrowCreekNearHayward | 2 | 16.9 | 97607.1 | 169583.6 | 73.7 |
| CullCkAboveCullCkReservoirNearCastroValley | 3 | 11.9 | 59049.3 | 93299.5 | 58.0 |
| ElCortedeMaderaAtVirginiaMillTrail | 1 | 2.3 | 6849.6 | 98967.6 | 1344.9 |
| EttieStreetPumpStation_A | 1 | 99.7 | 721.4 | 93.0 | -87.1 |
| EvergreenCreekatSanFelipeRoad | 1 | 29.1 | 545.6 | 1885.9 | 245.7 |
| EvergreenCreekatTuscanyCircle | 1 | 5.0 | 157.6 | 1688.0 | 970.8 |
| GuadalupeRAboveAlmadenExpresswayAtSanJose | 1 | 59.5 | 34805.3 | 202102.0 | 480.7 |
| GuadalupeRAboveHighway101AtSanJose | 2 | 78.4 | 207621.8 | 232502.2 | 12.0 |
| LagunitasCkAtSamuelPTaylorStatePark | 3 | 27.0 | 90754.9 | 90957.9 | 0.2 |
| LlagasCkAboveChesbroReserviorNrMorganHill | 2 | 1.4 | 19090.0 | 76081.8 | 298.5 |
| NapaRNearNapa | 1 | 9.7 | 4021956.9 | 1961934.5 | -51.2 |
| NorthRichmondPumpStation | 1 | 98.0 | 54.0 | 63.8 | 18.1 |
| PermanenteCkNearMonteVista | 1 | 42.1 | 77231.8 | 33042.9 | -57.2 |
| PescaderoCkNearPescadero | 1 | 5.2 | 444663.2 | 872935.8 | 96.3 |
| PineCkAtBolinas | 1 | 2.7 | 267199.8 | 113674.1 | -57.5 |
| ProspectCreekatSaratogaGolfCourseNearSaratoga | 1 | 0.9 | 998.6 | 4753.6 | 376.0 |
| SanFrancisquitoCkAtStanford | 1 | 57.5 | 282524.2 | 260821.1 | -7.7 |
| SanLorenzoCkAboveDonCastroReservoirNearCastroValley | 3 | 20.8 | 202384.8 | 105200.5 | -48.0 |
| SanLorenzoCkAtSanLorenzo | 2 | 39.3 | 204514.7 | 365631.3 | 78.8 |
| SonomaCreekAtAguaCaliente | 1 | 47.2 | 740205.4 | 734631.1 | -0.8 |
| ThompsonCreekatEarlyMorningLane | 1 | 2.6 | 3368.0 | 615.9 | -81.7 |
| ThompsonCreekatQuimbyRoad | 1 | 37.2 | 102239.7 | 38737.8 | -62.1 |
| WildcatCkAtValeRoadAtRichmond | 2 | 22.0 | 129688.4 | 120521.5 | -7.1 |
| Zone4LineA | 2 | 99.6 | 184.7 | 96.2 | -47.9 |

Further tests indicate the sediment model was unable to converge to a stable solution through the automatic calibration procedure (Table 3). Each scenario involving a different number of iterations for baseline calibration produces different calibration outcomes (5000 iterations, 10000 iterations, 20000 iterations tested). Difference between simulated and observed loads and the resulting loading coefficients occurred making it difficult to determine which parameter coefficients are stable and suitable for use to model sediment loads for the rest of the watersheds in the region. Further calibration tests removing nested watersheds or reducing the number of parameter choices also didn't improve the model calibration, further indications of an unstable model.

**Table 3. Summary of difference between modeled and observed loads for each testing scenario.**

| **Adjusted data watershed loads calibrations (% difference)** | Baseline 5000 | Baseline 10000 | Baseline 20000 | No Nesting | Close-Match Locations | Under-simulated Locations | Over-simulated Locations | Reduced Parameter Set (8) | Reduced Parameter Set (6) |
|---|---|---|---|---|---|---|---|---|---|
| High quality data watersheds | -17 | -8 | -11 | -70 | 17 | 13 | -90 | -86 | -4 |
| Medium quality data watersheds | 48 | 76 | 72 | -18 | -17 | 101 | -80 | -71 | 82 |
| Individual High/Medium watersheds calibrations (Min) | -48 | -90 | -96 | -97 | -53 | -70 | -100 | -98 | -29 |
| Individual High/Medium watersheds calibrations (Max) | 299 | 272 | 262 | -1 | 236 | 349 | 23 | -7 | 3697 |
| All 46 watersheds | 0 | 8 | 5 | | | | | | |
| All 32 non-nested watersheds | - | - | - | -55 | -10 | 71 | -88 | -83 | -2 |

Another challenge with the model calibration is that the loading coefficients estimated through the calibration process don't match the real world conceptual understanding in terms of their relative order of magnitude (Sarah Pearce, personal communication) (Table 4). For example, the loading coefficient for Quaternary agriculture obtained from the baseline calibration was 5844 tons/km$^2$ and was higher than Great Valley or Tertiary parameters except for the Tertiary steep parameter. This relative order didn't fit our conceptual model based on field observations of sediment production and ratified during our experts' advisory group workshop:

- Franciscan/Salinian = Tertiary > Great Valley > Quaternary
- Steeper slope > lower slope
- Agricultural land use > urban > open

This appears to be due to lack of constraints on loading coefficients during the calibration process but also may be associated with underlying flaws in the model parameterization that are yet not evident. The inverse optimization procedure that was applied to generate initial parameter choices and coefficients produced wide ranging and overlapping coefficients. Since the Box auto-calibration procedure picks a loading coefficient from each coefficient range randomly without knowledge of their relative magnitude, it could end up picking the combination of loading coefficients in a purely random nature resulting in an outcome that is not physically meaningful.

**Table 4. Summary of calibrated loading coefficients for each testing scenario.**

| Parameter Code Loading rates (t/km2) | FranSalin | GreatValley | QuatAgri | QuatOpen | QuatUrb | TertFlat | TertModAgri | TertModOpen | TertModUrb | TertSteep |
|---|---|---|---|---|---|---|---|---|---|---|
| Baseline 5000 | 3263 | 108 | 5844 | 185 | 23 | 5190 | 4813 | 5440 | 559 | 8691 |
| Baseline 10000 | 2406 | 1818 | 5984 | 857 | 5 | 558 | 9727 | 8023 | 425 | 8729 |
| Baseline 20000 | 2369 | 1827 | 5993 | 10 | 2 | 510 | 8769 | 8024 | 418 | 8734 |
| No Nesting | 127 | 321 | 5993 | 0 | 1 | 508 | 2 | 1 | 418 | 6090 |
| Close-Match Locations | 1465 | 3867 | 5987 | 1284 | 13 | 601 | 6 | 7964 | 466 | 8724 |
| Under-simulated Locations | 3663 | 18 | 5947 | 11 | 106 | 7743 | 26004 | 8027 | 21307 | 8732 |
| Over-simulated Locations | 726 | 1 | 0 | 0 | 509 | 508 | 3 | 2201 | 422 | 95 |
| Reduced Parameter Set (8) | 61 | 1 | 41 | | | 508 | 2 | 498 | 418 | 3270 |
| Reduced Parameter Set (6) | 2683 | 3961 | 1687 | | | 508 | 1849 | | | 8734 |

An important measurement of success for a well-calibrated sediment model is that it has stabilized parameters that reflect the physical characteristics of the simulated watershed. Previous estimates of regional scale sediment loads developed through the RMP relied on the simplifying assumption that sediment production in small watersheds where there was no existing sediment observations was a function of land use and a delivery ratio based on watershed area; a two factor model (Lewicki and McKee, 2009). For watersheds draining to the Bay where there were empirical measurements (n=12), empirical measurements were used to estimate annual average load. For other larger agricultural land use dominated watersheds, the regional regressions relating peak flow to annual sediment load were developed for each of three provinces and applied. Since the objective here is to “design a robust sediment delivery estimate/sediment budget for local tributaries and urban drainages” and, in a sense, do better than the previous methods, another way of thinking about success is to compare the results of the advanced model being developed here to the previous regression (Figure 3). The modeled loads that resulted from our unstable calibration appear to have a similar scatter when regressed against annual peak flow and overall appear to result in a positive bias of about 30% relative to the previous model of Lewicki and McKee (2009).

Given one of the primary uses of the sediment model is to support the PCB and mercury models, one of the options considered was optimizing sediment model calibration for the urban landscape. The result of such an optimization focus would be to lose accuracy on the regional sediment loads estimates but potentially to increase accuracy in relation to regional sediment loads generated from urban areas. A first attempt at doing this was achieved through adjusting the weighting factor in relation to percent urbanization (rather than data quality); areas with greater proportions of urbanization were given greater weights within the model calibration procedure - functionally 0 (completely non-urban watershed) to 100% (completely urban watershed). Somewhat surprisingly, this resulted in under simulation of the most urbanized watersheds in the calibration set (Colma Ck At South San Francisco, North Richmond Pump Station, Zone 4 Line A, and Ettie Street Pump Station). This either occurred as an inherent response of model instability or the way the Box method weights watersheds with larger sediment load more highly. To test this theory, the calibration procedure was reprogrammed with normalized waiting. The results of this calibration run also indicated under simulation however, overall it resulted in a narrower relation between simulated and observed sediment loads.

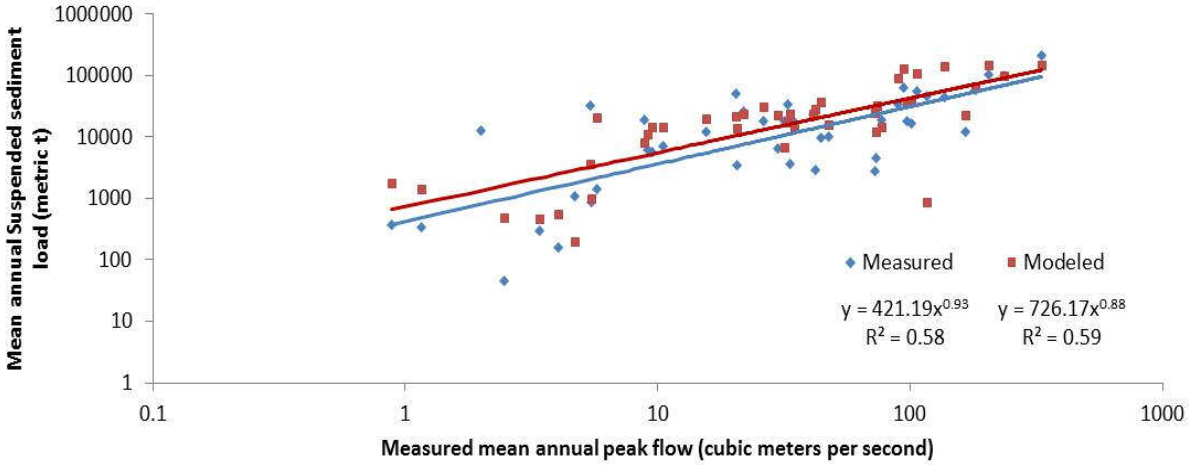


**Figure 3. Comparison between measured and modeled loads for the 46 calibration watersheds as a function of mean annual peak flow.**

In summary, the sediment model is not calibrated well to observed data and remains unstable. Therefore, the loading coefficients estimated from the model are not recommended to use for estimating watershed specific loads, or regional loads of sediment. The results from calibration runs designed to optimize sediment yields for urban areas did not make a conceptual sense probably due to a lack of some kind of parameterization. The sediment coefficients generated by this methodology remain preliminary at this time and were only evaluated at the watershed scale. Recipients of this interim report should not be tempted to use the results presented for site scale assessments for other purposes such as EIRs. In addition, the current and future versions of the model represent "normal circumstances", and not periods of sediment production after large earthquakes or forest fires.

Given both PCB (the extreme case) and mercury concentration in relation to land uses and source areas vary by a greater amount than sediment variability in the landscape, it is possible that the results from the existing uncalibrated unstable sediment model could still be used as a starting point for exploring PCB and mercury production from Bay Area watersheds.

## A6.4 Recommendations

Several improvements to the methodology were suggested during our experts' workshop including adding a model verification step (keeping some watersheds out of the calibration process for verification and potentially adding a storage component to the underlying model). Additionally, several bases or categories were proposed to refine the existing parameters and capture additional sediment yield drivers. The recommendations are summarized below in order of priority:

- Given rainfall is a major driver in sediment yield, investigate adding a factor representing climatic variability or differences in aridity between watersheds.

- Once a climatic factor is added in to the model parameterization, re-explore the choice of parameterization for geology-slope-land use combinations.
    - The default will be the existing 10 model parameter choices
    - If the default is found to be stable, we could explore an expanded/reduced set of parameters. This may improve model performance given that other parameters such as Franciscan and Great Valley for some slope and land use categories are represented in more than 10 out of the 46 watersheds for at least 10% of the watershed area.
- Decide on a subset of the watersheds for model verification.
- Investigate the possibility of incorporating a proxy for sediment storage, such as sediment delivery ratio (SDR) or travel distance into the statistical analysis, as an optimization variable.
- Given the high variability in Tertiary and Franciscan erosiveness, investigate the possibility of splitting out more erosive sub-units from less erosive sub-units.
- Further improving model performance requires better ways to constrain loading coefficients than just a simple range. Future model structures could incorporate important sediment generation processes - buildup, washoff, and supply and transport limitation, into modeling procedure.
- In parallel to developing improved sediment parameterization, we recommend going forward with exploring the PCB and mercury models based on the current sediment model outputs with the caveat that once improved sediment information is available; the PCB and mercury models would be recalibrated. This has the advantage of potentially narrowing down the parameterization for the PCB and mercury models in preparation for the final versions but has the disadvantage of consuming some of the available budget less efficiently.

## A6.5 References

Box, M. J. 1965. A new method of constraint optimization and a comparison with other methods. Computer Journal, 8(1965):42-52.

Brown, C.B., 1944. The control of reservoir silting. U.S. Department of Agriculture. Miscellaneous Publication 521. Washington, D.C.

Gilbreath, A., Yee, D., McKee, L.J., 2012. Concentrations and loads of trace contaminants in a small urban tributary, San Francisco Bay, California. A Technical Report of the Sources Pathways and Loading Work Group of the Regional Monitoring Program for Water Quality: Contribution No. 650. San Francisco Estuary Institute, Richmond, California. 40pp. http://www.sfei.org/sites/default/files/Z4LA_Final_2012May15.pdf

Hunt, J., Gluchowski, D., Gilbreath, A., and McKee, L.J., 2012. Pollutant Monitoring in the North Richmond Pump Station: A Pilot Study for Potential Dry Flow and Seasonal First Flush Diversion for Wastewater Treatment. A report for the Contra Costa County Watershed Program. Funded by a grant from the US Environmental Protection Agency, administered by the San Francisco Estuary

Project. San Francisco Estuary Institute, Richmond, CA. http://www.sfei.org/sites/default/files/NorthRichmondPumpStation_Final_19112012_ToCCCWP.pdf

Inman, D.L., and Jenkins, S.A., 1999. Climate change and the episodicity of sediment flux of small California rivers. Journal of Geology 107, 251-270.

Lent, M.A. and McKee, L.J., 2011. Development of regional suspended sediment and pollutant load estimates for San Francisco Bay Area tributaries using the regional watershed spreadsheet model (RWSM): Year 1 progress report. A technical report for the Regional Monitoring Program for Water Quality, Small Tributaries Loading Strategy (STLS). Contribution No. 666. San Francisco Estuary Institute, Richmond, CA. http://www.sfei.org/sites/default/files/RWSM_EMC_Year1_report_FINAL.pdf

Lent, M.A., Gilbreath, A.N., and McKee, L.J., 2012. Development of regional suspended sediment and pollutant load estimates for San Francisco Bay Area tributaries using the regional watershed spreadsheet model (RWSM): Year 2 progress report. A technical progress report prepared for the Regional Monitoring Program for Water Quality in San Francisco Bay (RMP), Small Tributaries Loading Strategy (STLS). Contribution No. 667. San Francisco Estuary Institute, Richmond, California. http://www.sfei.org/sites/default/files/RWSM_EMC_Year2_report_FINAL.pdf

Lewicki, M., and McKee, L.J, 2009. Watershed specific and regional scale suspended sediment loads for Bay Area small tributaries. A technical report for the Sources Pathways and Loading Workgroup of the Regional Monitoring Program for Water Quality: SFEI Contribution #566. San Francisco Estuary Institute, Oakland, CA. 28 pp + Appendices. http://www.sfei.org/sites/default/files/566_RMP_RegionalSedimentLoads_final_web.pdf

McKee, L.J., Leatherbarrow, J., Pearce, S., and Davis, J., 2003. A review of urban runoff processes in the Bay Area: Existing knowledge, conceptual models, and monitoring recommendations. A report prepared for the Sources, Pathways and Loading Workgroup of the Regional Monitoring Program for Trace Substances. SFEI Contribution 66. San Francisco Estuary Institute, Oakland, Ca. http://www.sfei.org/sites/default/files/Urban_runoff_literature~000.pdf

McKee, L.J., Gilbreath, A.N., Hunt, J.A., and Greenfield, B.K., 2012. Pollutants of concern (POC) loads monitoring data, Water Year (WY) 2011. A technical report prepared for the Regional Monitoring Program for Water Quality in San Francisco Bay (RMP), Small Tributaries Loading Strategy (STLS). Contribution No. 680. San Francisco Estuary Institute, Richmond, California. http://www.sfei.org/sites/default/files/POC%20loads%20WY%202011%202013-03-03%20FINAL%20with%20Cover.pdf

NRCS, 1983. Sediment sources, yields, and delivery ratios. Chapter 6. In: National Engineering Handbook, Section 3, Sedimentation. US Department of Agriculture, Natural Resources Conservation Service (SCS), 6.2–6.19. Washington DC, USA.

SFRWQCB, 2006. California Regional Water Quality Control Board San Francisco Bay Region Mercury in San Francisco Bay Proposed Basin Plan Amendment and Staff Report for Revised Total Maximum Daily Load (TMDL) and Proposed Mercury Water Quality Objectives. http://www.waterboards.ca.gov/sanfranciscobay/water_issues/programs/TMDLs/sfbaymercury/sr080906.pdf

SFRWQCB, 2008. California Regional Water Quality Control Board San Francisco Bay Region Total Maximum Daily Load for PCBs in San Francisco Bay Staff Report for Proposed Basin Plan Amendment. 134 pp. http://www.waterboards.ca.gov/sanfranciscobay/board_info/agendas/2008/february/tmdl/appc_pcbs_staffrept.pdf

SFRWQCB, 2009. California Regional Water Quality Control Board San Francisco Bay Region Municipal Regional Stormwater NPDES Permit, Order R2-2009-0074, NPDES Permit No. CAS612008. Adopted October 14, 2009. 279pp. http://www.waterboards.ca.gov/sanfranciscobay/water_issues/programs/stormwater/Municipal/index.shtml

# Appendix 6 Attachment 1. Suspended sediment model module methods

## A6A1.1 Suspended sediment model module architecture

The suspended sediment model is built upon the existing Spreadsheet Model framework. The model relates the physical characteristics of that watershed to the average annual suspended sediment load from each watershed. Based on available local data, a review of international information, and expert advice from a local sediment advisory group, suspended sediment generation in Bay Area watersheds is known to be highly variable both in time (2-4 orders of magnitude) and space (30 – 1600 t/km$^2$) (McKee et al., 2003). The factors influencing sediment production include geology, slope, land-use (both current and history), soil type, climate, and storage that is influenced by basin size, shape, slope, valley width, channel incision, and channel modifications such as hardening, straightening, and elevation control (weirs, dams, sills).

Given this tremendous complexity and limitations of available calibration data (collected in relatively many watersheds but for small snapshots of climatic variability), developing a calibrated regional scale average annual time step model for suspended sediments was challenging and simplifications were needed. In the model, sediment was produced based upon the type of bedrock, the slope of the hillslope, and the current land use; land use history was not considered largely because there is an absence of suitable regional geographic data. Sediment is then stored (or perhaps best described as not transported out of each watershed) based upon the delivery ratio of the watershed and any potential reservoirs that may be trapping sediment; other factors influencing storage such as shape, slope, valley width, and channel modifications were not considered. Model calibration used 54 watersheds where flow and suspended sediment data have been measured; inter-annual variability was not considered and explicitly removed by purposefully climatically averaging the available records. The geology, slope, and land use within a watershed were correlated to the amount of sediment measured or estimated being transported past the gage location. Using inverse optimization, the model has produced locally-derived land use coefficients based upon these measured loads, using them rather than published national coefficients which were derived in non-representative portions of the country (NRCS, 1983).

During model development, a decision to incorporate delivery ratios was made. Delivery ratio affects the amount of sediment that is transported out of a watershed; sediment has a higher chance of being stored (e.g. on a hillslope, in an alluvial fan, on a floodplain) in a larger watershed (low delivery ratio), compared to a small, typically steeper and more connected watershed (high delivery ratio). Using delivery ratios to adjust sediment loads removes the effect of watershed area, allowing the effects of other factors to be seen more clearly. Because of the variable sizes of watersheds in the Bay Area, we chose to modify the sediment data using the published delivery ratio equation (NRCS, 1983):

$$DR = 0.417762A^{-0.134958} - 0.127097$$

where DR is the delivery ratio, and A is the watershed area (mi$^2$).

In addition, we also chose to modify the sediment data for the effects of reservoirs. Watersheds with reservoirs can trap at least a portion, if not all, of the suspended sediment provided to the reservoir. The data was adjusted to reflect the proportion of sediment transported through the reservoir, or its trapping efficiency, as calculated by the Brown (1944) equation.

### A6A1.2 Available suspended sediment data

The suspended sediment data utilized is from 54 total gage stations gathered from three sources: USGS, Balance Hydrologics, and RMP/STLS studies (Table AI-1). The USGS has collected discharge and suspended sediment at 39 stations in the Bay Area since 1956, although collection periods are variable between stations (www.usgs.gov). Stations with at least four years of data were included. For each station, maximum instantaneous peak discharge (cfs) and suspended sediment total load (tons) for each Water Year was reported. Data from Balance Hydrologics Inc. for 12 new stations, plus additional data for an existing USGS station (Wildcat Creek), was provided by Barry Hecht and Jonathan Owens. For each of these stations, maximum instantaneous peak discharge (cfs) and annual total suspended sediment load (tons) for each period of record (data collection typically occurred only during the wet season) was reported. Data from three RMP/STLS studies were also included: North Richmond Pump Station, Ettie Street Pump Station, and Zone 4 Line A. North Richmond and Ettie Street only had one year of data for each, while Zone 4 Line A had four years of data, with data extracted from each respective project report (Gilbreath et al 2012; Hunt et al 2012; McKee et al 2012).

**Table A1-1. Available suspended sediment data sets in the Bay Area used in this project.**

| Station | Source of Data | USGS stn No. | County | Station Latitude | Station Longitude | Upstream Area ($km^2$) | Upstream Free Flowing Area ($km^2$) | Upstream Reservoirs |
|---|---|---|---|---|---|---|---|---|
| Alameda Ck. At Niles | USGS | 11179000 | Alameda | 37.58722 | -121.95972 | 1637.7 | 904.0 | San Antonio Res., Calaveras Res., Del Valle Res. |
| Alameda Ck. Below Welch Ck. Near Sunol | USGS | 11173575 | Alameda | 37.54056 | 121.85528 | 385.1 | 129.6 | Calaveras Res. |
| Arroyo De La Laguna at Verona | USGS | 11176900 | Alameda | 37.62667 | -121.88194 | 1043.6 | 665.2 | Del Valle Res. |
| Arroyo De La Laguna near Pleasanton | USGS | 11177000 | Alameda | 37.61528 | -121.88056 | 1045.7 | 667.3 | Del Valle Res. |
| Arroyo Valle Below Lang Canyon Near Livermore | USGS | 11176400 | Alameda | 37.56139 | -121.68278 | 337.0 | 337.0 | |
| Arroyo Valle Near Livermore | USGS | 11176500 | Alameda | 37.62333 | -121.75778 | 381.9 | 381.9 | Del Valle Res. |
| Berryessa Creek at Cropley Avenue | Balance Hydrologics | Balance | Santa Clara | 37.41667 | -121.85556 | 11.8 | 11.8 | |
| Berryessa Creek at Messina Drive | Balance Hydrologics | Balance | Santa Clara | 37.40972 | -121.86111 | 13.6 | 13.6 | |
| Berryessa Creek at North Hillview Drive | Balance Hydrologics | Balance | Santa Clara | 37.45194 | -121.89333 | 40.3 | 40.3 | |

| Station | Source of Data | USGS stn No. | County | Station Latitude | Station Longitude | Upstream Area ($km^2$) | Upstream Free Flowing Area ($km^2$) | Upstream Reservoirs |
|---|---|---|---|---|---|---|---|---|
| Calabazas Ck. At Rainbow Drive Near Cupertino | USGS | 11169616 | Santa Clara | 37.30083 | -122.02556 | 12.0 | 12.0 | |
| Calabazas Cr. Tributary at Mount Eden Road Near Saratgoa | USGS | 11169580 | Santa Clara | 37.26917 | -122.06000 | 0.9 | 0.9 | |
| Colma Ck. At South San Francisco | USGS | 11162720 | San Mateo | 37.65389 | -122.42528 | 26.4 | 26.4 | |
| Corte Madera Ck. Near Ross | USGS | 11460000 | Marin | 37.96306 | -122.55583 | 45.1 | 39.3 | Phoenix Lake |
| Coyote Ck. Above Highway 237 At Milpitas | USGS | 11172175 | Santa Clara | 37.42222 | -121.92639 | 831.2 | 320.5 | Coyote Lake, Anderson Lake, Cherry Flat Res. |
| Coyote Ck. Near Gilroy | USGS | 11169800 | Santa Clara | 37.07778 | -121.49333 | 282.5 | 282.5 | |
| Crow Creek Near Hayward | USGS | 11180900 | Alameda | 37.70500 | -122.04278 | 27.3 | 27.3 | |
| Cull Ck. Above Cull Ck. Reservoir Near Castro Valley | USGS | 11180960 | Alameda | 37.71778 | -122.05333 | 15.1 | 15.1 | |
| El Corte de Madera At Virginia Mill Trail | Balance Hydrologics | Balance | San Mateo | 37.38278 | -122.32750 | 12.7 | 12.7 | |
| Ettie Street Pump Station | RMP/STLS | RMP/STLS | Alameda | | | 4.0 | 4.0 | |
| Evergreen Creek at San Felipe Road | Balance Hydrologics | Balance | Santa Clara | 37.30278 | -121.77417 | 3.5 | 3.5 | |
| Evergreen Creek at Tuscany Circle | Balance Hydrologics | Balance | Santa Clara | 37.30472 | -121.75500 | 2.6 | 2.6 | |
| Guadalupe R. Above Almaden Expressway At San Jose | USGS | 11167800 | Santa Clara | 37.28083 | -121.87861 | 153.3 | 106.4 | Guadalupe Res., Alamaden Res., Calero Res. |
| Guadalupe R. Above Highway 101 At San Jose | USGS | 11169025 | Santa Clara | 37.37389 | -121.93194 | 393.0 | 231.8 | Vasona Res., Lexington Res., Guadalupe Res., Almaden Res. |
| Lagunitas Ck. At Samuel P. Taylor State Park | USGS | 11460400 | Marin | 38.02694 | -122.73528 | 32.8 | 88.9 | Kent Lake (Peters Dam) |
| Lagunitas Ck. Nr. Pt. Reyes Station | USGS | 11460600 | Marin | 38.08028 | -122.78333 | 211.4 | 62.3 | Kent Lake, Nicasio Res. |
| Llagas Ck. Above Chesbro Reservior Nr. Morgan Hill | USGS | 11153470 | Santa Clara | 37.14833 | -121.76722 | 24.9 | 24.9 | |
| Napa R. Near Napa | USGS | 11458000 | Napa | 38.36833 | -122.30222 | 567.4 | 380.8 | Kimball Canyon Res., Bell Canyon Res., Hennessey Res., Rector Res. |
| Napa River Near Saint Helena | USGS | 11456000 | Napa | 38.51139 | -122.45472 | 203.8 | 180.9 | Kimball Canyon Res., Bell Canyon Res. |
| North Richmond Pump Station | RMP/STLS | RMP/STLS | Contra Costa | | | 2.0 | 2.0 | |

| Station | Source of Data | USGS stn No. | County | Station Latitude | Station Longitude | Upstream Area ($km^2$) | Upstream Free Flowing Area ($km^2$) | Upstream Reservoirs |
|---|---|---|---|---|---|---|---|---|
| Permanente Ck. Near Monte Vista | USGS | 11166575 | Santa Clara | 37.33333 | -122.08694 | 10.0 | 10.0 | |
| Pescadero Ck. Near Pescadero | USGS | 11162500 | San Mateo | 37.26083 | -122.32778 | 118.9 | 118.9 | |
| Pine Ck. At Bolinas | USGS | 11460170 | Marin | 37.91861 | -122.69194 | 19.9 | 19.9 | |
| Prospect Creek at Saratoga Golf Course Near Saratoga | USGS | 11169600 | Santa Clara | 37.28583 | -122.05389 | 0.7 | 0.7 | |
| San Francisquito Ck. At Stanford | USGS | 11164500 | Santa Clara | 37.42333 | -122.18833 | 97.3 | 61.5 | Searsville Lake |
| San Lorenzo Ck. Above Don Castro Reservoir Near Castro Valley | USGS | 11180825 | Alameda | 37.69528 | -122.04389 | 46.7 | 46.7 | |
| San Lorenzo Ck. At San Lorenzo | USGS | 11181040 | Alameda | 37.68417 | -122.13889 | 124.7 | 56.2 | Don Castro Res., Cull Creek Res. |
| Sonoma Creek At Agua Caliente | USGS | 11458500 | Sonoma | 38.32333 | -122.49333 | 151.1 | 151.1 | |
| Sonoma Creek At Boyes hot spring | USGS | 11458500 | Sonoma | 38.31361 | -122.48583 | 161.7 | 161.7 | |
| Spruce Branch At South San Francisco | USGS | 11162722 | San Mateo | 37.64611 | -122.42083 | 2.0 | 2.0 | |
| Thompson Creek at Early Morning Lane | Balance Hydrologics | Balance | Santa Clara | 37.27250 | -121.74167 | 1.6 | 1.6 | |
| Thompson Creek at Quimby Road | Balance Hydrologics | Balance | Santa Clara | 37.32194 | -121.80667 | 46.1 | 46.1 | |
| Upper Penitencia Creek at Berryessa Road | Balance Hydrologics | Balance | Santa Clara | 37.37222 | -121.87472 | 60.2 | 54.1 | Cherry Flat Res. |
| Upper Penitencia Creek at Piedmont Avenue | Balance Hydrologics | Balance | Santa Clara | 37.39056 | -121.84278 | 57.1 | 51.0 | Cherry Flat Res. |
| Uvas Ck. Above Uvas Resersvoir Near Morgan Hill | USGS | 11153900 | Santa Clara | 37.09278 | -121.71722 | 55.3 | 55.3 | |
| Walker Ck. Near Marshall | USGS | 11460750 | Marin | 38.17583 | -122.81722 | 81.1 | 32.2 | Sausal Res. (Soulajule) |
| Walker Ck. Near Tomales | USGS | 11460800 | Marin | 38.20972 | -122.85972 | 104.2 | 55.2 | Sausal Res. (Soulajule) |
| Walnut Ck. At Concord | USGS | 11183600 | Contra Costa | 37.94528 | -122.04861 | 220.2 | 217.2 | Lafayette Res. |
| Walnut Ck at Walnut Creek | USGS | 11183500 | Contra Costa | 37.90583 | -122.05611 | 210.2 | 207.2 | Lafayette Res. |
| West Fork Permanente Ck. Near Monte Vista | USGS | 11166578 | Santa Clara | 37.33306 | -122.09944 | 7.9 | 7.9 | |
| Wildcat Ck. At Vale Road At Richmond | USGS and Balance Hydrologics | 11181390 | Contra Costa | 37.95333 | -122.33722 | 20.7 | 20.7 | |
| Yerba Buena Creek at San Felipe Road | Balance Hydrologics | Balance | Santa Clara | 37.29917 | -121.76889 | 7.1 | 7.1 | |

| Station | Source of Data | USGS stn No. | County | Station Latitude | Station Longitude | Upstream Area ($km^2$) | Upstream Free Flowing Area ($km^2$) | Upstream Reservoirs |
|---|---|---|---|---|---|---|---|---|
| Yerba Buena Creek at Villa Vista Road | Balance Hydrologics | Balance | Santa Clara | 37.29667 | -121.74944 | 4.6 | 4.6 | |
| Zone 4 Line A | RMP/STLS | RMP/STLS | Alameda | | | 4.2 | 4.2 | |
| Zone 6 Line B At Warm Springs Boulevard At Fremont | USGS | 11172365 | Alameda | 37.46972 | -121.91667 | 2.2 | 2.2 | |

### A6A1.3 Methods for climatic averaging

The existing suspended sediment data is from multiple stations, collected during various years, and together, the data represents the spectrum from very dry to very wet Water Years. In order for the data from different stations and different Water Years to be directly comparable, the data were climatically averaged to reduce, as much as possible, any climate-based variation. Averaging is based upon existing data, and assumes that this average remains valid into the future (no effects from climate change). Because of the variable Mediterranean climate of the Bay Area, a period of approximately 20 years was used, to cover three climatic cycles (Inman and Jenkins, 1999). Given the data available, the years 1992-2011 (the averaging period) were chosen for this effort. Three different methods of generating climatically averaged sediment loads were used, because of the variability of the existing empirical data. First, for nine watersheds where empirical flow records exist for the averaging period and at least four years of sediment data exist (for any period), a regression relationship was generated between peak annual flow and annual suspended sediment load, allowing the climatically averaged loads to be computed, and the mean and standard deviation statistics to be generated for these watersheds. Secondly, for watersheds that either had no peak flow data or only a partial record for the averaging period, Water Year-specific regional regressions were developed for three provinces (North Bay, East Bay, South Bay/Peninsula) relating watershed area to peak flow. Using these regressions, peak flow estimates were developed for each Water Year for 41 additional watersheds, allowing this flow data to be combined with the previous sediment load regression, thus calculating climatically averaged sediment loads, mean and standard deviation statistics. And finally, for four special-case watersheds, annual sediment loads were individually computed. In these cases, the sediment record appeared unreliable because it represented little of the climatic variability, was only collected for three or fewer years, or had evidence of a temporal trend.

### A6A1.4 Generation of watershed boundary layers

The sediment model used the existing watershed boundary layer created for the Proposition 13 project and used in the Spreadsheet Model, making only minor modifications or improvements as appropriate. In some of the 54 watersheds, the Prop 13 boundary was modified based upon more recent and accurate data. For example, the location of the drainage divide of some watersheds was adjusted based upon the new BAARI mapping that was not available when the Prop 13 boundaries were being developed. These modifications were very minor, but produce more accurate watershed boundaries.

For the watersheds with data provided by Balance Hydrologics, new watershed boundaries were created using relevant portions of the existing Prop 13 boundaries, and drawing new boundary segments by interpreting the 10m DEM, using BAARI stream lines, and using Oakland Museum stormdrain lines in the urban areas.

As a check on quality, for the 39 watersheds with USGS data, a comparison between the existing boundary layer and the boundary as defined by the USGS was completed. Comparing total watershed area as reported by the two boundary layers revealed that most were within 1% of each other, with only a few watersheds with differences as large as 5% (primarily reflecting storm drained portions of watersheds in urban areas). Closer inspection revealed that the Prop 13 boundaries were more precise, based upon 10m DEM or LiDAR, whereas the USGS boundaries were coarser, likely calculated decades ago based upon contours from topographic maps.

### A6A1.5 Influences of reservoirs

Although sediment can potentially be generated from all parts of a watershed, features such as reservoirs can prevent sediment from portions of a watershed from being transported downstream. Calculating suspended sediment load from a watershed thus must take into consideration potential trapping of a portion of the sediment load behind reservoirs. The many reservoirs that exist in Bay Area watersheds range in size, age, capacity, purpose, and management, with each of these features affecting the amount of sediment that is trapped. In this model, three options exist for considering reservoirs: 1) Reservoirs can be considered as fully pass-through, trapping zero sediment, thus the entire watershed area contributes to the total calculated load. 2) Reservoirs can be considered as fully trapping, thus the watershed area upstream of the reservoir does not contribute to the total calculated load, and should be removed. 3) Reservoirs can be considered as trapping variable amounts of sediment, based upon their trapping capacity, thus the upstream area is contributing to the total calculated load, however a portion of the sediment generated from that area is trapped behind the reservoir.

Option 3 is the most valid scientifically, and was chosen as the option for this model. The literature has multiple methods for calculating reservoir trapping efficiency, but one of the most simple and a widely-used method is by Brown (1944). Trapping efficiency is calculated using upstream contributing watershed area and the capacity of the reservoir:

$$C_T = 100\,[1 - 1\,(1+0.1\,C/W)]$$

where $C_T$ is reservoir trapping efficiency, C is reservoir capacity (acre/feet), and W is contributing watershed area ($mi^2$).

In the earlier Spreadsheet Model, only large reservoirs were included in the analysis. However, in this effort, additional reservoirs were added, including reservoirs that are registered in the Department of Water Resources Division of Safety of Dams (DSOD) database (http://www.water.ca.gov/damsafety/) that have an upstream contributing area greater than 3 $km^2$, for a total of 30 reservoirs. The trapping efficiency using the equation by Brown (1944) was used for each reservoir, and the resulting climatically averaged suspended sediment load for each watershed was adjusted accordingly.

### A6A1.6 Generation of watershed physical attributes

The sediment model relates physical attributes of each watershed to the calculated climatically averaged suspended sediment load. These attributes include geology (underlying bedrock lithology), slope (average percent slope of the hillslopes), and land use (lumped into three classes). The generalized geologic mapping by Graymer et al (2006) was gathered as kml files, and transformed into a seamless shapefile for use in GIS. Land use mapping by ABAG (2005) was used for both the Spreadsheet Model and this Sediment Model, however the classes were further lumped using best professional judgment for this purpose, into three categories (open, agriculture, and urban). The slope layer was calculated by SFEI staff using the USGS 10m digital elevation model (DEM), calculating average slope of each pixel, and outputting a slope map showing the pixel values summarized into the three broad slope categories.

The data layers were input in to ARC GIS for spatial analysis; for each of the 54 watersheds, a union was performed to output a number of polygons each with one of the unique combinations of physical attributes. A total of 60 unique combinations were possible; 3 slope classes, 5 geology classes (in addition to the four lithologies, the input data also had a "water" category), and 4 land use classes (in addition to the three categories, the input data also had a "water" category). Each unique combination was given a three digit code. After the union was performed, the area of the multiple polygons with each code was summed, producing a total area for each code for each watershed. Each code was then related to a specific amount of sediment production, providing the basis for estimating sediment loads from the other unmeasured watersheds in the model.

# Appendix 6 Attachment 2. Supporting documentation for optimization-based sediment coefficient development

## A6A2.1 Methods

### *A6A2.1.a Overall approach*

Parameter estimation, also known as inverse optimization, methods was used to derive land use-, geology-, and slope-specific sediment coefficients from local watershed sediment yield data. Initially, the bases (land use, geologic class, and slope class) were considered separately, but further investigation merged the bases for a multi-factor analysis. For all analyses, a sediment coefficient optimization was set up within a Monte Carlo loop that fed in a set of 20 randomly chosen watersheds sediment yields (out of 46 possible watersheds). The optimization then searched the parameter space of basis-specific sediment coefficients, and computed "simulated" downstream yields from these parameters, using a simple area-weighting model. The goal of the optimization was to minimize the difference between observed sediment yields and the simulated yields for each watershed while keeping the basis-specific sediment coefficients consistent across watersheds. The output was a distribution of sediment coefficients for each category under consideration. The optimization was performed in R and the basis analysis was performed in ArcGIS.

### *A6A2.1.b Input data*

All available watershed sediment loading data were assembled for the San Francisco Bay Area. After culling the data set and removing non-representative data (e.g., sediment loading from periods of extreme development), sediment yields were available for 46 watersheds. The sediment yield data for the 46 watersheds were then climate-normalized. Additionally the sediment yields were adjusted using delivery ratios (See Appendix I for details). The watershed yield data were rated according to confidence in the data quality in relation to length of observation period, robustness of the methods used for climatic averaging, and the representativeness of the data in relation to recent land use and management conditions. The resulting initial confidence rating was incorporated into the optimization using weighting factors. For the nine watersheds with high quality sediment data, their data were assigned full weight (w=1) in the optimization. Meanwhile, medium (n=16) and low (n=21) quality sediment data were assigned weighting factors of 0.5 and 0.25, respectively. In this way, less reliable sediment data could still be used, providing a larger data set, without overly impacting the results. Note, during the model calibration exercise, the initial confidence ratings were further evaluated and some were downgraded. Spatial analysis was performed on the 46 watersheds to compute the fractions of different land uses, geology classes, and slope classes in each watershed (See Appendix I for details).

### *A6A2.1.c Monte Carlo approach*

#### A6A2.1.c.i Underlying model

The underlying model provided the connection between the observed data and the parameters being optimized, i.e., the basis specific coefficients. A simple linear model was used to relate the coefficients being optimized to the downstream yields. Simulated downstream yields were approximated as area-weighted sums of contributing sediment coefficients:

$$Yield_{i,Sim} = \sum_{j=1}^{n} f_{i,C_j} * Sed.Coef_{i,C_j} \text{ where } f_{i,LU_j} = \frac{Area_{i,j}}{\sum_{j=1}^{n}(Area_{i,j})} \text{ and } C = category$$

A simplification in this approach is the lack of sediment storage in the system; all sediment suspended in runoff is assumed to be transported downstream. The same simplification was used in the current structure of the RWSM sediment and pollutant model.

#### A6A2.1.c.ii Optimization structure

One of the most important components of optimizations is the objective function, an equation that evaluates the state of the optimization. An optimization has arrived at an optimal solution when the objective function is at its global maxima or minima for the search space. The objective function developed for this work is as follows:

$$Minimize\ Z = \sum_{i=1}^{m} w_i\left(Yield_{i,Obs} - Yield_{i,Sim}\right)^2 + \lambda \sum_{j=1}^{n}\sum_{i=1}^{m}\left(Sed.Coef_{i,C_j} - \frac{\sum_{i=1}^{m} Sed.Coef_{i,C_j}}{m}\right)^2$$

The first term in the objective function serves to minimize the difference between observed yields and the simulated yields, and the second term forces convergence of coefficient values for each category.

The parameters being optimized (i.e., decision variables) are the basis-specific sediment coefficients ($Sed.Coef_C$). The simulated yields ($Yield_{Sim}$) are computed from the current set of sediment coefficients at each iteration of the optimization. The weights on the first term, $w_i$, can be set to represent confidence in observed data points (e.g., a questionable data point can be given a low weight, reducing its impact on the optimization). The weight on the second term, λ, sets the relative importance of the two objective function terms, controlling the level of convergence required of the sediment coefficients. No underlying distribution was assumed for the optimized concentrations, unlike in a maximum likelihood approach. Rather, the distributions of the land use specific concentrations were built up "blindly" via the Monte Carlo approach.

The optimization solver used was a limited-memory modification of the Boyd-Fletcher-Goldfarb-Shanno (BFGS) method with box constraints. The BFGS method is a quasi-Newton approach; it uses function values and gradients to build up a picture of the surface to be optimized. The major benefit of this approach was its compatibility with constraints; putting well-informed bounds on parameters being optimized reduces the searched parameter space (and thus computation time) and increases the likelihood of convergence to a stable solution. Here, bounds were used to focus the search space, not to serve as active constraints; when an optimization ran up against a bound, the bound was increased.

## A6A2.2 Results: Single-factor analysis

### *A6A2.2.a Slope*

Slope was binned in three categories: <10%, 10-30%, and >30% slope. Each slope class was well-represented in the input data set. The optimization found that the flatter areas (<10% slope) produced little sediment per unit area, while the steeper areas (>30% slope) produced moderate yields (Figure AII-1). The unexpected result was the moderate slope areas (10-30% slope) were predicted to produce large sediment yields. Generally, one would expect the steeper slopes to generate higher yields, but the optimization is estimating what actually makes it to the measurement location. Given that in-stream measurements are generally made in flatter areas, it is not surprising that some of the sediment produced in the steepest areas has had time to settle out by the measurement location. The optimization was re-run on two slope categories representing above and below 10% slope. Merging the two steeper slopes averaged out the effect of distance to the measurement station (Figure AII-2).

### *A6A2.2.b Geology*

Geology was grouped into four broad categories: Quaternary, Tertiary, Franciscan, and Great Valley (See Appendix I for details). These categories were adequately represented in the data set. The optimization found that Tertiary geology produced high yields, Franciscan and Great Valley geology produced moderate yields, and Quaternary geology produced small yields (Figure AII-3). From an erodibility perspective, one would expect Quaternary geology to produce greater yields; however, Quaternary geology tends to coincide with flatter areas (Table AII-1) and thus generally experiences smaller erosional forces. The predicted yields of the other geologic classes are also likely influenced by their tendencies to coincide with particular slope categories. Adding in the effect of distance to measurement location (increasing the opportunity to settle out) explains the results of the optimization (Figure AII-4).

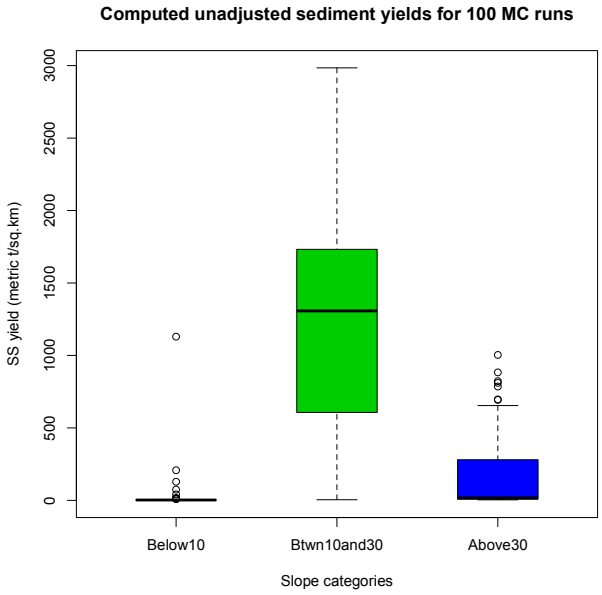


**Figure AII-1. Slope-based optimization results for three slope categories.**

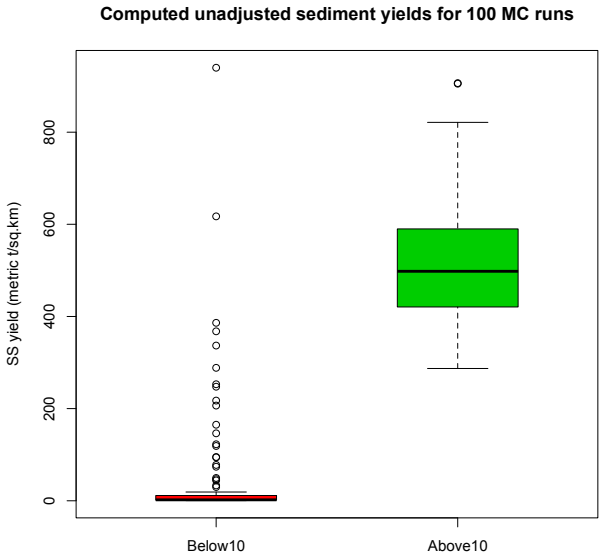


**Figure AII-2. Slope-based optimization results for two slope categories.**

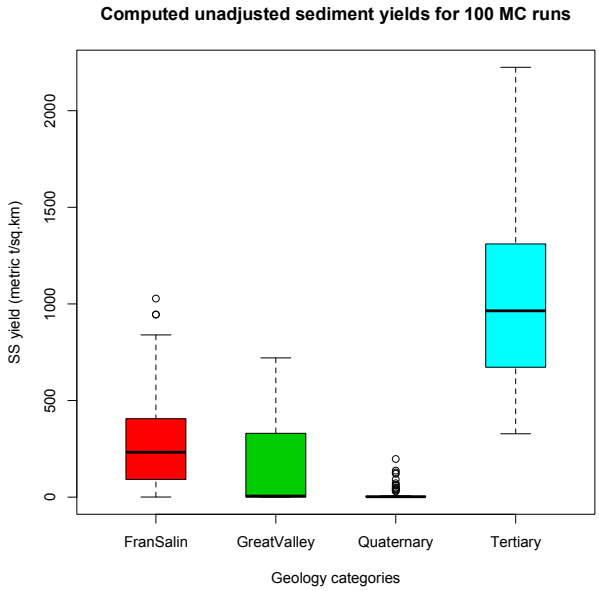


**Figure AII-3. Geology-based optimization results for four geologic categories.**

**Table AII-1. Representation of geologic classes in data set. Dominant geologic classes for each slope bin highlighted.**

| Geologic Class | Overall representation in data set | Representation in flat lands (<10% slope) | Representation in moderate slope areas (10-30%) | Representation in steepest areas (>30%) |
|---|---|---|---|---|
| Quaternary | 29% | **82%** | 14% | 5% |
| Tertiary | 36% | 12% | **46%** | **36%** |
| Franciscan | 24% | 4% | 26% | **42%** |
| Great Valley | 11% | 2% | 14% | 18% |

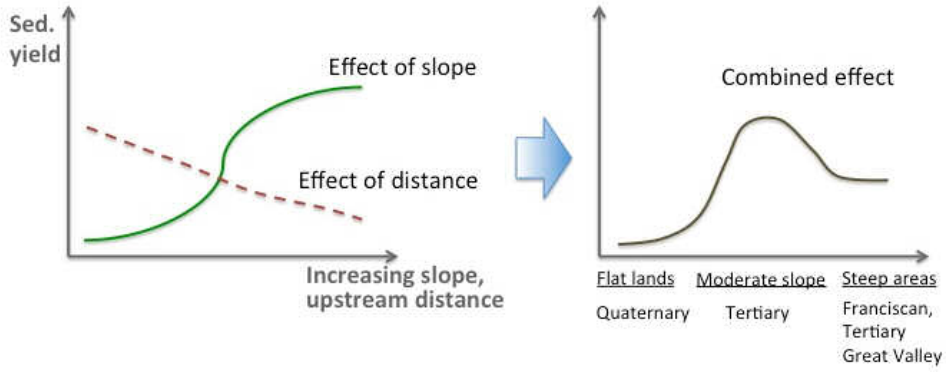


**Figure AII-4. Explaining competing effects on geology optimization results.**

### *A6A2.2.c Land use*

Land use was grouped into five categories: Open, Agricultural, Industrial, High- and Low-Density Urban. Open, agricultural, and low-density urban land use were well-represented in the input data set, but industrial and high-density urban land use were poorly represented in the data set at 7% and 5%, respectively. The optimization found that open and high-density urban areas produce small yields, low-density urban areas produce moderate yields, and agricultural areas produce larger yields (Figure AII-5). The optimization resulted in a very large range of yields for industrial areas (Figure AII-5), suggesting the results may not be robust. The large number of outliers on high-density urban yields also suggest a lack of robustness, which may be expected given the poor representation of the category in the input data set.

The optimization was re-run with aggregated land use categories. Once the land use categories were aggregated down to open, agricultural, and urban, the categories were adequately represented in the data set (Table AII-2). The optimization found that open areas produce small yields, urban areas produce moderate yields, and agricultural areas produce larger yields (Figure AII-6). These results are generally in line with our conceptual model of sediment production by land use type.

### *A6A2.2.d Comparing single-factor results*

The optimized sediment coefficients were then used to "simulate" downstream yields (computed as area-weighted sums of contributing sediment coefficients). The performance of the optimized sediment coefficients was evaluated by calculating the percent difference between the observed sediment yield and the simulated sediment yield (i.e., the error) for each of the 46 watersheds. Based on the distribution of errors for each optimization, geology appears to be the best classification scheme for predicting sediment yield (Figure AII-7). In part, this is because the geology categories inherently carry slope information (Quaternary correlates strongly with <10% slope; Franciscan correlates with >30% slope). For the slope results, it is interesting that reducing the slope categories from three to two does not reduce predictive power. And, finally, land use performed the worst in terms of single classification predictive abilities. But, the fact that the sediment yield results for land use are generally in line with our conceptual model suggests that the land use may be useful as a merged category with geology.

Additionally, the entire single factor analysis was also run with delivery ratio (DR) adjusted sediment yield data to see what impacts the modified input data has and to compare performance with unadjusted sediment yield data. The general patterns were similar using DR-adjusted sediment yields, but the estimated DR-adjusted sediment yields by category tended to be larger than the unadjusted estimated yields. Overall, the simulated watershed yields exhibited larger errors (Figure AII-8; note different y-axis from Figure AII-7). Geology still performed the best in terms of predictive power, but slope with three bins improved to the point of being a close second. Adjusting the watershed yields by the delivery ratio resulted in land use having more predictive power, although the classification scheme still lagged behind geology and three-bin slope (but not two-bin slope).

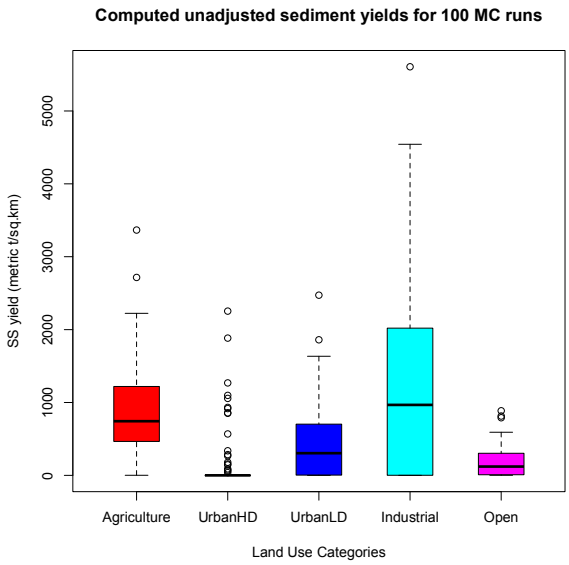


**Figure AII-5. Land use-based optimization results for five land use categories.**

**Table AII-2. Fractions of land use in aggregated categories.**

| Land Use | Representation in data set |
|---|---|
| Agriculture | 35% |
| Urban | 29% |
| Open | 36% |

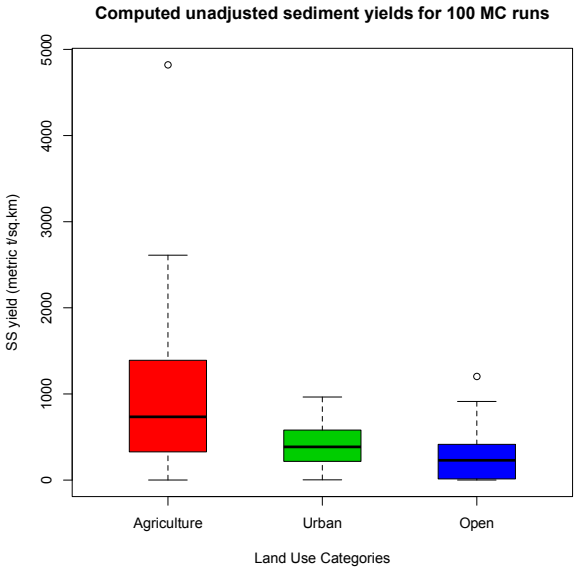


**Figure AII-6. Land use-based optimization results for three land use categories.**

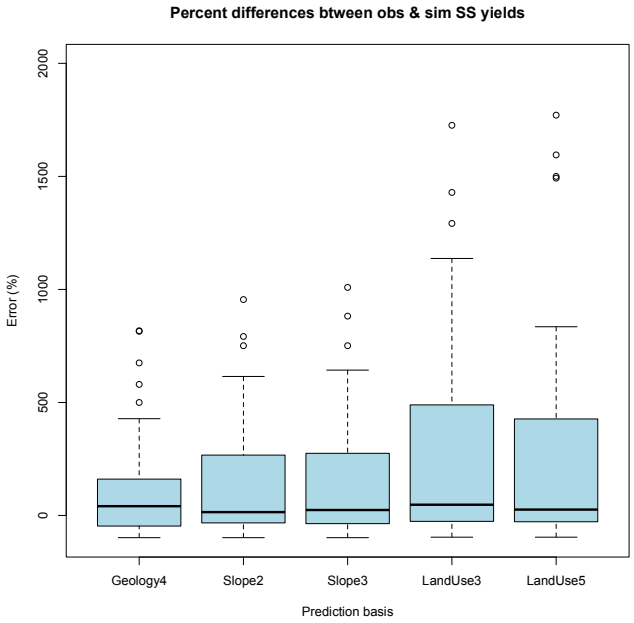


**Figure AII-7. Comparison of performance across optimizations using 100 iterations.**

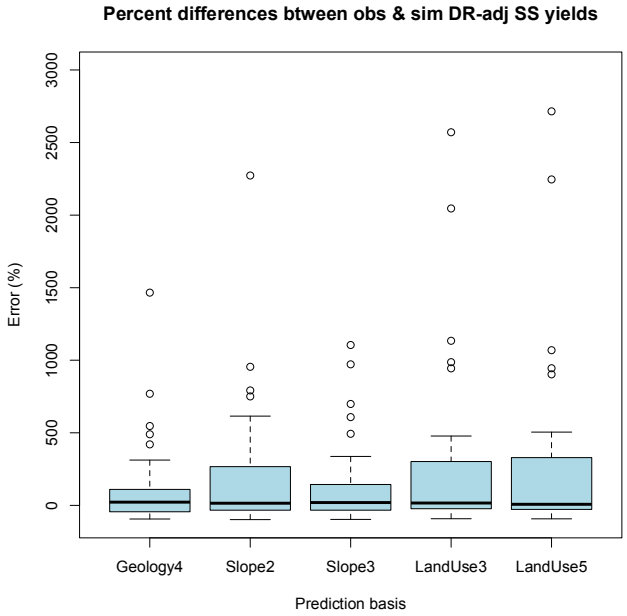


**Figure AII-8. Comparison of performance across optimizations for delivery ratio-adjusted sediment yields using 100 iterations.**

### A6A2.3 Results: Multi-factor analysis

While the single-factor analysis looked at one driver of sediment production at a time, the multi-factor analysis looked at multiple bases at once, taking into account the interactions between various drivers of sediment production. The goal of the multi-factor analysis was to find the minimal grouping of categories that best reproduced the observed sediment yields at the watershed scale. Unnecessary complexity (i.e., too many unsupported parameters) can lead to issues with excessive degrees of freedom and over-fitting the model.

The results of the single-factor analysis pointed to geology being the most important driver of sediment production, but with unexplained variation in the results for Quaternary (many outliers) and Tertiary (large range). Accordingly, Quaternary and Tertiary categories were split into further subcategories using various combinations of land use and slope. Since Quaternary geology predominantly occurs in flat areas, this geologic class was split with land use type (Figure AII-9 and Figure AII-10). Meanwhile the Tertiary class was split two different ways, by land use (Figure AII-9) and by slope (Figure AII-10). Splitting both Quaternary and Tertiary by land use only slightly improved the predictive power of the optimization over geology alone (Figure AII-11). Splitting Tertiary by slope instead performed similarly to splitting it by land use (Figure AII-11). The moderate slope Tertiary category exhibited a very large spread in sediment coefficient results, from close to zero to over 5000 metric tons/square km, suggesting unexplained variation was present. To try to capture this variation, the moderate slope Tertiary category was further split by land use (Figure AII-12), resulting in 10 optimization parameters (Table AII-3). Surprisingly, splitting the moderate slope Tertiary category by land use results in larger ranges in sediment coefficients. But the ten parameter optimization does show a slight improvement in performance over the eight parameter optimization (Figure AII-13). Overall, increasing classification complexity seems to be at the point of diminishing returns.

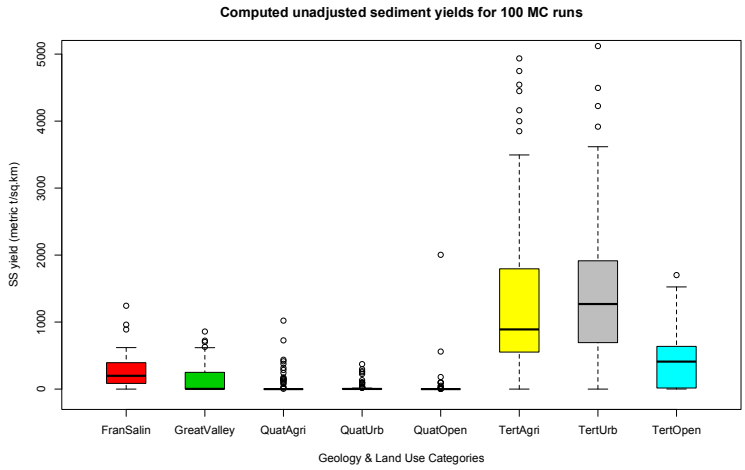


**Figure AII-9. Optimization results for eight categories (Geology plus land use).**

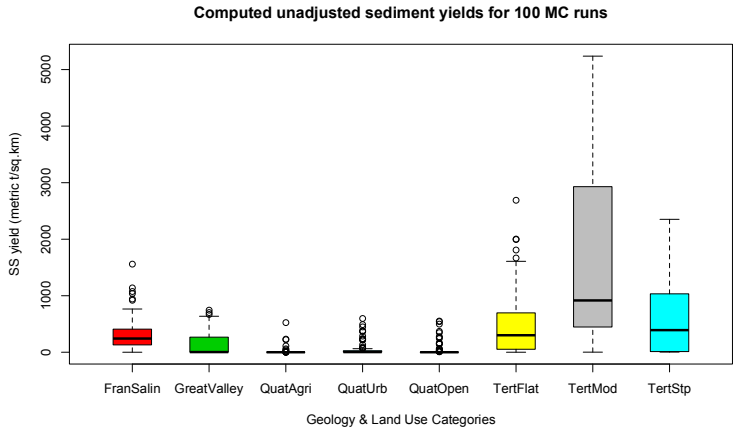


**Figure AII-10. Optimization results for eight categories (Geology plus land use and slope).**

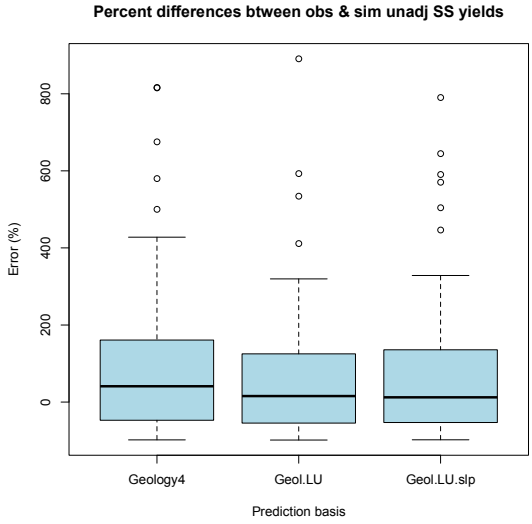


**Figure AII-11. Comparison of performance across optimizations using 100 iterations.**

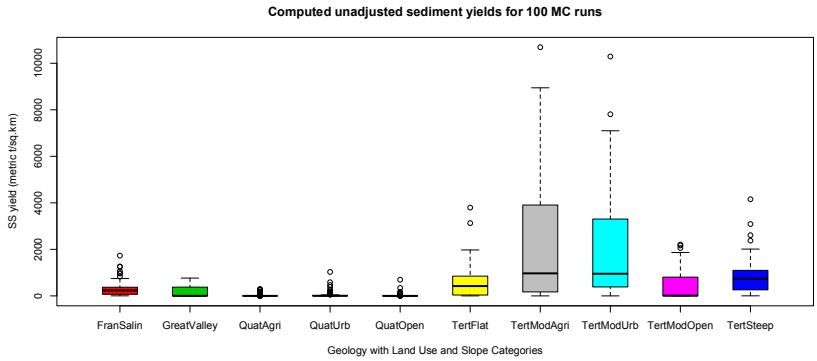


**Figure AII-12. Optimization results for ten categories (Geology plus land use and slope) based on unadjusted data and the initial proof of concept analysis using 100 iterations.**

**Table AII-3. Sediment coefficients (metric t/km$^2$) from 10-parameter optimization based on unadjusted data and the initial proof of concept analysis using 100 iterations.**

| Geology | Franciscan-Salinian | Great Valley | Quaternary | | | Tertiary | | | | |
|---|---|---|---|---|---|---|---|---|---|---|
| Slope | - | - | - | - | - | <10% | 10-30% | | | >30% |
| Land use | - | - | Ag | Urb | Open | - | Ag | Urb | Open | - |
| Mean | 292 | 161 | 19.4 | 42.7 | 17.3 | 584 | 2150 | 1970 | 424 | 801 |
| Median | 233 | 2.31 | 0.234 | 2.94 | 0.317 | 422 | 967 | 951 | 10.8 | 736 |

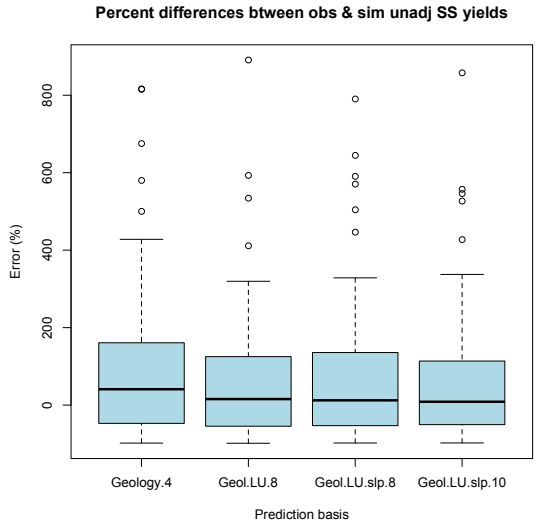


**Figure AII-13. Comparison of performance across optimizations using 100 iterations.**

# APPENDIX 7. COPPER MODULE

## A7.1 Copper pollutant profile

The modeling approach for each pollutant may be specific to the pollutant given specific sources, dispersal throughout the landscape, and transport characteristics. However, the Copper Model functions as a good introductory model for incorporating pollutants into the RWSM because, given the classical source build-up wash-off process, we may apply a Simple Method that estimates loads from the volume of stormwater runoff in a watershed multiplied by concentrations. A review of sources and use characteristics of copper in the urban landscape was completed to provide supporting evidence for the underlying geographic framework for a copper model (Lent and McKee 2011).

Copper appears to have a relatively even urban distribution and about 50% is transported in dissolved phase. Copper was used in building construction (49%), electric and electronic products (20%), transportation equipment (12%), consumer and general products (10%), and industrial machinery and equipment (9%). Most urban copper applications do not leach to urban stormwater (e.g. brass, electrical, and plumbing applications), however open applications such as roofing, external paints, biocides, and brake pads are known direct sources to stormwater.

The estimated order of importance for the Bay area is marine antifouling coating >> vehicle brake pads ≈copper use in pesticides ≈ atmospheric deposition ≈ soil erosion > architectural copper ≈ copper algaecides applied to surface water ≈ industrial copper use ≈ copper in domestic water discharged to storm drains > vehicle fluids leaks and dumping (Lent and McKee 2011). In the Bay Area, brakepad sources are estimated to comprise a median of 23% of the total supply to the Bay; in highly urbanized watersheds (e.g. Colma Creek, South San Francisco) the contribution was estimated at >50%. Copper is also found in high concentrations at some of our polluted sites that are undergoing regulatory cleanup, in particular, areas associated with manufacture of metals (copper ore smelter & pyrite roaster), military, and metals recycling. Marinas, marine repair yards, marine and general scrap metal recyclers, and military land uses may represent special source area categories for consideration in the spreadsheet model, however in most cases, these sources discharge directly to the Bay and not through urban drainage systems and our small tributaries. Therefore, as a starting point for the underlying geographic framework of a copper model, Lent and McKee (2011) proposed three land use categories: Industrial/commercial, other urban, and agricultural/open; evidence from Southern California suggests that industrial, recreational and open space sites are distinguishable from each other but that all other urban classes (high- and low-density residential, commercial, transportation) are indistinguishable.

## A7.2 Copper model module methods

### A7.2.a Copper module architecture

As described above, there is evidence that copper concentrations in urban runoff may be modeled by allocating varying concentrations to specific land use areas. This model structure is consistent with the current architecture of the hydrology model in which runoff coefficients are assigned to areas of land

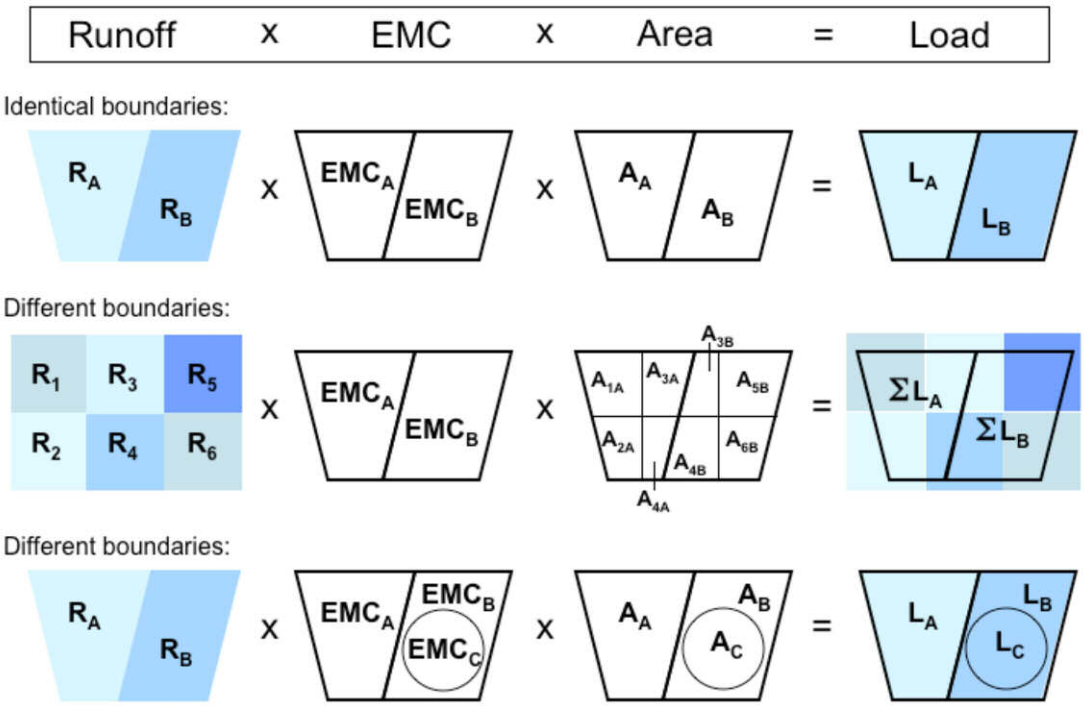


**Figure 6.3.1 Conceptual model of options for model architecture (after Lent and McKee 2011).**

use. Therefore the copper model architecture followed the first example of "identical boundaries" (Figure 6.3.1).

As such, copper loads were calculated by multiplying runoff volume by average concentration of pollutant in stormwater runoff for each distinct land area:

$V_j = RC_j * I * A_j$ Equation (1)
$L = \Sigma C_k * V_j$ Equation (2)

Where V = annual stormwater volume for unit of land *j*, RC = runoff coefficient for land unit *j*, I = average rainfall, A = Area of land unit *j*, L = pollutant load, and C = stormwater pollutant concentration for land use or pollutant source *k*. This model structure is a simple structure also used previously in Southern California (Ackerman and Schiff, 2003). Results for Equation (1) have already been developed in the RWSM hydrology model (see RWSM Year 1 (Lent and McKee 2011) and Year 2 (Lent et al., 2012) reports for further detail) with $V_j$ the key output.

## A7.2.b Review of the transportation land use layer for the copper model

Transportation is an important land use layer in the copper model in part because copper brakepads are estimated to account for 23% of the estimated copper load to the San Francisco Bay (Donigian and Bicknell, 2007), and also because the loading from pollutants widely dispersed in the environment that follow a buildup-wash-off process (like copper) are disproportionately influenced by the relatively higher runoff from more impervious landscapes (Tiefenthaler et al., 2008), and transportation is the most impervious land use category. As discussed in the Year 1 report (Lent and McKee, 2011), roads often present a particular challenge in modeling because roads may be lumped in with the land use that is surrounding them (e.g. residential areas) or they may be lines as opposed to polygons with area associated. Because of these challenges, a subgoal of this task was to review the characteristics of the ABAG 2005 land use layer (Table 6.3.2) and consider potential improvements to the Transportation class. Although developed here in relation to the copper model, this review and suggest in future improvements will likely support future models for other pollutants.

**Table 6.3.1. Transportation categories in the ABAG, 2005 database.**

| | |
|---|---|
| Military Airport | Unspecified Airport |
| Freeways, Highways, and Interchanges | Truck or Bus Maintenance Yard |
| Marina | Local Streets and Roads |
| Commercial Port-Other Terminal and Ship Repair | Commercial Port Passenger Terminal |
| Ferry Terminal | Park and Ride Lots |
| Marine Transportation Facilities | Parking Garages and Lots |
| Commercial Port Storage and Warehousing | Rail Yards |
| Tow Boat (Tug) Facility | Commercial Port Oil and Liquid Bulk Terminal |
| Commercial Port Container Terminal | Commercial Airport Runway |
| Military Port | Commercial Airport-Other |
| Road Transportation Facilities | Rail Passenger Stations |
| Inspection and Weigh Stations | City, County, or Utility Corporation Yard |
| Unspecified Transportation Communication and Utilities | Commercial Airport Passenger Terminal |
| Rail Transportation Facilities | Commercial Airport Airline Maintenance |
| Private Airfield | Commercial Airport Utilities |
| General Aviation (public) Airfield | Commercial Airport Air Cargo Facility |

Overall, the ABAG 2005 transportation land use layer appears pretty good. All of the transportation (and other land use classes) areas are polygons in the shapefile, thus every road for example has a width. The roads do have different widths depending on the size of the road and appear to be relatively accurate. Additionally, as opposed to the ABAG 2000 land use layer upon which version 1 of the Hydrology Model was based (Lent and McKee, 2011; Lent et al 2012), the transportation land use classes in ABAG 2005 are mapped at a pretty consistent scale across the entire region. However, there are some problems.

First, in areas where a polygon feature class was created from a raster, there are some remaining vestiges. In Figure 6.3.2 below, transportation polygons are extracted from all other land uses, and the

location is where Hwy 13 and 580 merge. Obviously raster vestiges are exuding beyond where the highways actually are. The result in the model would be that transportation areas are inflated. Second, there are some areas in the ABAG 2005 land use layer that are just not very resolved and the transportation is lumped in with the surrounding land use. We see an example of this in the area northwest of Codornices Ck (Figure 6.3.3, the bottom watershed outlined in red), as well as in the western portion of Codornices Ck itself, which flows through an area of Albany where the land use units are quite large despite that area being very residential. These areas are lacking in the transportation category altogether.

**Figure 6.3.2. Example of how raster vestiges may inaccurately inflate the transportation area.**

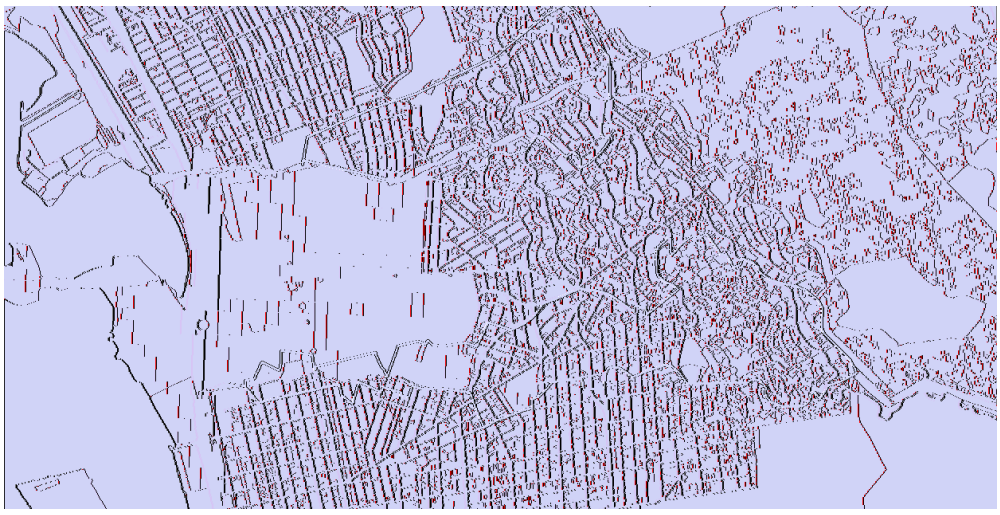

**Figure 6.3.3. Example of an area with lower resolution than the rest of the dataset.**

Finally, when zooming in on the roads with aerial imagery behind, it is clear that the roads include open space areas adjacent to the roads (Figure 6.3.4 below, roads outlined in yellow). This would affect the total area considered to be transportation, unduly biasing the area high. If transportation is allotted a concentration factor much larger than other urban areas yet is based on EMC data which is only representative of road runoff and not road+adjacent open area runoff, the total estimated load would be oversimulated. Alternatively, in some cases the roadside buffer areas may have similar pollutant concentrations as the road itself due to its proximity to the road, however the runoff coefficient used in the hydrology model would be high and consequently bias the load high.

**Figure 6.3.4. Transportation areas outlined in yellow; areas in adjacent open space.**

We thought of no easy upgrades that could be made to the transportation layer under this task budget. In the future, and particularly if we want to model any pollutants highly linked to roads or transportation, we could improve the roads layer by importing roads layers attained from the counties. Such datasets are generally available on county websites. However, these are mostly in line form and we would have to apply buffer-widths. It would also therefore be important that the county lines are attributed by type so that an appropriate buffer width may be applied. Further, if we improve the roads layer by removing vestiges, we would need to replace the open spaces with something (e.g. local land use data). All-told, this could be an intensive process. Presumably these defects would be improved upon in the next release of the ABAG land use dataset. Therefore, we queried ABAG as to when their next land use layer was expected to be completed and what improvements they were expecting to make over the 2005 dataset. The response from the GIS coordinator: “There are no plans for ABAG to

produce existing land use feature sets in the future. From now on the agency will gather land use information it needs for specific projects, but it is no longer going to produce regional feature sets for public consumption."

### A7.2.c Copper model inputs

The stormwater input concentration is defined by land use ($C_k$) is the key input parameter for the copper model. An input concentration must be defined for each land use category in the regional land use dataset. For simplification, the 100+ specific land use categories are generalized into the more commonly reported land use categories (Transportation, Industrial, Commercial, Residential, Open, Agriculture; see Appendix 7 Attachment 1). The general reclassification matched how the Hydrology Model was reclassified except that more specific subcategories of the Hydrology Model (Lent and McKee, 2011; Lent et al., 2012) were lumped (e.g. the "Open-Infiltrative" and "Open-Compacted" subcategories of the Hydrology Model are both lumped together under "Open" in the Copper Model). This was done because the input concentration data did not support any greater splitting of the land use data. It is noted that *how* the specific land use categories get lumped can be very important (depending on the pollutant) (Stenstrom, M, pers. comm.). For some models, for example, some land uses may have similar enough EMCs that splitting is not warranted (i.e. there is no statistical difference). In this test case process, we do not exclude splitting due to insignificant statistical differences; rather we explore the possibilities of splitting and lumping, and compare the differences.

The copper pollutant profile (Lent and McKee 2011) included land use specific concentration data for these land use categories and additionally the more general land use category, "urban". Each land use category includes between 11 and 28 data points of central tendency (average concentration, EMC, FWMC, or other), while the general urban category includes 31 data points. This database includes data from local gray literature as well as peer reviewed studies from Southern California and the world. Per the recommendation of Terry Cooke, as a default we first developed the input parameters with local source data which is likely more representative of our climatic and geographic conditions. Where source data for a particular land use was missing from the local data, data from Southern California was used to supplement. As last resort, the greater world literature was consulted.

The table of the central tendency data and references from which input concentrations were initially developed are compiled in Appendix 7 Attachment 2, and a summary of that data is presented in Table 6.3.2. Local land-use specific data is available for all of the generalized land use classes excluding agriculture, though few studies comprise the local dataset. Studies from the Arid West are primarily from Southern California and generally include much higher maximum central tendency data points per land use category, though when coupled with the local data the median concentrations are not much higher than the median of the local data alone, except in the transportation category. When adding in data from the greater world literature, median concentrations in each of the land use categories decreases except in the commercial class. Agricultural land uses have central tendency data with greater variability within and between studies, and this fits with our conceptual model that copper concentrations are more dependent on total sediment load (erosivity of the landscape) as opposed to particle concentrations.

We qualitatively assessed whether the rank order of concentrations between the different land uses was consistent between references that reported concentrations for multiple land uses (e.g. were open space land use concentrations always lower than urban land uses?). We found that the pattern was not without anomalies, however, concentrations generally ranked in the following order:

Industrial ≈ Transportation > Commercial ≥ Residential > Open

Agricultural concentrations were so inconsistently ranked that the land use category could not be inserted into the pattern noted above.

**Table 6.3.2. A comparison of copper concentrations (µ/l) in relation to land use for different geographic regions.**

| Local | | | | | | |
|---|---|---|---|---|---|---|
| Summary of local data points | | | | | | |
| | Agriculture | Commercial | Industrial | Open | Residential | Transportation |
| Minimum | - | 28 | 44 | 3 | 31 | 31 |
| Median | - | 31 | 49 | 10 | 33 | 45 |
| Maximum | - | 51 | 53 | 11 | 51 | 59 |
| n | 0 | 3 | 3 | 4 | 3 | 2 |

| Local + Arid West | | | | | | |
|---|---|---|---|---|---|---|
| Summary of local and Arid West data points | | | | | | |
| | Agriculture | Commercial | Industrial | Open | Residential | Transportation |
| Minimum | 33 | 23 | 30 | 3 | 16 | 9 |
| Median | 64 | 35 | 51 | 9 | 32 | 29 |
| Maximum | 96 | 72 | 72 | 55 | 100 | 59 |
| n | 2 | 6 | 6 | 7 | 8 | 8 |

| Local + Arid West + World | | | | | | |
|---|---|---|---|---|---|---|
| Summary of all data points | | | | | | |
| | Agriculture | Commercial | Industrial | Open | Residential | Transportation |
| Minimum | 1 | 17 | 14 | 0 | 7 | 0 |
| Median | 4 | 32 | 30 | 5 | 18 | 17 |
| Maximum | 96 | 87 | 108 | 55 | 100 | 135 |
| n | 12 | 11 | 21 | 15 | 22 | 28 |

*Weaknesses of the input concentration data:*

Although copper was chosen as a test case model specifically because of the wealth of available copper data to aid in developing initial input concentrations as well as in the calibration process, two notable weaknesses exist in the input concentration dataset. Central tendency of urban run-off data is described using a variety of methods including arithmetic mean, geometric mean or median concentration, EMC, or FWMC from watersheds in the specific land use. The single data points in our resulting database in some cases represent one watershed studied, in other cases many watersheds within the land use, and were included regardless of the statistical methods used to describe central tendency. Further, some of these central tendencies may even be back-calculated numbers from sampling in mixed-use watersheds. From these inconsistent data statistic types we selected the median in each land use category as the starting place for the initial input concentrations. Doing this could disproportionately weight some reference datasets over others. To reality check whether the medians appeared to produce believable

estimates for each land use category, we ensured that the resulting initial input concentrations followed similar patterns of ranking as reported in the references with multiple land use categories.

A second potential weakness involves possible time trends in the data (non-stationarity). McKee et al (unpublished) compiled an extensive literature review of copper concentrations reported in the literature from 1970 to 1995 (these are dates of actual sampling as opposed to dates of publication). Several metals in this review have strong declining trends. Copper has a slightly declining trend (Figure 6.3.5). Most of our local copper data was collected in the late 80's and early 90's. The BASMAA data collected at Zone 4 Line A includes copper results that are much higher in magnitude than the later-collected data under the RMP study (period 2007-2010) for the same location. It was difficult to calibrate the data using both the more recent and older local calibration data. To improve the calibration on the watersheds in which data was collected in the 2000's, these had to be split from the BASMAA calibration watersheds and the calibrated concentration factors decreased (discussed more below within this Cu model section). Non-stationarity may explain why this split seemed to improve the calibration process.

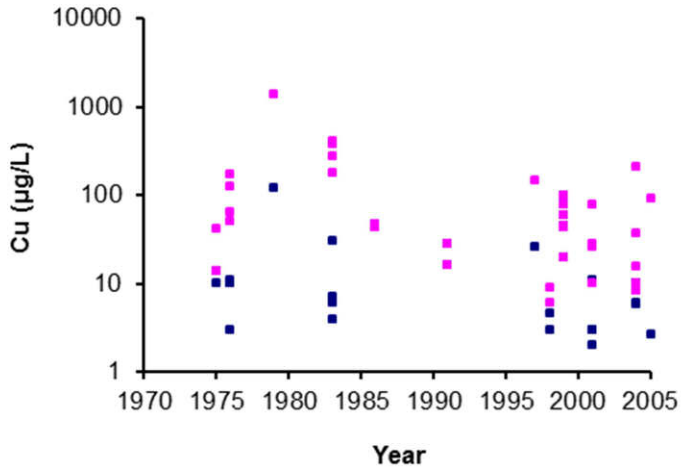


**Figure 6.3.5. Minimum (blue) and maximum (pink) copper concentrations reported in each individual study of urban stormwater between 1975 and 2005 (note the log scale). Please contact Lester McKee if you would like the list of literature behind this graphic.**

## A7.2.d Running the copper model

The Copper Model was developed in an ArcGIS platform using Python scripting language. Like the previously developed Hydrology Model (Lent and McKee 2011; Lent et al 2012), the Copper Model is a tool box function accessed through ArcCatalogue and can be utilized by beginning/intermediate GIS users. The Copper Model creates results based on an interface with the results of the Hydrology Model.

The Copper Model applies a lookup table of copper concentrations based on land use category to the intersected polygons created in the Hydrology Model. Each unique intersected polygon of the Hydrology Model has among other attributes a land use and an annual volume of runoff. Based on the land use, the Copper Model applies a copper concentration, and then multiplies that concentration by the annual volume of runoff for the polygon. The model then sums all of the resulting annual loads for each set of polygons within a watershed to compute the total watershed load.

To run a set of watersheds through the copper model, first the user must send those watersheds through the hydrology model. The copper model tool box (development described above) then provides a user-friendly interface (Figure 6.3.6) that calls upon the user to input the following files:

- Hydrology results geodatabase: this geodatabase is created after running the watershed shapefile through the hydrology model; the user must further select from that geodatabase the correct field that references the runoff volumes.
- Copper Lookup Table: this table (e.g. Figure 6.3.7) specifies an input concentration per land use; the user must further select from this lookup table the field that references the land use code associated with the land use dataset and then must also select which field bins the land uses into more generalized categories (the summary tables output from the model are based on these more generalized categories, though there is no limit to the number of categories and may include all of the more specific land uses); finally, the user must select which fields include the input concentrations. The user may input as many input concentration fields as desired in a single run and an output load will be created for each set of input concentrations.
- Tables.mdb database: this summary database is first created when running the watersheds through the hydrology model. Copper loads for each set of input concentrations are appended to these summary tables (Figure 6.3.8).

At this time, the Hg and PCB models are expected to have slightly different model architectures, but similar toolbox interface and style of input requirements.

### A7.2.e Copper model calibration

In total, there were 15 local watersheds with copper data distinct from the data that was used for developing the input concentrations (Figure 6.3.10). We had two different types of local calibration data for the copper model. Three watersheds (Zone 4 Line A, Guadalupe River (at San Jose Airport), and Ettie St Pump Station) have data collected in the last 10 years and include actual loads estimates. Both the Guadalupe River and Zone 4 Line A loads are based on multi-year RMP studies and the quality is considered high. The Ettie St. Pump Station load was based on a less complete dataset and the accuracy of the load estimate is considered lower. Calibration was performed by manually altering the input concentrations based on the comparison of the empirically estimated loads and the model-simulated loads.

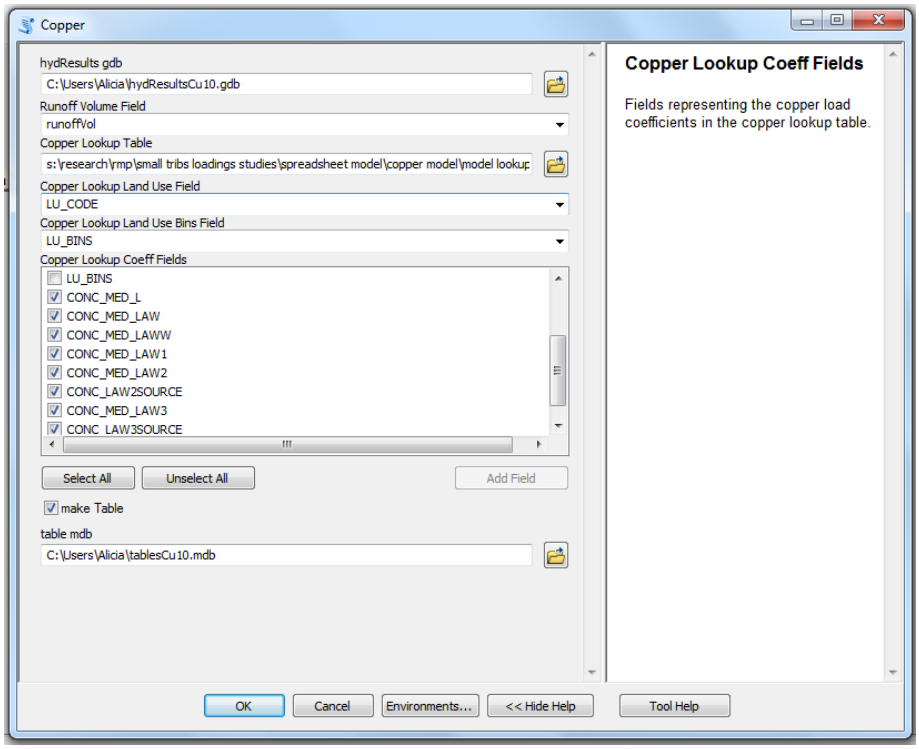


**Figure 6.3.6. The copper model user interface is a single page interface that guides the user through selecting the proper inputs into the model runs.**

| | A | B | C | D | E |
|---|---|---|---|---|---|
| | LU Code | LU Description | General Reclassification | LU Bin | Copper (ug/l) |
| 8 | 148 | Communication Facilities | Commercial - low | 5 | 23 |
| 9 | 126 | Unspecified Institutional Facilities | Commercial - low | 5 | 23 |
| 0 | 1262 | Religious Institution | Commercial - low | 5 | 23 |
| 1 | 751 | Strip Mines and Quarries | Industrial | 6 | 49 |
| 2 | 1473 | Water Storage-Covered | Industrial | 6 | 49 |
| 3 | 134 | Food Processing | Industrial | 6 | 49 |
| 4 | 147 | Municipal Water Supply Facilities | Industrial | 6 | 49 |
| 5 | 1461 | Wastewater Treatment Plant | Industrial | 6 | 49 |
| 6 | 1471 | Water Treatment Plant | Industrial | 6 | 49 |
| 7 | 752 | Earthworks not Associated with a Commercial Operation | Industrial | 6 | 49 |
| 8 | 1753 | Vacant Industrial | Industrial | 6 | 49 |
| 9 | 1453 | Electricity-Other | Industrial | 6 | 49 |
| 0 | 1452 | Electricity-Substation | Industrial | 6 | 49 |
| 1 | 131 | Heavy Industrial | Industrial | 6 | 49 |
| 2 | 1463 | Wastewater Storage | Industrial | 6 | 49 |
| 3 | 132 | Light industrial | Industrial | 6 | 49 |
| 4 | 1462 | Wastewater Pumping Station | Industrial | 6 | 49 |
| 5 | 13 | Unspecified Industrial | Industrial | 6 | 49 |
| 6 | 1451 | Electricity-Power Plant | Industrial | 6 | 49 |
| 7 | 1483 | Media Broadcast Tower and Communication Facilities | Industrial | 6 | 49 |
| 8 | 0 | <null> | Null | 1 | 0 |
| 9 | 75 | Strip Mines, Quarries, Gravel Pits | Open | 2 | 18 |
| 0 | 62 | Nonforested Wetlands | Open | 2 | 18 |
| 1 | 431 | Protected Mixed Forest | Open | 2 | 18 |
| 2 | 421 | Protected Evergreen Forest | Open | 2 | 18 |

**Figure 6.3.7. Example of the lookup table required by the copper model that associates the input concentrations per specific land use and also shows how land uses are aggregated into generalized categories.**

wsStats

| OBJECTID | watershed | totArea | totRunoffVol | cuCONC_AGSENSRUNLoadTot | avgWtSlope | avgWtPrecip | pctSlp |
|---|---|---|---|---|---|---|---|
| 1 | AlamedaCreek | 902,876,327 | 132,751,699 | 2,695,336 | 24.3 | 532 | |
| 2 | CalabazasCreekatWilcoxHS | 36,930,617 | 6,858,352 | 167,222 | 11.2 | 550 | |
| 3 | CastroValleyCk | 14,900,115 | 3,362,716 | 80,457 | 12.7 | 586 | |
| 4 | CerritoCreek | 1,921,113 | 608,244 | 14,915 | 14.5 | 629 | |
| 5 | CodornicesCk | 3,050,873 | 859,091 | 21,248 | 16.2 | 644 | |
| 6 | CoyoteCreekatMontagueExpswy | 323,149,840 | 53,771,817 | 1,163,020 | 18.2 | 530 | |
| 7 | EastSunnyvaleUPDATED | 14,783,657 | 2,701,885 | 69,667 | 1.1 | 422 | |
| 8 | EttieStreetPumpStation_A | 4,031,114 | 1,177,748 | 34,453 | 0.6 | 539 | |
| 9 | GuadalupeRiveratLostGatosCk | 207,341,175 | 38,731,110 | 947,316 | 12.1 | 555 | |
| 10 | GuadalupeRiveratSJAirport | 232,718,057 | 43,788,734 | 1,094,508 | 10.9 | 537 | |
| 11 | RheemCreekWatershed | 4,823,873 | 1,406,563 | 37,654 | 8.7 | 579 | |
| 12 | SanLorenzoCk | 109,734,785 | 19,467,271 | 380,513 | 33.1 | 658 | |
| 13 | WalnutCreek | 219,630,135 | 44,485,336 | 946,588 | 24.0 | 601 | |
| 14 | Zone4LineA | 4,172,155 | 1,027,414 | 31,138 | 0.8 | 486 | |
| 15 | Zone5LineD | 6,952,999 | 1,227,414 | 30,350 | 0.6 | 416 | |
| (New) | | | | | | | |

**Figure 6.3.8. Example of the table output after running the copper model. The column showing the copper loads for this particular model run is highlighted in light blue.**

The second type of calibration data includes EMC data collected for 12 local watersheds between the years 1987-1995 (BASMAA, 1996). Four of these watersheds were removed from the calibration because 5 or fewer events were sampled, and as previously discussed, “upwards of 11 storms might be a good starting point for field development of EMC data but upwards of 20 and typically 30 might be necessary to adequately increase confidence in the resulting EMC and coefficient of variation around the mean” (excerpted from RWSM Year 1 Progress Report (Lent and McKee, 2011)). All other watersheds (n=8) had between 10 and 32 composite samples. This dataset is considered high quality. Calibration of the model based on these watersheds was also performed by manually altering the input concentrations. Using this type of data, comparison was made between the EMCs for each watershed and an estimated FWMC calculated using the model simulated load and total discharge volume. Similar to the distribution of median EMCs from a large number of sites, at a particular site, EMCs over many storms generally have a log-normal distribution and so average conditions are best described the geometric mean rather than the arithmetic mean (Minton, 2005). Therefore, the geometric mean of the BASMAA dataset EMCs was selected as the metric for comparison against the back-calculated FWMC from the model-simulated load and discharge.

Calibration on the two different types of calibration watersheds was performed separately. We did this because when we tried to calibrate them altogether, we found that the EMC watersheds tended to drive the calibration since there were more of that type, and the loads watersheds were being relatively oversimulated. Of particular note, Zone 4 Line A was sampled both for EMCs with the BASMAA 1996 study as well as for loads with the RMP study. Although Zone 4 Line A was ultimately removed from the EMC calibration because only 4 events had been sampled there, interestingly the BASMAA EMC datapoints are much higher than FWMC concentration that was estimated from the total load and discharge reported by the RMP loading study (Gilbreath et al., 2012). In fact, the BASMAA EMCs are on par with the highest discrete grab sample concentrations collected through the RMP loading study. In the copper methods section above (subsection: *Weaknesses of the input concentration data*) we have already discussed a potential time trend issue that may be affecting the decreased concentrations from

the chronologically later RMP loadings study. Additionally, build-up and dilution may be affecting the concentrations between the two datasets. BASMAA data was comprised of 4 storm EMCs collected in January, February, March and December of 1990. WYs 1990 and 1991 were very dry years, only 53 and 68% of normal at the Oakland Museum rainfall gauge (Figure 6.3.9). Consequently, EMCs may have been higher due to less dilution effects. Copper, dispersed reasonably ubiquitously throughout the landscape, has a very short pathway to the storm drain system, and therefore a low-intensity rainfall may have the effect of higher concentrations whereas the greater volumes associated with a more intense rainfall and wetter season may result in dilution (Davis et al., 2000). The RMP loadings study was during WYs 2007-2010, which was also not during a particularly wet period (62, 87, 92, and 111% of normal, respectively), however wetter than the BASMAA collection period. Furthermore, the SFEI study period followed two wetter years (122 and 137% of normal), whereas the BASMAA study followed 3 drier years. Consequently, we found it useful and reasonable to separate the earlier period EMC calibration watersheds from the later period loads calibration watersheds.

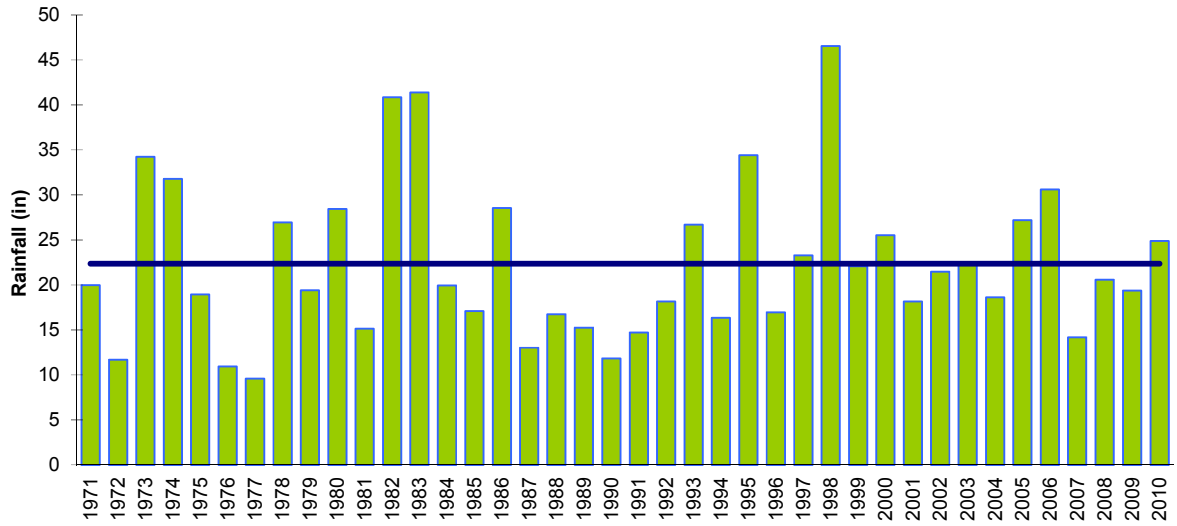


**Figure 6.3.9. Annual precipitation at the Oakland Museum rainfall gauge (WRCC, 2012) as an indicator of climatic variability in the Bay area.**

The calibration procedure involved comparing the difference between empirical estimates and simulated outputs to land use distributions in the watersheds and adjusting input concentrations per land use based on patterns of over- or under simulation for each land use. Calibration was performed manually. When altering the land use input concentrations, we aimed to remain consistent with the general ranking pattern noted in the reference datasets (Industrial ≈ Transportation > Commercial ≥ Residential > Open). Bias was calculated as the median percentage difference between the expected estimate and the actual results. We calibrated to bring the median and mean as close to zero as we could, while also minimizing the spread in the deviation between empirical and simulated estimates.

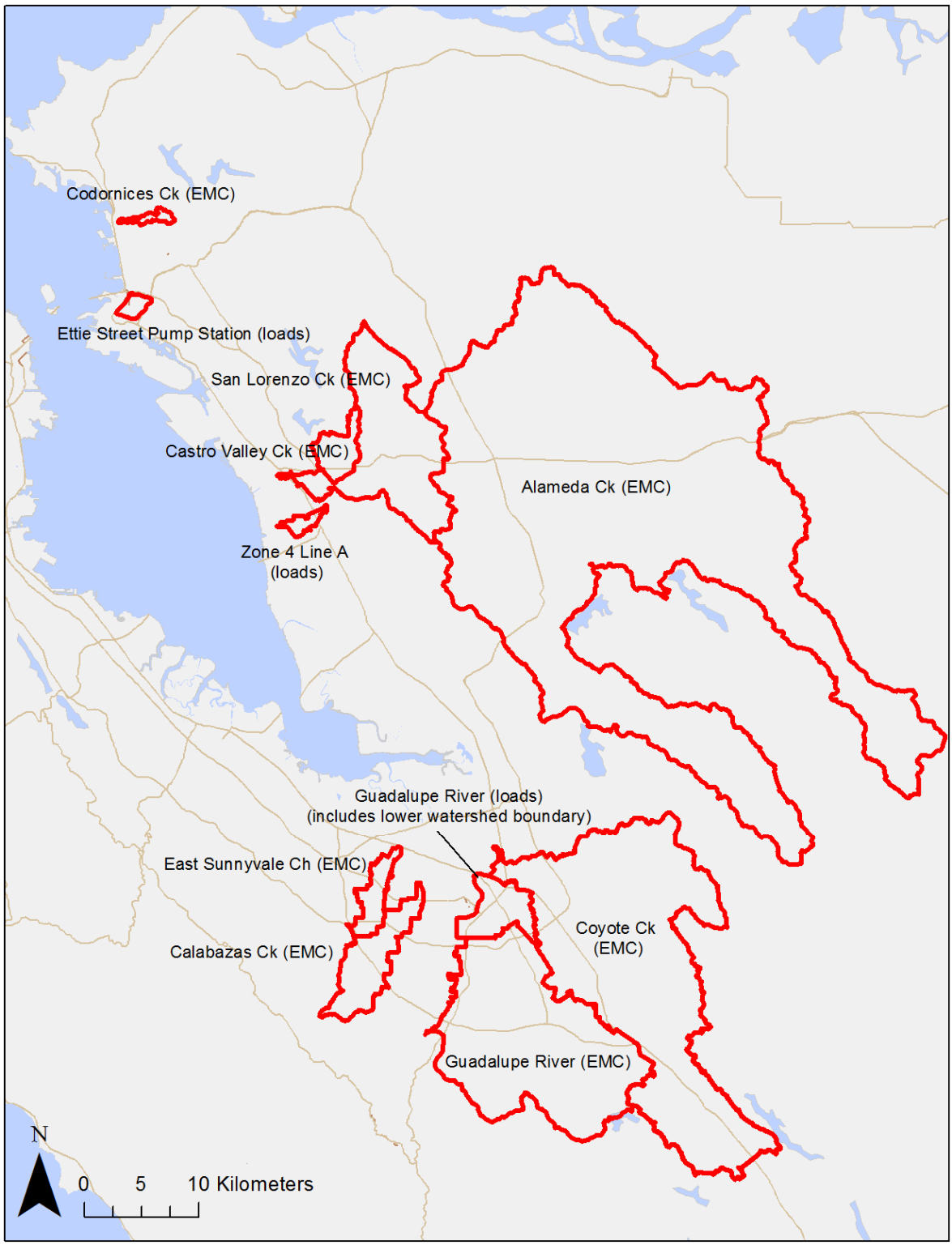


**Figure 6.3.10. The copper model calibration watersheds.**

# A7.3 Copper model module results

## A7.3.a Copper model module runs

The model was initially run on three sets of concentration parameters. The first set was comprised of the median concentrations in each land use category based only on local data. Because no data was available locally for agriculture, we used the "next best" source region to fill that gap, which we considered to be the data from the Arid West. The next set of concentration parameters included median concentrations in each land use category based on local data and data from the Arid West. And the final dataset included median concentrations from all available studies (local, Arid West, World). The initial input parameters are summarized in the upper portion of Table 6.3.3 below.

The best performing input parameters on the initial run for the EMC watersheds were the local only and the local + arid west median concentrations. Those parameter sets were more similar to one another, while the input concentrations based on all the data (local + arid west+ world) generally undersimulated the loads (see Table 6.3.4). Additionally, those watersheds with greater amounts of open space were undersimulated while those with more residential were oversimulated. We used the local and the local + arid west input parameters as a starting point and performed multiple iterative re-calibrations of the input concentrations. The loads calibration watersheds were more difficult to calibrate because there were only three watersheds in the set. Overall, the local and local+arid west input parameters oversimulated the loads. We largely decreased the input concentrations to bring the mean and median towards zero, but our confidence in the input concentrations is low given the few watersheds in this calibration dataset. The final calibrated input concentrations for the EMC watersheds and the loads watersheds are shown in the lower portion of Table 6.3.3 below.

**Table 6.3.3. Initially tested input concentrations and final calibrated concentrations.**

| Initial Input Concentrations | Agriculture | Commercial | Industrial | Open | Residential | Transportation |
|---|---|---|---|---|---|---|
| Local | 64 | 31 | 49 | 10 | 33 | 45 |
| Local + Arid West | 64 | 35 | 51 | 9 | 32 | 29 |
| Local + Arid West +World | 4 | 32 | 30 | 5 | 18 | 17 |
| **Calibrated Input Concentrations** | | | | | | |
| EMC Watersheds - Calibrated | 64 | 23 | 49 | 18 | 20 | 30 |
| Loads Watersheds - Calibrated | 64 | 20 | 20 | 16 | 20 | 20 |

Differences between the empirically estimated loads or flow weighted mean concentrations and the simulated results for each set of watersheds are shown below (Figures 6.3.11-12). Table 6.3.4 summarizes these differences. The loads watersheds were calibrated to within +/- 70%, with the simulation results of the bracketing watersheds nearly identically matching the simulation results of those watersheds in the hydrology model (Guadalupe River was not evaluated as a calibration

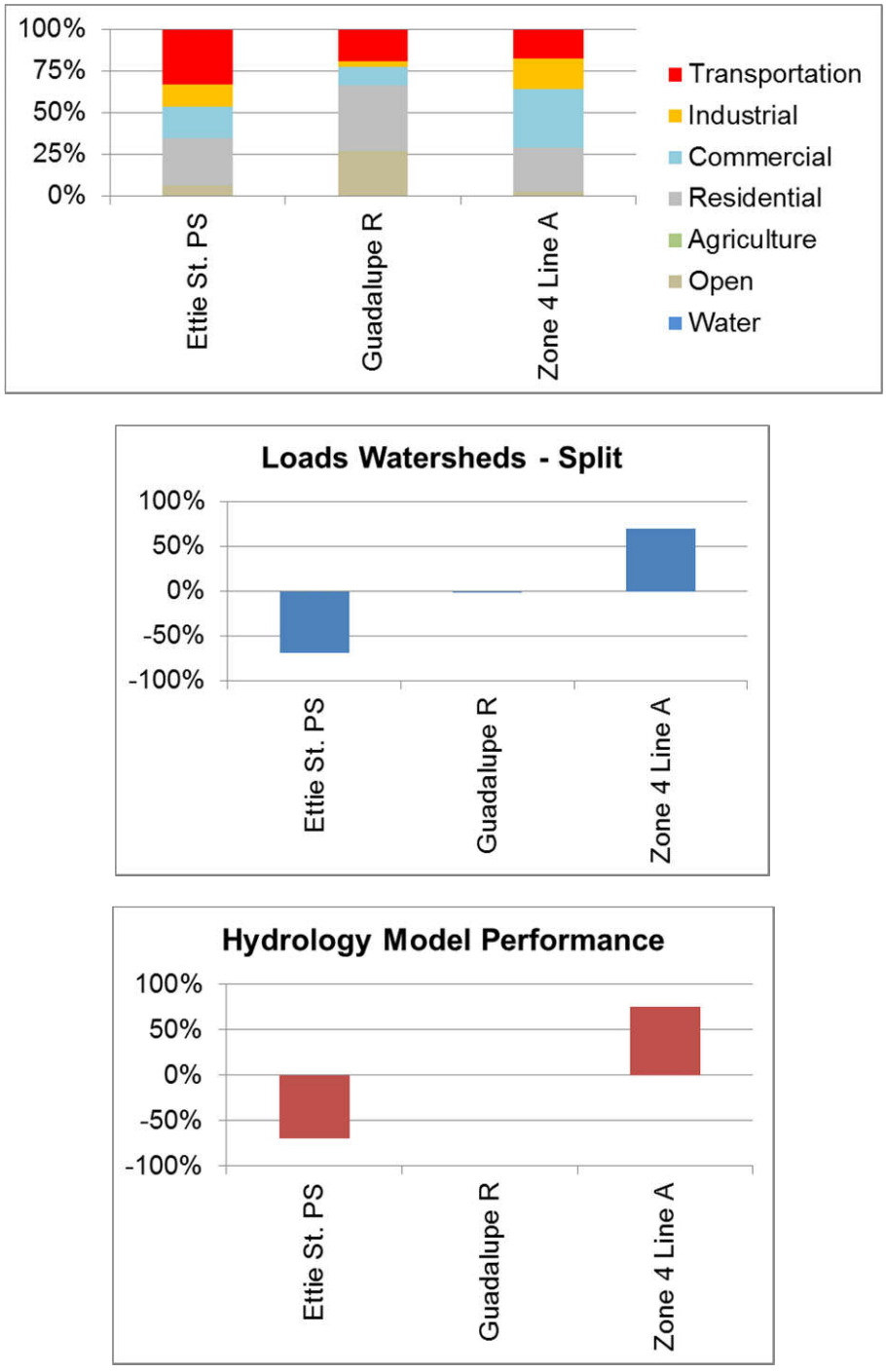


**Figure 6.3.11. Final calibration results of the loads watersheds and the corresponding land uses characteristics and hydrology model results. The hydrology model performance for two of the three loads watersheds (Guadalupe River hydrology model performance not evaluated in the hydrology modeling reports) nearly identically matches the copper model performance for those watersheds.**

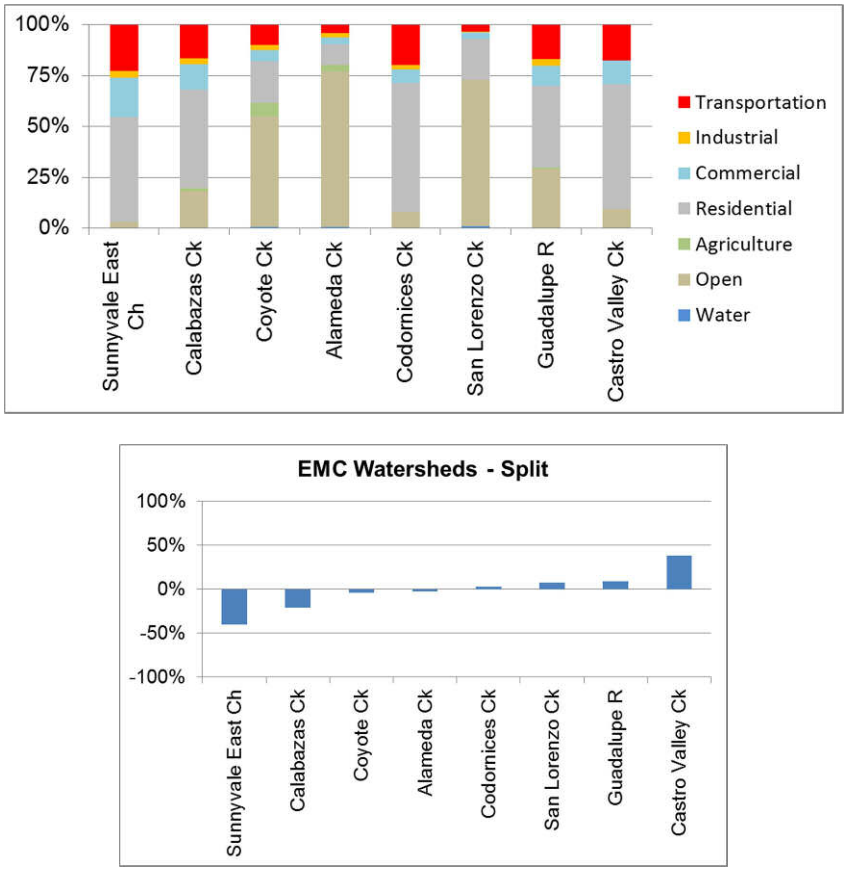


**Figure 6.3.12. Final calibration results of the EMC watersheds and corresponding land use characteristics.**

**Table 6.3.4. Statistical results of the calibration watersheds simulated loads or FWMCs versus empirically derived loads and EMCs. The white columns include the results on the uncalibrated input concentrations and the light grey columns include the results for the calibrated concentrations.**

| EMC Watersheds | | | | | | Loads Watersheds | | | | |
|---|---|---|---|---|---|---|---|---|---|---|
| | Local | Local + Arid West | Local + Arid West +World | EMC Watersheds Lumped | EMC Watersheds Split | Local | Local + Arid West | Local + Arid West +World | Loads Watersheds Lumped | Loads Watersheds Split |
| Mean | 18% | 1% | -38% | -1% | -1% | 86% | 68% | 15% | 0% | 0% |
| Median | 1% | -13% | -46% | -1% | 1% | 66% | 40% | -10% | -1% | 0% |
| Min | -18% | -29% | -57% | -41% | -40% | -39% | -48% | -66% | -69% | -69% |
| Max | 100% | 69% | 9% | 49% | 38% | 231% | 212% | 121% | 71% | 70% |

watershed in the hydrology model). This indicates that the runoff estimated in the hydrology model is likely driving the copper loading for these watersheds. The EMC watersheds were calibrated to +/- 40%.

### A7.3.b Copper model module sensitivity analysis

Agriculture was not represented in the local input concentration dataset and not well represented in Southern California. So we estimated the regional difference between using the Southern Californian median copper concentration (64 ug/l) and using the median when considering all of the data available in our database (4 ug/l). The difference in input concentrations had little impact on the calibration since very little agriculture is present in those watersheds, a primary factor for why we could not calibrate the agricultural input concentration. However, on a regional scale, the agricultural input concentration played an important role. Agriculture within the Region 2 boundary (inclusive of areas upstream of dams) accounts for 15% of the land area. By decreasing the input concentration from 64 to 4 ug/l, loads decreased 40% and 47% based on the EMC and loads input concentration sets, respectively. The corresponding regional annual loads when 4 ug/L is the agricultural input are 28,000,000 and 22,000,000 kg, respectively.

We tested on the calibration watersheds how splitting the data into the land uses chosen and allowing for different input concentrations per land use compared with forcing all of the urban land uses to be lumped. We found that lumping all of the urban land uses (residential, commercial, industrial, and transportation) and applying an input concentration of 20 and 27 µg/l for the loads and EMC watersheds, respectively, performed comparably well. The results were nearly identical for the loads watersheds because the split input concentrations were very similar to begin with, whereas the EMC watershed calibration benefited slightly by allowing industrial and transportation land uses to have higher input concentrations and residential land uses to have lower input concentrations. We propose two hypotheses for the comparable results: 1) transportation is the primary source of copper in the landscape and yet the land use layer is not at a fine enough resolution to tease apart all of the transportation land area from other urban areas (for example, commercial land use areas often include large parking lots), and/or 2) there is not enough variation of dominant land uses in the calibration watershed dataset to justify splitting rather than lumping the land uses.

We tested which input concentrations were playing the largest role and how deviating each land use input concentration by +/- 50% would affect the loads estimates for both our calibration watersheds and the region. The calibrated input concentrations based on the splitting option was used as the baseline from which to alter the concentrations up or down, and the EMC calibrated concentrations (split option) was used as the baseline in the regional run. Results are shown in Tables 6.3.5-7. For the EMC calibration watersheds, transportation, open and residential land uses have the largest effect on the mean because open and residential land uses comprise such a large percentage of the EMC calibration watersheds, and transportation has an impact because it combines a high input concentration with high runoff coefficient (RC). Open space land use has the largest effect on the median because it comprises a large percentage of the watersheds performing in the middle of the calibration. Likewise, transportation and residential land uses have the largest effect on the minimum and maximum differences because the watersheds that are the most under- and oversimulated (Sunnyvale East Channel and Castro Valley

Creek) both have a large proportion of residential area and the transportation again plays a significant role because of the high input concentrations combined with high RC.

For the loads calibration watersheds, transportation, commercial and industrial land use areas have the largest impact on the mean because they comprise a significant portion of the loads calibration watersheds and include higher RCs. Transportation, open, and residential land uses most affect the median because these are the largest land use categories in the watershed representing the median (Guadalupe River). For the loads watersheds, the maximum differences from the calibrated maximums are quite variable for the urban land uses categories, whereas the minimum differences are less affected. At first glance, this is a surprising outcome since the two watersheds that are the most under- and over-simulated loads watersheds have similar land uses. Results of the hydrology model are driving this outcome, and specifically it is the soil type in these watersheds that is causing the difference in their simulated discharge. While Zone 4 Line A is comprised of soil types B, C, and D, Ettie St. Pump Station does not have soils data available for it in the soils layer we are currently using in the model. Therefore the RCs applied to this watershed by the hydrology model are much lower than reality given how impervious we know the Ettie St. Pump Station watershed is (75%). Consequently, the +/- 50% changes to the copper concentrations by land use are having less of an impact on the loading because of the lower RCs. This finding suggests that when we revisit the hydrology model, we should strive to fill in the gaps in soils data and then re-calibrate, or at least remove watersheds with no soil data from the calibration dataset and again re-calibrate.

Regionally (modeled area of Region 2 excluding areas upstream of the dams), the land uses most affecting the loading estimate are agriculture, open space, and transportation (Table 6.3.7). Agriculture is highly affected by the +/- 50% exercise given how high the concentrations are relative to most of the other land uses combined with the fact that agriculture comprises 15% of the region. Open space is important because of how it dominates in area across the region. Whereas transportation only comprises 8% of the landscape, the +/- 50% has an impact because of how it combines a high input concentration with a high RC.

**Table 6.3.5. Differences between the empirically derived EMCs in the calibration watersheds versus the simulated FWMCs when altering each land use category by +/- 50%. The first number in each cell shows the statistic when decreasing the input concentration for that land use by 50%, and the second shows the statistic when increasing the concentration by 50%. Similar statistics are shown for the calibrated input concentrations for reference. All numbers are percentages.**

| EMC Watersheds | | | | | |
|---|---|---|---|---|---|
| | % in EMC dataset | Mean | Median | Min | Max |
| Calibrated Concentrations | | -1 | 1 | -40 | 38 |
| Agriculture | 3% | -3 - 1 | -2 - 3 | -40 - -40 | 38 - 38 |
| Commercial | 5% | -7 - 5 | -3 - 4 | -47 - -33 | 26 - 51 |
| Industrial | 2% | -5 - 3 | -4 - 5 | -43 - -37 | 38 - 39 |
| Open | 63% | -13 - 11 | -22 - 16 | -41 - -40 | 35 - 42 |
| Residential | 19% | -11 - 9 | -7 - 9 | -47 - -33 | 15 - 62 |
| Transportation | 8% | -17 - 15 | -13 - 11 | -53 - -28 | 8 - 69 |

**Table 6.3.6. Differences between the empirically derived loads estimates in the calibration watersheds versus the simulated loads when altering each land use category by +/- 50%. The first number in each cell shows the statistic when decreasing the input concentration for that land use by 50%, and the second shows the statistic when increasing the concentration by 50%. Similar statistics are shown for the calibrated input concentrations for reference. All numbers are percentages.**

| Loads Watersheds | | | | | |
|---|---|---|---|---|---|
| | % in loads dataset | Mean | Median | Min | Max |
| Calibrated Concentrations | | 0 | 0 | -69 | 70 |
| Agriculture | 1% | 0 - 1 | -1 - 1 | -69 - -69 | 70 - 70 |
| Commercial | 12% | -13 - 13 | -7 - 7 | -71 - -66 | 41 - 99 |
| Industrial | 4% | -9 - 10 | -4 - 3 | -71 - -66 | 48 - 92 |
| Open | 25% | -3 - 4 | -10 - 10 | -69 - -68 | 69 - 71 |
| Residential | 39% | -7 - 8 | -10 - 9 | -71 - -66 | 60 - 81 |
| Transportation | 19% | -16 - 17 | -19 - 18 | -76 - -61 | 48 - 93 |

**Table 6.3.7. The percentage change to the total regional loading estimate simulated by the copper model (excluding areas upstream of dams) when altering each land use category by +/- 50%.**

| Land Use | % of Region | % change in regional loading estimate |
|---|---|---|
| Agriculture | 15% | +/- 21 |
| Commercial | 6% | +/- 3 |
| Industrial | 3% | +/- 5 |
| Open | 46% | +/- 10 |
| Residential | 20% | +/- 4 |
| Transportation | 8% | +/- 7 |

## A7.3.c Regional/sub-regional loads estimates

Regional loads were estimated for three boundaries within Region 2 for watersheds which drain to the Bay. The first boundary was inclusive of the entire watershed area within Region 2 and draining to the Bay. In this boundary version, areas upstream of dams are treated the same as areas downstream of dams and do not currently take into account any changes to loads resulting from the obstruction of the dams to water and chemical transport. The second boundary was the same as the first except that it excluded areas upstream of dams. The third boundary included just watersheds within the Region 2 boundary that are within the jurisdiction of the four Phase I Permittees (San Mateo County, Santa Clara County, Alameda County, and Contra Costa County) and including the cities of Vallejo, Fairfield and Suisun, with areas upstream of the dams excluded. Land use characteristics for these three boundaries are shown in Tables 6.3.8-9, as well as the estimated loads. Generally, the loads estimated for the input concentrations from the EMC calibration were 20-25% higher than for the loads calibrated input parameters. Agriculture had a large impact in the full region boundaries, as seen by the dramatic decrease in loads when the agriculture input parameter was decreased to 4 ug/L (down from 64 ug/L).

Loads were also calculated for each of the Region 2 Bay Segments. Land use characteristics for each bay segment are shown in Table 6.3.10, and loads and yields are reported in Table 6.3.11. Loads and yields are highest in the San Pablo Bay Segment when the agricultural input concentration is set at 64 ug/L, whereas yields shift to being highest in the Central Bay Segment when the agricultural input concentration is decreased to 4 ug/L. The Central Bay Segment combines relatively high transportation and industrial areas along with moderately high rainfall for the region. While the Lower South Bay Segment mirrors the Central Bay in these land use characteristics, the average rainfall in the region is much lower, thereby decreasing the relative yields. Loads are highest in the San Pablo Bay Segment even when the agricultural input is decreased to 4 ug/L due to the fact that the total drainage area of this segment is larger than for any other segment, and the total annual runoff from the segment is nearly 2-7 times any other segment.

# A7.4 Copper model module discussion

## A7.4.a Copper model structure

The Copper Model is a pilot test case for incorporating pollutant modeling into the RWSM. Developing this test case helped us to better formulate the necessary inputs and ideal outputs for the pollutant models. The Copper Model architecture applies the simplest application of an EMC to

**Table 6.3.8. Land use characteristics for the three regional boundaries.**

| | Water | Open | Agriculture | Residential | Commercial | Industrial | Transportation |
|---|---|---|---|---|---|---|---|
| **Full Region 2 Boundary** | 2% | 55% | 12% | 16% | 5% | 2% | 7% |
| **Full Region 2 Boundary minus areas upstream of dams** | 2% | 46% | 15% | 20% | 6% | 3% | 8% |
| **4 Main Permittees + Fairfield, Suisun and Vallejo** | 1% | 47% | 2% | 26% | 9% | 4% | 12% |

**Table 6.3.9. Regional estimates of loads for the three regional boundaries using the EMC and Loads calibrated input concentrations (split option only).**

| **Full Region 2 Boundary** | Area ($km^2$) | Total Annual Runoff ($10^6 m^3$) | RWSM Load (kg/yr) | RWSM Load - Ag Decreased (kg/yr) |
|---|---|---|---|---|
| EMC Calibrated Concentrations (Split Option) | 8,804 | 1,802 | 55,000 | 35,000 |
| Loads Calibrated Concentrations (Split Option) | | | 47,000 | 27,000 |
| **Full Region 2 Boundary (minus areas upstream of dams)** | | | | |
| EMC Calibrated Concentrations (Split Option) | 6,901 | 1,491 | 49,000 | 29,000 |
| Loads Calibrated Concentrations (Split Option) | | | 41,000 | 22,000 |
| **4 Main Permittees + Fairfield, Suisun and Vallejo (minus areas upstream of dams)** | | | | |
| EMC Calibrated Concentrations (Split Option) | 4,044 | 764 | 20,000 | 19,000 |
| Loads Calibrated Concentrations (Split Option) | | | 15,000 | 14,000 |

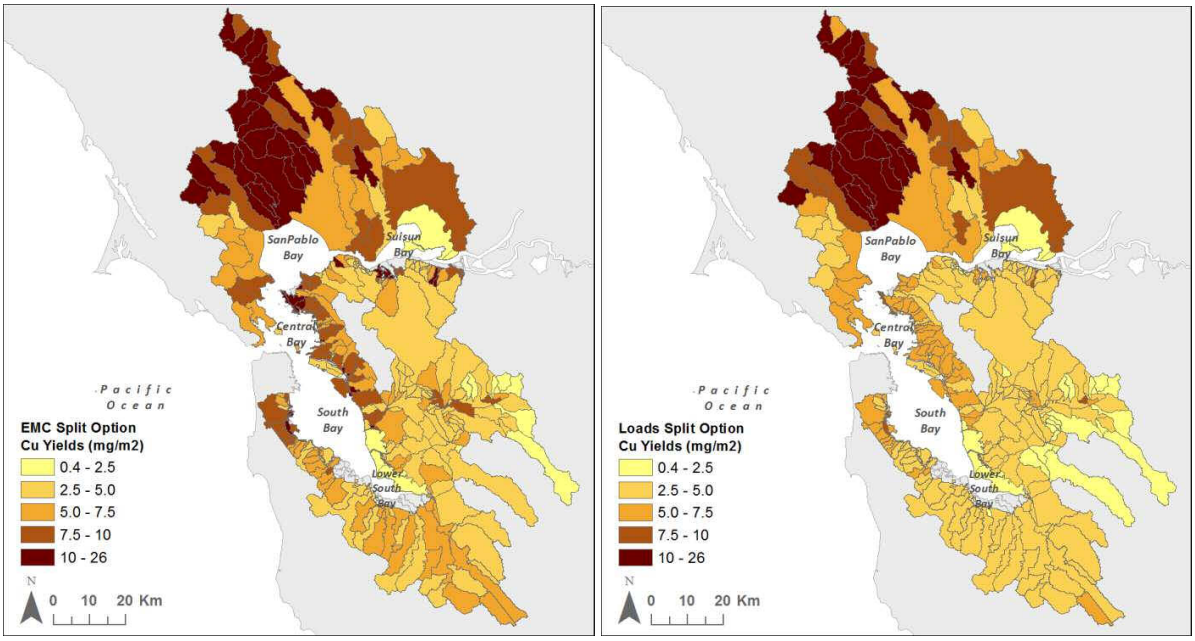


**Figure 6.3.13. Copper yields for watersheds downstream of dams for the EMC calibrated concentrations (split option) (left), and for the loads calibrated concentrations (split option) (right).**

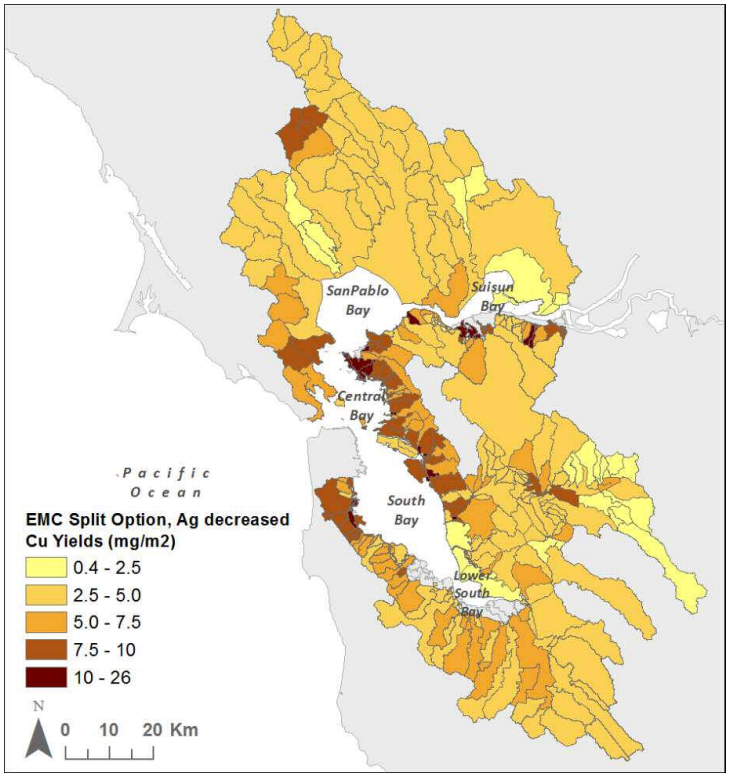


**Figure 6.3.14. . Copper yields for watersheds downstream of dams for the EMC calibrated concentrations (split option) using an agricultural input concentration of 4 ug/L (rather than 64 ug/L).**

**Table 6.3.10. Land use characteristics for Bay Segment areas (areas upstream of dams excluded).**

| Bay Segment | Area (km2) | Total Annual Runoff (10^6 m3) | Water | Open | Agriculture | Residential | Commercial | Industrial | Transportation |
|---|---|---|---|---|---|---|---|---|---|
| Suisun | 1,520 | 278 | 4% | 52% | 17% | 15% | 4% | 2% | 7% |
| San Pablo | 2,122 | 592 | 3% | 42% | 33% | 13% | 3% | 2% | 4% |
| Central | 255 | 78 | 1% | 32% | 0% | 37% | 10% | 4% | 16% |
| South | 1,686 | 308 | 1% | 55% | 2% | 21% | 8% | 3% | 11% |
| Lower South | 1,318 | 236 | 1% | 37% | 2% | 30% | 11% | 5% | 14% |

**Table 6.3.11. Loads and yields of copper for each Bay Segment (areas upstream of dams excluded) for four different input concentration scenarios.**

| | Loads (10^6 kg) | | | |
|---|---|---|---|---|
| Bay Segment | EMC Split Option | Loads Split Option | EMC Split, Ag decrease | Loads Split, Ag decrease |
| Suisun | 8.9 | 7.7 | 5.3 | 4.0 |
| San Pablo | 23.9 | 21.9 | 8.8 | 6.7 |
| Central | 2.0 | 1.5 | 2.0 | 1.5 |
| South | 7.6 | 5.8 | 7.3 | 5.5 |
| Lower South | 6.3 | 4.6 | 6.1 | 4.3 |
| | Yields (mg/m2) | | | |
| Suisun | 5.9 | 5.0 | 3.5 | 2.6 |
| San Pablo | 11.3 | 10.3 | 4.1 | 3.2 |
| Central | 7.8 | 5.8 | 7.8 | 5.8 |
| South | 4.5 | 3.4 | 4.3 | 3.3 |
| Lower South | 4.8 | 3.5 | 4.6 | 3.3 |

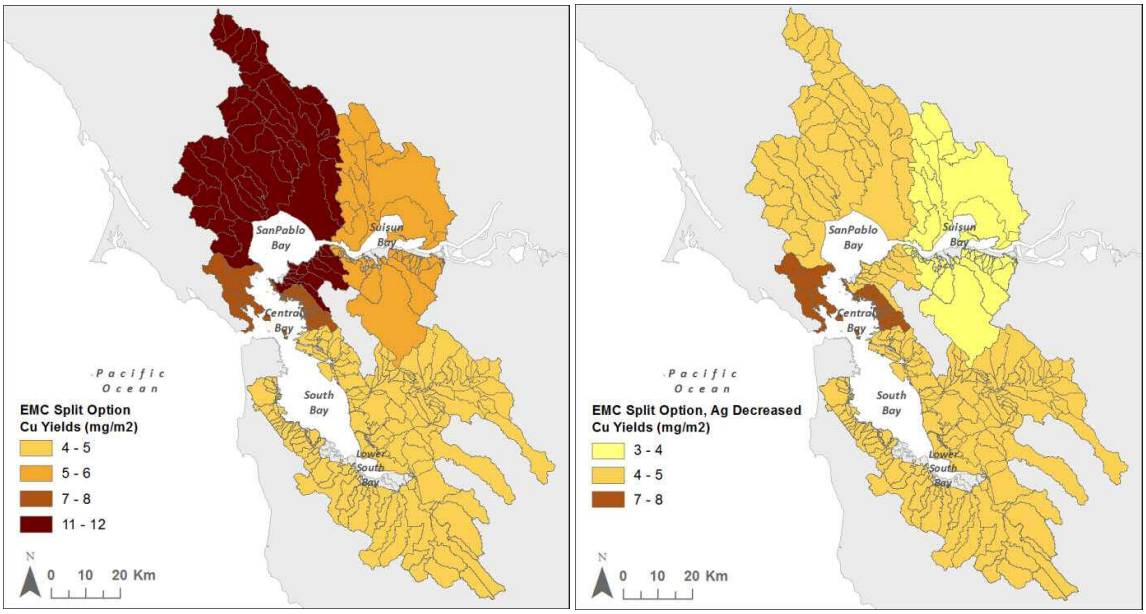


**Figure 6.3.15. Average copper yields by Bay Segment excluding areas upstream of dams for the EMC calibrated concentrations (split option) using an agricultural input concentration of 64 ug/L (left) and 4 ug/L (right).**

specific land uses which have already been parsed out in the Hydrology Model. In moving toward more complex applications such as integrating source area layers, we now understand that we will burn the source areas into the land use layer and add a specific concentration input for that source area in the model lookup table.

### A7.4.b Was copper EMC input data representative?

As described in the RWSM Year 1 Progress Report (Lent and McKee, 2011), copper land use and source areas could include older and newer industrial area, military land use, manufacture of steel or metals, metals recycling, marine repair and marine scrap yards, marinas, urban areas other than industrial, and nonurban areas. While EMC data exists for industrial areas, urban areas and nonurban areas, EMC data does not exist for manufacture of steel or metals, metals recycling, marine repair and marine scrap yards, and marinas. Therefore, a more complex model beyond application of concentration inputs on generalized land use categories was not possible at this time. However, had EMC data been available, the ABAG 2005 land use layer does include the following specific categories to which the EMCs could have been applied:

| Military-related land uses |
|---|
| Military Airport |
| Military Port |
| Military Residential |
| General Military Use |
| Military Open Areas |
| Closed Military Facilities |
| Unspecified Military |
| Military Hospital |
| **Marine/Marina land uses** |
| Marina |
| Marine Transportation Facilities |

Although agriculture is specified as a general land use category distinct from open spaces in the model, input data for agriculture was entirely lacking locally and few studies from Southern California existed. The data from the two Southern California studies did not represent very many agriculture watersheds: Ackerman and Schiff (2003) = 2 watersheds, Tiefenthaler et al. (2008) = 2 watersheds. Furthermore, our calibration watersheds included very little agricultural land use and therefore we were not able to calibrate the agriculture input concentration. Consequently, we ran a sensitivity analysis on the central and south bay region to understand how the agriculture input concentration would affect the regional load estimate. We found that the sub-regional total loading difference between when using the median of the local+Arid West data (64 ug/l) versus when using the median of all the data points in the database (4 ug/l) resulted in a relative difference of 7% and 9% based on the EMC and loads calibration watersheds, respectively.

### A7.4.c Was the copper model calibration adequate?

There were eight EMC watersheds to work with in the calibration. These exhibited transportation land uses ranging between 3 and 23%, and industrial between 0 and 3%, and commercial areas between 3 and 19%, all land uses possibly very important with regard to copper loading. Having watersheds in the calibration dataset that dominated one of these land uses would have been particularly useful to better justify splitting the urban input concentrations rather than lumping them. There were not enough loads calibration watersheds for a robust calibration process and under- and over-simulation by the hydrology model had a larger impact on the loads than any one of the input concentrations (based on the effects of altering the input concentrations by +/- 50%).

### A7.4.d Possible expectations for the other pollutants based on copper model outcomes

The test case copper model was calibrated to within +/- 70% for the loads stations and +/- 40 % for the EMC stations. However, we know that the model results for the loads stations were driven by the over- or undersimulation by the Hydrology Model. Given this, we feel that our best possible expectations for other pollutants will likely also be driven by the calibration of the hydrology model. However, given the unit run-off between watersheds on the industrialized Bay margin does not vary greatly, the determination of leverage should be more strongly based on larger variations in source area characteristics.

### A7.4.e Comparison to previous regional copper loads estimates

The regional load estimated using the EMC calibrated input concentrations inputs (assuming agriculture input concentration = 64 ug/L) compared well with previous regional copper loads estimates. Davis et al. (2000) used a simple model similar in nature to the RWSM and the best estimate was 66,000 kg/yr. This report's estimate (49,000 kg/yr) is lower than the Davis et al. best estimate, but within the estimated range (36,000 – 110,000 kg/year). The Davis et al. simple model did indeed use higher input concentration values for most of the land uses, which could be the primary explanation for the higher best load estimate. In 2007, Donigian et al. used HSPF modeling to estimate loads from the region for work associated with the Brake Pad Partnership, and estimated a total load of about 56,000 kg/yr. These other estimates corroborate the results of this report.

Tetra Tech developed loadings estimates for the Lower South Bay Segment based on scaling up the loads estimated for the Guadalupe River. Their estimate was 3.76 kg/yr of total copper (Tetra Tech, 1999). This estimate is 40% and 18% lower than the RWSM result for the EMC and Loads Split options, respectively (6.3 and 4.6 x10^6 kg/yr).

### A7.4.f Copper high leverage watersheds

High leverage watersheds (watersheds where there is a greater portion of the load coming from smaller areas; Stenstrom et al., 1984; Park and Stenstrom, 2007; Park et al., 2009) were evaluated for all watersheds for the EMC input concentrations (split option) both with the agricultural input as 64 ug/L and 4 ug/L. Although mapped below for areas only downstream of dams. No areas above dams were in the highest leverage watersheds under any scenario. For the entire Region 2 area and with the

agricultural input concentration at 64 ug/L, the top 10 highest leverage watersheds are listed in Table 6.3.12 and shown in Figure 6.3.16. These watersheds are concentrated in the San Pablo Bay Segment, and generally characterized by high average watershed slope, high percentages of Soil Type D, and high percentages of agriculture or, in a few cases, a combination of industrial and transportation land uses. When the agricultural input concentration is lowered to 4 ug/L, most of these watersheds have a sharp decrease in yield.

When lowering the agricultural input concentration to 4 ug/L, the top 10 highest leverage watersheds for the entire Region 2 also matched the top 10 highest leverage watersheds in the area of only the 4 Main Permittees + Vellejo, Fairfield and Suisun under either agricultural input scenario (Table 6.3.13, Figure 6.3.17). These watersheds are dispersed throughout the Bay Segments, excepting the Lower South Bay where annual precipitation is lower. These watersheds are generally characterized by small drainage area (all < 10 km2), high percentages of Soil Type D, no agriculture, and a high percentage of the combination of industrial and transportation land uses.

One problem noted in reviewing the highest leverage watersheds has to do with the classification of industrial area. Point San Pablo West and North watersheds (amongst the highest leverage watersheds for both agricultural scenarios), have a very high percentage of industrial land use. However, while Chevron owns much of this area, we can see in an aerial that much of the area is pervious and probably does not deserve the runoff coefficient applied to the industrial classification. Therefore, the high runoff coefficient and high input concentration applied to these watersheds are probably falsely elevating the yields from these watersheds. This problem should encourage us to evaluate other similar cases of this discrepancy and somehow account for it in the hydrology volume output.

## A7.5 Copper model conclusions/ recommendations

The Copper Model serves as a simple Test Case model for integration of pollutants modeling into the RWSM. In the process of creating this model, we developed much of the basic structure that will be applied to other pollutants of more interest but which are more complex in source and transport processes. Although copper represents one of our richest datasets, we nevertheless found it difficult to justify splitting the input concentrations between urban land uses because we were lacking calibration watersheds with varied dominant land uses. Furthermore, the agriculture land use proved problematic because some Southern California studies have reported high concentrations of copper in runoff from agriculture, while literature from outside the Southern California region generally reports much lower concentrations. We were unable to justify lowering the agriculture input concentration because we did not have any calibration watersheds with very much agricultural land use, though on a regional scale agriculture comprises 15% of the landscape and decreasing the agriculture input concentration to the median of all the concentrations for agriculture in our database (4ug/l) would have decreased total copper loads estimated by 40-47%. Through the sensitivity analysis to input concentrations by specific land use, we found that in the calibration watersheds transportation, open space and residential land uses most often played the largest roles. Open space and residential have a sizable impact because both land uses comprise a large percentage of the calibration watersheds as well as the region.

**Table 6.3.12. Watersheds characteristics for the 10 highest yielding watersheds in Region 2 downstream of dams, assuming an agricultural input concentration of 64 ug/L.**

| Watershed | Bay Segment | 4 Main Permittees or Fairfield/ Suisun? | Area (km2) | Runoff (m3x10^6)) | Avg Slope (%) | Avg Precip (mm) | Soil Type D (%) | Agriculture (%) | Industrial (%) | Transportation (%) | EMC (Split Option) Yield ($mg/m^2$) | EMC (Split Option, Ag 4 ug/L) Yield ($mg/m^2$) |
|---|---|---|---|---|---|---|---|---|---|---|---|---|
| ChamplinCreek | San Pablo | N | 19.0 | 8.0 | 22 | 788 | 70% | 89% | 4% | 0% | 26.2 | 3.2 |
| AdobeCreekLakeville | San Pablo | N | 36.5 | 16.1 | 16 | 889 | 85% | 77% | 0% | 1% | 26.1 | 2.5 |
| TolayCreek | San Pablo | N | 30.4 | 12.8 | 15 | 812 | 77% | 88% | 0% | 0% | 25.5 | 2.3 |
| LynchCreek | San Pablo | N | 42.4 | 18.1 | 14 | 908 | 91% | 67% | 0% | 1% | 24.1 | 2.8 |
| PointSanPabloPeninsulaWest | Central | Y | 3.7 | 1.6 | 30 | 610 | 88% | 0% | 64% | 9% | 22.4 | 22.4 |
| PointSanPabloPeninsulaNorth | San Pablo | Y | 0.8 | 0.3 | 35 | 631 | 14% | 0% | 63% | 9% | 21.6 | 21.6 |
| CC_unk17 | Suisun | Y | 3.1 | 1.2 | 27 | 525 | 93% | 0% | 70% | 2% | 20.1 | 20.1 |
| NathansonCreek | San Pablo | N | 36.5 | 14.6 | 29 | 1017 | 72% | 43% | 3% | 1% | 19.7 | 5.0 |
| StageGulch | San Pablo | N | 30.3 | 10.4 | 13 | 727 | 80% | 78% | 0% | 1% | 19.6 | 2.2 |
| RedwoodCreek | San Pablo | N | 28.2 | 10.0 | 30 | 1035 | 9% | 55% | 0% | 1% | 18.1 | 2.9 |

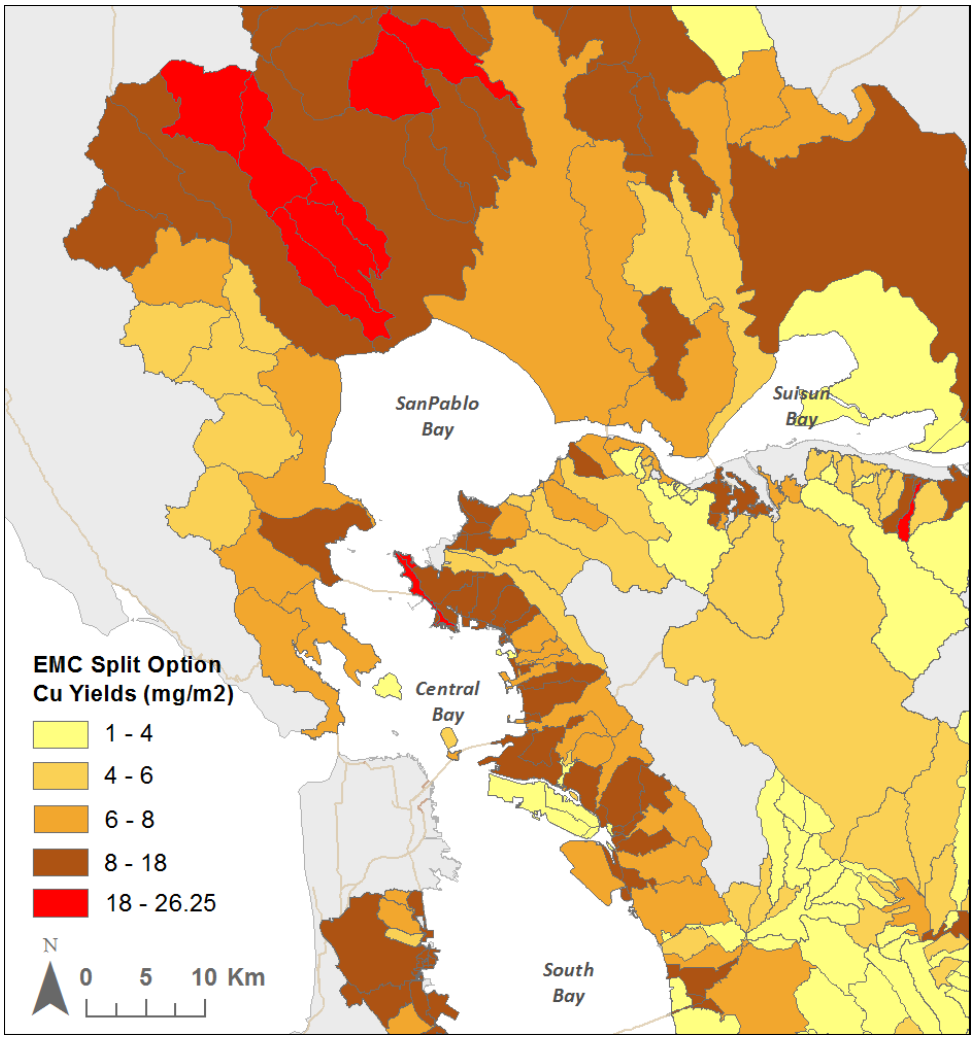


**Figure 6.3.16. Copper yields for watersheds (excluding areas upstream of dams) with the 10 highest yielding watersheds highlighted in red. This figure assumes an agricultural input concentration of 64 ug/L).**

**Table 6.3.13. Watersheds characteristics for the 10 highest yielding watersheds in Region 2 downstream of dams, assuming an agricultural input concentration of 4 ug/L. This list is identical to the 10 highest yielding watersheds in the area of the 4 Main Permittees + Vallejo, Fairfield and Suisun (agricultural input concentration is irrelevant).**

| Watershed | Bay Segment | 4 Main Permittees or Fairfield/ Suisun? | Area (km2) | Runoff (m3x10^6)) | Avg Slope (%) | Avg Precip (mm) | Soil Type D (%) | Agriculture (%) | Industrial (%) | Transportation (%) | EMC (Split Option) Yield ($mg/m^2$) | EMC (Split Option, Ag 4 ug/L) Yield ($mg/m^2$) |
|---|---|---|---|---|---|---|---|---|---|---|---|---|
| PointSanPabloPeninsulaWest | Central | Y | 3.7 | 1.6 | 30 | 610 | 88% | 0% | 64% | 9% | 22.4 | 22.4 |
| PointSanPabloPeninsulaNorth | San Pablo | Y | 0.8 | 0.3 | 35 | 631 | 14% | 0% | 63% | 9% | 21.6 | 21.6 |
| CC_unk17 | Suisun | Y | 3.1 | 1.2 | 27 | 525 | 93% | 0% | 70% | 2% | 20.1 | 20.1 |
| HermanSloughandCastroCreek | San Pablo | Y | 9.6 | 3.4 | 7 | 594 | 47% | 0% | 59% | 11% | 17.6 | 17.6 |
| PointIsabel | Central | Y | 0.3 | 0.1 | 3 | 557 | 0% | 0% | 69% | 10% | 17.3 | 17.3 |
| CC_unk27 | Suisun | Y | 0.2 | 0.0 | 2 | 467 | 99% | 0% | 80% | 0% | 15.4 | 15.4 |
| SanPablo | San Pablo | Y | 1.4 | 0.4 | 1 | 587 | 78% | 0% | 54% | 11% | 15.2 | 15.2 |
| AC_unk27 | South | Y | 0.9 | 0.3 | 1 | 464 | 83% | 0% | 66% | 14% | 15.1 | 15.1 |
| DavisPoint | San Pablo | Y | 4.9 | 1.4 | 16 | 545 | 56% | 0% | 41% | 7% | 13.2 | 13.2 |
| SMC_unk03 | South | Y | 0.6 | 0.2 | 9 | 530 | 100% | 0% | 10% | 11% | 12.6 | 12.6 |

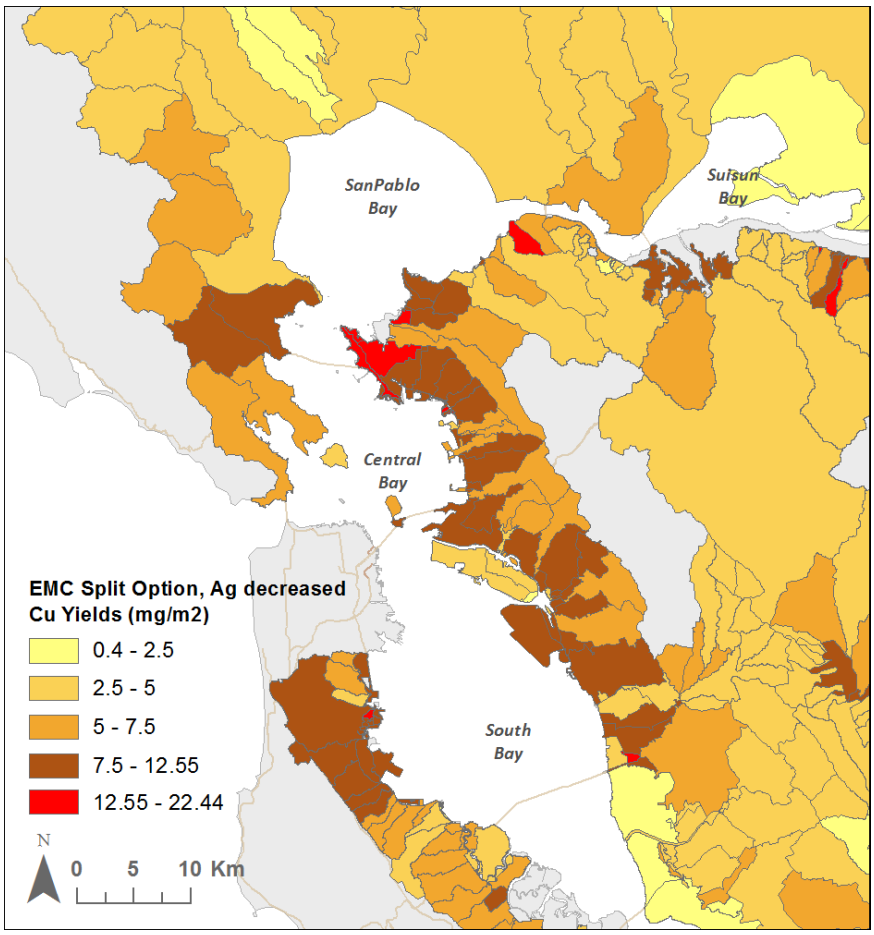


**Figure 6.3.17. Copper yields for watersheds (excluding areas upstream of dams) with the 10 highest yielding watersheds highlighted in red. This figure assumes an agricultural input concentration of 4 ug/L).**

Transportation plays a sizeable role because of how it combines a high input concentration with high a run-off coefficient. Across the region as a whole, residential has less of an impact but open space and transportation remain important for similar reasons as in the calibration watersheds. Additionally, altering the agriculture input by 50% has an impact because of how high the concentration is to begin with in combination with the fact that it represents 15% of the landscape. Based on the results, the copper loads can be modeled to within about +/-70% on a watershed basis, but regional scale loading estimates appear to be in reasonable agreement to other published estimates. Recommendations for moving forward include:

1) Quality check the hydrology model output to specifically check for situations in which watersheds have low imperviousness but high percentages of land use classes considered as highly impervious); we may even want to re-consider using impervious cover to underlie the hydrology model, or re-examine the general classification of the land uses.
2) Currently we are calibrating the model manually, however an automatic optimized calibration routine may improve the calibration process.
3) When considering the siting of future sampling watersheds intended to improve the RWSM model calibration, it would be helpful (to the greatest degree possible) to select watersheds that have a dominant land use different than the set of calibration watersheds already available.
4) If possible, we should consider the effects of time trends in stormwater concentrations and use this consideration to guide what data is used for input concentrations and what period of record is acceptable for calibration watersheds. It is also important to consider changes in land use in the calibration watersheds during the period of record of the data.
5) Should further Hydrology Model development be undertaken, a more comprehensive soils dataset might improve Hydrology Model calibration and all pollutants models based on the Hydrology Model.
6) An updated version of the PRISM rainfall datalayer was just released and should be used from this point forward.

## A7.6 References

Ackerman, D. and K. Schiff. 2003. Modeling stormwater mass emissions to the southern California Bight. *Journal of the American Society of Civil Engineers,* 129, 308-323.

BASMAA, 1996. San Francisco Bay Area Stormwater Runoff Monitoring Data Analysis 1988-1995. Prepared by Woodward Clyde Consultants. Final Report October 15, 1996. 112 pgs.

Davis, J.A., L. McKee, J. Leatherbarrow, and T. Daum. 2000. Contaminant Loads from Stormwater to Coastal Waters in the San Francisco Bay Region: Comparison to Other Pathways and Recommended Approach for Future Evaluation. San Francisco Estuary Institute, Richmond, CA.

Donigian, A.S., Bricknell, B.R. (Aqua Terra Consultants). 2007. Modeling the Contribution of Copper from Brake Pad Wear Debris to the San Francisco Bay. Submitted to Association of Bay Area Governments San Francisco Estuary Project and California Department of Transportation. 62 pp. Available online at: http://www.suscon.org/bpp/pdfs/WatershedModelingFinalReport100207.pdf

Gilbreath, A., Yee, D., McKee, L., 2012. Concentrations and loads of trace contaminants in a small urban tributary, San Francisco Bay, California. A Technical Report of the Sources Pathways and Loading Work Group of the Regional Monitoring Program for Water Quality: Contribution No. 650. San Francisco Estuary Institute, Richmond, California. 40pp. http://www.sfei.org/sites/default/files/Z4LA_Final_2012May15.pdf

Ha, S.J. and M.K. Stenstrom. 2008. Predictive modeling of storm-water runoff quantity and quality for a large urban watershed. *Journal of Environmental Engineering, 134(9), 703-711.*

Lent, M.A., Gilbreath, A.N. and McKee, L.J., 2012. Development of regional suspended sediment and pollutant load estimates for San Francisco Bay Area tributaries using the regional watershed spreadsheet model (RWSM): Year 2 progress report. A technical progress report prepared for the Regional Monitoring Program for Water Quality in San Francisco Bay (RMP), Small Tributaries Loading Strategy (STLS). Contribution No. 667. San Francisco Estuary Institute, Richmond, CA.

Lent, M.A. and McKee, L.J., 2011. Development of regional suspended sediment and pollutant load estimates for San Francisco Bay Area tributaries using the regional watershed spreadsheet model (RWSM): Year 1 progress report. A technical progress report prepared for the Regional Monitoring Program for Water Quality in San Francisco Bay (RMP), Small Tributaries Loading Strategy (STLS). Contribution No. 666. San Francisco Estuary Institute, Richmond, CA.

Minton, G. 2005. Stormwater Treatment, Second Edition. Sheridan Books, Inc., MI, USA.

Park, M.-H., Stenstrom, M.K., 2007. Utility of LANDSAT-derived land use data for estimating storm-water pollutant loads in an urbanizing area. Journal of Environmental Engineering, ASCE 133 (2), 203–210.

Park, M.-H., Swamikannu X., and Stenstrom, M.K., 2009. Accuracy and precision of the volume-concentration method for urban stormwater modeling. Water Research 43, 2773-86.

Stenstrom, M.K., Silverman, G.S., Bursztynsky, T.A., 1984. Oil and grease in urban stormwaters. Journal of the Environmental Water Research 34 (18), Engineering, ASCE 110 (1), 58–72.

Tetra Tech, I.; Associates, R.; Eoa, I., 2001. Copper Action Plan for the Lower South San Francisco Bay. Prepared for City of San Jose and Copper Development Association Inc. 93 pp. Available online at: http://www.sanjoseca.gov/esd/PDFs/Copper%20Action%20Plan%20Report%20-%20March%202001.pdf).

Tiefenthaler L.L., Stein, E.D., and Schiff, K.C. 2008. Watershed and land use-based sources of trace metals in urban stormwater. *Environmental Toxicology and Chemistry,* 27(2), 277-287.

# Appendix 7 Attachment 1: Land use reclassification for the copper module

| ABAG 2005 Land Use Code | ABAG 2005 Land Use Description | Copper Model General Reclassification |
|---|---|---|
| 54 | Bays and Estuaries | Water |
| 52 | Lakes | Water |
| 53 | Reservoirs | Water |
| 5 | Unspecified Water | Water |
| 563 | Industrial Ports and Piers | Water |
| 561 | Residential on Water (Arks) | Water |
| 56 | Water on USGS Base Maps but Land on Other Maps | Water |
| 1474 | Water Storage (Open) | Water |
| 51 | Streams and Canals | Water |
| 0 | <null> | Null |
| 75 | Strip Mines, Quarries, Gravel Pits | Open |
| 62 | Non-forested Wetlands | Open |
| 431 | Protected Mixed Forest | Open |
| 421 | Protected Evergreen Forest | Open |
| 63 | Salt Evaporation Ponds | Open |
| 321 | Protected Shrub and Brush Rangeland | Open |
| 311 | Protected Herbaceous Rangeland | Open |
| 72 | Beaches | Open |
| 31 | Herbaceous Rangeland | Open |
| 43 | Mixed Forest | Open |
| 33 | Mixed Rangeland | Open |
| 331 | Protected Mixed Rangeland | Open |
| 61 | Forested Wetlands | Open |
| 411 | Protected Deciduous Forest | Open |
| 55 | Sedimentation Pond | Open |
| 64 | Land on USGS Base Maps but Wetland on Other Maps | Open |
| 41 | Deciduous Forest | Open |
| 42 | Evergreen Forest | Open |
| 77 | Mixed Sparsely Vegetated Land | Open |
| 32 | Shrub and Brush Rangeland | Open |
| 73 | Sand Other Than Beaches | Open |
| 1253 | General Military Use | Open |
| 174 | Open Space-Slated for Redevelopment | Open |
| 1249 | State Psychiatric Facilities | Open |
| 1713 | Campground | Open |
| 1248 | State Mental Health and Developmentally Disabled Facil | Open |

| ABAG 2005 Land Use Code | ABAG 2005 Land Use Description | Copper Model General Reclassification |
|---|---|---|
| 1257 | Military Open Areas | Open |
| 1711 | Golf Course | Open |
| 1712 | Racetrack | Open |
| 74 | Bare Exposed Rock | Open |
| 172 | Cemetery | Open |
| 1751 | Vacant Residential | Open |
| 173 | Urban Park | Open |
| 119 | Common Facilities | Open |
| 17 | Unspecified Urban Open | Open |
| 761 | Sanitary Land Fills | Open |
| 122 | Intensive Outdoor Recreation | Open |
| 175 | Undeveloped Vacant Land | Open |
| 21 | Cropland and Pasture | Agriculture |
| 211 | Cropland | Agriculture |
| 23 | Confined Feeding | Agriculture |
| 2112 | Small Grains | Agriculture |
| 212 | Pasture | Agriculture |
| 22 | Orchards, Groves, Vineyards, Nurseries | Agriculture |
| 2111 | Row Crops | Agriculture |
| 222 | Vineyards and Kiwi Fruit | Agriculture |
| 24 | Farmsteads and Agricultural Buildings | Agriculture |
| 221 | Orchard or Groves | Agriculture |
| 1242 | Community Hospitals (not Designated Trauma Centers) | Commercial |
| 1268 | Convention Centers | Commercial |
| 1235 | #N/A | Commercial |
| 124 | Hospitals, Rehabilitation, Health, and State Prison Fa | Commercial |
| 129 | Hotels and Motels | Commercial |
| 1261 | Stadium (not associated with a college or university) | Commercial |
| 127 | Research Centers | Commercial |
| 128 | Office | Commercial |
| 1241 | Designated Trauma Centers | Commercial |
| 1263 | Fire Station | Commercial |
| 162 | Mixed Residential and Commercial-Single Building | Commercial |
| 121 | Retail and Wholesale, Post Offices | Commercial |
| 1264 | Police Station | Commercial |
| 135 | Warehousing | Commercial |
| 1246 | Out-Patient Surgery Centers | Commercial |
| 1259 | Closed Military Facilities | Commercial |
| 125 | Unspecified Military | Commercial |
| 1254 | Military Hospital | Commercial |

| ABAG 2005 Land Use Code | ABAG 2005 Land Use Description | Copper Model General Reclassification |
|---|---|---|
| 161 | Mixed Residential and Commercial-Separate Buildings | Commercial |
| 1244 | Medical Clinics | Commercial |
| 1232 | Colleges and Universities | Commercial |
| 223 | Greenhouses and Floriculture, Wholesale Nurseries | Commercial |
| 1233 | Stadiums | Commercial |
| 1267 | Local Government Jails and Rehabilitation Centers | Commercial |
| 171 | Extensive Recreation | Commercial |
| 1247 | State Prisons | Commercial |
| 1243 | Medical Long-Term Care Facilities | Commercial |
| 76 | Transitional Areas | Commercial |
| 1265 | City Halls, County, State, Federal Government Centers | Commercial |
| 123 | Education | Commercial |
| 1231 | Primary Schools | Commercial |
| 15 | Mixed Commercial and Industrial | Commercial |
| 762 | Other Transitional | Commercial |
| 1752 | Vacant Commercial | Commercial |
| 1269 | Museums, Libraries, Community Centers | Commercial |
| 12 | Unspecified Commercial and Services | Commercial |
| 148 | Communication Facilities | Commercial |
| 126 | Unspecified Institutional Facilities | Commercial |
| 1262 | Religious Institution | Commercial |
| 751 | Strip Mines and Quarries | Industrial |
| 1473 | Water Storage-Covered | Industrial |
| 134 | Food Processing | Industrial |
| 147 | Municipal Water Supply Facilities | Industrial |
| 1461 | Wastewater Treatment Plant | Industrial |
| 1471 | Water Treatment Plant | Industrial |
| 752 | Earthworks not Associated with a Commercial Operation | Industrial |
| 1753 | Vacant Industrial | Industrial |
| 1453 | Electricity-Other | Industrial |
| 1452 | Electricity-Substation | Industrial |
| 131 | Heavy Industrial | Industrial |
| 1463 | Wastewater Storage | Industrial |
| 132 | Light industrial | Industrial |
| 1462 | Wastewater Pumping Station | Industrial |
| 13 | Unspecified Industrial | Industrial |
| 1451 | Electricity-Power Plant | Industrial |
| 1483 | Media Broadcast Tower and Communication Facilities | Industrial |
| 16 | Mixed Residential | Residential |
| 118 | Group Quarters | Residential |

| ABAG 2005 Land Use Code | ABAG 2005 Land Use Description | Copper Model General Reclassification |
|---|---|---|
| 114 | Mobile Homes and Mobile Home Parks | Residential |
| 115 | Less than .126 acre lots | Residential |
| 11 | Unspecified Residential | Residential |
| 112 | .334-1 acres/unit | Residential |
| 1251 | Military Residential | Residential |
| 1234 | University Housing | Residential |
| 113 | .126-.333 acres/unit | Residential |
| 111 | 1-5 acres/unit | Residential |
| 1256 | Military Airport | Transportation |
| 1411 | Freeways, Highways, and Interchanges | Transportation |
| 1448 | Marina | Transportation |
| 1444 | Commercial Port-Other Terminal and Ship Repair | Transportation |
| 1447 | Ferry Terminal | Transportation |
| 144 | Marine Transportation Facilities | Transportation |
| 1445 | Commercial Port Storage and Warehousing | Transportation |
| 1446 | Tow Boat (Tug) Facility | Transportation |
| 1442 | Commercial Port Container Terminal | Transportation |
| 1258 | Military Port | Transportation |
| 141 | Road Transportation Facilities | Transportation |
| 1417 | Inspection and Weigh Stations | Transportation |
| 14 | Unspecified Transportation Communication and Utilities | Transportation |
| 142 | Rail Transportation Facilities | Transportation |
| 1438 | Private Airfield | Transportation |
| 1437 | General Aviation (public) Airfield | Transportation |
| 143 | Unspecified Airport | Transportation |
| 1414 | Truck or Bus Maintenance Yard | Transportation |
| 1418 | Local Streets and Roads | Transportation |
| 1441 | Commercial Port Passenger Terminal | Transportation |
| 1413 | Park and Ride Lots | Transportation |
| 1416 | Parking Garages and Lots | Transportation |
| 1422 | Rail Yards | Transportation |
| 1443 | Commercial Port Oil and Liquid Bulk Terminal | Transportation |
| 1434 | Commercial Airport Runway | Transportation |
| 1436 | Commercial Airport-Other | Transportation |
| 1421 | Rail Passenger Stations | Transportation |
| 1415 | City, County, or Utility Corporation Yard | Transportation |
| 1431 | Commercial Airport Passenger Terminal | Transportation |
| 1433 | Commercial Airport Airline Maintenance | Transportation |
| 1435 | Commercial Airport Utilities | Transportation |
| 1432 | Commercial Airport Air Cargo Facility | Transportation |

# Appendix 7 Attachment 2: Copper EMC database to support the copper module

| Land Use Category | Reference | Location | Local/Arid West/World | "Central tendency" |
|---|---|---|---|---|
| Agriculture | Ackerman & Schiff, 2003 | S. CA | Arid West | 96 |
| Agriculture | Lawson et al., 2001 | Chesapeake Bay | World | 3 |
| Agriculture | Lawson et al., 2001 | Chesapeake Bay | World | 3 |
| Agriculture | Miller et al., 2003 | Chesapeake Bay (Chesterville branch) | World | 1 |
| Agriculture | Miller et al., 2003 | Chesapeake Bay (Nanticoke River) | World | 1 |
| Agriculture | Robson and Neal, 1997 | UK | World | 3 |
| Agriculture | Robson and Neal, 1997 | UK | World | 3 |
| Agriculture | Robson and Neal, 1997 | UK | World | 4 |
| Agriculture | Robson and Neal, 1997 | UK | World | 4 |
| Agriculture | Robson and Neal, 1997 | UK | World | 7 |
| Agriculture | Robson and Neal, 1997 | UK | World | 5 |
| Agriculture | Stein et al, 2007 | S. CA | Arid West | 24 |
| Agriculture | Tiefenthaler et al, 2008 | S. CA | Arid West | 33 |
| Commercial | Ackerman & Schiff, 2003 | S. CA | Arid West | 23 |
| Commercial | ACWA 1997 | Oregon | World | 32 |
| Commercial | BCDC, 1991 | N. CA | Local | 28 |
| Commercial | Choe et al., 2002 | Korea | World | 60 |
| Commercial | Flint 2007 | Maryland | World | 87 |
| Commercial | Pitt et al., 2004 (NSQD) | USA | World | 17 |
| Commercial | Stein et al, 2007 | S. CA | Arid West | 24 |
| Commercial | Stenstrom and Strecker, 1993 | S. California | Arid West | 72 |
| Commercial | Tiefenthaler et al, 2008 | S. CA | Arid West | 38 |
| Commercial | US EPA, 1983 (NURP) | USA | World | 29 |
| Commercial | WCC, 1991 (reference in BASMAA 1996) | Alameda, CA | Local | 31 |
| Commercial | WCC, 1991 (reference in BASMAA 1996) | Santa Clara, CA | Local | 51 |
| Industrial | Ackerman & Schiff, 2003 | S. CA | Arid West | 30 |
| Industrial | ACWA 1997 | Oregon | World | 24 |
| Industrial | Asaf et al., 2004 | Israel | World | 25 |
| Industrial | Bannerman et al., 1993 | Wisconsin | World | 28 |
| Industrial | BCDC, 1991 | N. CA | Local | 49 |
| Industrial | Choe et al., 2002 | Korea | World | 44 |
| Industrial | Choe et al., 2002 | Korea | World | 45 |
| Industrial | Choe et al., 2002 | Korea | World | 20 |
| Industrial | City of Austin, 1995 | TX | World | 22 |

| Land Use Category | Reference | Location | Local/Arid West/World | "Central tendency" |
|---|---|---|---|---|
| Industrial | Pitt et al., 2004 (NSQD) | USA | World | 22 |
| Industrial | Robson and Neal, 1997 | UK | World | 14 |
| Industrial | Robson and Neal, 1997 | UK | World | 17 |
| Industrial | Robson and Neal, 1997 | UK | World | 14 |
| Industrial | Rule et al., 2006 | UK | World | 108 |
| Industrial | Stein et al, 2007 | S. CA | Arid West | 33 |
| Industrial | Stenstrom and Strecker, 1993 | S. California | Arid West | 72 |
| Industrial | Tiefenthaler et al, 2008 | S. CA | Arid West | 70 |
| Industrial | US EPA, 1983 (NURP) | USA | World | 27 |
| Industrial | WCC, 1991 (reference in BASMAA 1996) | Alameda, CA | Local | 44 |
| Industrial | WCC, 1991 (reference in BASMAA 1996) | Santa Clara, CA | Local | 53 |
| Industrial | Wilber and Hunter, 1977 | New Jersey | World | 44 |
| Industrial | Wilber and Hunter, 1977 | New Jersey | World | 31 |
| Open | Ackerman & Schiff, 2003 | S. CA | Arid West | 7 |
| Open | ACWA 1997 | Oregon | World | 4 |
| Open | BASMAA, 1995 | N. CA | Local | 11 |
| Open | BCDC, 1991 | N. CA | Local | 11 |
| Open | Lawson et al., 2001 | Chesapeake Bay | World | 4 |
| Open | Lawson et al., 2001 | Chesapeake Bay | World | 4 |
| Open | Lawson et al., 2001 | Chesapeake Bay | World | 11 |
| Open | Lazerte et al., 1989 | Canada | World | 1 |
| Open | Pitt et al., 2004 (NSQD) | USA | World | 5 |
| Open | Robson and Neal, 1997 | UK | World | 4 |
| Open | Schut et al., 1986 | Canada | World | 0 |
| Open | Stein et al, 2007 | S. CA | Arid West | 8 |
| Open | Stenstrom and Strecker, 1993 | S. California | Arid West | 55 |
| Open | Tiefenthaler et al, 2008 | S. CA | Arid West | 8 |
| Open | WCC, 1991 (reference in BASMAA 1996) | Alameda, CA | Local | 3 |
| Open | WCC, 1991 (reference in BASMAA 1996) | Santa Clara, CA | Local | 9 |
| Residential | Ackerman & Schiff, 2003 | S. CA | Arid West | 16 |
| Residential | ACWA 1997 | Oregon | World | 14 |
| Residential | Asaf et al., 2004 | Israel | World | 9 |
| Residential | Asaf et al., 2004 | Israel | World | 7 |
| Residential | Asaf et al., 2004 | Israel | World | 10 |
| Residential | Bannerman et al., 1993 | Wisconsin | World | 16 |
| Residential | BCDC, 1991 | N. CA | Local | 33 |
| Residential | Choe et al., 2002 | Korea | World | 99 |

| Land Use Category | Reference | Location | Local/Arid West/World | "Central tendency" |
|---|---|---|---|---|
| Residential | Choe et al., 2002 | Korea | World | 77 |
| Residential | City of Austin, 1995 | TX | World | 10 |
| Residential | Mattraw and Sherwood, 1977 | Florida | World | 21 |
| Residential | Pitt et al., 2004 (NSQD) | USA | World | 12 |
| Residential | Roberts et al., 1977 | Switzerland | World | 14 |
| Residential | Rule et al., 2006 | UK | World | 11 |
| Residential | Smith 2010 | Florida | World | 7 |
| Residential | Stein et al, 2007 | S. CA | Arid West | 18 |
| Residential | Stenstrom and Strecker, 1993 | S. California | Arid West | 95 |
| Residential | Stenstrom and Strecker, 1993 | S. California | Arid West | 100 |
| Residential | Tiefenthaler et al, 2008 | S. CA | Arid West | 26 |
| Residential | Tiefenthaler et al, 2008 | S. CA | Arid West | 30 |
| Residential | US EPA, 1983 (NURP) | USA | World | 33 |
| Residential | WCC, 1991 (reference in BASMAA 1996) | Alameda, CA | Local | 31 |
| Residential | WCC, 1991 (reference in BASMAA 1996) | Santa Clara, CA | Local | 51 |
| Transportation | Baeckstroem et al., 2003 | Sweden | World | 44 |
| Transportation | Barrett et al., 1998 | TX | World | 37 |
| Transportation | Barrett et al., 1998 | TX | World | 7 |
| Transportation | Barrett et al., 1998 | TX | World | 12 |
| Transportation | David et al., 2011 | N. CA | Local | 59 |
| Transportation | Driscoll et al., 1990a | ? | World | 54 |
| Transportation | Driscoll et al., 1990a | ? | World | 22 |
| Transportation | Gnecco et al., 2005 | Italy | World | 19 |
| Transportation | Kayhanian et al., 2003 | CA | Arid West | 9 |
| Transportation | Kayhanian et al., 2003 | CA | Arid West | 59 |
| Transportation | Kayhanian et al., 2007 | CA | Arid West | 12 |
| Transportation | Kayhanian et al., 2007 | CA | Arid West | 27 |
| Transportation | Kayhanian et al., 2007 | CA | Arid West | 50 |
| Transportation | Legret and Pagotto, 1999 | France | World | 45 |
| Transportation | Maniquiz et al., 2009 | Korea | World | 104 |
| Transportation | Pitt et al., 2004 (NSQD) | USA | World | 35 |
| Transportation | Prestes et al., 2006 | Brazil | World | 8 |
| Transportation | Rushton 2001 | Florida | World | 10 |
| Transportation | Rushton 2001 | Florida | World | 9 |
| Transportation | Rushton 2001 | Florida | World | 4 |
| Transportation | Rushton 2001 | Florida | World | 3 |
| Transportation | Sansalone and Buchberger, 1997 | OH | World | 135 |
| Transportation | Shinya et al., 2000 | Japan | World | 0 |

| Land Use Category | Reference | Location | Local/Arid West/World | "Central tendency" |
|---|---|---|---|---|
| Transportation | Tiefenthaler et al, 2008 | S. CA | Arid West | 10 |
| Transportation | WCC, 1991 (reference in BASMAA 1996) | Alameda, CA | Local | 31 |
| Transportation | Wu et al., 1998 | NC | World | 15 |
| Transportation | Wu et al., 1998 | NC | World | 12 |
| Transportation | Wu et al., 1998 | NC | World | 3 |
| Urban | Ashley and Napier, 2005 | Australia | World | 10 |
| Urban | BASMAA, 1995 | N. CA | Local | 45 |
| Urban | Behera et al., 2006 | Toronto | World | 30 |
| Urban | Bodo, 1989 | Canada | World | 10 |
| Urban | Bodo, 1989 | Canada | World | 31 |
| Urban | Buffleben et al., 2002 | S. California | Arid West | 85 |
| Urban | Domagalski and Dileanis, 2000; Domagalski, 2001 | Sacramento, CA | Arid West | 5 |
| Urban | Gromaire et al., 2001 | Paris | World | 43 |
| Urban | Gromaire et al., 2001 | Paris | World | 27 |
| Urban | Gromaire et al., 2001 | Paris | World | 63 |
| Urban | Gromaire et al., 2001 | Paris | World | 117 |
| Urban | Lawson et al., 2001 | Chesapeake | World | 7 |
| Urban | Lawson et al., 2001 | Chesapeake Bay | World | 7 |
| Urban | Marsalek and Ng, 1989 | Canada | World | 47 |
| Urban | Marsalek and Ng, 1989 | Canada | World | 43 |
| Urban | Marsalek and Ng, 1989 | Canada | World | 44 |
| Urban | Robson and Neal, 1997 | UK | World | 18 |
| Urban | Robson and Neal, 1997 | UK | World | 3 |
| Urban | Robson and Neal, 1997 | UK | World | 2 |
| Urban | Sabin et al., 2005 | California | Arid West | 27 |
| Urban | Smullen et al., 1999 | USA | World | 14 |
| Urban | Smullen et al., 1999 | USA | World | 11 |
| Urban | Smullen et al., 1999 | USA | World | 67 |
| Urban | Smullen et al., 1999 | USA | World | 55 |
| Urban | Soller et al., 2005 | san Jose, CA | Local | 16 |
| Urban | Soller et al., 2005 | san Jose, CA | Local | 16 |
| Urban | Stenstrom and Strecker, 1993 | S. California | Arid West | 72 |
| Urban | Stenstrom and Strecker, 1993 | S. California | Arid West | 100 |
| Urban | Stenstrom and Strecker, 1993 | S. California | Arid West | 100 |
| Urban | Wilber and Hunter, 1977 | New Jersey | World | 20 |
| Urban | Wilber and Hunter, 1977 | New Jersey | World | 26 |

# APPENDIX 8. PCBS AND MERCURY MODULE

## A8.1 PCB and Hg model methods

### A8.1.a PCB and Hg pollutant profiles

The first step for each analyte was to review what is known locally or internationally about the sources or use characteristics and processes of release and transport, of these contaminants, in order to identify the appropriate basis for estimating landscape scale pollutant loads. The decisions that need to be made were:

1. What land uses or source areas most influence mercury or PCB pollution on the landscape?
2. What GIS layers are available to support the model structure?

In the case of PCBs and mercury, decisions about the structural basis for the model were largely recorded in the y1 report (Lent and McKee 2011). A variety of different land uses and source areas were identified as potentially having a contribution on PCB and mercury loads (Table P&M1). These were ranked qualitatively from very high (for example PCBs in relation to electrical transmission and generation of mercury in relation to various recycling practices) to very low (in the case of PCBs - agriculture and mercury -open-space land use) (Table P&M1). Lent and McKee (2011) also discussed available GIS layers to support the development of the PCB or mercury regional watershed spreadsheet model and identified layers that needed further development (indicated by the letter N, Table P&M1). Many of these GIS layers have been improved through a joint effort between EOA and SFEI (see Appendix 1 of this report). As can be seen, there are now many more layers in the GIS data base to choose from for the current version of the PCB and mercury RWSM. However as described in Appendix 1, the data for each land-use or source area have been ascribed varying levels of data quality based on how the data were developed; continued improvements are expected in coming years.

### A8.1.b PCB and Hg model architecture

Functionally, the model architecture allows for unique definitions of land uses or source areas for a contaminant model using either the water model or the sediment model whereby differing concentration could feasibly be applied to areas with similar unit run-off. These spatial “land units” generate unique loading functions for estimating bottom of the watershed pollutant loads. Conversely, non-unique concentrations can be assigned to differing source areas that are modeled uniquely within the hydrology RWSM thus also generating unique loading functions.

The PCB and mercury models are built upon the existing Spreadsheet Model framework. The models relate physical characteristics in each watershed (suspended sediment production, land uses, and source areas) to the average annual PCB or mercury load. In the model, sediment production was based upon the type of bedrock, the slope of the hillslope, and land use (Appendix 6: suspended sediment module). Coefficients (mass of PCBs or mercury in relation to mass of sediment) were applied to sediment to compute spatial PCB and Hg release from all the thousands -millions of individual land units of each watershed.

**Table P&M1. Proposed potential land use / source area categories for PCBs and mercury based on Lent and McKee (2011) and availability of geographic information system (GIS) databases to support the basis of the model. Known or estimated magnitude of emission factor: Very High (VH), High (H), Medium (M), Low (L), Very Low (VL)*.**

| | PCBs | Mercury | GIS data available in 2011 | GIS data available in 2013 |
|---|---|---|---|---|
| All industrial | | H | | Y |
| Older industrial | M | H | | Improved |
| Newer industrial | M/L | | | Improved |
| Military | H | | N | Y |
| Electrical transformer and capacitor (manufacture/repair/testing/storage/use) | VH | | | Improved |
| Electric power generation | | MH | N | Y |
| Cement production | | | N | Y |
| Cremation | | | | Improved |
| Oil refineries / petrochemicals | M | | N | Y |
| Manufacture (steel or metals) | M | | N | Y |
| Recycling (drum) | H | VH | N | Y |
| Metals recycling | M/L | | N | Y |
| Marine repair and marine scrap yards | | | N | Y |
| Auto recycling/ refurbishing | | | | Improved |
| General waste recycling / disposal | | | N | Y |
| All transportation | | | | |
| Marina's | | | N | Y |
| Transport (ship) | M | M | N | Y |
| Transport (rail) | | | | Improved |
| Transport (air) | ? | ? | N | Improved |
| Freeways | | L | | Improved |
| Streets | | | | Improved |
| Urban (except industrial) | L | | | Y |
| Commercial | | | | Y |
| Older urban | | M | | Improved |
| High density residential | | | | Y |
| Low density residential | | | | Y |
| All nonurban | VL | VL | | Y |
| Agriculture | | | | Y |
| Open space | | | | Y |

*Note, the range of these high, medium and low qualifiers are pollutant specific – for example concentrations of PCBs in soils and water span 3-4 orders of magnitude whereas concentration ranges for copper span 1-2 orders of magnitude. 'N' indicates data were not available in 2011, 'Y' indicates data now developed, and 'improved' indicates the data have been improved since 2011 through an EOA/SFEI collaboration (see Appendix 1 of this report).

Given that net sediment or pollutant load leaving the watershed and entering the Bay is a function of both production and storage, a delivery ratio (NRCS, 1983) was applied to simulate storage and estimate loads to the Bay. Sediment and pollutants have a higher chance of being stored (e.g. on a hillslope, in an alluvial fan, on a floodplain, or within channels) in a larger watershed (low delivery ratio), compared to a small, typically steeper and more connected watershed (high delivery ratio). Given that urban drainage systems are designed not to store sediment in large quantities, delivery ratio was based on the percentage of area that is nonurban. In effect, larger, but fully urbanized watersheds still have near 100% delivery. The published delivery ratio equation (NRCS, 1983) was applied:

$$DR = 0.417762A^{-0.134958} - 0.127097$$

where DR is the delivery ratio, and A is the area of nonurban land use in each watershed ($mi^2$).

Using delivery ratios to adjust loads removes the effect of watershed area, allowing other factors such as pollutant sources to dominate the model output. In addition, we also chose to modify the sediment and pollutant loads for the effects of reservoirs. Watersheds with reservoirs can trap at least a portion, if not all, of the suspended sediment provided to the reservoir. The data were adjusted to reflect the proportion of sediment transported through the reservoir, or its trapping efficiency, as calculated by the Brown (1944) equation. Trapping efficiency was calculated using upstream contributing watershed area and the capacity of the reservoir:

$$CT = 100\ [1 - 1\ (1+0.1\ C/W)]$$

where CT is reservoir trapping efficiency (as a decimal fraction), C is reservoir capacity (acre/feet), and W is contributing watershed area ($mi^2$). Most reservoirs in the Bay Area were estimated to have a trapping efficiency of >95% (assuming they are not full of sediment). In the earlier Spreadsheet Model, only large reservoirs were included in the analysis and 100% trapping efficiency was assumed (e.g. Davis et al., 2000; Lewicki and McKee, 2009). However, in this effort, additional reservoirs were considered for area exclusion/adjustment, including reservoirs that are registered in the Department of Water Resources Division of Safety of Dams (DSOD) database (http://www.water.ca.gov/damsafety/) that have an upstream contributing area greater than 3 $km^2$, for a total of 30 reservoirs. The trapping efficiency using the equation by Brown (1944) was used for each reservoir, and the resulting climatically averaged PCB or mercury load for each watershed was adjusted accordingly consistent with the sediment RWSM.

The final component of the architecture was to determine which geographic land use or source area layers for mercury and PCBs were contained within the calibration watershed dataset with sufficient area to potentially influence the particle ratios or loads observed at the outlet of the watershed (Table P&M2). Land-use categories can be considered those essentially generated from coalescing categories within the ABAG land use dataset. Open space as a land-use category is represented in all of our calibration watersheds as is residential, commercial, and transportation. Industrial land use is present in more than two thirds of the watersheds whereas agriculture is less prevalent. Source area categories represent geographic information that was generated from a variety of sources including State databases, heads up digitization and other methods, as well as manipulations of multiple datasets (see Appendix 1 of this report for details). In relation to the source area categories, Old Urban and

**Table P&M2. The potential for each land use or source area category to have an influence on the calibration process for the PCB and mercury models.**

| Land use or Source Area | | Percentage of calibration watersheds with at least 0.5% of the area represented | |
|---|---|---|---|
| | | PCB | Hg |
| Land Use | Open % WS Area | 100 | 100 |
| | Residential % WS Area | 100 | 100 |
| | Commercial % WS Area | 100 | 100 |
| | Transportation % WS Area | 100 | 100 |
| | Industrial % WS Area | 68 | 67 |
| | Agriculture % WS Area | 23 | 14 |
| Soure Area | streets % WS Area | 100 | 100 |
| | oldUrbanAndIndustrial % WS Area | 95 | 95 |
| | highways % WS Area | 91 | 90 |
| | transpRail % WS Area | 68 | 71 |
| | crematoria % WS Area | 41 | 33 |
| | manufMetals % WS Area | 27 | 29 |
| | recycWaste % WS Area | 27 | 29 |
| | recycAuto % WS Area | 14 | 14 |
| | recycMetals % WS Area | 9 | 10 |
| | transpAir % WS Area | 9 | 5 |
| | cement % WS Area | 5 | 5 |
| | electricTransf % WS Area | 5 | 5 |
| | electricPower % WS Area | 0 | 0 |
| | military % WS Area | 0 | 0 |
| | oilRefineries % WS Area | 0 | 0 |
| | recycDrums % WS Area | 0 | 0 |
| | transpShip % WS Area | 0 | 0 |

Old Industrial, TransP Rail (rail transport), crematoria, Manuf Metals (metal manufacturing facilities), Recyc Waste (waste recycling facilities), Recycle Auto (auto recycling facilities), and Recyc Metals (metals recycling facilities) are all represented in the calibration model space. An additional category, Electric Transf (electrical power distribution facilities) is less well represented but as discussed later was also included due to the potential for legacy soil contamination in the vicinity of these facilities.

### A8.1.c PCB and Hg model input data

The input concentration (Ck) for each land use or source area is the key input parameter for the PCB model and was explicitly defined or estimated based on available data. As described the above section A8.1.b, the PCB RWSM can conceptually be based on either the outputs from the hydrology RWSM and water concentrations (ng/L) or the outputs from the sediment RWSM and particle based concentrations (mg/kg). We made no a priori decision on either a water or sediment basis for each land-use or source area category before running early versions of the model; rather our intent was to use the model to explore and justify the basis. However, conceptually, the preference initially was to use sediment as the basis for the PCB model in watersheds or landscape components that have higher sediment production rates such as our agricultural and open space areas. Doing this would preserve variability of PCB supply associated with the erosion of clean sediments in the model structure.

A literature review was completed on PCB concentrations in water and in urban sediments and soils to support a recommendation for the proposed model architecture (Lent and McKee 2011). They found that PCB data on concentrations in both water and sediment/soils were lacking for the land uses and source areas in relation to the proposed model architecture. In response, they recommended a mix of

further targeted literature review, further exploration of local data using “back-calculation methods”, or estimation techniques partly based on best professional judgment and statistical distributions of either or both water and sediment/soil concentration data from world literature and local data combined (Lent and McKee, 2011). These methods were applied (see section A2.1.b of this report for details) to generate the initial input data. Despite considerable effort, the outcome was still a lack of information available for concentrations in flowing stormwater in relation to land uses or source areas. Thus, a decision was made to base the PCB and mercury models on sediment and use particle ratios as the basis (Table P&M3). A range or tolerance of upper and lower limits of the coefficient for each land use and source area category is shown. These limits became the starting point for initial calibration runs of the PCB and Hg models. There was considerable overlap in the coefficients between different categories indicating the likelihood for relatively loose constraint on the calibration process. However, the relatively large variation between the most polluted categories for PCBs and Hg and the cleanest category (all nonurban) suggests that despite challenges with calibrating the sediment model (see Appendix 6 of this report), using the current version of the sediment model as a basis for the PCB and mercury models may still be reasonable given that sediment production in the urban landscape is represented by only one parameter.

### A8.1.d Available PCB and Hg calibration and verification data

Beginning WY 2002, a systematic effort has occurred in the Bay Area to generate information on concentrations and loads of PCBs and mercury in stormwater at a variety of landscape scales. The majority of this information has been generated through efforts by the RMP but additional data have also been generated by local agencies such as EBMUD, and through grants obtained by SFEI in relation to evaluating the performance of management practices.

The model was calibrated based on particle ratios which are available for PCBs in 22 watersheds and mercury in 21 watersheds (Table P&M4). The set of watersheds is essentially the same for mercury and PCBs with the exception of either of the locations in the Guadalupe River watershed which are inappropriate for calibration of the mercury model due to historic mining and the lack of parameterization in the model for mining sources, and San Pedro Creek storm drain watershed which was lacking PCB data. Although there are definitely uncertainties in the quality of the particle ratio data used in the calibration procedure, these are harder to quantify. Making more effort to qualify the uncertainty for the particle ratio data and using a weighting factor in future calibration processes is a possible future improvement.

The loading data that are currently available were used as one of the verification methods. Although all of the current loading estimates have been generated from watersheds where there is also particle ratio data, the loading data differs from the particle ratio data in that it is a derivation of the flow of water from a watershed area rather than the concentration of sediment in the water column. It is asserted that this derivation difference is large enough to use the loading data as an independent verification. That assertion made, there is varying confidence in the quality of the loads data ranging from low to high, with most data being of low certainty (Table P&M4) in relation to the climatic representative of the

**Table P&M3. PCB and mercury input data for calibration of the spreadsheet model. Green indicates the base model that was trialed first and orange indicates additional source areas that were trialed during the calibration runs.**

| Land use or Source Area | Proposed categories | PCB calibration boundaries (mg/kg) | | | | | | Hg calibration boundaries (mg/kg) | | | | | |
|---|---|---|---|---|---|---|---|---|---|---|---|---|---|
| | | Mean | Min | 10%ile | Median | 90%ile | Max | Mean | Min | 10%ile | Median | 90%ile | Max |
| **All industrial** | | 0.13 | | | | | | 1.7 | | | | | |
| Older industrial | Older Industrial | 1.2 | 0.010 | 0.029 | 0.60 | 4.2 | 36 | 0.92 | 0.13 | 0.22 | 0.68 | 5.6 | 9.0 |
| Newer industrial | | 0.1 | | | | | | 1.2 | | | | | |
| Military | | 1.5 | | | | | | 0.35 | | | | | |
| Electrical transformer and capacitor (manufacture/repair/testing/storage/use) | electricTransf | 10 | 0.010 | 0.19 | 1.3 | 26 | 36 | 1.5 | 0.28 | 0.30 | 0.84 | 3.34 | 5.5 |
| Electric power generation | | 10 | | | | | | 0.84 | | | | | |
| Cement production | | | | | | | | 1.0 | | | | | |
| Cremation | crematoria | | | | | | | 0.44 | 0.14 | 0.15 | 0.18 | 0.84 | 1.00 |
| Oil refineries / petrochemicals | | 0.13 | | | | | | 0.98 | | | | | |
| Manufacture (steel or metals) | manufMetals | 0.80 | 0.060 | 0.086 | 0.38 | 1.9 | 3.2 | 0.75 | 0.29 | 0.30 | 0.48 | 1.47 | 1.9 |
| Recycling (drum) | | 1.3 | | | | | | 2.5 | | | | | |
| Metals recycling | | 0.60 | | | | | | 3.0 | | | | | |
| Marine repair and marine scrap yards | | 0.093 | | | | | | 9.0 | | | | | |
| Auto recycling/ refurbishing | recycAuto | 0.23 | 0.020 | 0.057 | 0.14 | 0.49 | 0.60 | 2.5 | 0.17 | 0.24 | 0.45 | 6.78 | 9.0 |
| General waste recycling / disposal | recycWaste | 3.2 | 0.093 | 0.52 | 2.2 | 6.2 | 7.1 | 2.1 | 0.31 | 0.37 | 0.70 | 5.35 | 9.0 |
| **All transportation** | | | | | | | | | | | | | |
| Marina's | | | | | | | | | | | | | |
| Transport (ship) | | 1.1 | | | | | | 1.2 | | | | | |
| Transport (rail) | transpRail | 0.66 | 0.00061 | 0.084 | 0.50 | 1.4 | 1.5 | 0.45 | 0.32 | 0.32 | 0.36 | 0.65 | 0.76 |
| Transport (air) | | 0.060 | | | | | | 0.13 | | | | | |
| Freeways | | | | | | | | 0.13 | | | | | |
| Streets | | | | | | | | 0.13 | | | | | |
| **Urban (except industrial)** | Urban_other | 0.050 | 0.00017 | 0.0027 | 0.22 | 1.3 | 3.0 | 0.21 | 0.11 | 0.13 | 0.32 | 0.89 | 4.3 |
| Commercial | | 0.56 | | | | | | 0.39 | | | | | |
| Older urban | Older Urban | 0.15 | 0.0034 | 0.015 | 0.28 | 1.9 | 13 | 0.16 | 0.12 | 0.18 | 0.50 | 3.2 | 6.6 |
| High density residential | | 0.063 | | | | | | 0.63 | | | | | |
| Low density residential | | | | | | | | 0.18 | | | | | |
| **All nonurban** | Ag/Open | 0.007 | 0.0002 | 0.014 | 0.030 | 0.19 | 0.23 | 0.091 | 0.070 | 0.079 | 0.12 | 0.26 | 0.32 |
| Agriculture | | 0.030 | | | | | | 0.10 | | | | | |
| Open space | | 0.12 | | | | | | 0.21 | | | | | |
| | | | | | | | | | | | | | |
| Variation (Max/Min) | | 1,437 | | | | | | 99 | | | | | |

**Table P&M4. Available calibration data and watersheds of the Bay Area for the PCB and mercury spreadsheet models.**

| | Calibration data | | Varification data | | | | |
|---|---|---|---|---|---|---|---|
| Watershed name | PCB Particle ratio | Hg Particle ratio | PCB loads | Hg Loads | Certainty | Possible bias | Reference |
| Belmont Creek | x | x | | | | | McKee et al., 2012 |
| Borel Creek | x | x | | | | | McKee et al., 2012 |
| Calabazas Creek | x | x | | | | | McKee et al., 2012 |
| Coyote Creek at Hwy 237 | x | x | x | x | Low | Low | McKee et al., unpublished |
| Ettie Street Pump Station | x | x | x | x | Low | Low | McKee et al., 2012 |
| Glen Echo Creek | x | x | | | | | McKee et al., 2012 |
| Guadalupe River at Almaden Expressway | x | | x | | Moderate | Low | McKee et al., unpublished |
| Guadalupe River at Hwy 101 | x | | x | | Moderate | | McKee et al., 2004; 2005; 2006a; 2010; 2013; Gilbreath et al., in review |
| Lower Marsh Creek | x | x | x | x | Low | Low | McKee et al., 2012; McKee et al., 2013; Gilbreath et al., in review |
| Lower Penetencia Creek | x | x | | | | | McKee et al., 2012 |
| North Richmond Pump Station | x | x | x | x | Moderate | | Hunt et al., 2012; Gilbreath et al., in review |
| Pulgas Creek Pump Station - North | x | x | | | | | McKee et al., 2012 |
| Pulgas Creek Pump Station - South | x | x | x | x | Low | Low | McKee et al., 2012; Gilbreath et al., in review |
| San Leandro Creek at San Leandro Blvd | x | x | x | x | Low | Low | McKee et al., 2012; McKee et al., 2013; Gilbreath et al., in review |
| San Lorenzo Creek | x | x | x | x | Low | Low | McKee et al., 2012 |
| San Pedro Stormdrain | | x | | | | | McKee et al., unpublished |
| San Tomas Creek | x | x | | | | | McKee et al., 2012 |
| Santa Fe Channel | x | x | | | | | McKee et al., 2012 |
| Stevens Creek | x | x | | | | | McKee et al., 2012 |
| Sunnyvale East Channel | x | x | x | x | Low | Low | McKee et al., 2012; McKee et al., 2013; Gilbreath et al., in review |
| Walnut Creek | x | x | x | x | Low | | McKee et al., 2012 |
| Zone 4 Line A at Cabot Blvd | x | x | x | x | High | | Gilbreath et al. 2012 |
| Zone 5 Line M | x | x | | | | | McKee et al., 2012 |

dataset, and the effort made to date to climatically adjust whatever limited data are available. In general, most of the loads data currently available are likely biased low due to a lack of observations during moderate to more intense storm events. In addition, loads data for verification are limited to a small subset of watersheds that are not those identified as high priority management areas, adding yet another challenge to determine the confidence of the model for its primary purposes. These topics will be discussed more below.

### A8.1.e PCB and Hg model calibration procedure

The calibration was carried out through a constrained optimization method ("Complex Method", Box 1965). Functionally, this was done by randomly sampling particle ratios (coefficients) starting with the $10^{th}$ percentile to $90^{th}$ percentile (Table P&M3) as the lower and upper boundary conditions for each parameter, combining this with the sediment load for each parameter in each watershed generated from the sediment model (see section A6), and running an auto-calibration procedure. The auto-calibration procedure mathematically searches for the optimum combination of particle ratios that produce the minimum difference between observed particle ratio (obtained from field observations) (Table P&M4) and the simulated particle ratio (derived from the simulated pollutant load normalized by the total sediment load) for each watershed simultaneously. An initial analysis to determine the appropriate number of iterations (loops) for each trial was performed using 50, 500, and 5000 iterations and 500 iterations were deemed sufficient. Unlike for sediment (see section A6), a weighting factor (e.g. 3= high quality; 2=medium quality; 1= low quality) was not assigned to each watershed to reflect the quality of the observed data. This could be explored in the future since there are moderate differences between the representativeness of the available particle ratio data from one watershed to another.

To evaluate model performance, it was necessary to define some general success criteria for determining if the calibration results were reasonable for each group of land uses and source areas investigated:

1. The relative order of magnitude of each of the coefficients should be logical; source area coefficients should in most cases be greater than the coefficients for land uses
2. The calibrated coefficients should not reach the lower or upper initial starting boundary unless there is a preconceived rationale as to why the coefficient should have been fixed (for example field observations)
3. Repeated calibrations using the same input boundary conditions for the same set of parameters should produce the same calibrated coefficients (within 5%)

#### *A8.1.e.i PCB model calibration procedure*

A total of 17 calibration trials were conducted to explore which set of parameters and coefficients can best describe PCBs observed in Bay Area stormwater runoff (Table P&M5). During trial runs 1-9 (Table P&M6), the upper and lower limits for each parameter coefficient were set to the $10^{th}$ and $90^{th}$ percentiles (Table P&M3). The initial parameter choice for the base run (two land uses: Ag/Open, Other Urban; two source areas: Old Industrial, Old Urban) was based on work completed in the summer of 2012 using inverse optimization techniques (see section A2.1.b. of this report) and was the same.

**Table P&M5. Calibration trials completed for the PCB regional watershed spreadsheet model. "Lower" and "Upper" indicate the lower and upper limits for each of the parameters in milligrams per kilogram that were set as the boundary conditions for each calibration trial. Initially, quite narrow lower and upper limits were set for each parameter based on the 10$^{th}$ and 90$^{th}$ percentiles of the available data (see Table P&M 3), but as discoveries were made, boundaries were widened to the minimum and maximum for each parameter (Table P&M3), and eventually to the overall minimum and maximum observed in any literature (Table P&M3).**

| Calibration trial description | Trial run # | All urban | | Ag/Open | | Other urban | | Old urban | | Old Industrial | | manufMetals | | recycAuto | | transpRail | | electricTransf | | recycWaste | | Allrecycle | |
|---|---|---|---|---|---|---|---|---|---|---|---|---|---|---|---|---|---|---|---|---|---|---|---|
| | | Lower | Upper | Lower | Upper | Lower | Upper | Lower | Upper | Lower | Upper | Lower | Upper | Lower | Upper | Lower | Upper | Lower | Upper | Lower | Upper | Lower | Upper |
| Base | 1 | | | 0.014 | 0.19 | 0.0027 | 1.3 | 0.015 | 1.9 | 0.029 | 4.2 | | | | | | | | | | | | |
| Base (rerun) | 2 | | | 0.014 | 0.19 | 0.0027 | 1.3 | 0.015 | 1.9 | 0.029 | 4.2 | | | | | | | | | | | | |
| Base plus manufMetals | 3 | | | 0.014 | 0.19 | 0.0027 | 1.3 | 0.015 | 1.9 | 0.029 | 4.2 | 0.086 | 1.9 | | | | | | | | | | |
| Base plus recycAuto | 4 | | | 0.014 | 0.19 | 0.0027 | 1.3 | 0.015 | 1.9 | 0.029 | 4.2 | | | 0.057 | 0.49 | | | | | | | | |
| Base plus transpRail | 5 | | | 0.014 | 0.19 | 0.0027 | 1.3 | 0.015 | 1.9 | 0.029 | 4.2 | | | | | 0.084 | 1.4 | | | | | | |
| Base plus electricTransf | 6 | | | 0.014 | 0.19 | 0.0027 | 1.3 | 0.015 | 1.9 | 0.029 | 4.2 | | | | | | | 0.19 | 26 | | | | |
| Base plus recycWaste | 7 | | | 0.014 | 0.19 | 0.0027 | 1.3 | 0.015 | 1.9 | 0.029 | 4.2 | | | | | | | | | 0.52 | 6.2 | | |
| Base - new ag/open lower limit | 8 | | | 0.0020 | 0.190 | 0.0027 | 1.3 | 0.015 | 1.9 | 0.029 | 4.2 | | | | | | | | | | | | |
| Base plus transpRail higher upper limit | 9 | | | 0.014 | 0.19 | 0.0027 | 1.3 | 0.015 | 1.9 | 0.029 | 4.2 | | | | | 0.084 | 36 | | | | | | |
| Base - new ag/open lower limit plus transpRail higher upper limit | 10 | | | 0.0020 | 0.190 | 0.0027 | 1.3 | 0.015 | 1.9 | 0.029 | 4.2 | | | | | 0.084 | 36 | | | | | | |
| Base plus all parameters with parameter specific limits | 11 | | | 0.00017 | 0.23 | 0.00017 | 3.0 | 0.0034 | 13 | 0.010 | 36 | 0.060 | 3.2 | 0.020 | 0.60 | 0.00061 | 1.5 | 0.010 | 36 | 0.093 | 7.1 | | |
| Base plus all Parameters maximum wide limits | 12 | | | 0.00017 | 36 | 0.00017 | 36 | 0.00017 | 36 | 0.00017 | 36 | 0.00017 | 36 | 0.00017 | 36 | 0.00017 | 36 | 0.00017 | 36 | 0.00017 | 36 | | |
| Simplified base plus best two plus all recycle | 13 | 0.00017 | 36 | 0.00017 | 36 | | | | | 0.00017 | 36 | | | | | 0.00017 | 36 | 0.00017 | 36 | | | 0.00017 | 36 |
| Simplified base plus best two plus all recycle (rerun) | 14 | 0.00017 | 36 | 0.00017 | 36 | | | | | 0.00017 | 36 | | | | | 0.00017 | 36 | 0.00017 | 36 | | | 0.00017 | 36 |
| Simplified new base plus best two plus all recycle | 15 | 0.00017 | 36 | 0.00017 | 36 | | | | | 0.00017 | 36 | | | | | 0.00017 | 36 | 0.00017 | 36 | | | | |
| Simplified new base plus best two plus all recycle (rerun) | 16 | 0.00017 | 36 | 0.00017 | 36 | | | | | 0.00017 | 36 | | | | | 0.00017 | 36 | 0.00017 | 36 | | | | |

**Table P&M6. Coefficients for each calibration trial for the PCB regional watershed spreadsheet model. Red indicates a boundary violation during a calibration trial. Purple indicate a stability violation when a calibration trial was repeated with the same initial starting conditions.**

| Calibration trial description | Trial run # | All urban | Ag/ Open | Other urban | Old urban | Old Industrial | manuf Metals | recyc Auto | transp Rail | electric Transf | recyc Waste | All recycle | Comments |
|---|---|---|---|---|---|---|---|---|---|---|---|---|---|
| Base | 1 | | 0.014 | 0.24 | 0.022 | 1.5 | | | | | | | The coefficient for ag/open met lower boundary and old urban< other urban does not fit the expected order. Same results between the base trial and the rerun of the base trial show that calibration trial was stable. |
| Base (rerun) | 2 | | 0.014 | 0.24 | 0.015 | 1.5 | | | | | | | |
| Base plus manufMetals | 3 | | 0.014 | 0.24 | 0.022 | 1.6 | 0.086 | | | | | | The coefficient for ag/open and manufMetals met lower boundaries and old urban < other urban does not fit the expected order. |
| Base plus recycAuto | 4 | | 0.014 | 0.24 | 0.022 | 1.5 | | 0.057 | | | | | The coefficient for ag/open and auto recycle met lower boundaries and old urban < other urban does not fit the expected order. |
| Base plus transpRail | 5 | | 0.014 | 0.19 | 0.022 | 1.32 | | | 1.4 | | | | The coefficient for ag/open and auto recycle met lower boundaries and old urban < other urban does not fit the expected order. TranspRail seems to have an influence of particle ratios. |
| Base plus electricTransf | 6 | | 0.014 | 0.24 | 0.022 | 1.5 | | | | 0.19 | | | The coefficient for ag/open and electricTransf met lower boundaries and old urban < other urban does not fit the expected order. It is surprising that electricTrans did not have an influence on old industrial. |
| Base plus recycWaste | 7 | | 0.014 | 0.24 | 0.022 | 1.6 | | | | | 0.52 | | The coefficient for ag/open and recycWaste met lower boundaries and old urban < other urban does not fit the expected order. It is surprising that recycWaste did not have an influence on old industrial. |
| Base - new ag/open lower limit | 8 | | 0.0020 | 0.25 | 0.022 | 1.4 | | | | | | | The coefficient for ag/open met the even lower boundary and old urban < other urban does not fit the expected order. |
| Base plus transpRail higher upper limit | 9 | | 0.014 | 0.18 | 0.022 | 1.1 | | | 2.1 | | | | The coefficient for ag/open met lower boundary and old urban > other urban now fits the expected order. Transport rail is clearly associated with other urban and old industrial. This is the first calibration trial where results behave well relative to each other. |
| Base - new ag/open lower limit plus transpRail higher upper limit | 10 | | 0.0020 | 0.18 | 0.022 | 1.1 | | | 2.1 | | | | The coefficient for ag/open met lower further relaxed boundary and old urban > other urban now fits the expected order. Transport rail is clearly associated with other urban and old industrial. This is the first calibration trial where results behave well relative to each other. |
| Base plus all parameters with parameter specific but wide limits | 11 | | 0.00098 | 0.20 | 0.0041 | 1.6 | 0.074 | 0.071 | 1.5 | 0.15 | 0.10 | | Likely unstable but stability not tested since relative order illogical. |
| Base plus all Parameters maximum wide limits | 12 | | 0.037 | 0.093 | 0.051 | 0.034 | 5.1 | 1.6 | 3.3 | 36 | 0.15 | | Large differences between the coefficients for each of the parameters indicate calibration trial was unstable. |
| Base plus all Parameters maximum wide limits (rerun) | 13 | | 0.00017 | 0.16 | 0.075 | 1.2 | 1.3 | 2.3 | 2.0 | 0.18 | 0.00017 | | |
| Simplified base plus best two plus all recycle | 14 | 0.083 | 0.0020 | | | 1.8 | | | 3.4 | 9.2 | | 0.0002 | Moderate differences between the first trial run and the rerun show that calibration trial was unstable; Five parameters appears to be the current limit of the calibration data set (see Hg section trial runs #13 and #14). |
| Simplified base plus best two plus all recycle (rerun) | 15 | 0.092 | 0.00023 | | | 1.8 | | | 3.2 | 5.8 | | 0.0003 | |
| Simplified new base plus best two plus all recycle | 16 | 0.095 | 0.00024 | | | 1.6 | | | 3.0 | 11 | | | The coefficients make sense in relation to each other and to the empirical observations we have for the Bay Area. Same results between the first run and the rerun show that calibration trial was stable. |
| Simplified new base plus best two plus all recycle (rerun) | 17 | 0.096 | 0.00017 | | | 1.6 | | | 3.0 | 11 | | | |

for PCBs and Hg. The relative order of the baseline coefficients from the initial baseline run was Old Industrial>Other Urban>Old Urban>Ag/Open. Although consistent coefficients between calibration trial runs #1 and #2 indicated calibration stability, the relative order with Other Urban greater than Old Urban seemed illogical. The results indicated that the model was over predicting particle concentrations for the less contaminated watersheds. Upon looking at the coefficients, it was clear that Ag/Open was pushing against the lower limit set in the initial parameter boundary conditions. It was hypothesized that relaxing the lower limit below 0.014 mg/kg could result in improved calibration for cleaner watersheds.

In the initial set, a series of trials were also performed exploring five-parameter models that included an additional source area (Table P&M6: runs #3 - #7). For PCBs, these included the source areas Electric Transf, Manuf Metals, Recyc Auto, Recyc Waste, and Transp Rail. Santa Fe channel and other systems that have a higher rail component were under predicted by the initial calibration run. The calibrated coefficients for Transp Rail pushed up against the upper boundary of the initial coefficient boundary. Thus it was hypothesized that relaxing the upper boundary for Transp Rail may result in improved calibration for the more polluted (higher particle ratio) watersheds. Initial input coefficients for Older Urban and Other Urban were similar. Calibrated coefficients for Older Urban in all cases is approximately 10-fold lower than for Other Urban. This was not consistent with our conceptual model. Upon looking at sediment input data, Old Urban does occur in most watersheds but in general it is not a large portion of the sediment generation from any of the watersheds. The exceptions are North Richmond Pump Station, Borel Creek, East Sunnyvale Channel, and Zone 4 Line A. All four of these watersheds showed over prediction suggesting that maintaining Old Urban as a category in the PCB model was not warranted. Interestingly, adding an additional source area category in all cases improved the ratio of observed to predicted particle ratios and resulted in improved correlation coefficients.

Based on the results from calibration trials #1 - #7 (Table P&M6), the lower limit of Ag/Open was relaxed to 0.002 mg/L (the PCB TMDL “conceptual target” for pristine watersheds), and the upper limit for Transp Rail was relaxed to attempt to allow that parameter coefficient to find its optimal calibrated magnitude. The results of these calibration trial runs indicated that indeed even with the Ag/Open limit relaxed, the model again pushed against the lower boundary. It was hard to justify going much lower. The lowest concentrations measured in the world average 0.0006 mg/kg (McKee et al., 2006b). This represents perhaps the lowest possible boundary to try. The results for the Trans Rail calibration trial run indicated that with complete relaxation of the upper limit, the model did not push to the upper parameter boundary and calibrated at approximately 2.1 mg/kg and greater than the coefficient for Old Industrial. It was also interesting to note that the addition of the source area Trans Rail lowered the coefficients for both Other Urban and Old Urban, indicating part of the cause of Other Urban calibrating greater than Old Urban during trial runs #1 - #8. The results of the combined new Ag/Open and Transp Rail limits resulted in a slightly worse ratio between observed and predicted particle ratios, a slightly lower correlation coefficient, and a slightly improved overall range between the most under predicted and the most over predicted watersheds relative to the baseline run; not ideal outcomes.

The next two calibration trial runs were for a complex multi-parameter model that included Old Industrial, Old Urban, Other Urban, Ag/Open, and all the source area parameters (Electric Transf, Manuf

Metals, Recyc Auto, Recyc Waste, and Transp Rail). Trial #11 was done with very wide parameter ranges that were specific for each parameter and based on the minimum and maximum concentrations found either locally, back-calculated using various techniques, or in other parts of the world (Table P&M3). The lower bound for any parameter was set at 0.00017 mg/kg, which was the back-calculated concentration for high density residential derived from Lent's work using inverse optimization back calculation methods (see section A2.1.b. of this report) and the upper bound was set at 36 mg/kg. Note, the lowest concentration was lower than the lowest concentration found from literature review (0.0006 mg/kg: McKee et al 2006, Table 3-1, Catalonia, Spain) but the highest concentration is within the range of concentrations observed in soils in West Oakland.

The results of these runs were very interesting and unexpected. It appeared that once each parameter was given a wide (functionally unlimited) boundary range, high particle ratios were assigned to the source areas as opposed to the way the calibration was functioning in trials #1 - #10 when greater particle ratio coefficients were, perhaps somewhat forcibly in hindsight, optimized into the land use parameters. The results seem consistent with observations of sediment concentrations around the Bay Area; in general Old Industrial areas are more polluted with PCBs but within those old industrial areas, particle concentrations can range from the background to highly polluted in association with true source areas. The Electric Transf parameter was rated very high, followed by Recyc Waste, Manuf Metals, Transp Rail, and Recyc Auto. The Old Industrial source area parameter was rated medium; Other Urban was rated low and Ag/Open was rated very low. Unfortunately, rerunning the calibration with the same starting parameters showed instability; the coefficients changed dramatically with the subsequent rerun. It appeared that the optimal number of parameters was somewhere between five and nine and probably closer to five.

Based on this whole series of trial runs, the next trial runs were focused on simplifying the land use definitions and reducing the number of source areas. The following structure was trialed and checked for stability using a wide range (relatively unconstrained) for the coefficients (0.00017-36 mg/kg):

| **Land uses** | **Source areas** |
|---|---|
| All urban | All recycle |
| Ag/Open | Transp Rail |
| | Electric Transf |
| | Old industrial |

The moderate differences between the first trial run and the rerun (#14 and #15) show instability; a five parameter model appears to be the current limit of the calibration data set (a conclusion also reached for mercury). Since the parameter All Recycle met its lower bound for these trial runs it was hypothesized that removing this parameter would increase model stability which influenced the magnitude of the other parameters remarkably. The resulting final calibrated set of parameter coefficients makes sense in relation to each other and to the observations made in the Bay Area to date. The slight differences in the Ag/Open and All Urban coefficients were probably caused by the Ag/Open parameter calibrating right at its lower boundary. The consistency of the Old Industrial parameter across all of the trial calibration runs (except run #12) is encouraging and helps to suggest that the magnitude

of this parameter coefficient is close to optimal based on the number and characteristics of the current set of calibration watersheds Similarly, the magnitude and relative stability of the parameter Transp Rail across a number of runs in relation to old industrial tends to suggest this parameter may be calibrated relatively reliable as well (given the same caveats of the number and characteristics of the available calibration watershed particle ratio data). The results indicate that the most polluted source areas for PCBs may be more than 10,000-fold more polluted than the average condition of the Ag/Open land-use category. If this is true, identifying these areas will be extremely important for effectively managing PCBs in Bay Area. This differs from the proposed calibrated parameters for mercury where the variation in particle ratios between less polluted land use areas and the most polluted source areas are predicted to be just 10-fold.

Since most field observations in the Bay Area have been made in, at least, moderately polluted watersheds, the resulting calibrated set of parameters tended to over-predict the cleaner end members of the calibration set (Figure P&M1). This is likely an artefact with a variety of potential causes:

1. The available data tend to be biased towards urban watersheds of moderately polluted level; and truly clean watersheds are not strongly represented in the calibration dataset,
2. The spreadsheet model fails to capture stochastic processes such as rainfall/run-off, wind, and other pollutant off-site transport mechanisms because of its relatively simple architecture.

The calibrated parameters collectively resulted in a range of over and under prediction between 30% and 1200% of the observed particle ratios (Figure P&M1b). At first glance this appears to be a worse calibration than for mercury (see section A8.1.e.ii). However, with the exception of the “cleaner” eight watersheds (Lower Marsh Ck, Borel Creek, Belmont Creek, Guadalupe R Above Almaden Expressway in San Jose, Lower Penetencia, Walnut Creek, San Tomas Creek, and Stevens Creek below reservoir) the model based on the final proposed calibrated parameters appears to both under- and over-simulate moderate to relatively “dirtier” watersheds with greater observed particle ratios. Although the three watersheds with the highest particle ratios are all under simulated (Pulgas Creek Pump Station South, Pulgas Creek Pump Station North, and Santa Fe Channel), the most under simulated watershed happened to be San Lorenzo Creek which has a moderate particle ratio of 0.07 mg/kg. With the exception of just four watersheds (Stevens Creek, Borel Creek, Belmont Creek, and Lower Penetencia Creek) which have very low observed particle ratios (<0.034 mg/kg) based on available Bay Area data, the model appears to calibrate between 3-fold too high and 3-fold too low (Figure P&M1b).

Given the model has an additional step of applying a delivery ratio, the over-prediction of particle ratios for less polluted, larger watersheds is somewhat offset by the later modelling step. The final choice of parameters was largely a result of land uses/ source areas within the available calibration watersheds rather than a parameter set that is necessarily representative at a regional level. To include a greater number of source area parameters, a larger variety of watersheds are needed for the calibration dataset that include these source areas. To reduce the over prediction of cleaner watersheds, larger representation may be needed in the calibration dataset for these areas unless future modelling is focused on optimizing the results for the moderately to more polluted watersheds.

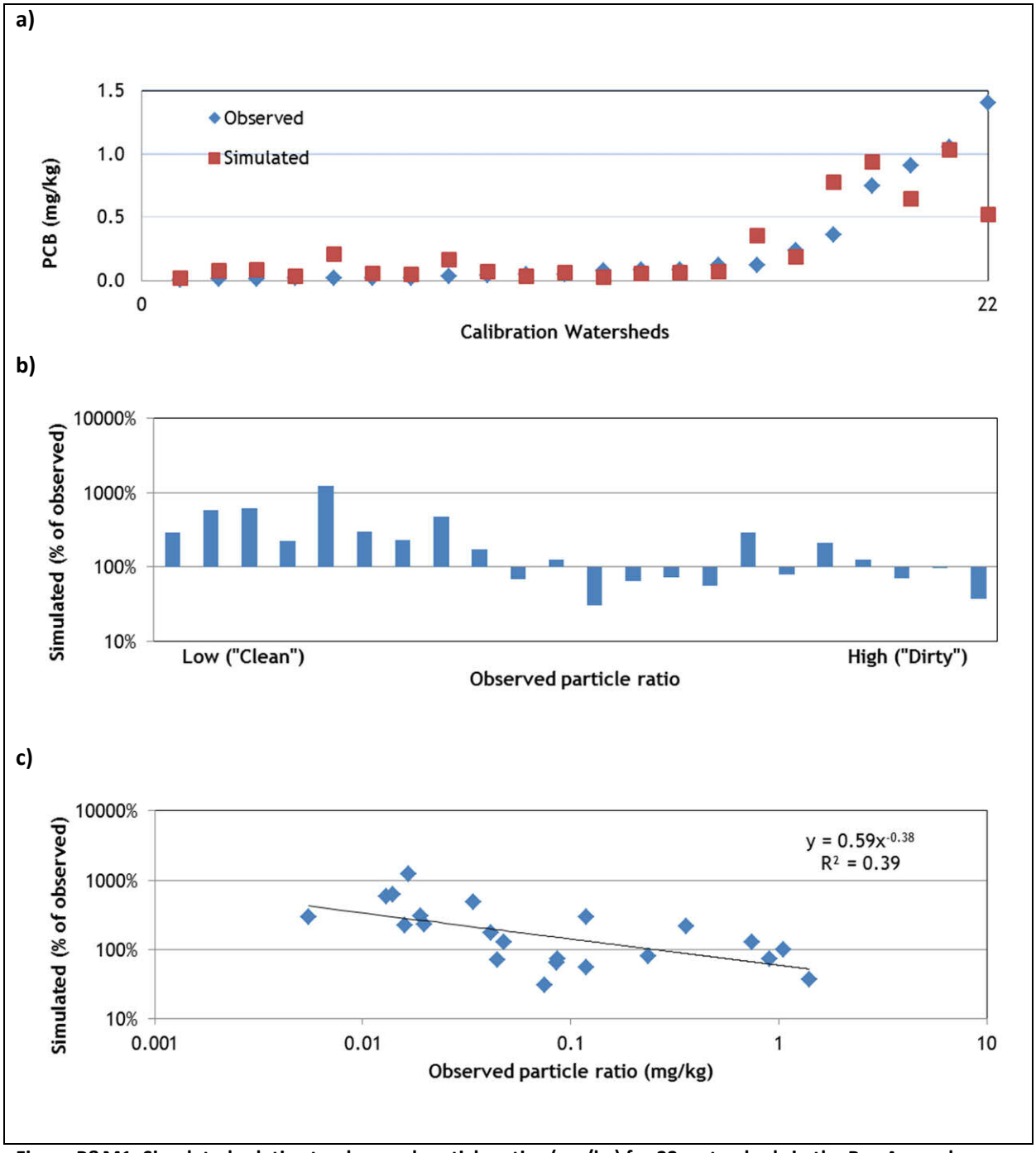


**Figure P&M1. Simulated relative to observed particle ratios (mg/kg) for 22 watersheds in the Bay Area where data are available. Note generally, the calibration, although stable, tends to over predict relatively "clean" low particle ratio watersheds and appears to both under- and over-simulate moderate to relatively "dirtier" watersheds with greater observed particle ratios. Although the three watersheds with the highest particle ratios are all under simulated, the most under simulated watershed happened to be one with a moderate particle ratio.**

### *A8.1.e.ii Hg model calibration procedure*

In a similar fashion, a large number of calibration trials were conducted for Hg to find the set of parameters and their coefficients that best describe the Hg particle ratios observed in stormwater runoff from Bay Area watersheds (Table P&M7). For trial runs 1-9 (Table P&M7), the upper and lower limits of each parameter coefficient were set to the $10^{th}$ and $90^{th}$ percentiles (Table P&M3). The parameter choice for the base run (two land uses: Ag/Open, Other Urban; two source areas: Old Industrial, Old Urban) was based on previous work as described in section A2.1.b of this report and was the same for PCBs and Hg. For each trial run, the calibration process was restarted with another set of random coefficients to test the stability of model calibration. The relative order of the calibrated coefficients for the base run was Old Industrial > Other Urban > Old Urban > Ag/Open, which does not fit our conceptual model of higher mercury generation in old urban than other general urban. In addition, the calibrated coefficients were against the lower boundary for older urban, suggesting that the coefficient would go even lower if not constrained. It is possible that Other Urban contains areas of light industrial and commercial space that are more polluted than old urban areas, or we have overestimated the influence of age of urbanization based on interpretation of relatively sparse data.

The examination of sediment input data reveals that older urban is present in almost all watersheds but generally the sediment generated from this source area is small. The exceptions are North Richmond Pump Station, Borel Creek, East Sunnyvale Channel, and Zone 4 Line A. The baseline calibration run over-predicted Hg for all these watersheds except North Richmond pump station. Therefore reducing the coefficient for Old Urban would likely push the model in the right direction for three out of four of these watersheds. North Richmond pump station is under-predicted for Hg and has a large proportion of sediment supply from source areas including Recyc Waste, Manuf Metals, and Transp Rail, and to a lesser extent Recyc Auto. Given the small proportion of sediment associated with Old Urban, it was hypothesized that removing the parameter altogether would probably have little impact.

The most under-predicted watersheds were San Pedro storm drain and San Leandro Creek below Lake Chabot. San Pedro storm drain contains a large amount of recycle waste but San Leandro Creek is not dominated by any particular source areas. Overall, the most over-predicted watersheds for the base run were Borel Creek, Belmont Creek, Calabazas Creek, Walnut Creek, and Lower Penetencia. This was very similar to the PCB model calibration. These are in general more pristine watersheds with more benign land uses, and it appears that the calibrated parameters for Ag/Open might be too high. These watersheds are also dominated by “Other Urban”. The calibration for Other Urban is in the middle to upper range and could easily be pushed lower and still fit our conceptual model. Therefore it was hypothesized that adding parameterization for source areas in watersheds with plenty of Other Urban could help to push the coefficient and therefore improve the calibration for these relative clean watersheds.

Rail transport and Recyc Waste met this criterion, and trial runs were performed by adding these two source areas to baseline one by one. Adding Recyc Waste produced the best calibration results of all five parameter trials (Table P&M8; trials 3-8) but adding Transp Rail didn’t improve model calibration even when coefficients for Transp Rail was pushed against the upper boundary. The slope of a scatter plot

**Table P&M7. Calibration trials completed for the mercury regional watershed spreadsheet model. "Lower" and "Upper" indicate the lower and upper limits for each of the parameters in milligrams per kilogram that were set as the boundary conditions for each calibration trial. Initially, quite narrow lower and upper limits were set for each parameter based on the 10$^{th}$ and 90$^{th}$ percentiles of the available data (see Table P&M 3), but as discoveries were made, boundaries were widened to the minimum and maximum for each parameter (Table P&M3), and eventually to the overall minimum and maximum observed in any literature (Table P&M3).**

| Calibration trial description | Trial run # | All urban | | Ag/Open | | Other urban | | Old urban | | Old Industrial | | Old urban and industrial | | crematoria | | manufMetals | | recycAuto | | transpRail | | electricTransf | | recycWaste | | Allrecycle | |
|---|---|---|---|---|---|---|---|---|---|---|---|---|---|---|---|---|---|---|---|---|---|---|---|---|---|---|---|
| | | Lower | Upper | Lower | Upper | Lower | Upper | Lower | Upper | Lower | Upper | Lower | Upper | Lower | Upper | Lower | Upper | Lower | Upper | Lower | Upper | Lower | Upper | Lower | Upper | Lower | Upper |
| Base | 1 | | | 0.08 | 0.26 | 0.13 | 0.89 | 0.18 | 3.2 | 0.22 | 5.6 | | | | | | | | | | | | | | | | |
| Base (rerun) | 2 | | | 0.08 | 0.26 | 0.13 | 0.89 | 0.18 | 3.2 | 0.22 | 5.6 | | | | | | | | | | | | | | | | |
| Base plus crematoria | 3 | | | 0.08 | 0.26 | 0.13 | 0.89 | 0.18 | 3.2 | 0.22 | 5.6 | | | 0.15 | 0.84 | | | | | | | | | | | | |
| Base plus manufMetals | 4 | | | 0.08 | 0.26 | 0.13 | 0.89 | 0.18 | 3.2 | 0.22 | 5.6 | | | | | 0.30 | 1.5 | | | | | | | | | | |
| Base plus recycAuto | 5 | | | 0.08 | 0.26 | 0.13 | 0.89 | 0.18 | 3.2 | 0.22 | 5.6 | | | | | | | 0.24 | 6.78 | | | | | | | | |
| Base plus transpRail | 6 | | | 0.08 | 0.26 | 0.13 | 0.89 | 0.18 | 3.2 | 0.22 | 5.6 | | | | | | | | | 0.32 | 0.65 | | | | | | |
| Base plus electricTransf | 7 | | | 0.08 | 0.26 | 0.13 | 0.89 | 0.18 | 3.2 | 0.22 | 5.6 | | | | | | | | | | | 0.30 | 3.34 | | | | |
| Base plus recycWaste | 8 | | | 0.08 | 0.26 | 0.13 | 0.89 | 0.18 | 3.2 | 0.22 | 5.6 | | | | | | | | | | | | | 0.37 | 5.4 | | |
| Base plus best two (six params) | 9 | | | 0.08 | 0.26 | 0.13 | 0.89 | 0.12 | 3.2 | 0.22 | 5.6 | | | | | | | | | 0.32 | 9.0 | | | 0.37 | 9.0 | | |
| Base plus all Parameters wide limits | 10 | | | 0.07 | 0.32 | 0.11 | 4.3 | 0.12 | 6.6 | 0.13 | 9.0 | | | 0.14 | 1.0 | 0.29 | 1.9 | 0.17 | 9.0 | 0.32 | 0.80 | 0.28 | 5.5 | 0.31 | 9.0 | | |
| Base plus all Parameters same wide limits | 11 | | | 0.006 | 230 | 0.006 | 230 | 0.006 | 230 | 0.006 | 230 | | | 0.006 | 230 | 0.006 | 230 | 0.006 | 230 | 0.006 | 230 | 0.006 | 230 | 0.006 | 230 | | |
| Base plus all Parameters same wide limits (rerun) | 12 | | | 0.006 | 230 | 0.006 | 230 | 0.006 | 230 | 0.006 | 230 | | | 0.006 | 230 | 0.006 | 230 | 0.006 | 230 | 0.006 | 230 | 0.006 | 230 | 0.006 | 230 | | |
| New base plus best two plus all recycle | 13 | 0.006 | 230 | 0.006 | 230 | | | | | | | 0.006 | 230 | | | 0.006 | 230 | | | 0.006 | 230 | | | | | 0.006 | 230 |
| New base plus best two plus all recycle (rerun) | 14 | 0.006 | 230 | 0.006 | 230 | | | | | | | 0.006 | 230 | | | 0.006 | 230 | | | 0.006 | 230 | | | | | 0.006 | 230 |
| Simplified new base plus best two plus all recycle | 15 | 0.006 | 230 | 0.006 | 230 | | | | | | | | | | | 0.006 | 230 | | | 0.006 | 230 | | | | | 0.006 | 230 |
| Simplified new base plus best two plus all recycle (rerun) | 16 | 0.006 | 230 | 0.006 | 230 | | | | | | | | | | | 0.006 | 230 | | | 0.006 | 230 | | | | | 0.006 | 230 |

**Table P&M8. Coefficients for each calibration trial for the mercury regional watershed spreadsheet model. Red indicates a boundary violation during a calibration trial. Purple indicate a stability violation when a calibration trial was repeated with the same initial starting conditions.**

| Calibration trial description | Trial run # | All urban | Ag/ Open | Other urban | Old urban | Old Industrial | Old urban and industrial combined | crematoria | manuf Metals | recyc Auto | transp Rail | electric Transf | recyc Waste | Allrecycle | Comments |
|---|---|---|---|---|---|---|---|---|---|---|---|---|---|---|---|
| Base | 1 | | 0.14 | 0.66 | 0.18 | 1.18 | | | | | | | | | The coefficient for old urban met lower boundary and old urban< other urban does not fit the expected order. Same results between the base trial and the rerun of the base trial show that calibration trial was stable. |
| Base (rerun) | 2 | | 0.14 | 0.66 | 0.18 | 1.18 | | | | | | | | | |
| Base plus crematoria | 3 | | 0.14 | 0.65 | 0.18 | 1.33 | | 0.51 | | | | | | | The coefficient for old urban met lower boundary and old urban < other urban does not fit the expected order. Coefficient for crematoria seems plausible. |
| Base plus manufMetals | 4 | | 0.14 | 0.66 | 0.18 | 1.28 | | | 0.30 | | | | | | The coefficient for old urban and manufMetals met lower boundaries and old urban < other urban does not fit the expected order. |
| Base plus recycAuto | 5 | | 0.14 | 0.66 | 0.18 | 1.21 | | | | 0.24 | | | | | The coefficient for old urban and recycAuto met lower boundaries and old urban < other urban does not fit the expected order. |
| Base plus transpRail | 6 | | 0.16 | 0.62 | 0.18 | 1.31 | | | | | 0.65 | | | | The coefficient for old urban met lower boundary and old urban < other urban does not fit the expected order. TranspRail seems to have an influence of particle ratios but reaches the upper limit of the range set in the initial trial. |
| Base plus electricTransf | 7 | | 0.14 | 0.66 | 0.18 | 1.18 | | | | | | 0.30 | | | The coefficient for old urban and electricTransf met lower boundaries and old urban < other urban does not fit the expected order. |
| Base plus recycWaste | 8 | | 0.16 | 0.61 | 0.18 | 0.88 | | | | | | | 2.55 | | The coefficient for old urban met lower boundary and old urban < other urban does not fit the expected order. recycWaste seems to have a strong influence of particle ratios taking some of the share away from Old Industrial. |
| Base plus best two (six params) | 9 | | 0.20 | 0.53 | 0.12 | 0.59 | | | | | 2.22 | | 2.45 | | Even when the lower boundary was relaxed further, the coefficient for old urban met lower boundary and old urban < other urban does not fit the expected order. transpRail and recycWaste seem to have a strong influence of particle ratios taking a larger share away from Old Industrial than each do individually. |
| Base plus all Parameters wide limits | 10 | | 0.25 | 0.48 | 0.12 | 0.99 | | 0.14 | 0.33 | 0.21 | 0.79 | 0.37 | 8.35 | | The coefficients for old urban and crematoria met lower boundaries set for this trial and old urban < other urban does not fit the expected order. transpRail and recycWaste seem to have a strong influence of particle ratios although both reached the upper limits set for the trial. |
| Base plus all Parameters same very wide limits | 11 | | 0.72 | 0.12 | 0.24 | 0.29 | | 0.91 | 4.42 | 4.39 | 2.28 | 1.66 | 10.45 | | Wide difference between the coefficients for each of the parameters indicate calibration trial was unstable. |
| Base plus all Parameters same very wide limits (rerun) | 12 | | 0.28 | 0.28 | 1.24 | 0.24 | | 0.63 | 1.10 | 1.73 | 1.90 | 5.96 | 1.09 | | |
| New base plus best two plus all recycle | 13 | 0.43 | 0.24 | | | | 0.01 | | 3.01 | | 4.01 | | | 3.01 | Moderate difference between the coefficients for each of the parameters indicate calibration trial was unstable. Five parameters appears to be the current limit of the calibration data set (see PCB section trial runs #14 and #15). |
| New base plus best two plus all recycle (rerun) | 14 | 0.48 | 0.20 | | | | 0.12 | | 2.00 | | 3.83 | | | 2.65 | |
| Simplified new base plus best two plus all recycle | 15 | 0.42 | 0.25 | | | | | | 1.42 | | 2.57 | | | 2.21 | The coefficients make sense in relation to each other and to the empirical observations we have for the Bay Area. Same results between the first run and the rerun show that calibration trial was stable. |
| Simplified new base plus best two plus all recycle (rerun) | 16 | 0.42 | 0.25 | | | | | | 1.42 | | 2.56 | | | 2.21 | |

between observed and predicted particle ratios was well less than 1:1 for all of these trials and the correlation coefficients were low.

To further improve model calibration, a six parameter model (run#9) that included the four base parameters plus Transp Rail and Recyc Waste was explored, with wider limits for Old Urban (relaxed lower limit) and Transp Rail and Recyc Waste (relaxed upper limit). The coefficient was calibrated at 2.2 milligrams per kilogram for Transp Rail 2.4 milligrams per kilogram for Recyc Waste, respectively, and the coefficient for Old Urban was again pushed to the lower limit. The calibration results showed an overall slight improvement for over-predicted watersheds. However, the fact that the coefficient for Old Urban was calibrated lower than that of Other Urban continued to violate current field observation that Old Urban is in general more polluted than Other Urban. The slope of an XY scatter plot between measured and modeled particle concentration was also well less than 1:1 for this trial and the correlation coefficient was low.

Since calibrated coefficients for some parameters were forced against either the lower or upper limit during the trial runs 1-9 (Table P&M7), the limits were widened to the minimum and maximum possible particle ratios for all parameters (functionally, a 10 parameter model) (Table P&M3) in order to explore how far coefficients for each parameter can go if left unconstrained. The upper and lower bound was set the same for all parameters, with the lower bound of 0.006 milligrams per kilogram (McKee et al 2006b, table 3.1, Four Corners, NM) and the upper bound of 230 milligrams per kilogram (McKee et al 2006b, table 3.1, Turner Valley, Canada) from literature review. The relative order of the magnitude of resulting parameter coefficients from this trial run, however, was illogical. For example, the coefficient for Ag/Open was 0.72 mg per kilogram, greater than that of Other Urban. In addition, this trial appeared to be unstable; the magnitude of the coefficients as well as their relative order changed significantly between the initial trial run and a rerun. It was concluded that the 10 parameter model was too complex for the current number and characteristics of the calibration watersheds; some of the parameters are not well represented in these watersheds. A good compromise between model complexity and stability appears to be found by adding a few representative source areas to a simple land use based model.

To find a balance between model complexity and stability, the next two trials tested a simplified definition of the base land uses (lumping all urban together) and a reduced set of source areas. Initially four source areas were considered (All recycle, Transp Rail, Manuf Metals, and combined Old Urban/Old Industrial) but a rerun of trials #13 with different starting points (#14) indicated model is not stable as the coefficients between these two runs were moderately different (Table P&M8). Given that the influence of Old Urban and Old Industrial combined was relatively small in comparison to the other parameters, during trial 15 and 16, Old Urban and Industrial combined was dropped and model was proven stable. The resulting model coefficients appeared to follow a logical order with source area coefficients greater than the coefficients for land uses.

The final model calibration results (#15 & #16) indicate that the most polluted source areas for mercury may be only 10-fold more polluted than the average condition of the Ag/Open land-use category. This differs from the PCB model where much greater differences in the particle ratios between less polluted land use areas and the most polluted source areas are predicted. Based on the calibration trial runs investigated, it appears that a five parameter model may be compatible with the current set of calibration watersheds and the characteristics of those watersheds. It is possible that with a greater number of iterations during the calibration procedure (perhaps 1000 or more), a stable set of parameter coefficients could be found for a greater number of parameters (six or maybe even seven), but this could be explored in the future.

Given the nature of the PCB/Hg model as designed to simulate the long-term average condition, it is not surprising that the model tended to predict better for the watersheds with moderate level of pollution that is more closely representative of average condition, than the cleaner and dirtier watersheds as they represented more extreme situations (Figure P&M2). The calibration parameters tends to over-predict particle ratios for relatively “clean” watersheds and appears to both under- and over-simulate relatively “dirty” watersheds with higher observed particle ratios. This is likely caused by a combination of factors:

1. The available data tend to be biased towards urban watersheds of moderate pollution level, as such truly clean or very polluted watersheds are not strongly represented in the calibration dataset,
2. The spreadsheet model fails to capture or describe stochastic processes such as rainfall and run-off, wind, and other mechanisms of off-site transport of pollutants because of its relatively simple architecture.

The difference between the absolute magnitude of particle ratios in cleaner watersheds is large but the model calibration procedure produced coefficients that are in a conceptually logical order. Even though the model overall over-simulated cleaner watersheds and under-simulated dirtier watersheds, the overall regional pattern of clean watersheds being clean and dirty watersheds being dirty still holds. The calibrated parameters collectively resulted in a range of over and under prediction between 30% and 330% of the observed particle ratios (Figure P&M2b). Even as big as these errors appear, the model calibration could still be considered satisfactory , considering the varying quality of the observed calibration data and the relative consistency between over and under prediction (between 3-fold too high and 3-fold too low).

These findings accepted, the over prediction of relatively clean particle ratios may be somewhat offset in a later modelling step, when a delivery ratio is applied to adjust sediment loads (especially larger watersheds with less urban area). The final choice of parameters to include was a combination of land uses and source areas within the current calibration watersheds, not necessarily the most polluting source areas in the Bay Area. To include a greater number of potential polluting source areas in the model, a larger calibration dataset that includes watersheds with these source areas is needed. Similarly, a larger representation of cleaner

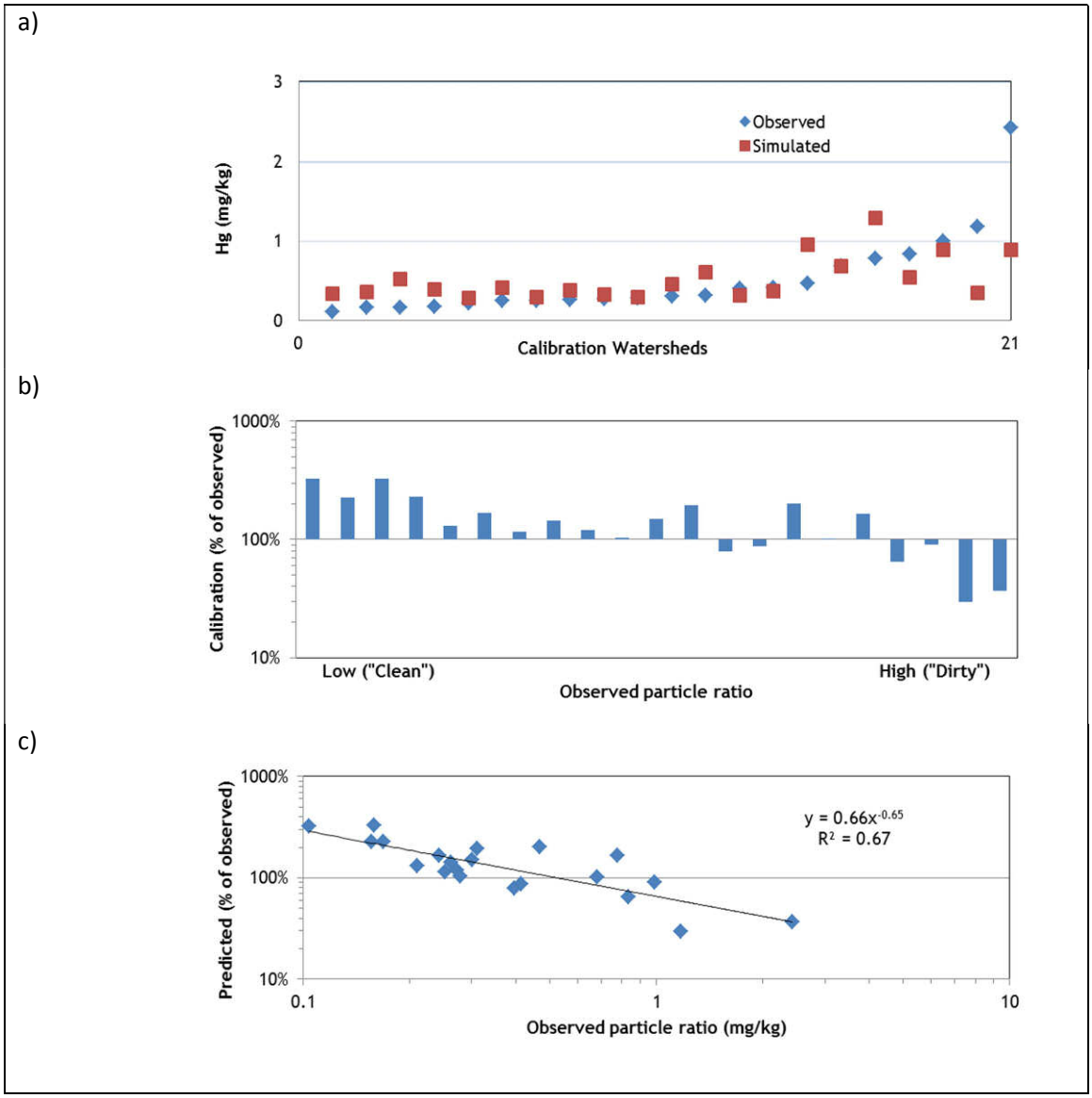


**Figure P&M2. Simulated in relation to observed particle ratios (mg/kg) for 21 watersheds in the Bay Area where data are available. Note generally, the calibration, although stable, tends to over predict relatively "clean" low particle ratio watersheds and appears to both under- and over-simulate relatively "dirty" watersheds with greater observed particle ratios.**

watersheds in the calibration dataset is needed in order to reduce the over prediction of cleaner watersheds in the current model. Constraining the Ag/Open land use parameter is not considered the best option. Future calibrations could explore separating Agriculture and Open land uses or differentiating between open spaces in urban areas that may be more polluted from open spaces in less urban areas to investigate if the open space parameter has more complexity. This could help legitimately reduce over-simulation of particle ratios in larger rural watersheds and reduce overall imbalances between cleaner land uses and dirtier source areas.

### A8.1.f. Running the PCB and Hg models

The PCB and Hg Models were developed in an ArcGIS platform using Python scripting language. Like the previously developed Hydrology Model (Lent and McKee 2011; Lent et al 2012) and the Copper Model (Section A7), the PCB and Hg Models are a tool box function accessed through ArcCatalogue and can be utilized by intermediate GIS users. The PCB and Hg Models interface with the output from the Sediment Model (Section A6). The PCB and Hg Models apply PCB or Hg coefficients based on land use and source area categories to the intersected polygons created in the Sediment Model. Each unique intersected polygon of the Sediment Model has, among other attributes, a landscape unit and an annual average sediment erosion mass (kg). Pollution coefficients (or potency factors: mg/kg) for each of the land use and source area parameters chosen during the calibration procedures described above, are multiplied by the sediment erosion associated with each parameter land unit to derive an annual average PCB and mercury erosion mass for each parameter. The model then sums the resulting annual erosion loads (kg) for the whole set of parameters within a watershed. The last step is to apply adjustment factors (a delivery ratio and a reservoir trapping efficiency) to compute the total watershed load.

To run a set of watersheds through the PCB and Hg Models, first the user must send those watersheds through the Sediment Model. The PCB and Hg Models tool box (development described in Section A4) then provides a user-friendly interface that calls upon the user to input the following files:

1. Sediment results geodatabase: this geodatabase is created after running the watershed shape file through the Sediment Model; the user must further select from that geodatabase the correct field that references the sediment loads.
2. PCB or Hg Coefficient Lookup Table: this table specifies an input concentration per land use or source area; the user must further select from this lookup table the field that references the land use or source area code associated with the land use/source area dataset and then must also select which field bins the land uses/source areas into more generalized categories (the summary tables output from the model are based on these more generalized categories, though there is no limit to the number of categories and may include all of the more specific land uses); finally, the user must select which fields include the input concentrations. The user may input as many input concentration fields as desired in a single run (although ideally all would be well calibrated) and an output load will be created for each set of input concentrations.
3. Results.gdb: this summary database is first created when running the watersheds through the Sediment Model. PCB or Hg loads for each set of input concentrations are appended to these summary tables.

At this time, the Hg and PCB models have slightly different model architectures (differing choices of land use and source areas), but a similar toolbox interface and style of input requirements.

## A8.2 PCB and Hg model performance verification

As described in the PCB and Hg methods, one method of model verification is afforded by a comparison of the load outputs from the model to measured loads for a subset of our local watersheds. There is varying confidence in the quality of the measured loads which have been computed using various techniques from data generated using various sampling designs that may or may not have captured concentration variability in relation to storms appropriately. In addition, the small subset of watersheds for which there is an estimated load available don't necessarily correspond to watersheds of high management priority. Therefore, although the results of this primary verification step are encouraging, verification does not necessarily portend further improvements are not possible; indeed further improvements exploring many of the suggestions described are quite likely and needed.

Loads simulated by the PCB model are primarily derived from the All Urban land use parameter in the larger watersheds such as Coyote Creek, Guadalupe River, Walnut Creek and San Lorenzo Creek (Figure P&M3). Even in Marsh Creek, where urban land use is minimal, the distribution of simulated PCB load between each land use and source area in the current version of the model is primarily associated with urban land use. This suggests that that the calibrated coefficient for the Ag/Open land-use parameter is presently too low or that for future model developments, nonurban land-use could be dropped altogether with little impact on the results. In contrast, the results suggest that for smaller watersheds like Zone 4 Line A and the three pump station watersheds (Ettie, Richmond and Pulgas) loads are dominated by industrial sources.

Based on the model outcomes for mercury for the set of verification watersheds, the Ag/Open parameter is estimated to play a larger role in the loads from our larger watersheds than urban sources. Although this makes conceptual sense, the magnitude of the coefficient for Ag/Open may need some further verification. The contribution of Ag/Open land use to the watershed scale load of mercury contrasts considerably from PCBs not only in the structural basis of the chosen model that resulted from the calibration process, but also in our conceptual understanding of the dispersion of mercury in the landscape. Similar to PCBs however, in smaller urbanized watersheds like Zone 4 Line A and the three pump station watersheds (Ettie, Richmond and Pulgas), the general All Urban land use parameter plays a larger role in simulated loads production as do the presence of the other source areas including recycling, metallurgy and rail transport. Overall, the relative contribution from each land use or source area further supports a hypothesis for the more ubiquitous dispersion of Hg relative to PCBs.

## A8.3 PCB and Hg loads estimates

### A8.3.a Regional PCB and Hg loads

One of the primary objectives of the spreadsheet model was to generate improved estimates of regional scale loads. Functionally this is done by simply adding up all of the simulated PCB and mercury load for each of the individual watersheds. Given the basic parameterization of the spreadsheet model, even if some of the individual watershed loads are spurious, the regional

loads, or sub-regional loads may be considered a little bit more representative of real conditions. Rather than providing single loading numbers only, to illustrate the utility of the model for estimating sub-regional loads, we collated the loads based on RMP Bay segments, and summed them for the region (Table P&M9). It is seen that the new estimate of regional scale PCB loads is 117 kg. This is about 6-fold greater than the load previously estimated (from McKee by scaling loading data from Guadalupe River and Coyote Creek to the area of urban land use in the Bay Area) and published in the San Francisco Bay PCB TMDL (20 kg: Water Board, 2008). Similarly, the simulated mercury load of 487 kg is about 2.6-fold greater than the estimate published in the San Francisco Bay mercury TMDL (160 kg urban; 25 kg non-urban: Water Board, 2006).

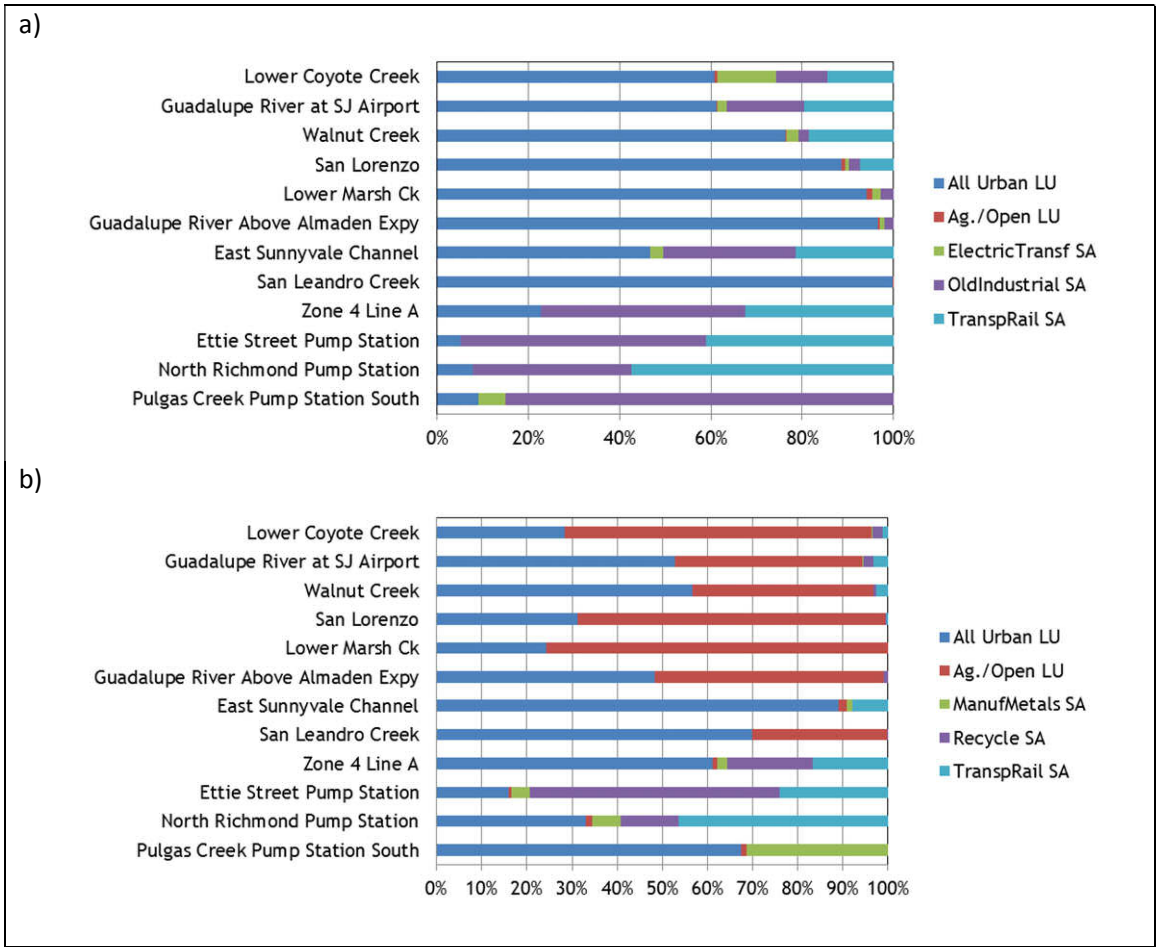


**Figure P&M3. Relative contribution of mass from each of the land use and source areas in the PCB model (a) and the mercury model (b).**

**Table P&M9. Sub-regional and regional scale loads (kg) of PCBs and mercury for the Bay Area in relation to RMP Bay segments.**

| Bay Segment | Total Hg Load (kg) | Total PCB Load (kg) |
|---|---|---|
| Lower South Bay | 87 | 19 |
| South Bay (East) | 61 | 14 |
| South Bay (West) | 39 | 12 |
| Central Bay (East) | 13 | 8 |
| Central Bay (West) | 15 | 3 |
| San Pablo Bay (South East) | 44 | 22 |
| San Pablo Bay (North West) | 98 | 8 |
| Suisun Bay (South East) | 85 | 26 |
| Suisun Bay (North West) | 46 | 5 |
| Total regional load | 487 | 116 |

Are these RWSM simulated loads estimates reasonable? The current best estimate of mean annual total regional flow is 1.525 thousand million meters cubed (Lent et al., 2012). Using this estimate and combining it with the RWSM simulations equate to an annual average regional concentration of 76 and 319 ng/L for PCBs and Hg respectively. A mean annual concentration of 76 ng/L is much greater than observed in any of our loads observation watersheds to-date (Gilbreath et al., in review); with further sampling this may end up being about the magnitude of flow-weighted mean concentration of either Sunnyvale East Channel or Pulgas Creek Pump Station watersheds. Similarly, PCB flow-weighted mean concentrations of 319 ng/L are observed in some of the more polluted watersheds in the Bay Area such as Guadalupe River or San Leandro Creek (Gilbreath et al., in review) or in San Lorenzo Creek, Zone 5 Line M (several of the urbanized watersheds) or Walnut Creek (an example of a high sediment load watershed) (McKee et al., 2012).

The current best estimate of regional scale sediment loads is 1.269 million metric t (Lewicki and McKee, 2009). Equating this with the model simulations suggests regional average particle ratios of 0.092 and 0.38 mg/kg for PCB and Hg respectively. San Lorenzo Creek, San Leandro Creek, Glen Echo Creek, Guadalupe River at Hwy 101, and Zone 4 Line A all have PCB particle ratios within approximately 25% of 0.092 mg/kg. Although these fall in the middle of the range of observations made so far in the Bay Area, these might be considered above average due to the sampling bias towards more polluted areas that was built into the sampling design. Similarly for Hg, East Sunnyvale Channel, Zone 4 Line A, Zone 5 Line M, Glen Echo Creek, and Pulgas Creek Pump Station North have measured particle ratios within 25% of 0.38 mg/kg. These are probably

representative of above average particle ratios for the region as a whole. The model appears to be calibrating as it should to the available calibration data but the data are inherently biased towards more polluted watersheds. During the next phases of model development, adding a weighting factor during calibration based on the exploratory categorization of watersheds into watershed classes (Greenfield et al., 2010) could be trialed.

### A8.3.b Spatial distribution of regional loads

The same simulated loading information can be viewed on a map to illustrate the spatially nuanced distribution of loads. Although the absolute accuracy of these loads should be considered questionable at this time (see previous section), individual watershed loads are presented to provide a proof of concept to provoke further discussion on how to improve the RWSM. The overall magnitude of annual average load has ramifications for pollution of the Bay. Large loads of relatively clean sediment may be helpful for diluting the particle concentrations in the Bay, and assuming fish tissue and wildlife endpoints are linked to sediment concentrations (Water Board, 2006; Water Board, 2008), may help to cause trends towards improved environmental quality of the Bay.

As was expected, the model simulations predicted that the larger watersheds in the Bay Area contribute generally larger PCB loads (Figure P&M4). This was also generally true for mercury (Figure P&M5) although mercury simulated loads were a little more influenced by sediment production and PCB loads were a little more influenced by urban and industrial land uses. As such, there are another group of smaller watersheds in the size range between a few square kilometers up to a few 10s of square kilometers where the presence of more polluting land uses in combination with medium watershed size also resulted in high simulated loads from individual watersheds.

For PCBs, the 25 watersheds with the largest loads (Table P&M10) account for 57% of the total regional load (Figure P&M6a). In contrast, the 25 watersheds that are estimated to produce the largest mercury loads account for 62% of the total regional load (Figure P&M6b). This result was not expected and is counter to the previous notions of PCB and mercury behavior in the region. Prior to this modelling exercise, it was anticipated that mercury would be more dispersed than PCBs and therefore overall more watersheds would contribute more evenly to the overall regional load. Stating it differently, 50% of the PCB and mercury load is estimated to be delivered by just 14 watersheds (Table P&M10); although the watershed list is different for mercury and PCBs.

### A8.3.c Watershed with greater loads per unit area

Watersheds with high area normalized loads may contribute loads disproportionally to smaller or semi-enclosed areas on the Bay margin. In these areas where water circulation and mixing and water and sediment dispersion may be less rapid, localized toxic impacts (due to either or both high water or sediment concentrations) may be more prevalent. Areas with this type of disproportional impact and their attending watersheds have been referred to as high leverage;

management actions focused in these areas may be more cost effective and have a greater chance of achieving improved Bay environmental quality relative to trying to manage areas with more dispersed pollution. A few such areas have been identified previously (the watersheds of Richmond, Pulgas and Ettie Street Pump Stations, Santa Fe Channel, and Leo Avenue) all of which are presently undergoing further investigations and enhanced management effort.

The simulated results from the RWSM indicate that for PCBs, area normalized loads (yields: ug/m$^2$) range from 221-2223 ug/m$^2$ in the top 25 simulated watersheds (Figure P&M7; Table P&M 11). Similarly, mercury yields range between 1962-344 ug/m$^2$ (note that the list of 25 watersheds are unique to each pollutant; Figure P&M8; Table P&M 11). Although not outside the realm of possibility, reported yields of this magnitude are rare and with the exception of Ettie Street Pump Station for PCBs and Guadalupe River for mercury, are at least 10-fold greater than any place observed in the Bay Area. That said, further sampling of the more industrialized watersheds in the Bay Area could reveal yields of this magnitude if concentrations like those observed in Santa Fe channel are observed elsewhere.

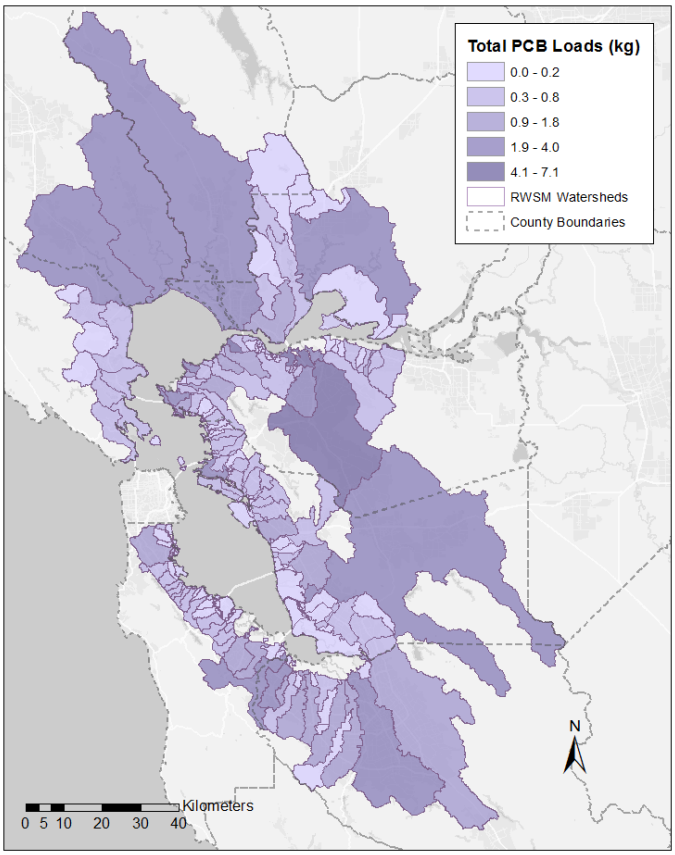


**Figure P&M4. The distribution of PCB loads in watersheds of the Bay Area estimated from the regional watershed spreadsheet model.**

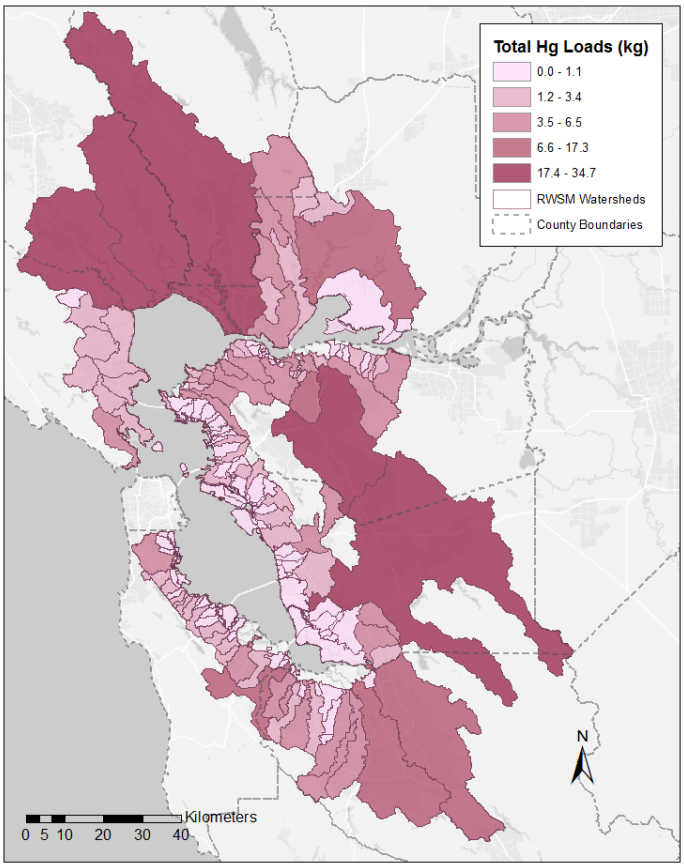


**Figure P&M5. The distribution of mercury loads in watersheds of the Bay Area estimated from the regional watershed spreadsheet model.**

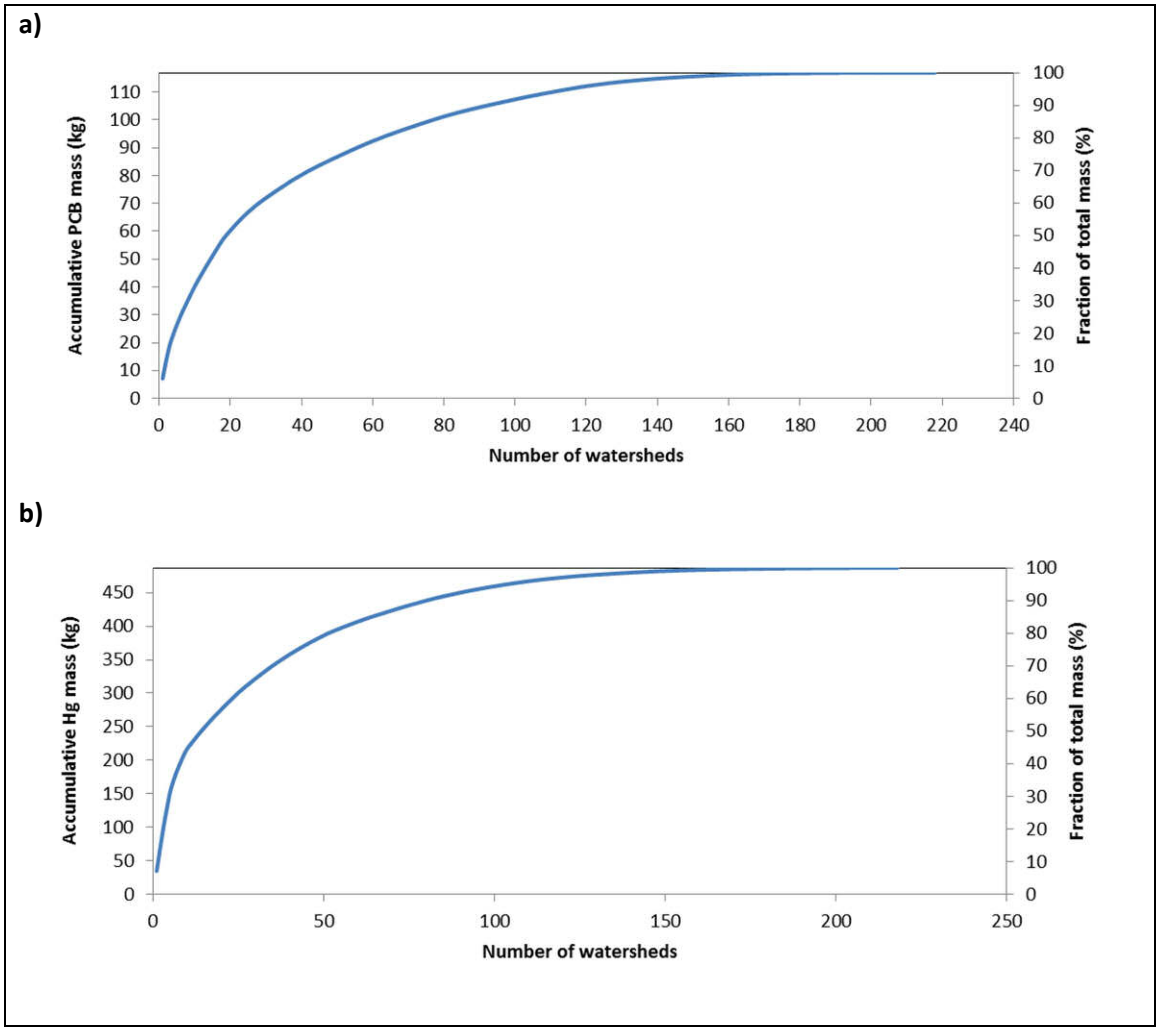


**Figure P&M6. Cumulative mass delivered to the Bay from each watershed based on outputs from the PCB model (a) and the mercury model (b).**

**Table P&M10. Watersheds with the largest PCB and mercury loads for the Bay Area estimated by the regional watershed spreadsheet model.**

| Watershed | PCB Estimated Load (kg) | | Watershed | Hg Estimated Load (kg) |
|---|---|---|---|---|
| Davis Point | 7.1 | | Napa River | 35 |
| Martinez Creek 4 | 6.6 | | Alameda Creek | 33 |
| Mallard Reservoir | 5.5 | | Mallard Reservoir | 32 |
| Walnut Creek | 3.9 | | Sonoma Creek | 29 |
| Matadero Creek | 3.3 | | Petaluma River | 25 |
| Point San Pablo Peninsula West | 3.2 | | Suisun Slough | 17 |
| Point Pinole | 2.8 | | Lower Coyote Creek | 14 |
| Petaluma River | 2.7 | | San Francisquito Creek | 12 |
| Grayson Creek | 2.6 | | Grayson Creek | 11 |
| Herman Slough and Castro Creek | 2.6 | | Guadalupe River | 9.4 |
| Sonoma Creek | 2.3 | | DonnerCreek | 6.5 |
| Napa River | 2.2 | | Matadero Creek | 6.4 |
| Suisun Slough | 2.2 | | PinoleCreek | 6.3 |
| Guadalupe River | 2.1 | | GreenValleyCreek | 6.3 |
| Alameda Creek | 2.1 | | SanPabloCreek | 5.8 |
| Alameda County unk09 | 2.1 | | San Lorenzo Creek | 5.7 |
| San Francisquito Creek | 2.1 | | San Tomas | 5.7 |
| Colma Creek | 1.8 | | Suisun Reservoir | 5.4 |
| Hercules | 1.6 | | Hercules | 5.2 |
| Pine Lake | 1.4 | | Martinez Creek 4 | 5.2 |
| Lower Coyote Creek | 1.4 | | Redwood Creek and Arroyo Ojode Agua Creek | 5.1 |
| Stevens Creek | 1.4 | | RodeoCreek5 | 5.0 |
| Parchester | 1.3 | | KirkerCreek | 5.0 |
| Redwood Creek and Arroyo Ojode Agua Creek | 1.3 | | PermanenteCreek | 5.0 |
| San Tomas | 1.2 | | Colma Creek | 4.9 |
| Total | 67 | | | 301 |

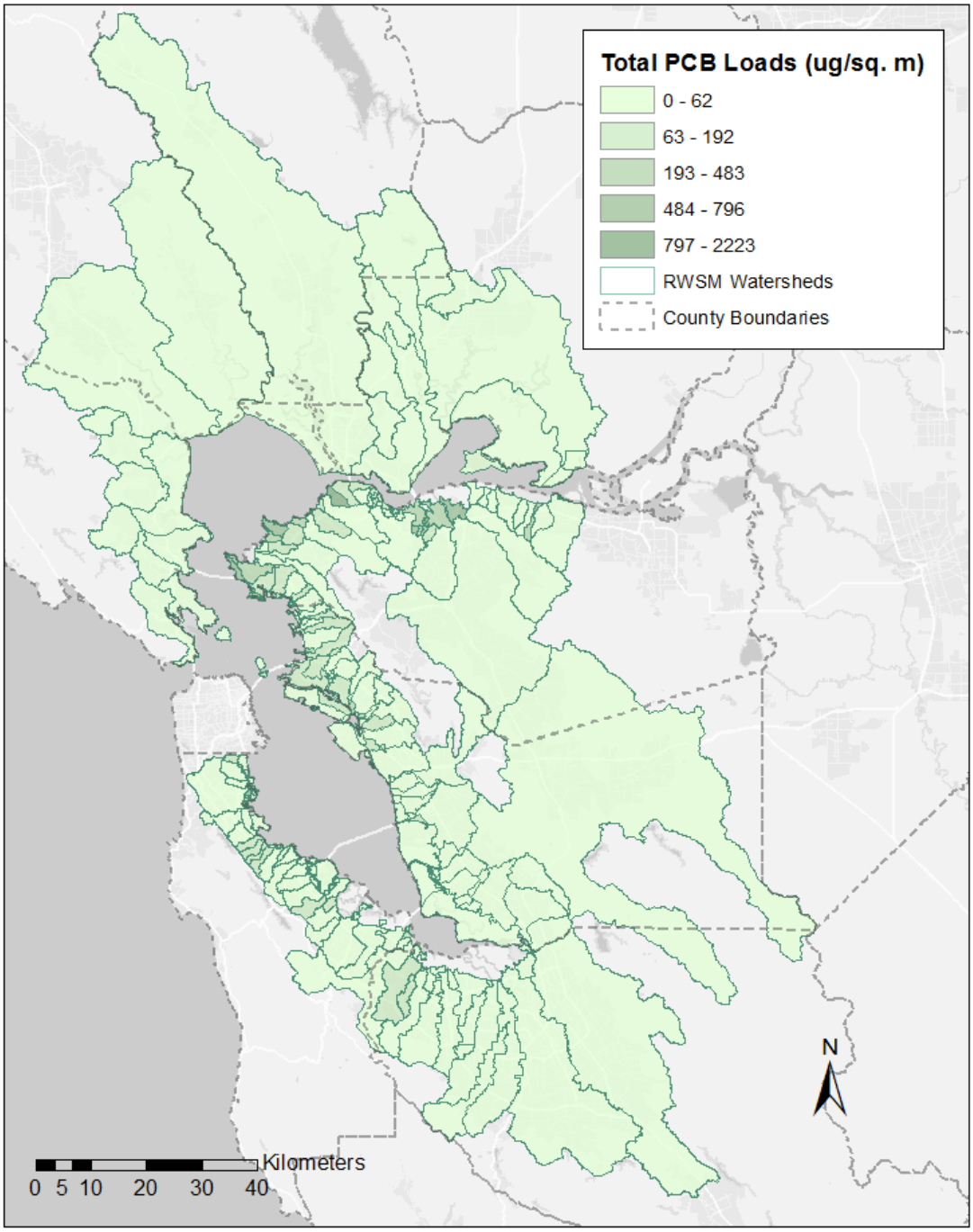


**Figure P&M7. High leverage watersheds (high unit area normalized PCBs loads) for the Bay Area estimated from the regional watershed spreadsheet model.**

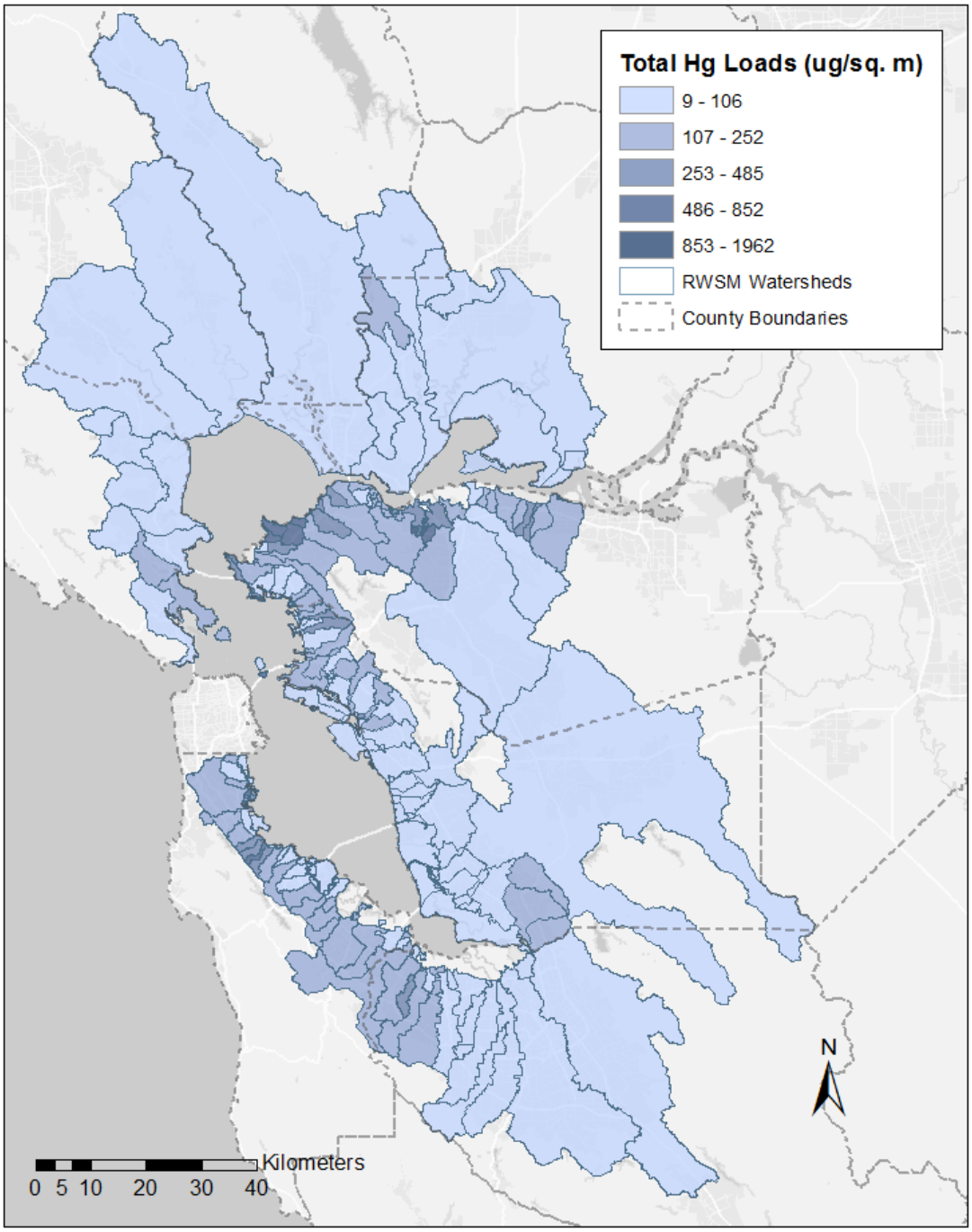


**Figure P&M8. High leverage watersheds (high unit area normalized mercury loads) for the Bay Area estimated from the regional watershed spreadsheet model.**

**Table P&M11. Watersheds in the Bay Area with the largest simulated PCB and mercury yields estimated by the regional watershed spreadsheet model.**

| Watershed | Total watershed area (km2) | PCB total load simulated (kg) | PCB total load simulated (ug/m2) | | Watershed | Total watershed area (km2) | Total simulated Hg load (kg) | Total simulated Hg load (ug/m2) |
|---|---|---|---|---|---|---|---|---|
| HerculesCreekandRefugioCreek | 0.196 | 0.435 | 2223 | | MartinezCreek6 | 0.490 | 0.962 | 1962 |
| DavisPoint | 4.90 | 7.13 | 1456 | | MartinezCreek5 | 0.713 | 0.954 | 1338 |
| MartinezCreek6 | 0.490 | 0.624 | 1273 | | HerculesCreekandRefugioCreek | 0.196 | 0.228 | 1166 |
| PointSanPabloPeninsulaWest | 4.01 | 3.19 | 796 | | MartinezCreek2 | 1.07 | 1.19 | 1117 |
| SMC_unk03 | 0.577 | 0.457 | 791 | | MartinezCreek1 | 0.898 | 0.765 | 852 |
| MartinezCreek2 | 1.07 | 0.713 | 669 | | MartinezCreek3 | 3.26 | 2.68 | 823 |
| WalnutCreek | 6.34 | 3.87 | 610 | | YerbaBuenaIsland | 0.576 | 0.418 | 725 |
| AC_unk12 | 0.133 | 0.0810 | 608 | | PointPinole | 4.67 | 3.31 | 707 |
| PointPinole | 4.67 | 2.78 | 596 | | Parchester | 2.67 | 1.71 | 639 |
| OysterPoint | 0.183 | 0.104 | 566 | | PinoleShores | 2.22 | 1.33 | 597 |
| Parchester | 2.67 | 1.29 | 483 | | EastonCreek | 2.76 | 1.56 | 565 |
| AC_unk06 | 0.110 | 0.0491 | 448 | | SMC_unk03 | 0.577 | 0.307 | 532 |
| PointSanPabloPeninsulaNorth | 0.795 | 0.337 | 425 | | GarrityCreek | 7.73 | 4.00 | 518 |
| MartinezCreek4 | 15.8 | 6.57 | 415 | | BarronCreek | 8.04 | 3.90 | 485 |
| AC_unk04 | 0.877 | 0.349 | 398 | | LawlorRavine1 | 3.43 | 1.62 | 471 |
| MartinezCreek5 | 0.713 | 0.237 | 332 | | AC_unk12 | 0.133 | 0.0624 | 468 |
| PinoleShores | 2.22 | 0.735 | 331 | | AC_unk01 | 0.136 | 0.0627 | 460 |
| MartinezCreek1 | 0.898 | 0.273 | 304 | | PointSanPabloPeninsulaNorth | 0.795 | 0.357 | 449 |
| LawlorRavine1 | 3.43 | 0.975 | 284 | | RodeoCreek11 | 0.126 | 0.0544 | 430 |
| HermanSloughandCastroCreek | 9.74 | 2.58 | 265 | | DavisPoint | 4.90 | 2.06 | 420 |
| AC_unk17 | 0.496 | 0.129 | 260 | | RefugioNorth | 1.37 | 0.572 | 418 |
| SMC_unk09 | 0.130 | 0.0338 | 260 | | RheemCreek | 5.27 | 2.16 | 410 |
| SMC_unk07 | 0.172 | 0.0413 | 241 | | MillsCreek | 4.13 | 1.53 | 370 |
| AC_unk15 | 1.30 | 0.297 | 229 | | PointSanPabloPeninsulaWest | 4.01 | 1.42 | 353 |
| AC_unk01 | 0.136 | 0.0302 | 221 | | SanchezCreek | 4.66 | 1.61 | 344 |
| Total | 62.1 | 33.3 | - | | Total | 64.8 | 34.8 | - |

From a management perspective, it is easier to manage and reduce loads when they emanate from concentrated sources and smaller watershed areas. The model predicts that 33.3 kg of PCBs emulates from watersheds with a total area of 62.1 km² into the Bay from the top 25 high leverage (high yielding) watersheds (Table P&M 11). This is equivalent to 28% of the simulated annual average PCB load emulating from just 0.93% of the modeling area. Similarly, the model predicts that as much as 7.1% of the annual average mercury load enters the Bay from high leverage watersheds (specific and unique to Hg) accounting for just 0.93% of the modeled area. This is consistent with our conceptual models of the relative nature of PCBs relative to Hg and

elusive nature and challenges associated with finding and managing watersheds polluted with PCBs and mercury from a legacy of past industrial, commercial and residential activities.

## A8.4 PCB and Hg model summary and recommendations

Five key questions were identified by the Small Tributaries Loading Strategy Team that can be utilized to help summarize the model development and simulations completed to-date:

- **What are the limitations of the PCB and Hg model structure?**

Summary:

The structural basis of the PCB and mercury RWSM is presently a combination of sediment loads from the sediment RWSM, a set of parameters based on land uses and source areas derived from previous literature reviews, and a set of coefficients for those parameters based initially on literature review and a series of model calibration runs specific to PCBs and mercury. The sediment model remains unverified and calibration runs for parameterization appear unstable. The addition of a climatic parameter may improve stability as would additional calibration data.

Recommendation:

- Complete the development of the sediment RWSM by adding a climatic parameter to the model and re-calibrating and verifying model performance. Use the new model to generate the regional, sub-regional, and watersheds specific sediment loads and complete documentation.
- The current set of land use and source area parameters, to a large degree, are limited by whether they are present in the calibration watersheds. Adding additional calibration watersheds with observed data specifically focused on the source area categories that are currently under-represented would allow an increased number of parameters to be included in the final model structure and have the potential to improve model performance. We recommend additional reconnaissance level stormwater monitoring during wet season conditions in industrial watersheds that contain the source area categories that are poorly represented in current calibration dataset. Such data could be collected at small pump station watersheds near the Bay margin using the methods developed by McKee et al (2011), or if possible, at even smaller scales for specific land uses and source areas to verify coefficients derived from the model calibration.
- The number of parameters that are possible for a stable model performance appears to be restricted to around five to seven. In the case of PCBs, one of these parameter slots is presently taken up for Ag/Open land-use. Since very little load is generated from this parameter, including this parameter in future model structures may not be warranted. In the case of mercury, given that much of the simulated load is associated with Ag/Open land use, there may be

justification for splitting this land use parameter further during future model development.

- When a larger number of parameters are included in the model calibration, increasing the number of iterations from 500 to 1000 or more during each calibration trial run may help to increase stability. The future model calibration will focus on exploring increasing the number of model parameters from five (the current level) to seven or ideally more (so that a wider variety of land use/source area combinations are represented in the model) using an increased number of iterations during the calibration procedure. As more calibration data become available, model structures with even greater number of parameters can be explored and an even greater number of iterations may be required to improve model performance and ensure calibration stability.

- **Were PCB and Hg EMC parameter coefficients (input data) representative?**

Summary:

The present version of the PCB and mercury RWSM uses a set of parameter coefficients that resulted from the mathematical auto calibration procedure. Initial boundary conditions for the auto calibration procedure were based on particle ratio data summarized during previous literature reviews.

- There is no land-use or source areas specific particle ratio data available for stormwater run-off in the Bay Area.
- The parameter coefficient for Ag/Open land-use for mercury is 0.24 mg/kg. This is very high compared to both empirical observations in some of the cleaner watersheds and baseline concentrations found in deep cores in the Bay. Given the fact that the model structure and the calibration process both gravitated toward representing average conditions, it is not surprising that the model over simulated mercury loads in more rural areas which represent the extremely clean end member conditions.
- The exclusion of Old Urban source areas as a model parameter for mercury was a surprise and defies our previous conceptual model for the distribution of mercury pollution. Perhaps our conceptual model needs to be reevaluated, or the lack of representative data in the calibration watersheds obscured the relevance of Old Urban source areas.
- The parameter coefficient for Ag/Open land use for PCBs is currently 0.00017 mg/kg. This seems unreasonably low. It is possible that the contribution loads associated with soil erosion from Ag/Open areas has been under-estimated.
- The parameter coefficient for Electric Transf for PCBs is currently 11 mg/kg. Although the calibration trial that generated this parameter coefficient was stable, and this magnitude is not unreasonable, in general this source area is poorly represented in the available calibration watersheds.

- The overall variation between the most polluted parameters and the least polluted parameters was approximately 50,000-fold for PCBs and 10-fold for mercury, respectively. This variation between parameter coefficients may be too large for PCBs and too small for mercury.
- The lack of inclusion of a broader range of parameters for both mercury and PCB models may lead to spurious conclusions regarding which watersheds may be considered high leverage.

Recommendation: Perform a sensitivity analysis to explore how the list of high leverage watersheds changes with the choice of coefficients. Include as many parameters as possible into model structure and where possible, verify the magnitude of the calibrated coefficients with field reconnaissance data and literature values.

- **Was the PCB and Hg model calibration adequate?**

Summary:

The model was calibrated based on particle ratio data available for 22 watersheds for PCBs and 21 watersheds for mercury, essentially the same set of watersheds for both pollutants.

- The quality of the particle ratio data in each watershed varies considerably due to the sample size and the rainfall run-off characteristics experienced during sampling in relation to heterogeneous land use and source area characteristics for each watershed.
- The available particle ratio data is biased towards moderately polluted watersheds; data for both less polluted watersheds and highly polluted watersheds are very sparse. As a result, the auto calibration process tended to calibrate well for the general urban category (moderately polluted) watersheds.

Recommendation: Further development and improvement of calibration data for the PCB and mercury RWSMs could be achieved through adding weighting factors to each calibration watershed based on the quality of data. Although adding weighting factors in relation to data quality may help improve the model calibration, adding some kind of weighting factors to represent the distribution of land uses or source areas of the Bay Area would likely yield a more representative calibration. One proposed method would be to derive weighting factors from the results of the regional watershed characterization study completed by Greenfield et al (2010).

- **Are the simulated PCB and Hg loads estimates likely accurate?**

Summary:

Verification to-date has been limited to loading data of variable quality available for just 12 watersheds for PCBs and 10 watersheds for mercury. Measured loads data are limited to a small subset of watersheds that do not coincide with nor are very representative of high priority

management areas. Therefore, it is a challenging to verify the confidence of the model for its primary purposes. The total regional loads currently simulated by the model are greater than the previous estimates reported in the PCB and mercury TMDLs for San Francisco Bay, and the back calculated regional scale particle ratios and flow weighted mean concentrations appear elevated as well. In addition, although plausible, the area normalized loads for individual watersheds (yields: ug/$m^2$) are greater than any observations currently available in the Bay Area. These outcomes suggest that the loads estimates are unreasonably high. The model, as it currently stands, is over-estimating loads from cleaner, larger watersheds, and under-estimating loads from more polluted watersheds. Since larger watersheds are few but cover the majority of land area and smaller watersheds are many but cover only a small area, these calibration issues need to be resolved.

- **Despite modeling challenges, can PCB and Hg high leverage watersheds be identified?**

Summary:

At the very least, the current model simulations can be considered a proof of concept for future model capabilities with improved calibration and verification based on the recommendations outlined above. Given the rather limited parameterization for the full range of source areas originally considered important for PCB and mercury loads in Bay Area watersheds, it is possible that some high leverage watersheds have been omitted from the current list, or that the list contains some watersheds that are not necessarily important from a management standpoint.

Recommendation: Further exploration of the source area fingerprint for the 25 identified high leverage watersheds should be carried out. Assuming this exploration does not demonstrate a strong bias towards the choice of model parameterization, this list could be used as a starting point for further reconnaissance verification. But it is always important to recognize the limitations of any modeling tool as an empirical approximation of the real world, and take this fact into account when evaluating the model performance or using the outputs for management purposes.

## A8.5 References

Box, M. J. 1965. A new method of constraint optimization and a comparison with other methods. Computer Journal, 8(1965):42-52.

Brown, C.B., 1944. The control of reservoir silting. U.S. Department of Agriculture. Miscellaneous Publication 521. Washington, D.C.

Davis, J.A., L. McKee, J. Leatherbarrow, and T. Daum. 2000. Contaminant Loads from Stormwater to Coastal Waters in the San Francisco Bay Region: Comparison to Other Pathways and

Recommended Approach for Future Evaluation. San Francisco Estuary Institute, Richmond, CA. http://www.sfei.org/sites/default/files/AB1429_Final_wcover.pdf

Gilbreath, A., Yee, D., McKee, L.J., 2012. Concentrations and loads of trace contaminants in a small urban tributary, San Francisco Bay, California. A Technical Report of the Sources Pathways and Loading Work Group of the Regional Monitoring Program for Water Quality: Contribution No. 650. San Francisco Estuary Institute, Richmond, California. 40pp. http://www.sfei.org/sites/default/files/Z4LA_Final_2012May15.pdf

Gilbreath, A.N., Gluchowski, D.C., Wu, J., Hunt, J.A., and McKee, L.J. (in review). Pollutants of concern (POC) loads monitoring data progress report, water year (WYs) 2012 and 2013. A technical report prepared for the Regional Monitoring Program for Water Quality in San Francisco Bay (RMP), Sources, Pathways and Loadings Workgroup (SPLWG), Small Tributaries Loading Strategy (STLS). Contribution No. xxx. San Francisco Estuary Institute, Richmond, California.

Greenfield, B., Klatt, M., Leatherbarrow, J.E., and McKee, L., 2010. Exploratory categorization of watersheds for potential stormwater monitoring in San Francisco Bay. A technical memo for the Sources Pathways and Loading Workgroup of the Regional Monitoring Program for Water Quality. San Francisco Estuary Institute, Oakland, CA. http://www.waterboards.ca.gov/sanfranciscobay/water_issues/programs/stormwater/MRP/2011_AR/BASMAA/B2d_2010-11_MRP_AR.pdf

Hunt, J., Gluchowski, D., Gilbreath, A., and McKee, L.J., 2012. Pollutant Monitoring in the North Richmond Pump Station: A Pilot Study for Potential Dry Flow and Seasonal First Flush Diversion for Wastewater Treatment. A report for the Contra Costa County Watershed Program. Funded by a grant from the US Environmental Protection Agency, administered by the San Francisco Estuary Project. San Francisco Estuary Institute, Richmond, CA. http://www.sfei.org/sites/default/files/NorthRichmondPumpStation_Final_19112012_ToCCCWP.pdf

Lent, M.A., Gilbreath, A.N., and McKee, L.J., 2012. Development of regional suspended sediment and pollutant load estimates for San Francisco Bay Area tributaries using the regional watershed spreadsheet model (RWSM): Year 2 progress report. A technical progress report prepared for the Regional Monitoring Program for Water Quality in San Francisco Bay (RMP), Small Tributaries Loading Strategy (STLS). Contribution No. 667. San Francisco Estuary Institute, Richmond, California. http://www.sfei.org/sites/default/files/RWSM_EMC_Year2_report_FINAL.pdf

Lewicki, M., and McKee, L.J, 2009. Watershed specific and regional scale suspended sediment loads for Bay Area small tributaries. A technical report for the Sources Pathways and Loading Workgroup of the Regional Monitoring Program for Water Quality: SFEI Contribution #566. San Francisco Estuary Institute, Oakland, CA. 28 pp + Appendices. http://www.sfei.org/sites/default/files/566_RMP_RegionalSedimentLoads_final_web.pdf

McKee, L., Leatherbarrow, J., Eads, R., and Freeman, L., 2004. Concentrations and loads of PCBs, OC pesticides, and mercury associated with suspended sediments in the lower Guadalupe River, San Jose, California. A Technical Report of the Regional Watershed Program: SFEI Contribution #86. San Francisco Estuary Institute, Oakland, CA. 79pp. http://www.sfei.org/sites/default/files/GuadalupeYear1final.pdf

McKee, L., Leatherbarrow, J., and Oram, J., 2005. Concentrations and loads of mercury, PCBs, and OC pesticides in the lower Guadalupe River, San Jose, California: Water Years 2003 and 2004. A Technical Report of the Regional Watershed Program: SFEI Contribution 409. San Francisco Estuary Institute, Oakland, CA. 72pp. http://www.sfei.org/sites/default/files/409_GuadalupeRiverLoadsYear2.pdf

McKee, L., Oram, J., Leatherbarrow, J., Bonnema, A., Heim, W., and Stephenson, M., 2006a. Concentrations and loads of mercury, PCBs, and PBDEs in the lower Guadalupe River, San Jose, California: Water Years 2003, 2004, and 2005. A Technical Report of the Regional Watershed Program: SFEI Contribution 424. San Francisco Estuary Institute, Oakland, CA. 47pp + Appendix A and B. http://www.sfei.org/sites/default/files/424_Guadalupe_2005Report_Final_0.pdf

McKee, L., Mangarella, P., Thompson, B., Hayworth, J., and Austin, L., 2006b. Review of methods used to reduce urban stormwater loads (Task 3.4). A Technical Report of the Regional Watershed Program: SFEI Contribution 429. San Francisco Estuary Institute, Oakland, CA. ~150pp http://www.sfei.org/sites/default/files/White%20Paper%20Review%20of%20methods%20to%20reduce%20urban%20stormwater%20loads.pdf

McKee, L.J., Hunt, J., Greenfield, B.J., 2010. Concentration and loads of mercury species in the Guadalupe River, San Jose, California, Water Year 2010. A report prepared for the Santa Clara Valley Water District in Compliance with California Regional Water Quality Control Board San Francisco Bay Region Order Number 01- 036 as Amended by Order Number R2-2009-0044, Requirement D. October 29, 2010. San Francisco Estuary Institute. http://www.sfei.org/sites/default/files/SFEI_Guadalupe_final_report_12_23_10_0.pdf

McKee, L.J., Gilbreath, A.N., Hunt, J.A., and Greenfield, B.K., 2012. Pollutants of concern (POC) loads monitoring data, Water Year (WY) 2011. A technical report prepared for the Regional Monitoring Program for Water Quality in San Francisco Bay (RMP), Small Tributaries Loading Strategy (STLS). Contribution No. 680. San Francisco Estuary Institute, Richmond, California. http://www.sfei.org/sites/default/files/POC%20loads%20WY%202011%202013-03-03%20FINAL%20with%20Cover.pdf

McKee, L.J., Gluchowski, D.C., Gilbreath, A.N., and Hunt, J.A., 2013. Pollutants of concern (POC) loads monitoring data progress report, water year (WY) 2012. A technical report prepared for the Regional Monitoring Program for Water Quality in San Francisco Bay (RMP), Sources, Pathways and Loadings Workgroup (SPLWG), Small Tributaries Loading Strategy (STLS).

Contribution No. 690. San Francisco Estuary Institute, Richmond, California. http://www.swrcb.ca.gov/rwqcb2/water_issues/programs/stormwater/UC_Monitoring_Report_2012.pdf

NRCS, 1983. Sediment sources, yields, and delivery ratios. Chapter 6. In: National Engineering Handbook, Section 3, Sedimentation. US Department of Agriculture, Natural Resources Conservation Service (SCS), 6.2–6.19. Washington DC, USA.

Water Board, 2006. Mercury in San Francisco Bay: Proposed Basin Plan Amendment and Staff Report for Revised Total Maximum Daily Load (TMDL) and Proposed Mercury Water Quality Objectives. Oakland (CA): California Regional Water Quality Control Board, San Francisco Bay Region 2. Accessed September 28, 2011 http://www.swrcb.ca.gov/rwqcb2/water_issues/programs/TMDLs/sfbaymercury/sr080906.pdf

Water Board, 2008. Total Maximum Daily Load for PCBs in San Francisco Bay: Final Staff Report for Proposed Basin Plan Amendment. Oakland (CA): California Regional Water Quality Control Board, San Francisco Bay Region 2. Accessed September 29, 2011 http://www.waterboards.ca.gov/sanfranciscobay/water_issues/programs/TMDLs/sfbaypcbs/Staff_Report.pdf

# APPENDIX 9. PBDE MODULE POLLUTANT PROFILE

## A9.1 Introduction and purpose

This profile was prepared by SFEI as one of a series supporting development of the Regional Watershed Spreadsheet Model (RWSM) for estimating pollutant loads to the San Francisco Bay per the joint RMP-BASMAA Small Tributaries Loading Strategy. The RWSM will be used to generate pollutant-specific sub-models using spatial datasets that define input runoff coefficients for local land use types and also pollutant-specific "source areas". The first step for each pollutant-specific sub-model is to review what is known locally and/or internationally about the sources or use characteristics and processes of release and transport of the San Francisco Bay. This information is then put together with what is known about available GIS layers on the proposed most important sources and a model structure and generalized work plan is recommended. This information for Polybrominated Diphenyl Ethers (PBDEs) is compiled into this profile.

BASMAA funded the preparation of this document to assist in fulfilling C.14 MRP requirements, but the profile's focus is on all potential sources to Bay, as well as conveyance by stormwater and local tributaries from the SF Bay watershed.

## A9.2 PBDEs: Description, historical usage, and behavior in environment

Polybrominated diphenyl ethers (PBDEs) are a group of flame retardant additives used in thermoplastics, polyurethane foam, and textiles. These materials are found in products within clothing, homes, offices, automobiles and airplanes. PBDEs are diphenyl ethers with one to ten bromine atoms attached (Figure 1) and although 209 congeners are possible, only some of the congeners are manufactured or result as degradation products.

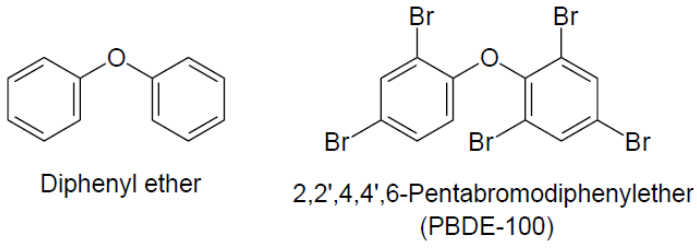


Diphenyl ether

2,2',4,4',6-Pentabromodiphenylether
(PBDE-100)

**Figure 1. Diphenyl ether structure and structure of BDE-100 (illustration from California Environmental Protection Agency, 2006).**

Over the last 60 years, concurrent with increasing applications of petroleum-based polymers, usage of flame retardants also increased as regulations led to their integration into the polymers to meet fire safety expectations. Organobromine compounds are the most effective of the halogenated organic flame retardants, and widespread usage and commercial production of PBDEs as a flame retardant began in the 1970s. There are three commercial mixtures of PBDEs, each named for the average bromination level of the various congeners that comprise the mixture ("penta-", "octa-", and "deca-BDE"; Table 1).

**Table 1. Commercial mixtures of PBDE flame retardants, congeners comprising each mixture, and the predominant usage of each mixture.**

| Commercial Mixture | Congeners present, listed in order of dominant composition (greatest to least)[a] | Predominant usage |
|---|---|---|
| **pentaBDE**[b] (commercially known as DE-71 and Bromkal 70-5DE) | BDE 99 (35-50%), 47 (25-37%), 100, 153, 154 and possibly minor amounts of 17, 28, 66, 85, 138 and 183 | Approx 95% used in polyurethane foam in furniture cushions, automobile seats and head rests, and mattresses; Approx 5% used in foam-based packaging and carpet padding |
| **octaBDE**[b] (commercially known as DE-79) | BDE 183 (40%), 197 (21%), 203 (5-35%), 196, 208, 207, 153 and 154. | Approx 95% used in ABS resins; Approx 5% used in other plastics for computers and kitchen appliances |
| **decaBDE**[b] (commercially known as DE-83R and Saytex 102E) | BDE 209 (97.5%), 206, 207 and 208. | General purpose flame retardant used in virtually any type of polymer, including thermoplastics, textiles, and back-coatings of consumer electronics, the backs of television sets, wire insulations, upholstery, electrical boxes, and high impact polystyrene (HIPS) plastic |

[a]Congener composition information from Alaee et al. 2003 and U. S. Environmental Protection Agency 2010.
[b]For this report, "pentaBDE", "octaBDE", and "decaBDE" will refer to the commercial mixtures and not the homologue group.

Scarce data on market demand for PBDEs is available (Table 2). The period of peak usage of each formulation is not well-known and likely varies across regions of the world. As described in a review by Hale et al. (2006), sediment core data from Europe and Japan show peaks in the early to mid-1990's, suggesting that peak market demand and usage occurred sometime prior given the time required for PBDEs to cycle from their products into sediments where they would be observed in sediment core data. In contrast, total self-reported environmental releases of decaBDE in the United States (U.S.) peaked in 1999 (53.9 metric tons (metric t)), and stayed at similar levels through 2002 (Toxic Release Inventory, accessed January 2013). There has since been a steady decline down to 21.1 metric t in 2007 and 8.4 metric t in 2011, likely due to the imminent ban on production and usage (in 2013, discussed later). If the US market tracks self-reported releases by US production/processing entities, this may suggest

**Table 2. Market demand statistics for PBDEs. Data in metric tons (metric t).**

| | 1991 | 1999[a] | | | 2001[b] | | | 2003[c] |
|---|---|---|---|---|---|---|---|---|
| | PentaBDE | PentaBDE | OctaBDE | DecaBDE | PentaBDE | OctaBDE | DecaBDE | All PBDEs |
| Americas | 4,000 | 8,290 | 1,375 | 24,300 | 7,100 | 1,500 | 24,500 | not reported |
| Europe | unknown | 210 | 450 | 7,500 | 150 | 610 | 7,600 | not reported |
| Asia | unknown | --- | 2,000 | 23,000 | 150 | 1,500 | 23,000 | not reported |
| Rest of world | unknown | unknown | unknown | unknown | 100 | 180 | 1,050 | not reported |
| Total | 4,000 | 8,500 | 3,825 | 54,800 | 7,500 | 3,790 | 56,100 | 56,418 |

[a] = Watanabe and Sakai, 2003
[b] = U.S. Department of Health and Human Services, 2004
[c] = U.S. Environmental Protection Agency, 2010

concentrations in the U.S. environment may not be expected to peak until post-2002, although it is unclear whether or not environmental peaks have yet occur ed. Indeed, core data from two out of three wetland areas in the San Francisco (SF) Bay collected in 2005-2006 showed increasing trends in PBDE concentrations without any sign of plateau (Yee et al., 2011). On the other hand, in a recent review of PBDEs in the SF Bay, Sutton et al., (in prep) reported that concentrations in water and sediment over the ten year period of record have not shown distinct trends, while concentrations in Bay wildlife are trending downward.

### A9.2.a Recent History of Environmental Concerns and Regulatory Response

Studies of PBDEs in laboratory animals have suggested potential concerns about liver toxicity, thyroid toxicity, developmental and reproductive toxicity, and developmental neurotoxicity (reviewed in U.S. Environmental Protection Agency, 2010). There is concern over human exposure to PBDEs, especially in children given the typical exposure mechanism being indoor dust coupled with the increased hand-to-mouth frequency for children. Studies of human blood, breastmilk and adipose tissue samples indicated rapidly increasing concentrations of PBDEs over the last two decades, with concentrations in North Americans generally several times higher than those seen in Europeans (U.S. Environmental Protection Agency, 2010). Although the most recent findings suggest that concentrations in SF Bay biota are decreasing (Sutton et al., 2013), PBDEs measured in humans and wildlife in the SF Bay Area are amongst the highest concentrations reported anywhere in the world (She et al., 2007; reviewed in Shaw and Kannan, 2009). One hypothesis for these elevated concentrations is the existence of California Technical Bulletin 117 (Zota et al., 2008) first passed in 1975, which requires a stricter degree of flame retardation in upholstered furniture than fire safety regulations elsewhere. Until phase-out in 2006, pentaBDE was the predominant flame retardant used to comply with TB 117.

Governments have responded to the rising environmental concerns over PBDEs with bans on production and usage (Table 3). The earliest bans went into effect in parts of Europe, and focused on the penta- and octa-BDE formulations due to the evidence that lower-brominated congeners bioconcentrate more readily than the higher-brominated congeners. Nevertheless, bans on deca-BDE have followed in some locations. In 2003, California passed Assembly Bill 302, becoming the first U.S. state to prohibit the manufacture, distribution, and processing of products containing the penta- and octaBDE formulations. This phase-out was originally scheduled for 2008, although the Legislature later accelerated that timeframe for phase-out to begin as of June 1, 2006. The United Stated Environmental Protection Agency (USEPA) has now negotiated with the two major U.S. manufacturers to end production, importation, and sales of decaBDE for most uses by December 31, 2012, and to end all uses by late 2013 (U.S. Environmental Protection Agency, 2010). The USEPA has also encouraged the other minor importers of decaBDE to join this initiative, although the ban does not prevent decaBDE importation.

**Table 3. Years when bans on PBDEs went into effect in various parts of the world.**

| | Year of Ban | | |
|---|---|---|---|
| **Location** | **pentaBDE** | **octaBDE** | **decaBDE** |
| California | 2006 | 2006 | 2013[1] |
| European Union | 2004 | 2004 | 2008 |
| Sweden | 1999 | unknown | 2007 |
| Australia | 2007 | 2007 | unknown |
| China | 2006 | 2006 | unknown |

## A9.2.b How do PBDEs behave in the environment?

PBDEs enter our surface waters primarily from stormwater runoff and sewage treatment plant discharges, as well as in minor amounts from rainfall and direct atmospheric deposition. PBDEs in the terrestrial landscape are primarily atmospherically deposited after emissions from production, use, and disposal/recycling. PBDEs are semivolatile organic compounds and have low water solubilities, however their vapor pressures differ enough from one another to affect their movement into and within various media of the environment. At air temperatures of 25°C, > 98% of the mono-, di-, triBDE (homologue group) congeners may be present in the vapor phase, tetra- and pentaBDE (homologue group) congeners begin to distribute more to atmospheric particles (e.g. BDE-47 is 10% particle phase, BDE-99 is 39% particle phase), hexa- and hepta- congeners are 87 - 99% particle phase, and 99% of BDE-209 is expected to be associated with airborne particles. This vapor versus particle phase distribution has important implications for how and where different BDEs move and settle in the environment.

[1] As described in the text above Table 3, this "ban" is actually a negotiation between the U.S. EPA and the two major U.S. manufacturers to end production, importation, and sales of all decaBDE by the end of 2013. This does not effectively ban importation of decaBDE by smaller importers.

***Air:*** Lower-brominated homologs (e.g., tri- and tetraBDE) are volatile and persistent enough to permit long-range transport. In fact, the tetra-brominated BDE-47 has even been detected in environmental samples in remote regions of the world such as the Arctic and Tibetan Plateau (de Wit et al., 2006; Wang et al., 2009a). Higher-brominated congeners (e.g. BDE-209) may also be found in air samples, but are more likely to deposit closer to their sources as they are more prone to wet and dry atmospheric deposition. For example, in a study of atmospheric concentrations of PBDEs in urban and rural areas of the Great Lakes region, Strandberg et al. (2001) found that the dominant congeners in air samples were BDE-47, -99, and -100, while BDE-209 was only detected in the Chicago area, likely near to point sources. Ambient and near source air monitoring has been conducted by the California Air Resources Board (CARB) in California urban areas and near automobile shredders and electronics recycling facilities. While all urban areas contained background levels, the near source areas were highly elevated in comparison (results discussed in greater detail later).

***Soil/sediment:*** Adsorption of PBDEs increases with bromination and organic carbon content of soil and sediment. PBDEs in soils across the landscape are therefore expected to be in greater concentrations nearest to point sources – urban areas, and source areas within the urban environment. In particular, decaBDE (predominantly BDE-209) is expected to deposit near its source and not be particularly mobile in the environment. DecaBDE will transport however, via the particle it is bound to as that particle is mobilized through the environment (e.g. in stormwater runoff).

***Water:*** In water, greater proportions of the lower-brominated homologs will remain suspended in the water column as compared to the higher-brominated homologs that are more likely to settle out on sediment particles. In the SF Bay, BDE-47 is the congener found in the highest concentrations in the water column, whereas BDE-209 is the dominant congener in the Bay's surficial sediment samples (Klosterhaus et al., 2012).

***Stormwater:*** Stormwater represents an important pathway particularly for the particle-bound higher-brominated PBDEs (e.g. BDE-209) to move from the terrestrial landscape to the Bay. Stormwater concentrations in Zone 4 Line A, a 100% urban tributary in Hayward, showed a strong correlation with turbidity, for both the sum of PBDEs as well as the individual congeners BDE-47 and BDE-209 ($r^2$ = 0.88, 0.9, and 0.86, respectively; Gilbreath et al., 2012). In this watershed, an estimated 99.3% of the total PBDE load was transported during storm flow conditions and 58% of the total load was BDE-209 and 6% was BDE-47 thus the majority of PBDEs in stormwater are accounted for with these two BDEs alone. BDE-99, 206, 207 and 208 contributed another 5-10% of the load. These observations are consistent with other local urbanized tributaries in the SF Bay Area well (Oram et al., 2008).

***Debromination and transformation:*** Lower-brominated PBDEs are more lipophilic, and hence more likely to accumulate in aquatic organisms, than their higher-brominated

counterparts. However, studies suggest that transformation of higher-brominated congeners to more bioaccumulative forms may occur through microbial degradation, metabolic debromination, photodegradation, and possibly reaction with the hydroxyl radical (reviewed in U.S. Environmental Protection Agency, 2010).

## A9.3 Release mechanisms to the environment and possible pollutant source areas

Environmental sediment core data from numerous studies generally show increases in PBDEs beginning in the late 1960's or early 70's (Qiu et al., 2010; Zegers et al., 2003), concurrent with the beginnings of commercial production. Although in California the penta- and octa-formulations were banned in 2006, and production, importation, and sales of decaBDE by the two major US manufacturers will end for all uses by the end of 2013, the volume of PBDEs still in use in products manufactured prior to these bans is enormous. Steadily over the next several years to decades, this standing stock will be disposed of or recycled, creating still further opportunities for PBDEs to enter the environment. Releases of PBDEs to the environment can occur during initial synthesis of the compounds, during its incorporation into polymers, during the usage of products containing PBDEs, and as the result of disposal, recycling or incineration of PBDE-containing products. These pathways of release into the SF Bay Area environment are explored in this report subsection.

**Initial synthesis:** There are no locations of manufacture of PBDEs in the SF Bay Area. PBDEs were historically manufactured within the U.S. only in Arkansas and will no longer be manufactured at all in the U.S. after 2013.

**Releases from incorporation processes into polymers:** Given the recent bans on usage in consumer products, sites of PBDE incorporation into polymers should not be a continuing mechanism of release into the environment. However, legacy contamination may exist around areas where such manufacture occurred in the past. While not an exhaustive list of decaBDE sources as only certain emitters are required to self-report, the USEPA Toxic Release Inventory (TRI) includes two business locations within the Bay Area that self-report on- and off-site releases of decaBDE. Both locations are in the Peninsula region (Redwood City and Menlo Park) and are associated with Tyco Thermal Controls. While the majority of decaBDE disposal from these businesses has been done through landfilling and recycling, air emission releases have also been reported. At the Redwood City location for nearly the entire period between 1991 and 2005, Tyco self-reported air emission releases of 113 kg of decaBDE each year. This is a significant load in relation to the previously estimated annual load to the SF Bay of 33-52 kg (BDEs 47+209; Oram et al., 2008). Other business types that may be important source areas include manufacturers of electronics equipment, plastics, cars, carpet and furniture.

**During product usage:** Degradation of in-use products containing PBDEs is an important mechanism of exposure for humans and release particularly to the indoor environment. PBDEs

are additive flame retardants, meaning they are simply blended into polymers rather than chemically bonded, enabling them to readily leach out of products. As a result, indoor dust represents the primary exposure pathway for most humans. Some of this dust migrates outside, some goes down our drains to sewage treatment plants, and some goes into the garbage can (e.g. through disposal of waste from vacuum cleaners) for disposal at a landfill. In addition, clothing is both a source as well as a filter for air and thus dryer lint is enriched with PBDEs (Stapleton et al., 2005), which is usually partially trapped in the dryer lint trap and disposed of in the garbage and partially vented to an outside wall of each house. In the outdoor environment, PBDEs are found ubiquitously, with more densely populated urban areas generally containing higher concentrations of PBDEs than agricultural and rural areas (with the exception of sewage sludge-applied lands (e.g. Strandberg et al., 2001)).

Source areas of in-use products that may have concentrations of PBDEs greater than the general urban signal might include:

- Carpet, upholstery and furniture manufacturers and warehouses
- Electronics manufacturers and distribution warehouses
- Foam manufacturers and distributors

Due to recent bans on PBDEs, these source areas are not expected to continue to release PBDEs at the same rates in the future, however, the immediate surrounding landscapes of the above-listed areas may have elevated PBDE concentrations due to a legacy build-up of leached PBDEs.

**Disposal and recycling:** The most important remaining pathway for PBDE release into the environment is in the process of disposal – into landfills, recycling, or in sewage sludge. Landfill disposal is not expected to result in significant environmental releases because of the US laws for municipal solid waste landfills aimed at creating conditions to prevent such releases (liners, treated leachate[2]) (U.S. Environmental Protection Agency, 2010). However, environmental releases are expected or have been shown to result for all of the following source areas:

- E-waste recycling facilities
- Automobile shredding and recycling facilities or “Autoshredders”
- Carpet and foam recycling facilities
- Sewage Sludge application to rural lands
- Publicly Owned Treatment Works (POTW) sewage sludge incinerators

California e-waste is estimated at 1200 metric t/yr (Petreas and Oros, 2009) and comprises the largest proportion of PBDEs in the California waste stream. E-waste today is reflective of the magnitude of electronics sold in previous years, which increased (by weight, see Figure 2) steadily in the 1980’s, and sharply in the 1990’s to a peak of nearly 3 million short tons (2.92 M

[2] Untreated leachate has been found to contain PBDEs, however in the one study that addressed PBDE concentrations in treated leachate, no PBDEs were detected (reviewed in U.S. Environmental Protection Agency, 2010).

metric t) in 2000, and has since plateaued (U.S. Environmental Protection Agency, 2011). The USEPA estimates the average lifespan of most electronic products to range between 5 and 15 years, depending on the product. Therefore, despite the recent PBDE bans in California, we would expect PBDEs to remain in the e-waste stream for many years to come, and BDE-209 is expected to dominate the congener profile for these products. E-wastes are usually recycled, landfilled or incinerated, and a large proportion of e-wastes are exported to China. Elevated PBDE concentrations in runoff from e-waste recycling facilities may be expected, however the only studies to report sample data near such facilities are from China (see Table 4) where e-waste recycling practices may differ from practices in the U.S.

Autoshredders may pose as another important source area for PBDE releases given that PBDEs have been used in the plastics and foam within automobiles. Seven autoshredder facilities in California, two of which are in the SF Bay Area (Sims Metal Recycling in Redwood City and Schnitzer Steel in Oakland), generate an estimated 300,000 tons of waste (including millable components of automobiles, refrigerators, and ovens) each year (Department of Toxic Substances Control, 2002) primarily to be used as alternative daily cover (ADC; material other than soil placed on the surface of municipal solid-waste

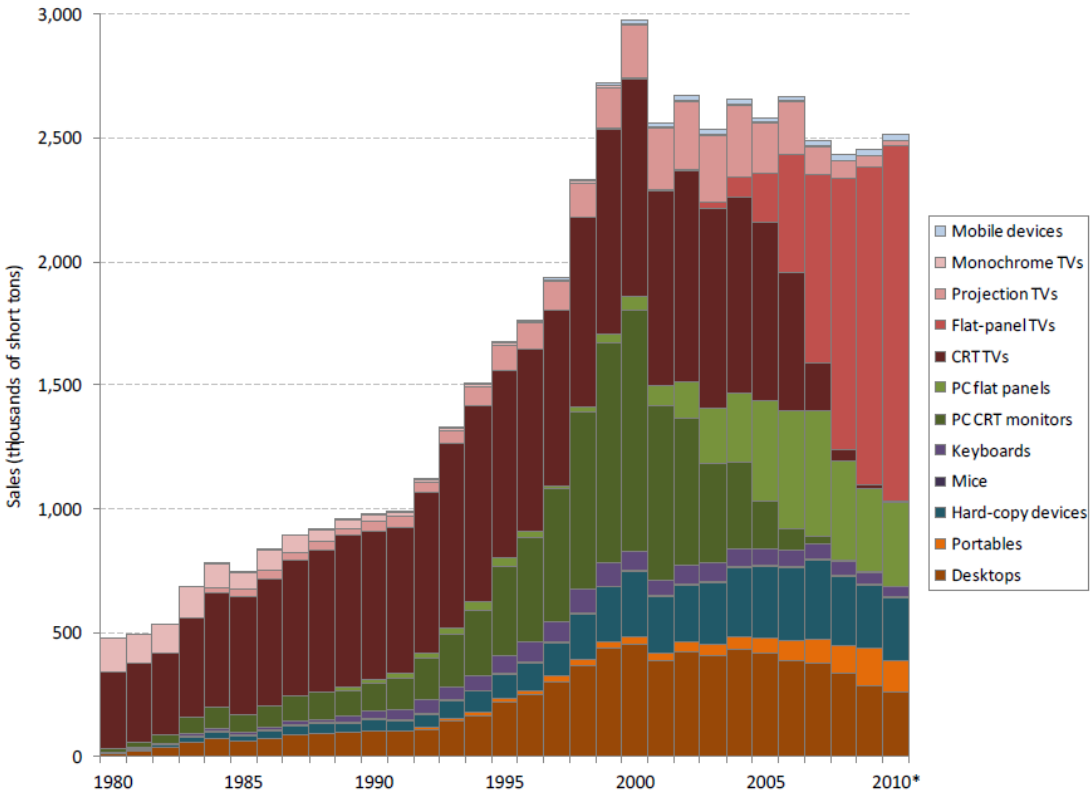


**Figure 2. Annual sales of electronic products (in thousands of short tons) (from U.S. Environmental Protection Agency, 2011, without permission). PBDEs in these products range up to 30% by weight (Hale et al., 2003).**

landfills at the end of each operating day). Shredder waste consists of glass, fiber, rubber, automobile fluids, dirt and plastics found in automobiles and household appliances that remain after the recyclable metals have been removed (Department of Toxic Substances Control, 2002). Autoshredder waste sampled in the SF Bay Area contained approximately 50,000 ng/g of total PBDEs (Petreas and Oros, 2009), though higher levels have been reported elsewhere (310,000 ng/g in Japan, Sakai et al., 2006). While usage as ADC in lined landfills is not expected to release PBDEs into the environment (U.S. Department of Health and Human Services, 2004) such that it would be available for transport to surface waters, autoshredder facilities can be an important local source when wind blows shredder residue or "auto fluff" onto surface waters or surrounding areas).

The CARB conducted ambient air monitoring in urban areas of California and near e-waste recycling and autoshredder facilities. BDE-209 near an electronics recycling facility measured up to 11,000 pg/$m^3$ and up to 1,900 pg/$m^3$ near an auto-shredding facility (Charles et al., 2005). These elevated near-source concentrations contrast sharply with ambient urban concentrations averaging 25 pg/$m^3$ of BDE-209 in six SF Bay Area and Southern California cities (average of 160 pg/$m^3$ for the sum of PBDEs in 2004 monitoring; CARB website http://www.arb.ca.gov/app/dioxin/cadamp.php).

No data could be found on water or soil concentrations of PBDEs in or around carpet, carpet padding and foam recycling facilities. However, exposure to these sources has been shown to cause significantly elevated blood serum levels of PBDEs in humans (Stapleton et al., 2008) and thus areas surrounding these facilities may have elevated concentrations due to PBDE releases through the crumbling of this material at the end of its life and as it is being physically manipulated for disposal. A simple hypothetical scenario (inclusive of numerous untested assumptions) illustrates the potential magnitude of PBDEs that may be released into the environment from this source. An estimated 175,000 metric t of carpet and carpet padding was discarded to landfills and recycling in California in 2011 (CARE, http://www.carpetrecovery.org/, accessed Jan.2013). Assuming carpet padding represents approximately one quarter of the total discarded mass by weight, PBDEs in the carpet padding equal approximately 0.3% by weight (based on studies overseen by Dr. Robert Hale and reported by the Carpet Cushion Council, http://www.carpetcushion.org/bonded-cushion.cfm), 0.5%[3] of the PBDEs in that material are released to the environment during the disposal or recycling process, and then weighting the resulting load by the percentage of the California population living in the Bay Area (19%), then 125 kg of PBDEs would be released annually from discarded carpet padding. Again, this is a significant load in relation to the previously estimated annual load to the SF Bay of 33-52 kg (BDEs 47+209; Oram et al., 2008).

PBDEs have been found in high concentrations in sewage sludge. Land application of biosolids is generally viewed as beneficial (e.g. the U.S. EPA: http://water.epa.gov/polwaste/wastewater/treatment/biosolids/genqa.cfm), however, it also is

[3] It is unknown how realistic this assumption is.

a mechanism of redistribution of PBDEs out into the rural environment. Hale et al. (2001) tested 11 sludge samples from four different states and found that the sum concentrations of the -47, -99, -100, -153, and -154 congeners were relatively consistent regardless of location of pre-treatment, ranging from 1,100 to 2,290 ng/g. This exceeds some European sludge concentrations of these congeners by 10 to 100-fold (Hale et al., 2001; reviewed in de Wit, 2002). Concentrations of BDE-209 in the Hale et al. (2001) samples varied more greatly between 84.8–4,890 ng/g. Measurements of PBDEs in sewage sludge of the SF Bay Area are within a similar range: one POTW sampled in 2002 (North, 2004) and three others sampled in 2005 (Petreas and Oros, 2009) contained average total PBDE concentrations of 2,600 ng/g, and biosolids measured from two SF Bay Area treatment plants were 2,917 and 3,651 ng/g (County of Solano, 2012).

A report commissioned by the Bay Area Clean Water Agencies noted that the SF Bay Area produced 158,000 metric t of sewage sludge in 2007, and this number is projected to rise with increasing population (Mitchell, 2009). Of this, 19% (~30,000 metric t) was land applied (Figure 3; Mitchell, 2009). At an average concentration of 2,800 ng/g, an estimated total of 84 kg of PBDEs are annually released through sewage sludge land application. Although it is unknown how much of this load is applied within the Region 2 boundary, Solano County reported an approximate average of 10,000 tons being land applied annually between 2002 and 2011 (County of Solano, 2012), so at least approximately 25-30 kg of PBDEs are being land applied within Solano County. Again, as compared with the previously estimated annual loads to the SF Bay, this back-of-the-envelope calculation shows that sewage sludge land application may have a significant role in PBDE loading to the Bay from at least certain small tributaries. Note however, that Solano has a higher proportion of crop agricultural land than most other Bay Area counties thus Solano is not necessarily typical.

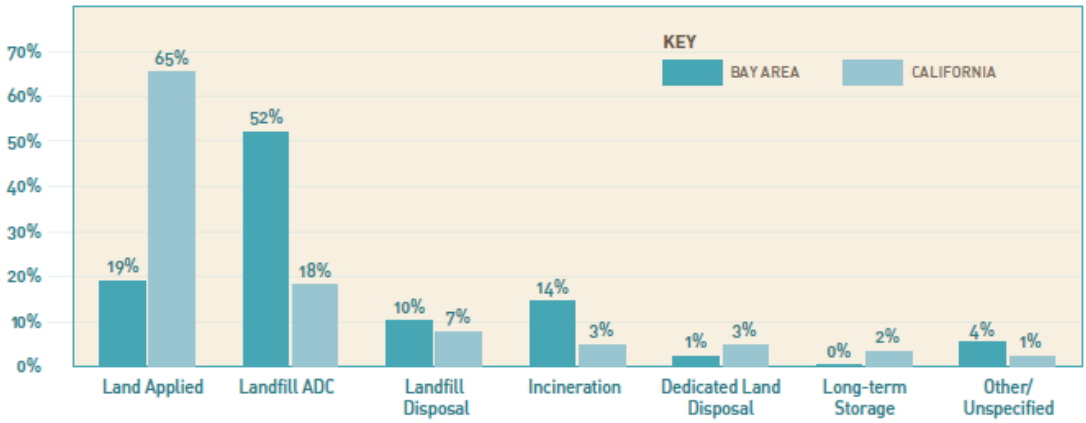


**Figure 3. Bay Area and California biosolids management practices in 2007 (figure from Mitchell, 2009 without permission).**

Landfilling of sewage sludge (as ADC) is not expected to result in environmental release, but incineration may. Only two POTWs in California incinerate biosolids, both of which are located in the SF Bay Area, explaining why a much greater portion of biosolids in the SF Bay Area are incinerated as compared to California as a whole (Figure 3). In a 2004 study in which stack emissions from a SF Bay Area POTW incineration facility were analyzed for brominated dioxins and furans, North noted that PBDEs were not measured because it was assumed all PBDEs would be transformed to dioxins during the process. Given that this study reported 96% of the PBDEs entering the POTW were trapped within the sludge, a follow-up study to verify that assumption may be warranted. Areas surrounding the two POTW incinerators located in the cities of Palo Alto and Concord may therefore represent source areas, however this hypothesis has not been studied.

## A9.4 Source areas and pollutant concentrations in soils

Soils data from a survey of the world literature supports the hypothesis that higher PBDE concentrations are generally found in the urban environment relative to the rural environment. The world literature on PBDE concentrations in soils is dominated by studies conducted in Europe (UK, Sweden, Norway, France) and China. Few studies have reported soils concentrations in the U.S. and to our knowledge, no soils data is available for the SF Bay Area. In the following tables, we report statistics on soils data collected in individual studies (Table 4), as well as summarize this data into land use classes (Table 5) that may be considered for our regional modeling efforts.

The ordering scheme was chosen because most of the studies reported mean concentration data, whereas fewer studies reported medians (Table 5). The ordering would be very similar if the classes had instead been organized by maximum concentrations measured in each class, though the “urban” category would have moved farther down the list. This general ordering matches the conceptual model of PBDEs as a relatively ubiquitous urban contaminant, with a few important source areas. However, there is much deviation within this scheme when considering the individual studies (Table 4), and in part this is due to the variable definitions for land use terms. For example, Duan et al. (2010) looked at PBDE concentrations on a small island in China where the mean concentrations sampled amongst the various rural land uses there (5.5-14 ng/g) are elevated above some urban areas in France, the UK, and even other locations in China (Muresan et al., 2010; Harrad, 2006; Jiang et al., 2010). Likely, these more elevated concentrations are the result of Chongming Island’s proximity to a very urban landscape (Chongming Island is part of the Shanghai municipal area and includes modern shipbuilding, port machinery and communications equipment manufacturing, and biopharmaceutical manufacturing). Other agricultural areas in China also indicate more elevated concentrations (e.g., Luo et al., 2009; Zou et al., 2007) and again, this may be due to the proximity to urban centers, or in the case of agriculture, it may be due to practices in biosolids application. With this in mind, there may be good justification to create a new land use category that describes

open spaces that are in close proximity to urban (e.g. “rural with urban influence”), and to recognize that agricultural lands may have widely varying concentrations depending on biosolids application practices.

The very elevated levels of PBDEs in sludge applied lands are striking in that it provides further support for the hypothesis that PBDE distributions in soils are not isolated to the urban environment alone and PDBEs are being redistributed at high concentrations into portions of the rural environment. Commensurate with usage and market demand statistics, PBDE concentrations in sewage sludge tend to be higher in the U.S. than in Europe (Hale et al., 2001; Andrade et al., 2010), and therefore sludge applied lands in and near the SF Bay Area may have concentrations elevated beyond those reported outside the US. Ironically, of the studies reported here, the U.S. sludge applied lands return some of the lower concentrations. Complicating the understanding of PBDE concentrations in sludge applied lands, Andrade et al. (2010) demonstrated that multiple applications over the years leads to greater PBDE concentrations in the soil, and Gorgy et al. (2013) found that PBDE concentrations decrease exponentially with time following the application of biosolids with part of the losses attributed to downward migration of the PBDEs into the soil and hypothesizing that a large proportion of the PBDEs degrade. One might also hypothesize that some of the losses may be attributed to mobilization in stormwater runoff or irrigation runoff. Further additional factors such as the tonnage of biosolids applied per acre or differences in crop practices that enhance local degradation, resuspension, or wash-off of PBDEs may alter PBDE mass that may find its way into stormwater and result in elevated concentrations from sewage applied lands.

Given the differences in usage of PBDEs between the U.S. and Europe (see market demand in Table 2), and the differences in end-use disposal practices between the U.S. and China (the U.S. typically exporting large quantities of e-waste to China), extrapolation from the world literature to the SF Bay should be done with caution. Although magnitude of use may be elevated in California relative to European countries, the use categories should be the same perhaps leading to generally similar land use relationships.

It should be noted that the PBDE concentrations presented in these two tables are generally much less than seen in the SF Bay Area for PCBs in soils and sediments (e.g. Yee and McKee, 2010). For example, the open space and urban soil concentrations for PCBs are approximately 0.02 mg/kg and 0.06 mg/kg or 20 ng/g and 60 ng/g respectively. Given we generally see higher concentrations and loads of PBDEs relative to PCBs in our mixed land use urban areas, it is a little surprising that PBDE soil concentrations are not at least as high if not higher than the PCB concentrations. If PBDEs are not in the soils at the same magnitude as PCBs and yet they are in urban stormwater at 2-3 times the concentrations of PCBs, they must be coming from real source areas that are specific to PBDEs or from atmospheric fallout onto impervious surfaces such as roadways and rooftops and being washed off during storm events and particulate phase. At this time we cannot be certain of the pathways and processes.

**Table 4. PBDE concentrations in soils data from a search of world literature.**

| Class | Description | Specific Location | PBDE concentrations (ng/g) | | | | Reference |
|---|---|---|---|---|---|---|---|
| | | | Min | Max | Mean | Median | |
| Background | Arctic | Russian Arctic | 0.16 | 0.23 | 0.20[a] | | de Wit et al., 2006 |
| | Reference soils | Sweden | 0.03 | 1.9 | 0.15 | 0.61 | Sellström et al., 2005 |
| | Upland soils | Tibetan Plateau, China | 0.004 | 0.04 | 0.0111 | | Wang et al., 2009a |
| Open Space | Woodland | Chongming Island, China | 7.0 | 16 | 12 | | Duan et al., 2010 |
| | Woodland | France | 0.23 | 5.1 | 1.2 | 0.59 | Muresan et al., 2010 |
| | Woodland | UK | 0.11 | 12 | 6.1[a] | 2.5 | Hassanin et al., 2003 |
| | Woodland | Norway | 0.13 | 3.0 | 1.6[a] | 0.97 | Hassanin et al., 2003 |
| | Grassland | Chongming Island, China | 0.48 | 9.5 | 5.5 | | Duan et al., 2010 |
| | Grassland | UK | 0.07 | 6.0 | 3.0[a] | 0.61 | Hassanin et al., 2003 |
| Agriculture | Agriculture | Pearl River Delta, China | | | 15 | | Zou et al., 2007 |
| | Agriculture | USA | < MDL | 11 | 2.2 | < MDL | Andrade et al., 2010 |
| | Agriculture | USA | | | 0.5 | | Rieck, 2004 |
| | Agriculture | Canada | | | 0.3 | | Gorgy et al., 2013 |
| | Agriculture | France | 0.24 | 44 | 1.9 | 0.66 | Muresan et al., 2010 |
| | Agriculture | Sweden | 0.03 | 0.10 | 0.066 | 0.06 | Matscheko et al., 2002 |
| | Agriculture | Surabaya, Indonesia | 0.08 | 0.35 | 0.23 | | Ilyas et al., 2010 |
| | Agriculture (near urbanized area) | Chongming Island, China | 0.32 | 37 | 14 | | Duan et al., 2010 |
| | Agriculture (rural) | Qingyuan,China | 5.3 | 29 | 20 | | Luo et al., 2009 |
| | Agriculture near an electric and electronic manufacturing zone | Qingyuan,China | 50 | 81 | 64 | | Luo et al., 2009 |
| Rural | Rural | UK | 0.07 | 0.29 | 0.22 | 0.24 | Harrad, 2006 |
| | Road - Rural (near urbanized area) | Chongming Island, China | 5.7 | 26 | 14 | | Duan et al., 2010 |
| Urban | Suburban | UK | 0.24 | 0.40 | 0.32 | 0.32 | Harrad, 2006 |
| | Urban | Taiyuan city, China | 0.02 | 211 | 26 | 2.1 | Li et al., 2008 |
| | Urban | France | 0.32 | 18 | 2.2 | 1.1 | Muresan et al., 2010 |
| | Urban | UK | 0.54 | 3.9 | 1.8 | 0.84 | Harrad, 2006 |
| | Urban | Shanghai, China | 0.02 | 3.8 | 0.74 | | Jiang et al., 2010 |
| | Urban | Harbin, China | 0.002 | 0.06 | 0.026 | | Wang et al., 2009b |
| | Urban | Ningbo, China | 1.0 | 20 | 11[a] | 10 | Wang et al., 2011 |

[a] The mean reported here was calculated as the average of the minimum and maximum concentrations reported in each reference.

**Table 4 (cont). PBDE concentrations in soils data from a search of world literature.**

| Class | Description | Specific Location | PBDE concentrations (ng/g) | | | | Reference |
|---|---|---|---|---|---|---|---|
| | | | Min | Max | Mean | Median | |
| Urban (cont.) | Urban roads | Surabaya, Indonesia | 1 | 22 | 10 | | Ilyas et al., 2010 |
| | Urban sewer sediments | Hochiminh city | 55 | 119 | 82 | 83 | Minh et al., 2010 |
| | Urban | 15 states in USA | 0.09 | 1200 | 82 | 5.3 | Offenberg et al., 2006 *in* U.S. Environmental Protection Agency, 2010 |
| | Mixed urban/rural: Floodplain soils | Shiawassee R, Michigan | 0.94 | 55 | 14 | | Yun et al., 2008 |
| | Mixed urban/rural: Floodplain soils | Saginaw R, Michigan | 0.09 | 19 | 3.0 | | Yun et al., 2008 |
| Industrial | Industrial | Taiyuan city, China | 6.0 | 144 | 46 | 28 | Li et al., 2008 |
| | Urban/Low-voltage electrical industrial area | Liushi, China | 1.0 | 155 | 78[a] | 30 | Wang et al., 2011 |
| Sludge Applied Lands | Sludge Applied Lands (1x application) | USA | 0.51 | 34 | 14 | 11 | Andrade et al., 2010 |
| | Sludge Applied Lands (2x applications) | USA | 8.5 | 140 | 58 | 55 | Andrade et al., 2010 |
| | Sludge Applied Lands | Sweden | 0.06 | 3900 | 608 | 1.2 | Sellström et al., 2005 |
| | Sludge Applied Lands | Spain | 30 | 689 | 266 | 184 | Eljarrat et al., 2008 |
| | Sludge Applied Lands | USA | 140 | 7600 | 3870[a] | | Rieck, 2004 |
| | Sludge Applied Lands | Canada | 30 | 600 | 315[a] | | Gorgy et al., 2013 |
| At and Near E-waste Centers | E-waste site soils | China | 858 | 991 | 940 | 961 | Cai and Jiang, 2006 |
| | E-waste site soils (acid leaching and printer-roller dump site) | Guiyu, China | 1440 | 3570 | 2505 | | Leung et al., 2007 |
| | Near E-waste site soils | Pearl River Delta, China | 28 | 122 | 79 | 86 | Zou et al., 2007 |
| | Road soils of e-waste recycling area | Qingyuan, China | 191 | 9156 | 2689 | | Luo et al., 2009 |
| | Urban/E-waste heavy area | Fengjiang, China | 95 | 220 | 158[a] | 140 | Wang et al., 2011 |
| | Ag soils near e-waste recycling area | Qingyuan, China | 5.0 | 207 | 42 | | Luo et al., 2009 |
| Near Polyurethane Foam (PUF) Plant | Near PUF manufacturing plant | USA | ND | 76 | 30 | 14 | Hale et al., 2002 |

[a] The mean reported here was calculated as the average of the minimum and maximum concentrations reported in each reference.

**Table 5. Summary of PBDE concentrations by class and organized from least to greatest by the mean of the mean4 concentrations within each class.**

| Class | N studies | PBDE concentrations (ng/g) | | |
|---|---|---|---|---|
| | | Minimum | Maximum | Mean of Means |
| Background | 3 | 0.004 | 1.9 | 0.12 |
| Open Space | 6 | 0.065 | 16.2 | 4.9 |
| Rural | 2 | 0.073 | 26.0 | 7.3 |
| Agriculture | 10 | ND | 81.2 | 12 |
| Urban | 12 | 0.002 | 1200 | 20 |
| Near PUF Plant | 1 | ND | 76.0 | 30 |
| Industrial | 2 | 1.00 | 155 | 62 |
| Sludge Applied Lands | 6 | 0.063 | 7600 | 855 |
| At and Near E-waste Centers | 6 | 5.00 | 9156 | 1250 |

## A9.5 Pollutant concentrations in stormwater

Little data exist in the world literature on PBDE concentrations in stormwater, and where PBDEs have been sampled in stormwater, it has been done in mixed-use urban areas (Table 6 & 7). Only two studies from outside of the SF Bay Area were found to report on concentrations in small tributaries in Washington and Oregon. Through funding from the RMP, SFEI has sampled 10 mixed-use watersheds around the SF Bay Area for PBDEs in stormwater runoff. Most of the SF Bay Area watersheds have only been studied at a pilot level, with <8 samples collected. In two of these watersheds, more concentration and loading information exists (Guadalupe and Zone 4 Line A).

Although stormwater data does not exist for homogenous land uses, we preliminarily explore concentrations in the SF Bay Area watersheds with the land use in those watersheds. This exploration yielded strong correlations with the combined sum of High Residential and Open Compacted spaces (Figure 4). The linear trendline in these graphs excludes the one high outlier watershed, Zone 5 Line M in Union City. Zone 5 Line M also had elevated median concentrations, particularly for total mercury (HgT) and to a lesser degree PCBs relative to other watersheds sampled in WY 2011 reconnaissance study (McKee et al., 2012). Although Zone 5 Line M represents an anomaly relative to the other nine Bay Area watersheds with PBDE data, it also represents an opportunity to investigate possible sources. The watershed land uses are approximately 31% residential, 11% transportation, 36% open, 15% commercial, and 7 % industrial. The watershed includes former industrial areas that have been re-zoned and are being redeveloped into a mixed-use transit village. Additionally, a cursory review of the current

[4] This includes central tendency figures calculated by averaging the minimum and maximum concentrations provided by each reference for those cases in which no average concentration was reported.

**Table 6. PBDE concentrations in stormwater based on review of peer-reviewed literature and locally collected data by the RMP. All watersheds include mixed-urban land uses. White and light gray highlighted data are from studies outside of the SF Bay Area, and dark gray highlighted data are from local small tributaries.**

| Specific Location | N | PBDE concentrations (ng/L) | | | | Reference |
|---|---|---|---|---|---|---|
| | | Min | Max | Mean | Median | |
| Spokane River, WA | 14 | | | 7 | 5 | Lubliner, 2009 |
| Columbia River Basin | 16 | ND | 53 | 9 | 0.2 | Morace, 2012 |
| Borel Ck, Peninsula Bay Area, CA | 3 | 9 | 20 | 14 | 12 | McKee et al., 2012 |
| Coyote Ck, Santa Clara County, CA | 7 | 7 | 36 | 15 | 13 | SFEI unpublished |
| Guadalupe River, San Jose, CA | 13 | 15 | 369 | 88 | 38 | SFEI unpublished (WY 2012); McKee et al., 2006 |
| Lower Marsh Ck, Brentwood, CA | 1 | 20 | 20 | 20 | 20 | SFEI unpublished |
| Lower Penetencia Ck, Milpitas, CA | 4 | 13 | 22 | 18 | 19 | McKee et al., 2012 |
| San Leandro Ck, San Leandro, CA | 3 | 41 | 80 | 57 | 50 | SFEI unpublished |
| Santa Fe Channel, Richmond, CA | 2 | 24 | 30 | 27 | 27 | McKee et al., 2012 |
| Sunnyvale East Channel, Sunnyvale, CA | 6 | 5 | 100 | 48 | 42 | McKee et al., 2012; SFEI unpublished (WY 2012) |
| Zone 4 Line A, Hayward, CA | 38 | 0 | 430 | 47 | 27 | Gilbreath et al., 2012 |
| Zone 5 Line M, Union City, CA | 4 | 34 | 128 | 75 | 69 | McKee et al., 2012 |

**Table 7. Summary table of PBDE concentrations in SF Bay Area stormwater runoff data.**

| | Bay Area Data (N=10) |
|---|---|
| **Minimum of dataset (all watersheds, all samples) (ng/L)** | **0.4** |
| **Maximum of dataset (all watersheds, all samples) (ng/L)** | **430** |
| **Mean of the Means (ng/L)** | **41** |
| | |
| **Mean of the Means % BDE-47** | **8** |
| **Mean of the Means % BDE-209** | **58** |
| **Mean of the Means Ratio BDE-209:BDE-47** | **10** |

industrial sector of this small watershed using Google Maps and Google Earth revealed several parcels that may be contributing to the PBDEs or HgT concentrations. These parcels included two custom plastics manufacturers, and a furniture distribution warehouse plus possible small-scale furniture recycling at this location. The most elevated sample concentration at this location was unlike the other samples collected in the same watershed and unlike the rest of the

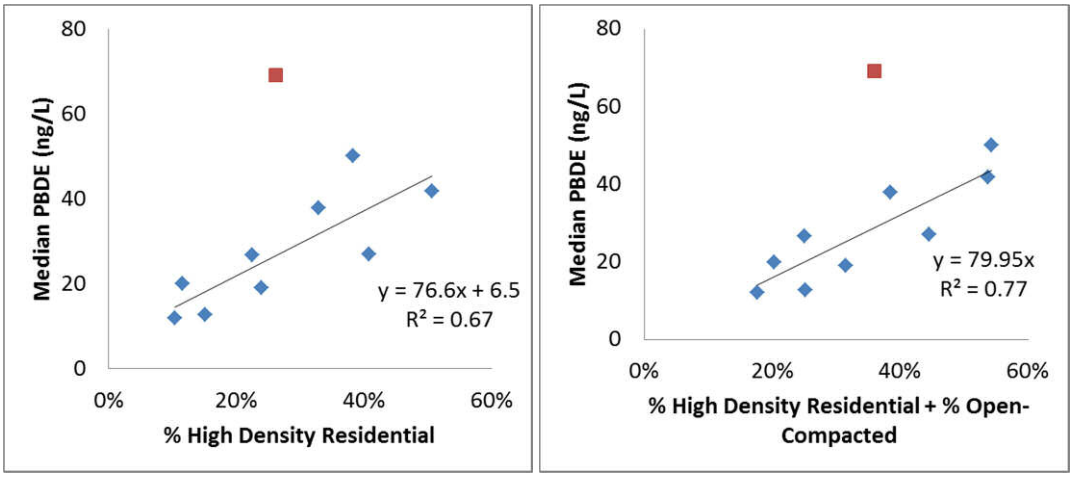


**Figure 4. Median PBDE concentrations in relation to the % high density residential (< 0.333 acres/unit) and % compacted open space in nine Bay Area watersheds. The linear trendline is related only to the nine watersheds represented by blue markers; the red marker is Zone 5 Line M.**

Bay Area samples in that the ratio BDE-209:BDE-47 was 38, as opposed to the SF Bay Area average ratio of 10, and 90% of the sample was comprised of BDEs 206-209, indicating that decaBDE was the dominant source. Further investigation could be done in this watershed to identify important source areas for the regional modeling effort. Particle ratios of PBDEs to suspended sediment concentration (SSC) in local stormwater data was also analyzed for relationships to land uses. No strong correlation was noted. The relationship to percent high density residential was only $R^2$=0.05. The strongest relationship was to industrial land use ($R^2$=0.42).

For perspective, Oram et al. (2008) completed a first effort at estimating PBDE loads into SF Bay from various sources. In this study, Oram and colleagues estimated that the small tributaries contributed 11-27% of the BDE-47 load to SF Bay, and 74% of the BDE-209 load. In contrast, effluent from POTWs has concentrations similar to stormwater runoff in the SF Bay Area (mean 29 ng/L; North, 2004) but is dominated by BDE-47 and other pentaBDE congeners (North, 2004). POTW effluent contributes an estimated 36-75% of the BDE-47 load to the Bay, and only 9% of the BDE-209 load (Oram et al., 2008). Presumably most of the BDE-209 load into POTWs is settled out in the sewage sludge. These concentrations in effluent from POTWs and stormwater runoff from small tributaries are about 3 orders of magnitude greater than concentrations sampled in SF Bay waters (Werme et al., 2007).

Local PBDEs in stormwater data was regressed with total mercury (HgT) and PCBs (sum of 40 congeners) to provide preliminary evidence if, at a regional average scale, targeting the clean-up of either of these high priority pollutants of concern would result in multiple benefits for management of PBDEs. On a water concentration basis, PBDEs were correlated with HgT, but not with PCBs (Figure 5). When normalized to suspended sediment concentration, PBDEs did not

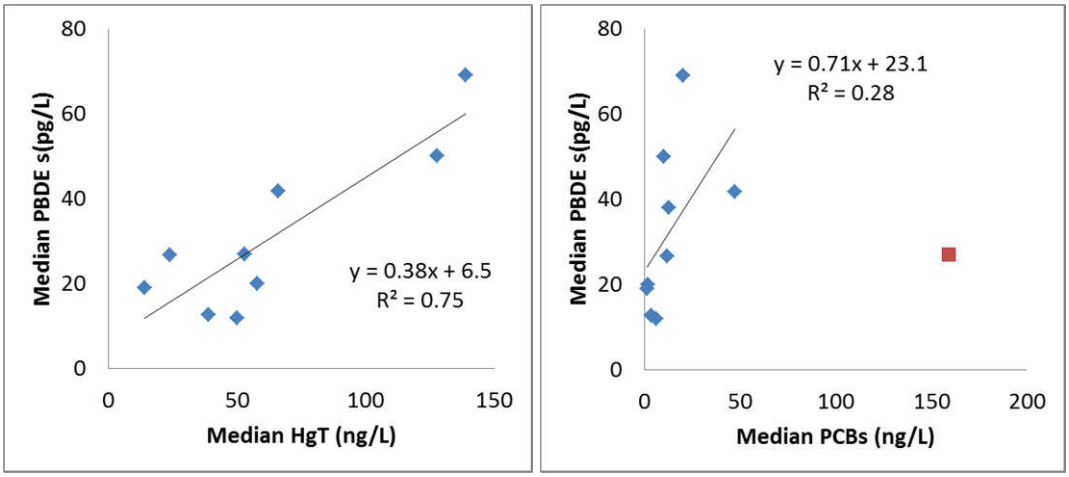


**Figure 5. Median PBDE concentrations in relation to median HgT and median PCB concentrations in Bay Area watersheds. The Guadalupe River watershed data is excluded as anomalous from the regression with median HgT due to Hg mining influence in this watershed. The outlier datapoint in red for median PCBs is the PCB hot spot watershed, Santa Fe Channel.**

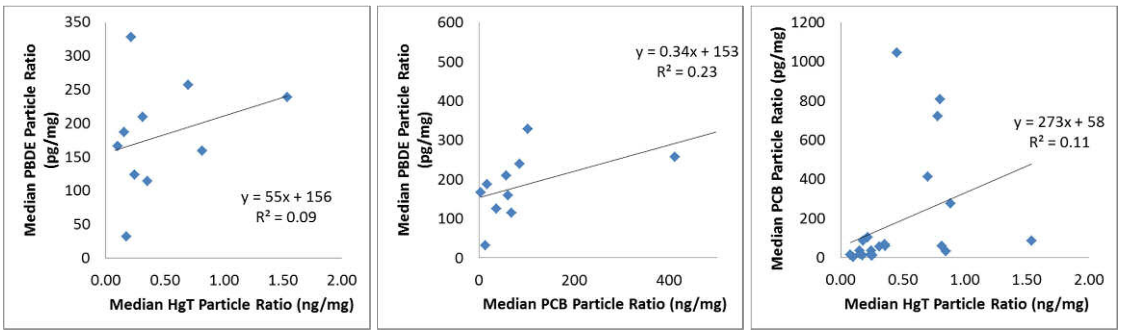


**Figure 6. Relationships of median PBDE, HgT and PCB particle ratios in Bay Area watersheds.**

correlate well with either HgT or PCBs, nor did HgT and PCBs correlate well with one another (Figure 6). The relationship between median particle ratios for PBDEs and PCBs (Figure 6, center graph) is improved when removing the high PCB outlier (Santa Fe Channel) on the far right of the graph, in which the $R^2$ raises to 0.45 and the equation line is y = 1.64x + 92.4. No relationship could be found between land use and the ratio of PCBs to PBDEs (median particle ratios), nor between HgT and PBDEs (median particle ratios), for local watersheds. This data suggests that management of PBDEs may coordinate with management of HgT, but not with PCBs. This matches our conceptual models of HgT as being a largely ubiquitous, atmospherically derived source versus PCBs being very much associated with very specific source areas. This is further corroborated by regression of the ratio of median PBDE:PCB water concentrations in stormwater and landscape characteristics (imperviousness, open space, and residential land use) (Figure 7). If we accept the standing hypothesis that PCBs are associated most strongly with

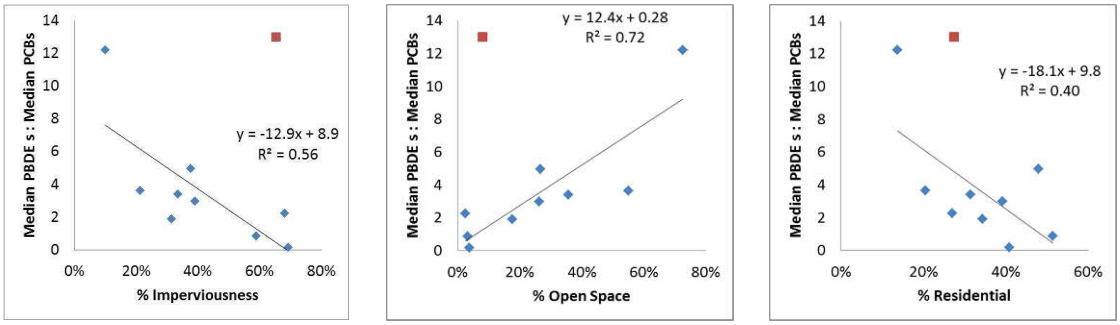


**Figure 7. Relationships between landscape characteristics and median PBDE:PCB concentrations in stormwater during rain storms in Bay Area watersheds. The outlier in red is Lower Penetencia Creek.**

sources and source areas in older industrial settings, these relationships appear to suggest that PBDEs are not strongly associated with local old industrial sources/source areas. Instead, more ubiquitous urban use and atmospheric deposition play a stronger role in PBDE concentrations observed in SF Bay Area stormwater.

## A9.6 Summary and options for event mean concentration (EMC) development for pollutant

PBDEs have been widely used as a flame retardant in textiles, plastics, and polyurethane foam products since the 1970's and are now both ubiquitous in the urban environment and also possibly being redistributed to the rural environment through application of biosolids and atmospheric deposition. PBDE loads to SF Bay have been previously estimated (Oram et al., 2008). However, since that time, more local empirical data has been collected for input, calibration, and verification for an improved estimate of loads from the small tributaries, and through the development of this contaminant profile, at least two important sources (sludge applied lands and areas surrounding Tyco Thermal Controls in the Peninsula) have been identified that were not previously captured by the input data into the previous estimate.

To model loads of PBDEs in stormwater runoff from the small tributaries to the SF Bay, unique PBDE concentration/loadings factors could be applied to select land use and source area classes. The systematic review of synthesis, product incorporation and uses, disposal processes, and soil and water concentration data supports a general distinction in PBDE concentrations between urban and rural areas, as well as select source areas. A strong correlation exists between PBDE concentrations in stormwater runoff from nine SF Bay watersheds and the percentage of high residential and compacted open spaces in those watersheds. This correlation alone may provide a good basis for an improved estimation of regional loads, however the one high outlier watershed (Zone 5 Line M) highlights the potential importance of adding in source areas to the PBDE model, to be weighed against the effort needed to identify and obtain reliable data for each type of source area. The potential source areas of most interest for PBDEs and the estimated magnitude of emission factor for each category is presented in Table 8.

**Table 8. Proposed land use / source area categories for PBDE based on our present conceptual model generated through this review.**

<table>
<tr><th>Land use / source areas</th><th>Estimate emission factor[1]</th><th>GIS layer created?[2]</th><th>Particle concentration data? [2]</th><th>Water concentration data? [2]</th></tr>
<tr><td>All industrial</td><td>M/H</td><td>Y</td><td>Y</td><td rowspan="15">N</td></tr>
<tr><td>Plastics, Electronics, Cars and Textiles Manufacturers</td><td rowspan="5">H</td><td rowspan="5">N</td><td rowspan="3">N</td></tr>
<tr><td>Autoshredders</td></tr>
<tr><td>Carpet/Foam Recycling Facilities</td></tr>
<tr><td>Electronics Recycling Facilities</td><td>Y</td></tr>
<tr><td>Area surrounding Tyco Thermal Controls</td><td rowspan="3">N</td></tr>
<tr><td>Auto recycling/ refurbishing</td><td>M/H</td><td>Y</td></tr>
<tr><td>Landfills that use auto-shredder fluff as daily alternative cover</td><td rowspan="3">M</td><td>N</td></tr>
<tr><td>All transportation</td><td rowspan="6">Y</td></tr>
<tr><td>Urban (except industrial)</td><td>Y</td></tr>
<tr><td>Commercial</td><td rowspan="3">N</td></tr>
<tr><td>High density residential</td><td>M/H</td></tr>
<tr><td>Low density residential</td><td>L/M</td></tr>
<tr><td>All nonurban (except sludge applied lands)</td><td>L</td><td rowspan="2">Y</td></tr>
<tr><td>Sludge Applied Lands</td><td>H</td><td>N</td></tr>
</table>

[1] Estimated magnitude of emission factor: High (H); Medium (M); Low (L).
[2] Indication of current availability of GIS shapefile and concentration data for each source area category: Yes (Y); No (N). An "N" indicates additional effort is needed to integrate this category into the RWSM.

To support the development of a regional PBDE loads model, GIS databases and shapefiles of the above listed source areas could be developed, and average soils, suspended particulate matter, or stormwater concentrations in those areas would need to be defined. Differences in usage patterns between the U.S. and elsewhere, and even California versus the rest of the U.S., confounds the usage of concentration data from outside areas but the general pattern of more highly versus less contaminated areas might hold true for the SF Bay Area more than the magnitude of concentrations. Therefore, to the extent possible, we recommend the use of local data as a starting point and data from the rest of the U.S. and outside of the U.S. for making decisions about the relative order magnitude of EMCs or concentration factors. Where necessary, data from outside the SF Bay Area can be used to augment the local dataset with the expectation that initial model runs might indicate the need for development of local data for input into the model. Options for developing the SF Bay Area specific EMC estimates needed for input into the spreadsheet model include:

A. Back calculating the EMCs for both land uses and source areas from the current local stormwater datasets. This method has shown promise for the Hg and PCB versions of the RWSM, however the success of this method is in part dependent on the source area classes being present in the watersheds with empirical data and the size of the data set (number of locations sampled assuming a robust number of samples per location – at least 4 but ideally 6-8 samples collected during storm flow conditions).

B. Conduct empirical studies of PBDEs in runoff or soils from the above listed source areas. Such studies may have added benefit for sampling of other priority analytes in similar source area classes (e.g. metals near autoshredders). These source area

EMCs could potentially be added to the more generalized urban versus rural land use model, or a model that applies concentrations based on high residential and compacted open spaces.

C. Use air monitoring data and assumptions regarding particle settlement and air deposition of PBDEs to estimate EMCs for source areas where air sampling has occurred (near autoshredders, e-waste recyclers, etc.) assuming storage and runoff characteristics of the local landscape (e.g. perhaps scaling for the runoff coefficient).

## A9.7 Preliminary recommendations for pollutant RWSM development

Most studies reporting environmental concentrations of PBDEs are for soils. Unfortunately no local soils data have been collected for comparison to measurements from other parts of the world, and given differences in use and recycling practices, we suggest using the soils data in combination with a sediment model only as a line of basic QA. Fewer stormwater studies have been conducted and none for homogenous land use types, but we do have 10 local watershed datasets and preliminary analysis of this data shows concentrations correlate fairly strongly with some identified land uses. As a result, we suggest estimating regional loads of PBDEs based on the application of our local stormwater concentration data to the volume results of the hydrology model. In short, we recommend a land-use based volume-concentration model. This approach appears to be supported by the correlations with mercury and the lack of correlations with PCBs. Given that concentrations of PBDEs in stormwater are expected to be continually trending downward due to the effects of the recent bans on PBDEs, such modeling should be considered to represent baseline conditions and not to predict future loads.

To develop a baseline model of the regional PBDE load, we suggest the following steps:

1) Further explore land use correlations between the SF Bay Area specific stormwater runoff data and the >150 ABAG defined land use classes. This may be the simplest approach towards reaching a calibrated model with a level of uncertainty we can feel comfortable with in this first version of the PBDE model. This approach would allow us to utilize the already-developed land-use based volume-concentration model that was used for the test case copper model.

2) If the above approach does not produce strong enough results, develop GIS layers for some or all of the source areas identified and apply effort towards developing EMCs for those source areas (further updated literature review focused on recent studies to account for the expected downward trend in PBDE concentrations due to the effects of recent bans on PBDEs, back calculation, or – as a last resort – empirical field data collection). This type of model would also be a land-use based volume-concentration model; however it would require integration of the source areas into the land use layer as was done for the Hg and PCB models.

## A9.8 References

Alaee, M., P. Arias, A. Sjödin and Å. Bergman (2003). "An overview of commercially used brominated flame retardants, their applications, their use patterns in different countries/regions and possible modes of release." Environment International **29**(6): 683-689.

Andrade, N. A., L. L. McConnell, A. Torrents and M. Ramirez (2010). "Persistence of Polybrominated Diphenyl Ethers in Agricultural Soils after Biosolids Applications." Journal of Agricultural and Food Chemistry **58**(5): 3077-3084.

Cai, Z. and G. Jiang (2006). "Determination of polybrominated diphenyl ethers in soil from e-waste recycling site." Talanta **70**(1): 88-90.

California Environmental Protection Agency (2006). Polybrominated Diphenyl Ethers: Recommendations to Reduce Exposure in California. Sacramento, California**:** 53 pp.

Charles, M. J., D. Groskova and T. M. Cahill (2005). Near-Source Ambient Air Monitoring of Polybrominated Diphenyl Ethers. C. A. R. Board**:** 132.

County of Solano (2012). 2011 Annual Biosolids Land Application Report**:** 57 pp.

de Wit, C. A. (2002). "An overview of brominated flame retardants in the environment." Chemosphere **46**(5): 583-624.

de Wit, C. A., M. Alaee and D. C. G. Muir (2006). "Levels and trends of brominated flame retardants in the Arctic." Chemosphere **64**(2): 209-233.

Department of Toxic Substances Control (2002). California's Automobile Shredder Waste Initiative. Hazardous Waste Management Program**:** 44 pp.

Duan, Y.-P., X.-Z. Meng, C. Yang, Z.-Y. Pan, L. Chen, R. Yu and F.-T. Li (2010). "Polybrominated diphenyl ethers in background surface soils from the Yangtze River Delta (YRD), China: occurrence, sources, and inventory." Environmental Science and Pollution Research **17**(4): 948-956.

Eljarrat, E., G. Marsh, A. Labandeira and D. Barcelo (2008). "Effect of sewage sludges contaminated with polybrominated diphenylethers on agricultural soils." Chemosphere **71**(6): 1079-1086.

Gilbreath, A., D. Yee and L. McKee (2012). Concentrations and Loads of Trace Contaminants in a Small Urban Tributary, San Francisco Bay, California. A Technical Report of the Sources Pathways and Loading Work Group of the Regional Monitoring Program for Water Quality, San Francisco Estuary Institute**:** 40 pp.

Gorgy, T., L. Li, J. Grace and M. Ikonomou (2013). "Migration of polybrominated diphenyl ethers in biosolids-amended soil." Environ Pollut. **172**: 124-130. doi 110.1016/j.envpol.2012.1007.1047. Epub 2012 Sep 1026.

Hale, R. C., M. Alaee, J. B. Manchester-Neesvig, H. M. Stapleton and M. G. Ikonomou (2003). "Polybrominated diphenyl ether flame retardants in the North American environment." Environment International **29**(6): 771-779.

Hale, R. C., M. J. La Guardia, E. Harvey, M. O. Gaylor and T. M. Mainor (2006). "Brominated flame retardant concentrations and trends in abiotic media." Chemosphere **64**(2): 181-186.

Hale, R. C., M. J. La Guardia, E. Harvey and T. Matt Mainor (2002). "Potential role of fire retardant-treated polyurethane foam as a source of brominated diphenyl ethers to the US environment." Chemosphere **46**(5): 729-735.

Hale, R. C., M. J. La Guardia, E. P. Harvey, M. O. Gaylor, T. M. Mainor and W. H. Duff (2001). "Flame retardants: Persistent pollutants in land-applied sludges." Nature **412**(6843): 140-141.

Harrad, S. H., Stuart (2006). "Concentrations of Polybrominated Diphenyl Ethers in Air and Soil on a Rural−Urban Transect Across a Major UK Conurbation." Environmental Science & Technology **40**(15): 4548-4553.

Hassanin, A., K. Breivik, S. N. Meijer, E. Steinnes, G. O. Thomas and K. C. Jones (2003). "PBDEs in European Background Soils: Levels and Factors Controlling Their Distribution." Environmental Science & Technology **38**(3): 738-745.

Ilyas, M., A. Sudaryanto, I. E. Setiawan, A. S. Riady, T. Isobe, S. Takahashi and S. Tanabe (2010). Polybrominated Diphenyl Ethers in Soils from Various Locations in Surabaya City, Indonesia: Dumping Site and Urban Areas as Important Sources. Symposium on Brominated Flame Retardants. Kyoto, Japan.

Jiang, Y., X. Wang, K. Zhu, M. Wu, G. Sheng and J. Fu (2010). "Occurrence, compositional profiles and possible sources of polybrominated diphenyl ethers in urban soils of Shanghai, China." Chemosphere **80**(2): 131-136.

Klosterhaus, S. L., H. M. Stapleton, M. J. La Guardia and D. J. Greig (2012). "Brominated and chlorinated flame retardants in San Francisco Bay sediments and wildlife." Environment International **47**: 56-65.

Leung, A. O. W., W. J. Luksemburg, A. S. Wong and M. H. Wong (2007). "Spatial Distribution of Polybrominated Diphenyl Ethers and Polychlorinated Dibenzo-p-dioxins and Dibenzofurans in Soil and Combusted Residue at Guiyu, an Electronic Waste Recycling Site in Southeast China." Environmental Science & Technology **41**(8): 2730-2737.

Li, K., S. Fu, Z. Yang and X. Xu (2008). "Composition, Distribution and Characterization of Polybrominated Diphenyl Ethers (PBDEs) in the Soil in Taiyuan, China." Bulletin of Environmental Contamination and Toxicology **81**(6): 588-593.

Lubliner, B. (2009). PBDE and Dioxin/Furans in Spokane Stormwater. Olympia, Washington, Department of Ecology: State of Washington**:** 43.

Luo, Y., X.-J. Luo, Z. Lin, S.-J. Chen, J. Liu, B.-X. Mai and Z.-Y. Yang (2009). "Polybrominated diphenyl ethers in road and farmland soils from an e-waste recycling region in Southern China: Concentrations, source profiles, and potential dispersion and deposition." Science of The Total Environment **407**(3): 1105-1113.

Matscheko, N., M. Tysklind, C. de Wit, S. Bergek, R. Andersson and U. Sellstrom (2002). "Application of sewage sludge to arable land-soil concentrations of polybrominated diphenyl ethers and polychorinated dibenzo-p-dioxins, dibenzofurans, and biphenyls, and their accumulation in earthworms." Environmental Toxicology and Chemistry **21**(12): 2515-2525.

McKee, L., J. Oram, J. Leatherbarrow, A. Bonnema, W. Heim and M. Stephenson (2006). Concentrations and loads of mercury in the lower Guadalupe River, San Jose, California: Water Years 2003, 2004, and 2005. A Technical Report of the Regional Watershed Program. Oakland, CA**:** 47pp + Appendices A, B and C.

McKee, L. J., A. N. Gilbreath, J. A. Hunt and B. K. Greenfield (2012). Pollutants of concern (POC) loads monitoring data, water year (WY) 2011. A technical report prepared for the Regional Monitoring Program for Water Quality in San Francisco Bay (RMP), Small Tributaries Loading Strategy (STLS), San Francisco Estuary Institute.

Minh, N. H., T. B. Minh, T. Isobe and S. Tanabe (2010). Contamination of Polybromodiphenylethers (PBDEs) in Sewer system of Hochiminh City and Estuary of Saigon-Dongnai River. Symposium on Brominated Flame Retardants. Kyoto, Japan.

Mitchell, D. (2009). Bay Area Biosolids Management: Challenges, Opportunities, and Po licies**:** 51 pp.

Morace, J. L. (2012). Reconnaissance of contaminants in selected wastewater-treatment-plant effluent and stormwater runoff entering the Columbia River, Columbia River Basin, Washington and Oregon, 2008–10**::** 68 pp.

Muresan, B., C. Lorgeoux, J. Gasperi and R. Moilleron (2010). "Fate and spatial variations of polybrominated diphenyl ethers in the deposition within a heavily urbanized area: case of Paris (France)." Water Science and Technology **62**(4): 822-828.

North, K. D. (2004). "Tracking Polybrominated Diphenyl Ether Releases in a Wastewater Treatment Plant Effluent, Palo Alto, California." Environmental Science & Technology **38**(17): 4484-4488.

Oram, J. J., L. J. McKee, C. E. Werme, M. S. Connor, D. R. Oros, R. Grace and F. Rodigari (2008). "A mass budget of polybrominated diphenyl ethers in San Francisco Bay, CA." Environment International **34**(8): 1137-1147.

Petreas, M. and D. Oros (2009). Polybrominated diphenyl ethers in California wastestreams.

Qiu, Y.-W., G. Zhang, L.-L. Guo, G. J. Zheng and S.-Q. Cai (2010). "Bioaccumulation and historical deposition of polybrominated diphenyl ethers (PBDEs) in Deep Bay, South China." Marine Environmental Research **70**(2): 219-226.

Rieck, R. H. (2004). "Polybrominated Diphenyl Ether Analysis in Fish Tissue and Other Matrices by GC-ECD." LC-GC North America **22**(9).

Sakai, S., S. Takahashi, M. Osada and T. Miyazaki (2006). "Dioxin-related compounds, BFRs and heavy metals in automobile shredder residue (ASR) and their behavior in high-temperature melting process." Organohalogen Compounds **68**: 1824-1827.

Sellström, U., C. A. de Wit, N. Lundgren and M. Tysklind (2005). "Effect of Sewage-Sludge Application on Concentrations of Higher-Brominated Diphenyl Ethers in Soils and Earthworms." Environmental Science & Technology **39**(23): 9064-9070.

Shaw, S. D. and K. Kannan (2009). Polybrominated Diphenyl Ethers in Marine Ecosystems of the American Continents: Foresight from Current Knowledge. Reviews on Environmental Health. **24:** 157.

She, J., A. Holden, M. Sharp, M. Tanner, C. Williams-Derry and K. Hooper (2007). "Polybrominated diphenyl ethers (PBDEs) and polychlorinated biphenyls (PCBs) in breast milk from the Pacific Northwest." Chemosphere **67**(9): S307-S317.

Stapleton, H., N. Dodder, J. Offenberg, M. Schantz and S. Wise (2005). "Polybrominated diphenyl ethers in house dust and clothes dryer lint." Environ Sci Technol. **39**(4): 925-931.

Strandberg, B., N. G. Dodder, I. Basu and R. A. Hites (2001). "Concentrations and Spatial Variations of Polybrominated Diphenyl Ethers and Other Organohalogen Compounds in Great Lakes Air." Environmental Science & Technology **35**(6): 1078-1083.

Sutton, R., M. Sedlak and J. Davis (in prep). Polybrominated Diphenyl Ethers (PBDEs) in San Francisco Bay: A Summary of Occurrence and Trends. RMP Contribution XXX, San Francisco Estuary Institute, Richmond, CA**:** 64.

U.S. Department of Health and Human Services (2004). Toxicological Profile for Polybrominated Biphenyls and Polybrominated Diphenyl Ethers. Public Health Service: Agency for Toxic Substances and Disease Registry**:** 619 pp.

U.S. Environmental Protection Agency (2010). An Exposure Assessment of Polybrominated Diphenyl Ethers. National Center for Environmental Assessment. Washington, DC**:** 378 pp.

U.S. Environmental Protection Agency (2011). Electronics Waste Management in the United States Through 2009. Office of Resource Conservation and Recovery**:** 49 pp.

Wang, J. X., Z. K. Lin, K. F. Lin, C. Y. Wang, W. Zhang, C. Y. Cui, . . . C. J. Huang (2011). "Polybrominated diphenyl ethers in water, sediment, soil, and biological samples from different industrial areas in Zhejiang, China." Journal of Hazardous Materials **197**: 211-219.

Wang, P., Q. Zhang, Y. Wang, T. Wang, X. Li, Y. Li, . . . G. Jiang (2009a). "Altitude dependence of polychlorinated biphenyls (PCBs) and polybrominated diphenyl ethers (PBDEs) in surface soil from Tibetan Plateau, China." Chemosphere **76**(11): 1498-1504.

Wang, X., N. Q. Ren, H. Qi, W. L. Ma and Y. F. Li (2009b). "Levels and distribution of brominated flame retardants in the soil of Harbin in China." Journal of Environmental Sciences-China **21**(11): 1541-1546.

Watanabe, I. and S.-i. Sakai (2003). "Environmental release and behavior of brominated flame retardants." Environment International **29**(6): 665-682.

Werme, C., J. Oram, L. McKee, D. Oros and M. Connor (2007). PBDEs in San Francisco Bay: Conceptual Model/Impairment Assessment, San Francisco Estuary Institute; Prepared for the Clean Estuary Partnership.

Yee, D., B. Bemis, D. Hammond, W. Heim, B. Jaffe, A. Rattonetti and S. van Bergen (2011). Age Estimates and Pollutant Concentrations of Sediment Cores from San Francisco Bay and Wetlands, San Francisco Estuary Institute**:** 65.

Yee, D. and L. J. McKee (2010). Task 3.5: Concentrations of PCBs and Hg in soils, sediments and water in the urbanized Bay Area: Implications for best management. A technical report of the Watershed Program. SFEI Contribution 608, San Francisco Estuary Institute, Oakland CA 94621**:** 36 + Appendix.

Yun, S. H., R. Addink, J. M. McCabe, A. Ostaszewski, D. Mackenzie-Taylor, A. B. Taylor and K. Kannan (2008). "Polybrominated diphenyl ethers and polybrominated biphenyls in sediment and floodplain soils of the Saginaw River watershed, Michigan, USA." Archives of Environmental Contamination and Toxicology **55**(1): 1-10.

Zegers, B. N., W. E. Lewis, K. Booij, R. H. Smittenberg, W. Boer, J. de Boer and J. P. Boon (2003). "Levels of Polybrominated Diphenyl Ether Flame Retardants in Sediment Cores from Western Europe." Environmental Science & Technology **37**(17): 3803-3807.

Zota, A. R., R. A. Rudel, R. A. Morello-Frosch and J. G. Brody (2008). "Elevated House Dust and Serum Concentrations of PBDEs in California: Unintended Consequences of Furniture Flammability Standards?" Environmental Science & Technology **42**(21): 8158-8164.

Zou, M. Y., Y. Ran, J. Gong, B. X. Maw and E. Y. Zeng (2007). "Polybrominated diphenyl ethers in watershed soils of the Pearl River Delta, China: Occurrence, inventory, and fate." Environmental Science & Technology **41**(24): 8262-8267.

# APPENDIX 10. ORGANOCHLORINE PESTICIDES MODULE POLLUTANT PROFILE

## A10.1 Legacy Pesticides: description, historical usage, and behavior in the environment

### A10.1.a Description and historical usage

The legacy pesticides are a subset of organochlorine pollutants that were heavily used as insecticides in California up until their respective regulatory bans. These pollutants are highly toxic to wildlife and humans and are part of the dirty dozen variously chlorinated pollutants (aldrin, chlordane, DDT, dieldrin, endrin, heptachlor, mirex, toxaphene, dioxins, furans, hexachlorobenzene, and PCBs) that were banned or heavily regulated in the 1970s and 1980s (Werner and Hitzfeld 2012). All are considered legacy since they are no longer in use yet they still exist in the environment and continue to enter the Bay from local drainages. To support Provision C.14. of the Municipal Regional Stormwater Permit (MRP) (SFBRWQCB 2009), this report focuses on three organochlorine pesticides: Dichlorodiphenyltrichloroethane(DDT), chlordane, and dieldrin.

The term DDT (Figure 1) is generally used to describe six isomers which are a combination of technical grade DDT as well as degradation products (Mischke *et al.* 1985). DDT was used widely in the landscape during its period of usage. It was initially used as an agricultural pesticide and for controlling disease carrying vectors but then usage in residential applications became commonplace (Mischke *et al.* 1985). The use of DDT in California began around 1944, was restricted in 1963 and banned in 1972 consistent with the national ban (Mischke *et al.* 1985). California recordkeeping on pesticide use did not start until 1971 therefore County or even State resolution use statistics on DDTs are not available. However there are records of production for the whole of the US. It appears that more than 600,000 tonnes (1.35 billion lbs) was applied in the U.S. before the 1972 ban. Usage apparently peaked in 1962 at about 82,000 tonnes per year, coincidentally around the time of the publication of Rachel Carson's book "Silent Spring". Scaled to the US population of the 1960s census (181 million), the Bay Area was 2% of the US population and the total use of DDT in the nine county Bay Area was therefore approximately 12,000 metric tonnes (26.5 million lbs).

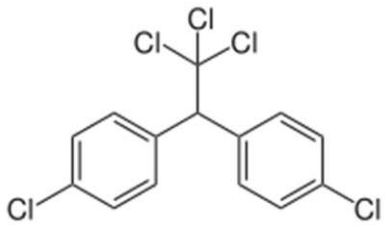


**Figure 1 . Chemical structure of DDT.**

The term Chlordane (Figure 2) also represents a pesticide category with multiple isomers. Chlordane was manufactured and sold in the United States from 1948 to 1988. In the Bay Area, this pesticide group had more structural (64%) applications than other legacy pesticides (Figure 3) and was primarily used in termite control. Early applications also included home/garden use (Dearth and Hites 1991). Over the period 1974-1980, Santa Clara County registered the highest Bay Area chlordane use accounting for about 30% of total use (Figure 4 and Figure 5). In the Bay Area, chlordane use declined from 117,000 pounds in 1975 to 53,000 pounds in 1980 – more than a 50% reduction in 5 years. Chlordane was restricted for use in California in 1975 and banned nationally in 1978 except for use in termite control (Dearth and Hites 1991; Kratzer 1999). The production of chlordane was ceased nationally in 1988.

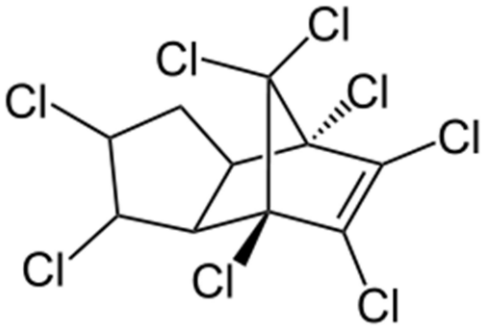


**Figure 2. Chemical structure of chlordane.**

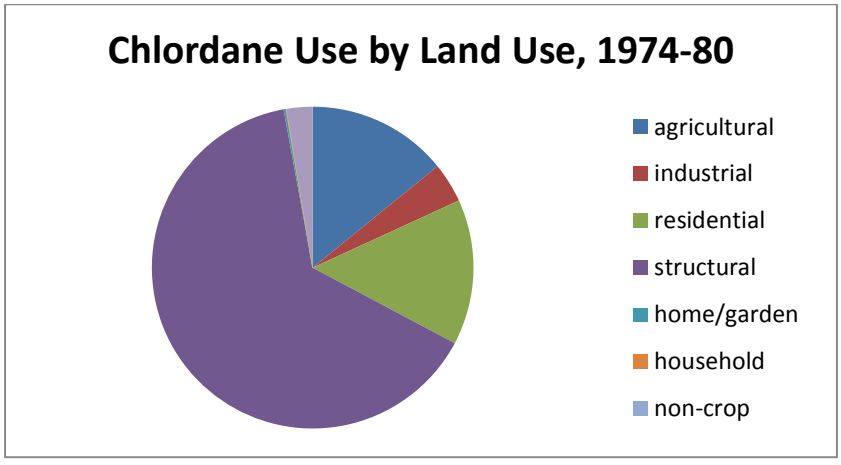


**Figure 3. Bay Area chlordane usage (in pounds) by land use 1974-1980 (California Department of Pesticide Regulation data).**

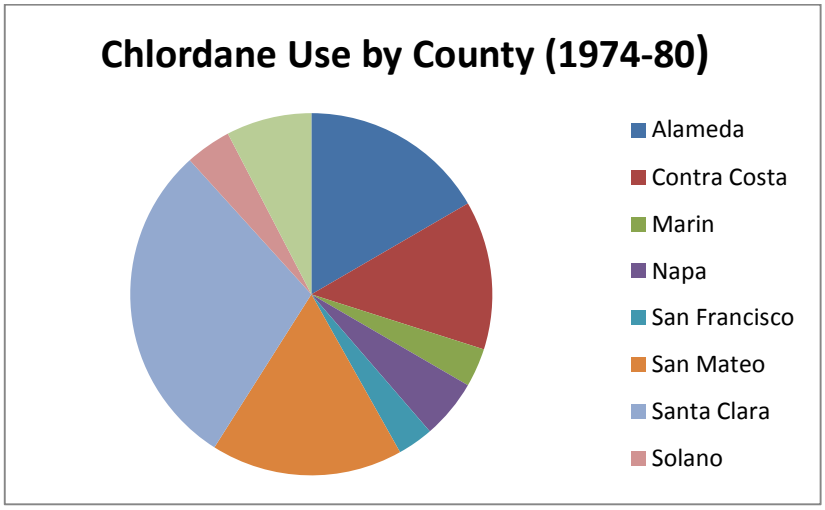


**Figure 4. Bay Area chlordane usage (in pounds) by county 1974-1980 (California Department of Pesticide Regulation Data).**

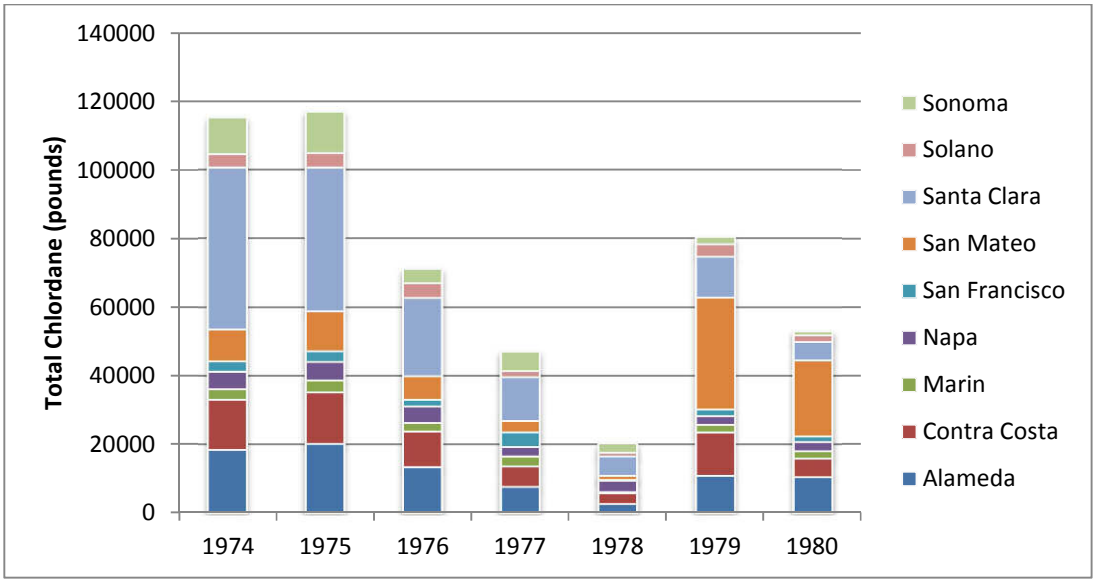


**Figure 5. Bay Area chlordane usage (in pounds) by county 1974-1980 (California Department of Pesticide Regulation Data).**

Dieldrin is a chlorinated hydrocarbon (Figure 6) originally produced in 1948 as an insecticide. Dieldrin is closely related to aldrin, which reacts further to form dieldrin. Aldrin is not toxic to insects; it is oxidized in the insect to form dieldrin which is the active compound. Both dieldrin and aldrin are named after the Diels-Alder reaction which is used to form aldrin from a mixture of norbornadiene and hexachlorocyclopentadiene. Dieldrin proved to be a highly effective insecticide and was very widely used during the 1950s to early1970s. Endrin is a stereoisomer of

dieldrin. However, it is an extremely persistent organic pollutant; it does not easily break down. Furthermore it tends to biomagnify as it is passed along the food chain. Long-term exposure has proven toxic to a very wide range of animals including humans, far greater than to the original insect targets. For this reason it is now banned in most of the world. It has been linked to health problems such as Parkinson's, breast cancer, and immune, reproductive, and nervous system damage.

Historically, dieldrin applications included termite control, wood preservation, and moth proofing, particularly by the textile industry (Meharg *et al.* 2000). Dieldrin use began in 1950 and, in the Bay Area, was primarily used in residential (47%), agriculture (29%), and commercial (24%) applications (Figure 7). Alameda and Solano counties (26% each) had the highest dieldrin use in the Bay Area over the period 1974-1980 (Figure 8 and Figure 9). The pesticide was restricted in 1974 and banned in 1985 except for underground termite control (Kratzer 1999). However, dieldrin use was effectively discontinued in the Bay Area in 1978 (Figure 9). A full national ban occurred in 1987.

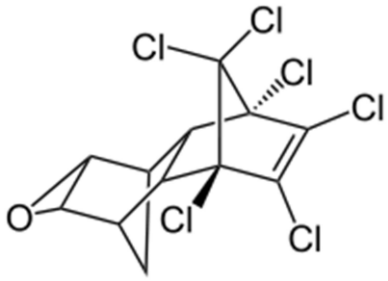


**Figure 6. Chemical structure of dieldrin.**

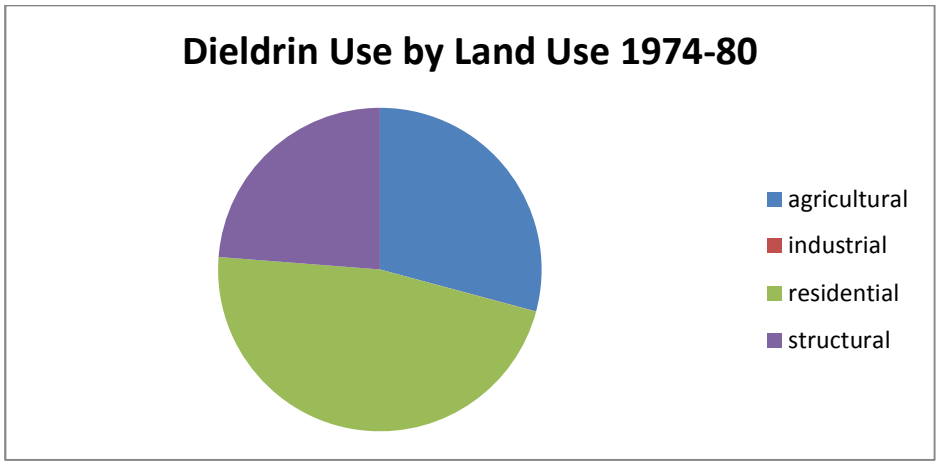


**Figure 7. Dieldrin usage by land use 1974-1980 (California Department of Pesticide Regulation data).**

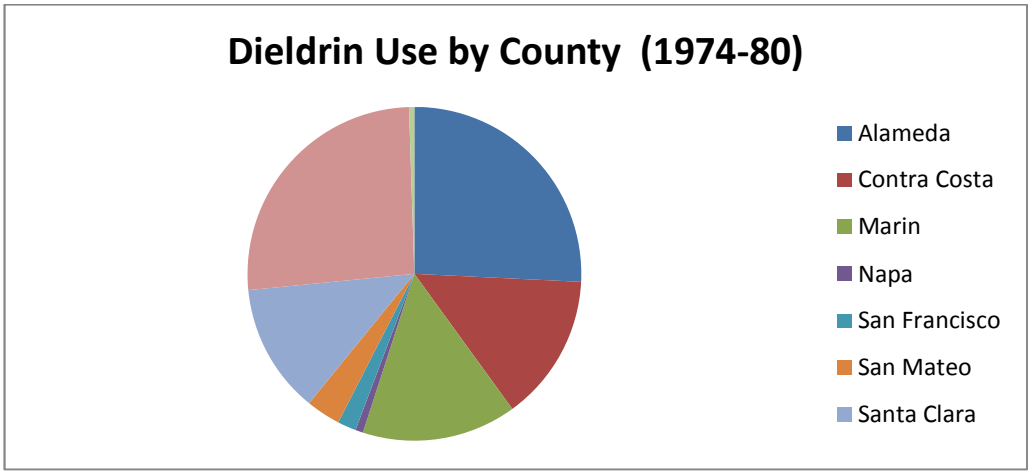


**Figure 8. Bay Area dieldrin usage (in pounds) by county 1974-1980 (California Department of Pesticide Regulation Data).**

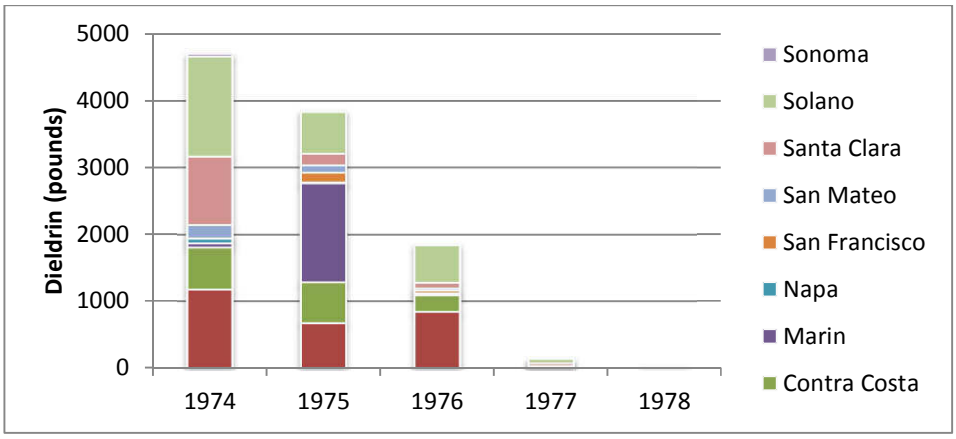


**Figure 9. Bay Area dieldrin usage (in pounds) by county 1974-1980 (California Department of Pesticide Regulation Data).**

## A10.1.b How do legacy pesticides behave in the environment?

Technical grade DDT is a mixture of three DDT isomers, p,p'-DDT (85%) and lower percentages of o,p'-DDT and o,o'-DDT (Network). DDE is the primary degradation product in oxygenated soils (Guenzi and Beard 1976). DDT and degradation products are persistent in the environment and, once in aquatic environments, have bioaccumulative properties (Kratzer 1999; Nowell *et al.* 1999). Soil half-lives for DDT and degradation products range from 110 days - 5690 days (0.3 – 15.6 years) (Nowell *et al.* 1999). Additionally, soil conditions can greatly affect chemical degradation (Guenzi and Beard 1976; Hitch and Day 1992).

Technical grade chlordane consists of an estimated 147 structurally related compounds (Dearth and Hites 1991). The most dominant isomers in technical grade are the cis- and trans-chlordanes which are also racemic in the mixture (Dearth and Hites 1991; Bidleman *et al.* 2004). Both isomers show low solubility in water, high affinity to bind with organic carbon in soils and have a half-life of about 365 days (Nowell *et al.* 1999; Medina *et al.* 2009). Other isomers, such as oxychlordane, are more water-soluble and have lower affinities for soil binding (Nowell *et al.* 1999). Legacy contaminated US Air Force sites showed high chlordane soil concentrations (up to 20 ppm) 20-60 years post application. Volatilization from soils is one of the primary pathways of transport (Bidleman *et al.* 2004; Scholtz and Bidleman 2007; Medina *et al.* 2009).

Dieldrin is more soluble (particularly at higher temperatures) than the other organochlorine pesticides discussed and has a lower affinity for binding with soils (Eye 1968; Nowell *et al.* 1999). However, dieldrin has been shown to remain in soils with half-lives ranging from 2 to 7 years depending on soil type (as reviewed in (Eye 1968). Flood events can mobilize dieldrin contaminated sediment particles from land based sources. When these are in a micro-particulate form (experimentally <32 µm) they can be prone to desorption, resulting in aqueous transport of dieldrin (Smit et al. 2008).

As noted above, as a general rule, all three chlorinated pesticides (DDT, chlordane, and dieldrin) can remain in soils for long periods of time and can be released to the atmosphere from contaminated soils or, through erosional processes, release to rivers, creeks, and other drainage systems via stormwater (Foster et al. 2000; McKee et al. 2004). Connor et al (2004) reviewed legacy pesticide transport pathways to San Francisco Bay. At that time, the authors estimated that local tributaries accounted for an estimated 71% of DDT loads, 91% of chlordane loads, and 33% of dieldrin loads to the Bay, the single largest pathway (

Table **1**). Keeping in mind that the errors and biases in the loads estimates may have been relatively large due to a lack of spatially and temporally resolute data, loads from the Central Valley Rivers were also identified as a larger contribution compared to direct atmospheric deposition or wastewater loads.

**Table 1. Legacy pesticide loading estimates including upper and lower bounds (kg/year) for San Francisco Bay (reproduced from Connor et al., 2004).**

| Pathway | DDTs | Chlordanes | Dieldrin |
|---|---|---|---|
| Central Valley | 15 (5–40) | 2 (0.7–5) | 5 (2–13) |
| Local Watershed | 40 (9–190) | 30 (7–160) | 3 (0.7–15) |
| Municipal Wastewater | 0.2 (0.02–2) | 0.1 (0.003–2) | 0.06 (0.008-0.4) |
| Industrial Wastewater | <0.2 | <0.1 | <0.06 |
| Atmospheric Deposition | 1 (0.02–2) | 0.9 | 1 (0.02–2) |
| Erosion of Sediment deposits | 9 (0.2 – 18) | 2 (0 – 4) | 0.2 (0 – 0.6) |
| Dredged material | -2 (-3 – -0.03) | -0.3 (-0.6 – 0) | -0.03 (-0.1-0) |
| **Total best estimate** | **60 (10 – 250)** | **30 (10-170)** | **10 (3-30)** |

## A10.2 Release mechanisms to the environment and possible pollutant source areas

Conceptually, release of organochlorine pesticides into the environment could have occurred during initial synthesis (true sources), contamination of soils due to spillage during transportation to market, (by definition) during usage, and during disposal of contaminated storage containers, equipment, or unused product. These conceptual categories will be explored in this report subsection.

**A10.2.a Initial synthesis:** That we are aware of, there are no legacy locations of manufacture of organochlorine pesticides in the Bay Area. United Heckathorn formulated, packaged, and shipped pesticides from a five acre site at the head of the Lauritzen and Parr channels of Richmond Harbor. No chemicals were manufactured on site. Heckathorn would receive technical grade pesticides from chemical manufacturers, grind them in air mills, mix them with other ingredients such as clays or solvents, and package them for final use in liquid or powder form. Although many pesticides were handled at United Heckathorn, DDT accounted for approximately 95% of the operations (EPA, 2013). We are not aware of any factories where mixing or alternative formulations were prepared. Thus, there are no true sources in the Bay Area.

**A10.2.b Contamination of soils due to spillage during transportation to market:** Given DDT use likely peaked in California in around 1962, the main transportation rout for DDT product would have been rail transport. Thus, historic rail yards and connected warehousing in older industrial areas could be considered legacy source areas. Production and use of chlordane and dieldrin occurred later but still within the same general period when rail transport was a strong component of Bay Area transport systems relative to today. Other legacy source areas may include wholesale and retail depots such as agricultural supply stores or supply depots for commercial pesticide applicators.

**A10.2.c Use area:** Given the use history of DDT, chlordane, and dieldrin, organochlorine pesticides are likely relatively ubiquitous in soil residues across Bay Area watersheds. However, despite the ubiquitous application and wind and atmospheric dispersion of these pollutants, there are potential land uses that can be identified in local watersheds. For example, soils in plant and tree nurseries have been found to contain excessively high concentrations of organochlorine pesticides (Mangiafico *et al.* 2008). From the Bay Area pesticide use data available, chlordanes were primarily used in structural applications for termite control while dieldrin was primarily used as a residential pesticide. These applications are spatially disparate in watersheds making source area identification more difficult.

**A10.2.d Disposal and recycling:** Like many chemicals, both in modern use and historic use, bulk product was delivered in metal drums. Source areas therefore likely include drum recycling facilities and perhaps more generally metals recycling facilities. There may also be

some legacy product still being discarded into landfills as packages containing pesticides, sometimes with obscured labels, are discarded from storage.

## A10.3 Source areas and pollutant concentrations in soils

Since no previous literature review was available on OC pesticides in soils for the Bay Area (the RMP nor and SFEI grant funded project competed such a review), we carried out a brief survey of peer-reviewed literature as well as reviewed data available locally based mainly on BASMAA studies carried out during 2000 and 2001.

Previous analyses of local DDT and chlordane storm drain sediment data found very limited statistical differences in chlordanes and DDTs by land use (KLI and Eisenberg 2002). In the following tables, concentrations and statistics on soils data collected in individual studies are shown (Table 2 - Table 4), as well as a summary based on simple land use classes (Table 5 - Table 7) that may be considered for our regional modeling efforts. For chlordanes, soil and sediment concentrations from residential/commercial land use were statistically higher than other land uses (industrial, mixed, and open). Chlordane was used more extensively as a structural pesticide which may partly explain why concentrations were highest in residential/commercial areas. However, there were no apparent statistical differences for DDT soil/sediment concentrations in these same land uses suggesting widespread usage and dispersion of DDTs. It is also interesting to note that concentration data from the historic study by Law and Goerlitz (1974) shows a similar range of concentrations for both DDT and chlordane compounds perhaps indicating no trend. Unfortunately, it is not possible to separate out specific source areas such as depots, railway loading areas, or nurseries and other possible source areas. Soils data from a survey of the local literature and local studies supports the hypothesis that:

- Maximum DDT concentrations were highest in soil and sediments from industrial land uses and lowest from open space. Residential/commercial land uses had the intermediate concentrations,
- Maximum chlordane concentrations were also highest in soil and sediment from industrial land uses and lowest in open space. Residential/commercial land uses also had intermediate concentrations,
- Dieldrin soil and sediment concentrations are highest in residential/commercial areas and lowest in open space.

## A10.4 Pollutant concentrations in stormwater

Despite regulatory actions banning use of these chemicals, legacy pesticides are still being found in Bay Area stormwater (KLI and Eisenberg 2002; Salop et al. 2002; McKee et al. 2004; Hunt et al. 2012). DDT isomer percentage (DDT: DDD and DDT: DDE) greater than 5% may indicate fresh sources of DDT or lower soil degradation rates from DDT to DDE (J Davis, personal communication). Based on this conceptual model, local data suggest that fresh DDT is still being transported from some watersheds (Guadalupe River, Zone 4 Line A, Richmond Pump Station).

**Table 2. Sediment and soil DDT concentrations, by land's use, from local studies and world literature. The fines fraction is <62.5 µm. For the tabulated data, DDT concentrations are comprised of p,p'-DDT, o,p'-DDT p,p'-DDD, o,p'-DDD, p,p'-DDE, and o,p'-DDE, unless otherwise noted. Zero (0) is entered for non-detect (ND) concentrations. Soil/sediment samples consist of grab and composite samples. Statistics are within study average, minimum, maximum, and median concentrations except where noted.**

| Land Use Source Category | Specific Location | Region (Bay Area, Arid West, US, World) | Reference | units | Media (stormwater, soil) | Type of Result (particle normalized, water concentration, sediment concentration) | Average | Maximum | Median | Minimum | Non-averaged result |
|---|---|---|---|---|---|---|---|---|---|---|---|
| Agricultural | Yolo Bypass | Central Valley California | Smalling et al., 2007 | µg/kg | Creek bed | Sediment Concentration | | | | | 263 |
| Agricultural | Yolo Bypass | Central Valley California | Smalling et al., 2007 | µg/kg | Soil | Sediment Concentration | 355 | 786 | 374 | 11 | |
| Industrial | Bay Area | Bay Area | KLI database | µg/kg | Sediment | Sediment Concentration | 244 | 4037 | 74 | 10 | |
| Industrial | Bay Area | Bay Area | KLI 2002 | µg/kg fines | Storm drain | Sediment Concentration | 881 | 24541 | | 19 | |
| Mixed | Bay Area | Bay Area | KLI database | µg/kg | Sediment | Sediment Concentration | 30 | 73 | 29 | 8 | |
| Mixed | Bay Area | Bay Area | KLI 2002 | µg/kg fines | Storm drain | Sediment Concentration | 123 | 734 | | 14 | |
| Open | Bay Area | Bay Area | KLI database | µg/kg | Sediment | Sediment Concentration | 6 | 15 | 1 | 1 | |
| Open | Bay Area | Bay Area | KLI 2002 | µg/kg fines | Storm drain | Sediment Concentration | 1 | 1 | | 1 | |
| Residential/commercial | Bay Area | Bay Area | KLI database | µg/kg | Sediment | Sediment Concentration | 267 | 2157 | 41 | 6 | |
| Residential/commercial | Bay Area | Bay Area | KLI 2002 | µg/kg fines | Storm drain | Sediment Concentration | 239 | 1307 | | 7 | |
| Unknown | Marin County | Bay Area | KLI database | µg/kg | Sediment | Sediment Concentration | 60 | 155 | 40 | 6 | |
| Unknown | San Mateo County | Bay Area | KLI database | µg/kg | Sediment | Sediment Concentration | 75 | 264 | 52 | 12 | |
| Urban | Ballona Creek | Arid West | Curren Et al. 2011 | µg/kg | Storm drain | Particulate concentration | | 70 | | 0 | |
| Urban | Beijing China | World | Zhang et al., 2010 | ng/g | Street dust | Sediment Concentration | 20 | 59 | | 1 | |
| Urban/Rural | 26 Bay Area creeks | Bay Area | Law and Goerlitz, 1974 | µg/kg | Creek bed | Sediment Concentration | 63 | | | | |
| Urban/Rural | Alameda Creek | Bay Area | Law and Goerlitz, 1974 | µg/kg | Creek bed | Sediment Concentration | 18 | | | | |
| Urban/Rural | Alamitos Creek | Bay Area | Law and Goerlitz, 1974 | µg/kg | Creek bed | Sediment Concentration | 60 | | | | |
| Urban/Rural | Arroyo Corte Madera del Persidio | Bay Area | Law and Goerlitz, 1974 | µg/kg | Creek bed | Sediment Concentration | 69 | | | | |
| Urban/Rural | Arroyo de la Laguna | Bay Area | Law and Goerlitz, 1974 | µg/kg | Creek bed | Sediment Concentration | 36 | | | | |
| Urban/Rural | Belmont Creek | Bay Area | Law and Goerlitz, 1974 | µg/kg | Creek bed | Sediment Concentration | 347 | | | | |
| Urban/Rural | Colma Creek | Bay Area | Law and Goerlitz, 1974 | µg/kg | Creek bed | Sediment Concentration | 11 | | | | |
| Urban/Rural | Cordilleros Creek | Bay Area | Law and Goerlitz, 1974 | µg/kg | Creek bed | Sediment Concentration | 46 | | | | |
| Urban/Rural | Corte Madera Creek | Bay Area | Law and Goerlitz, 1974 | µg/kg | Creek bed | Sediment Concentration | 106 | | | | |
| Urban/Rural | Coyote Creek | Bay Area | Law and Goerlitz, 1974 | µg/kg | Creek bed | Sediment Concentration | 99 | | | | |
| Urban/Rural | Green Valley Creek | Bay Area | Law and Goerlitz, 1974 | µg/kg | Creek bed | Sediment Concentration | 5 | | | | |
| Urban/Rural | Guadalupe River | Bay Area | Law and Goerlitz, 1974 | µg/kg | Creek bed | Sediment Concentration | 8 | | | | |
| Urban/Rural | Los Gatos Creek | Bay Area | Law and Goerlitz, 1974 | µg/kg | Creek bed | Sediment Concentration | 53 | | | | |
| Urban/Rural | Los Trancos Creek | Bay Area | Law and Goerlitz, 1974 | µg/kg | Creek bed | Sediment Concentration | 22 | | | | |
| Urban/Rural | Miller Creek | Bay Area | Law and Goerlitz, 1974 | µg/kg | Creek bed | Sediment Concentration | 48 | | | | |
| Urban/Rural | Napa River | Bay Area | Law and Goerlitz, 1974 | µg/kg | Creek bed | Sediment Concentration | 58 | | | | |
| Urban/Rural | Navato Creek | Bay Area | Law and Goerlitz, 1974 | µg/kg | Creek bed | Sediment Concentration | 20 | | | | |
| Urban/Rural | Petaluma River | Bay Area | Law and Goerlitz, 1974 | µg/kg | Creek bed | Sediment Concentration | 20 | | | | |
| Urban/Rural | Redwood Creek | Bay Area | Law and Goerlitz, 1974 | µg/kg | Creek bed | Sediment Concentration | 42 | | | | |
| Urban/Rural | San Francisquito Creek | Bay Area | Law and Goerlitz, 1974 | µg/kg | Creek bed | Sediment Concentration | 193 | | | | |
| Urban/Rural | San Lorenzo Creek | Bay Area | Law and Goerlitz, 1974 | µg/kg | Creek bed | Sediment Concentration | 16 | | | | |
| Urban/Rural | San Pablo Creek | Bay Area | Law and Goerlitz, 1974 | µg/kg | Creek bed | Sediment Concentration | 11 | | | | |
| Urban/Rural | San Rafael Creek | Bay Area | Law and Goerlitz, 1974 | µg/kg | Creek bed | Sediment Concentration | 270 | | | | |
| Urban/Rural | Sanoma Creek | Bay Area | Law and Goerlitz, 1974 | µg/kg | Creek bed | Sediment Concentration | 4 | | | | |
| Urban/Rural | Stevens Creek | Bay Area | Law and Goerlitz, 1974 | µg/kg | Creek bed | Sediment Concentration | 49 | | | | |
| Urban/Rural | Union Creek | Bay Area | Law and Goerlitz, 1974 | µg/kg | Creek bed | Sediment Concentration | 66 | | | | |
| Urban/Rural | Wildcat Creek | Bay Area | Law and Goerlitz, 1974 | µg/kg | Creek bed | Sediment Concentration | 29 | | | | |

**Table 3. Sediment and soil chlordane (sum of 6 isomers) concentrations by land use from local studies and world literature. Chlordane concentrations are comprised of Chlordane, cis-, Chlordane, trans-, Heptachlor, Nonachlor, cis-, Nonachlor, trans-, Oxychlordane, Heptachlor epoxide, unless otherwise noted. Zero (0) is entered for non-detect (ND) concentrations. Soil/sediment samples consist of grab and composite samples. Statistics are within study average, minimum, maximum, and median concentrations except where noted.**

| Land Use Source Category | Specific Location | Region (Bay Area, Arid West, US, World) | Reference | units | Media (stormwater, soil) | Type of Result (particle normalized, water concentration, sediment concentration) | Average | Maximum | Median | Minimum |
|---|---|---|---|---|---|---|---|---|---|---|
| Industrial | Bay Area | Bay Area | KLI database | µg/kg | Sediment | Sediment Concentration | 388 | 11496 | 55 | 9 |
| Industrial | Bay Area storm drains | Bay Area | KLI 2002 | µg/kg fines | Storm drain | Sediment Concentration | 1315 | 24296 | | 2 |
| Mixed | Bay Area | Bay Area | KLI database | µg/kg | Sediment | Sediment Concentration | 31 | 111 | 21 | 6 |
| Mixed | Bay Area storm drains | Bay Area | KLI 2002 | µg/kg fines | Storm drain | Sediment Concentration | 65 | 268 | | 5 |
| Open | Bay Area | Bay Area | KLI database | µg/kg | Sediment | Sediment Concentration | 5 | 13 | 1 | 1 |
| Open | Bay Area storm drains | Bay Area | KLI 2002 | µg/kg fines | Storm drain | Sediment Concentration | 2 | 4 | | 1 |
| Res/Com | Bay Area | Bay Area | KLI database | µg/kg | Sediment | Sediment Concentration | 363 | 2657 | 92 | 10 |
| Residential/commercial | Bay Area storm drains | Bay Area | KLI 2002 | µg/kg fines | Storm drain | Sediment Concentration | 964 | 3744 | | 54 |
| Unknown | Marin County | Bay Area | KLI database | µg/kg | Sediment | Sediment Concentration | 336 | 1125 | 106 | 7 |
| Unknown | San Mateo County | Bay Area | KLI database | µg/kg | Sediment | Sediment Concentration | 64 | 227 | 41 | 15 |
| Urban | Ballona Creek | Arid West | Curren Et al. 2011 | µg/kg | Storm drain | Particulate concentration | | 191 | | 0 |
| Urban/Rural | 26 Bay Area creeks | Bay Area | Law and Goerlitz, 1974 | µg/kg | Creek bed | Sediment Concentration | 122 | | | |
| Urban/Rural | Alameda Creek | Bay Area | Law and Goerlitz, 1974 | µg/kg | Creek bed | Sediment Concentration | 33 | | | |
| Urban/Rural | Alamitos Creek | Bay Area | Law and Goerlitz, 1974 | µg/kg | Creek bed | Sediment Concentration | 46 | | | |
| Urban/Rural | Arroyo Corte Madera del Persidio | Bay Area | Law and Goerlitz, 1974 | µg/kg | Creek bed | Sediment Concentration | 140 | | | |
| Urban/Rural | Arroyo de la Laguna | Bay Area | Law and Goerlitz, 1974 | µg/kg | Creek bed | Sediment Concentration | 111 | | | |
| Urban/Rural | Belmont Creek | Bay Area | Law and Goerlitz, 1974 | µg/kg | Creek bed | Sediment Concentration | 660 | | | |
| Urban/Rural | Colma Creek | Bay Area | Law and Goerlitz, 1974 | µg/kg | Creek bed | Sediment Concentration | 29 | | | |
| Urban/Rural | Cordilleros Creek | Bay Area | Law and Goerlitz, 1974 | µg/kg | Creek bed | Sediment Concentration | 27 | | | |
| Urban/Rural | Corte Madera Creek | Bay Area | Law and Goerlitz, 1974 | µg/kg | Creek bed | Sediment Concentration | 103 | | | |
| Urban/Rural | Coyote Creek | Bay Area | Law and Goerlitz, 1974 | µg/kg | Creek bed | Sediment Concentration | 77 | | | |
| Urban/Rural | Green Valley Creek | Bay Area | Law and Goerlitz, 1974 | µg/kg | Creek bed | Sediment Concentration | 0 | | | |
| Urban/Rural | Guadalupe River | Bay Area | Law and Goerlitz, 1974 | µg/kg | Creek bed | Sediment Concentration | 13 | | | |
| Urban/Rural | Los Gatos Creek | Bay Area | Law and Goerlitz, 1974 | µg/kg | Creek bed | Sediment Concentration | 140 | | | |
| Urban/Rural | Los Trancos Creek | Bay Area | Law and Goerlitz, 1974 | µg/kg | Creek bed | Sediment Concentration | 21 | | | |
| Urban/Rural | Miller Creek | Bay Area | Law and Goerlitz, 1974 | µg/kg | Creek bed | Sediment Concentration | 310 | | | |
| Urban/Rural | Napa River | Bay Area | Law and Goerlitz, 1974 | µg/kg | Creek bed | Sediment Concentration | 36 | | | |
| Urban/Rural | Navato Creek | Bay Area | Law and Goerlitz, 1974 | µg/kg | Creek bed | Sediment Concentration | 62 | | | |
| Urban/Rural | Petaluma River | Bay Area | Law and Goerlitz, 1974 | µg/kg | Creek bed | Sediment Concentration | 130 | | | |
| Urban/Rural | Redwood Creek | Bay Area | Law and Goerlitz, 1974 | µg/kg | Creek bed | Sediment Concentration | 40 | | | |
| Urban/Rural | San Francisquito Creek | Bay Area | Law and Goerlitz, 1974 | µg/kg | Creek bed | Sediment Concentration | 339 | | | |
| Urban/Rural | San Lorenzo Creek | Bay Area | Law and Goerlitz, 1974 | µg/kg | Creek bed | Sediment Concentration | 15 | | | |
| Urban/Rural | San Pablo Creek | Bay Area | Law and Goerlitz, 1974 | µg/kg | Creek bed | Sediment Concentration | 65 | | | |
| Urban/Rural | San Rafael Creek | Bay Area | Law and Goerlitz, 1974 | µg/kg | Creek bed | Sediment Concentration | 800 | | | |
| Urban/Rural | Sanoma Creek | Bay Area | Law and Goerlitz, 1974 | µg/kg | Creek bed | Sediment Concentration | 4 | | | |
| Urban/Rural | Stevens Creek | Bay Area | Law and Goerlitz, 1974 | µg/kg | Creek bed | Sediment Concentration | 99 | | | |
| Urban/Rural | Union Creek | Bay Area | Law and Goerlitz, 1974 | µg/kg | Creek bed | Sediment Concentration | 200 | | | |
| Urban/Rural | Wildcat Creek | Bay Area | Law and Goerlitz, 1974 | µg/kg | Creek bed | Sediment Concentration | 66 | | | |

**Table 4. Sediment and soil dieldrin concentrations by land use from local studies only. Zero (0) is entered for non-detect (ND) concentrations.**

| Land Use Source Category | Specific Location | Region (Bay Area, Arid West, US, World) | Reference | units | Media (stormwater, soil) | Type of Result (particle normalized, water concentration, sediment concentration) | Average | Maximum | Median | Minimum |
|---|---|---|---|---|---|---|---|---|---|---|
| Industrial | Bay Area | Bay Area | KLI database | µg/kg | Sediment | Sediment Concentration | 25 | 570 | 7 | 1 |
| Mixed | Bay Area | Bay Area | KLI database | µg/kg | Sediment | Sediment Concentration | 7 | 17 | 5 | 0 |
| Open | Bay Area | Bay Area | KLI database | µg/kg | Sediment | Sediment Concentration | 6 | 14 | 3 | 0 |
| Res/Com | Bay Area | Bay Area | KLI database | µg/kg | Sediment | Sediment Concentration | 118 | 1300 | 11 | 0 |
| Unknown | Marin County | Bay Area | KLI database | µg/kg | Sediment | Sediment Concentration | 8 | 14 | 6 | 0 |
| Unknown | San Mateo County | Bay Area | KLI database | µg/kg | Sediment | Sediment Concentration | 13 | 82 | 5 | 4 |

**Table 5. Summary statistics for DDTs in sediment and soils by land use for local studies only.**

| Land Use Source Category | units | Count | Minimum | Maximum | Average |
|---|---|---|---|---|---|
| Industrial | µg/kg | 4 | 10 | 4037 | 1091 |
| Residential/commercial | µg/kg | 4 | 6 | 2157 | 618 |
| Urban/Rural | µg/kg | 27 | 4 | 347 | 66 |
| Unknown | µg/kg | 8 | 6 | 264 | 83 |
| Mixed | µg/kg | 4 | 8 | 73 | 35 |
| Open | µg/kg | 4 | 1 | 15 | 6 |
| Industrial | µg/kg fines | 3 | 19 | 24,541 | 8480 |
| Residential/commercial | µg/kg fines | 3 | 7 | 1307 | 518 |
| Mixed | µg/kg fines | 3 | 14 | 734 | 290 |
| Open | µg/kg fines | 3 | 1 | 1 | 1 |

**Table 6. Summary statistics for chlordane and sediment in soils by land use our local studies only. Zero (0) is entered for non-detect (ND) concentrations.**

| Land Use Source Category | units | Count | Minimum | Maximum | Average |
|---|---|---|---|---|---|
| Industrial | µg/kg | 4 | 9 | 11496 | 2987 |
| Residential/commercial | µg/kg | 4 | 10 | 2657 | 781 |
| Unknown | µg/kg | 8 | 7 | 1125 | 240 |
| Urban/Rural | µg/kg | 27 | 0 | 800 | 137 |
| Mixed | µg/kg | 4 | 6 | 111 | 42 |
| Open | µg/kg | 4 | 1 | 13 | 5 |
| Industrial | µg/kg fines | 3 | 2 | 24296 | 8538 |
| Residential/commercial | µg/kg fines | 3 | 54 | 3744 | 1587 |
| Mixed | µg/kg fines | 3 | 5 | 268 | 113 |
| Open | µg/kg fines | 3 | 1 | 4 | 2 |

**Table 7. Summary statistics for dieldrin in sediment and soils by land use for local studies only. Zero (0) is entered for non-detect (ND) concentrations.**

| Land Use Source Category | units | Count | Minimum | Maximum | Average |
|---|---|---|---|---|---|
| Residential/commercial | µg/kg | 4 | 0 | 1300 | 357 |
| Industrial | µg/kg | 4 | 1 | 570 | 151 |
| Unknown | µg/kg | 8 | 0 | 82 | 16 |
| Mixed | µg/kg | 4 | 0 | 17 | 7 |
| Open | µg/kg | 4 | 0 | 14 | 6 |

Soil temperatures, oxygen levels, and other soil conditions can affect the degradation of DDT to DDE with higher temperatures resulting in higher degradation rates (Guenzi and Beard 1976; Hitch and Day 1992; Rinella et al. 1993). It is unclear if higher DDT isomer percentages, in stormwater, are a result of ongoing illegal applications of private stockpiles or from soil conditions that hinder degradation to DDE in the watershed.

OC pesticide data in stormwater are available from a number of Bay Area rivers, creeks, and stormdrains (Table 8-Table 11). However, since most of the sampling locations are at the downstream points of our systems, pollutant contributions from distinct land uses or source areas are not available. The local exception is the Heckathorn United Inc. Superfund site which can be considered a source area. Recent stormwater monitoring at this location, showed most stormwater samples below detection. But a storm event in May 2012 produced maximum stormwater concentrations for DDT (267 ng/L) and dieldrin (13 ng/L) (Services 2013). After this storm event, a cracked pipe in the stormwater collection system was found and believed to be the source of the pesticides in stormwater. As part of the Superfund remediation, the site has been engineered with a concrete cap covering the contaminated area as well as an extensive stormwater collection system. There is potential for additional leaking from the capped area if the engineered system becomes compromised.

There are also nonlocal pesticide findings that do provide some basis of pollutant contributions from land use/source areas, in particular from agricultural areas. DDT and dieldrin stormwater concentrations from plant nurseries in Southern California were elevated compared with local stormwater concentrations. Maximum DDT was measured at 620 ng/L and maximum dieldrin was measured at 20 ng/L (Mangiafico *et al.* 2009). An additional study at Southern California citrus/avocado groves also found elevated DDT concentrations of stormwater (136 ng/L) (Mangiafico *et al.* 2009). It is unclear why pesticide concentrations were elevated since property owners did not report using these pesticides. The papers hypothesized pollutants may be spray drift from adjacent properties or legacy contaminants that are continuing to be mobilized. No similar Bay Area studies were found. Therefore it is unclear if local nurseries and other agricultural areas are sources of organochlorine pesticides.

To explore possible regional scale variations in applications in relation to land use, the ratios of chlordane to dieldrin were computed for the local stormwater data as well as the available storm drain sediment data. No unequivocal patterns were isolated in relation to imperviousness or land use characteristics for the stormwater data except there appears to be an indication that older industrial areas exhibit less chlordane relative to dieldrin (Table 12). A better pattern may have been observed if the Richmond sampling location had more wet weather data (the data currently available is from the original Richmond pump station data set which was predominantly dry flow (Hunt et al., 2012)) or if data were available from more locations than just four. There appears to be a more robust pattern emerging from the bed sediment data (Table 13). Chlordane use in the Bay Area was mostly structural while dieldrin was residential. From the usage history, we might expect open spaces and residential/commercial land uses to have lower ratios and that does appear to bear out in the bed sediment data – although there

**Table 8. DDT concentrations in stormwater, by land use, from local studies and world literature**

| Analyte | Land Use Source Category | Specific Location | Region (Bay Area, Arid West, US, World) | Reference | units | Media (stormwater, soil) | Type of Result (particle normalized, water concentration, sediment concentration) | Average | Maximum | Median | Minimum |
|---|---|---|---|---|---|---|---|---|---|---|---|
| DDT-Sum | Agricultural | Orestimba Creek at River Road | Arid West | Kratzer 2007 | µg/kg | Stormwater | Particulate concentration | 316 | | | |
| DDT-Sum | Agricultural | San Joaquin River tributaries | Arid West | Kratzer 2007 | µg/kg | Dry Season Runoff | Sediment Concentration | 307 | 617 | 258 | 71 |
| DDT-Sum | Agricultural | San Joaquin River tributaries | Arid West | Kratzer 2007 | µg/kg | Stormwater | Particulate concentration | 205 | 458 | 193 | 4.6 |
| Sum p,p isomers | Hekathorn Superfund Site | Heckathorn Superfund Site | Bay Area | Environmental Technical Services, 2013 | ng/L | stormwater | Water Concentration | | 267 | | 0.0 |
| DDT-Sum | Mixed | Guadalupe River at hwy 101 | Bay Area | SFEI Loading Studies | ng/L | Stormwater | Water Concentration | 35 | 71 | 35 | 3.3 |
| DDT-Sum | Mixed | Mallard Island | Bay Area | SFEI Loading Studies | ng/L | Stormwater | Water Concentration | 0.8 | 1.6 | 0.5 | 0.3 |
| DDT-Sum | Mixed | Mallard Island | Central Valley | Bergamaschi et al., 2001 | µg/kg | Stormwater | Particulate concentration | 6.0 | 11 | | 4.0 |
| DDT-Sum | Mixed | Richmond Pumpstation | Bay Area | SFEI Loading Studies | ng/L | Stormwater | Water Concentration | 1.2 | 3.6 | 0.5 | 0.0 |
| DDT-Sum | Mixed | Zone 4 Line A | Bay Area | SFEI Loading Studies | ng/L | Stormwater | Water Concentration | 20 | 59 | 10 | 7.4 |
| DDT-Sum | Urban | Beijing China | World | Zhang et al., 2010 | ng/L | Stormwater | EMC | 12 | 1.3 | | 1.3 |
| Sum p,p isomers | Citrus/avocado grove | Ventura County | Arid West | Mangiafico et al., 2009 | ng/L | Stormwater | Water Concentration | | 136 | | |
| Sum p,p isomers | Plant nursery | Ventura County | Arid West | Mangiafico et al., 2008 | ng/L | Stormwater | Water Concentration | | 374 | | |
| Sum p,p isomers | Plant nursery | Ventura County | Arid West | Mangiafico et al., 2009 | ng/L | Stormwater | Water Concentration | | 620 | | |

**Table 9. Chlordane concentrations in stormwater, by land use, from local studies and world literature**

| Analyte | Land Use Source Category | Specific Location | Region (Bay Area, Arid West, US, World) | Reference | units | Media (stormwater, soil) | Type of Result (particle normalized, water concentration, sediment concentration) | Average | Maximum | Median | Minimum |
|---|---|---|---|---|---|---|---|---|---|---|---|
| Chlordane | Agricultural | Orestimba Creek at River Road | Arid West | Kratzer 2007 | µg/kg | Stormwater | Particulate concentration | 7 | | | |
| Chlordane | Agricultural | San Joaquin River tributaries | Arid West | Kratzer 2007 | µg/kg | Dry Season Runoff | Sediment Concentration | 11 | 31 | 6 | 0 |
| Chlordane | Agricultural | San Joaquin River tributaries | Arid West | Kratzer 2007 | µg/kg | Stormwater | Particulate concentration | 12 | 43 | 5 | 0 |
| Chlordane | Mixed | Guadalupe River at hwy 101 | Bay Area | SFEI Loading Studies | ng/L | Stormwater | Water Concentration | 29 | 64 | 26 | 3.4 |
| Chlordane | Mixed | Mallard Island | Bay Area | SFEI Loading Studies | ng/L | Stormwater | Water Concentration | 0.10 | 0.18 | 0.10 | 0.04 |
| Chlordane | Mixed | Mallard Island | Central Valley | Bergamaschi et al., 2001 | µg/kg | Stormwater | Particulate concentration | 0 | | | |
| Chlordane | Mixed | Richmond Pumpstation | Bay Area | SFEI Loading Studies | ng/L | Stormwater | Water Concentration | 1.8 | 5.6 | 0.73 | 0.27 |
| Chlordane | Mixed | Zone 4 Line A | Bay Area | SFEI Loading Studies | ng/L | Stormwater | Water Concentration | 9.3 | 16 | 9.3 | 3.5 |
| Heptachlor and trans chlordane | Plant nursery | Ventura County | Arid West | Mangiafico et al., 2008 | ng/L | Stormwater | Water Concentration | | 37 | | |
| Sum of cis,trans-chlordane, Heptachlor, heptachlor epoxide | Hekathorn Superfund Site | Heckathorn Superfund Site | Bay Area | Environmental Technical Services, 2013 | ng/L | stormwater | Water Concentration | | 0 | | 0 |
| Technical chlordane | Hekathorn Superfund Site | Heckathorn Superfund Site | Bay Area | Environmental Technical Services, 2013 | ng/L | stormwater | Water Concentration | | 0 | | 0 |
| Trans chlordane | Plant nursery | Ventura County | Arid West | Mangiafico et al., 2009 | ng/L | Stormwater | Water Concentration | | 12 | | |

**Table 10. Dieldrin concentrations in stormwater, by land use, from local studies and world literature**

| Land Use Source Category | Specific Location | Region (Bay Area, Arid West, US, World) | Reference | units | Media (stormwater, soil) | Type of Result (particle normalized, water concentration, sediment concentration) | Average | Maximum | Median | Minimum |
|---|---|---|---|---|---|---|---|---|---|---|
| Agricultural | England | England | Meharg et al., 2000 | ng/L | Water | Water Concentration | 3.0 | 13 | | 0.16 |
| Agricultural | Orestimba Creek at River Road | Arid West | Kratzer 2007 | µg/kg | Stormwater | Particulate concentratio | 4.6 | | | |
| Agricultural | San Joaquin River tributaries | Arid West | Kratzer 2007 | µg/kg | Dry Season Runoff | Sediment Concentration | 4.8 | 7.9 | 5.3 | 0 |
| Agricultural | San Joaquin River tributaries | Arid West | Kratzer 2007 | µg/kg | Stormwater | Particulate concentratio | 3.0 | 8.8 | 2.0 | 0 |
| Hekathorn Superfund Site | Heckathorn Superfund Site | Bay Area | Environmental Technical Services, 2013 | ng/L | stormwater | Water Concentration | | 13 | | 0 |
| Industrial | England | England | Meharg et al., 2000 | ng/L | Water | Water Concentration | 3.0 | 13 | 0 | 0.16 |
| Mixed | Guadalupe River at hwy 101 | Bay Area | SFEI Loading Studies | ng/L | Stormwater | Water Concentration | 2.8 | 6.0 | 2.7 | 0.64 |
| Mixed | Mallard Island | Bay Area | SFEI Loading Studies | ng/L | Stormwater | Water Concentration | 0.16 | 0.25 | 0.16 | 0.06 |
| Mixed | Richmond Pumpstation | Bay Area | SFEI Loading Studies | ng/L | Stormwater | Water Concentration | 0.85 | 1.1 | 0.90 | 0.46 |
| Mixed | Zone 4 Line A | Bay Area | SFEI Loading Studies | ng/L | Stormwater | Water Concentration | 1.5 | 4.6 | 0.85 | 0.71 |
| Plant nursery | Ventura County | Arid West | Mangiafico et al., 2008 | ng/L | Stormwater | Water Concentration | | 20 | | |

**Table 11. Summary statistics for DDT, dieldrin, chlordanes in stormwater by land use, from local studies. Sum of p,p isomers include DDT, DDD, and DDE.**

| Contaminant | Land Use Source Category | Units | Count of Sites | Maximum | Minimum | Average |
|---|---|---|---|---|---|---|
| Sum p,p isomers | Hekathorn Superfund Site | ng/L | 2 | 267 | 0 | 134 |
| DDT-Sum | Mixed | ng/L | 48 | 71 | 0 | 10 |
| Dieldrin | Hekathorn Superfund Site | ng/L | 2 | 13 | 0 | 6.5 |
| Dieldrin | Mixed | ng/L | 48 | 6 | 0.06 | 1.1 |
| Sum of cis,trans-chlordane, Heptachlor, heptachlor epoxide | Hekathorn Superfund Site | ng/L | 2 | 0 | 0 | 0 |
| Technical chlordane | Hekathorn Superfund Site | ng/L | 2 | 0 | 0 | 0 |
| Chlordane | Mixed | ng/L | 48 | 64 | 0 | 7.1 |

**Table 12. The ratio of chlordane to dieldrin based on stormwater loading studies in the Bay Area.**

| | Ratio of Chlordane/Dieldrin in Stormwater | % Impervious | % Old Industrial (1974) | % Res/Com |
|---|---|---|---|---|
| Guadalupe River at hwy 101 | 10 | 39 | 2 | 50 |
| Zone 4 Line A | 4.8 | 68 | 18 | 62 |
| Richmond Pumpstation* | 0.91 | 62 | 33 | 35 |
| Mallard Island | 0.73 | - | - | - |

*Based mostly on dry weather data.

**Table 13. The ratio of chlordane to dieldrin based on bed sediment studies in the Bay Area (KLI and EOA, 2002).**

| | Ratio of Chlordane/Dieldrin in Stormdrain Sediment |
|---|---|
| Unknown | 16 |
| Industrial | 15 |
| Mixed | 4.8 |
| Res/Com | 3.1 |
| Open | 0.93 |

are many structures in residential/commercial areas but perhaps dieldrin was used more in industrial applications - not in residential or commercial areas. This pattern appears to be directly opposite to the pattern seen in the stormwater data (although the n is small for the stormwater data).

## A10.5 Relationships with other pollutants

Investigating local data can provide information that can be used to identify relationships between hydrophobic contaminants. These relationships do not necessarily identify source areas but they can identify contaminants that co-occur spatially or are transported during storm water runoff following similar release and transport processes. DDTs, chlordanes, and dieldrin stormwater and storm drain concentrations were found to be highly correlated with PCB concentrations in local watersheds (Zone 4 Line A, Guadalupe River, Richmond Pump Station, and various watersheds in KLI 2002) suggesting that land/stream based transport mechanisms for organic pollutants, in these watersheds, are similar (Table 14 and Table 15). These correlations suggest that management actions, designed to remove PCBs, may also be effective in removing DDTs, chlordanes, and dieldrin. They suggest that management of Hg will not be as effective for removal of other contaminants.

**Table 14. Pearson correlation coefficients between legacy pesticides, PCBs, and Mercury for stormwater data from Zone 4 Line A, Guadalupe River, and Richmond Pump Station. Yellow highlights indicate well correlated data.**

| | *Dieldrin* | *Total Mercury* | *Sum of 40 PCBs (SFEI)* | *Sum of Chlordanes (SFEI)* | *Sum of DDTs (SFEI)* |
|---|---|---|---|---|---|
| Dieldrin | 1 | | | | |
| Mercury | 0.27 | 1 | | | |
| Sum of 40 PCBs (SFEI) | 0.87 | 0.28 | 1 | | |
| Sum of Chlordanes (SFEI) | 0.86 | 0.26 | 0.87 | 1 | |
| Sum of DDTs (SFEI) | 0.84 | 0.23 | 0.88 | 0.95 | 1 |

**Table 15. Pearson correlation coefficients between legacy pesticides, PCBs, and mercury for storm drain sediment data from KLI 2002 (utilizing data normalized to percent fines <62.5 µm). Yellow highlights indicate well correlated data.**

| | *Chlordane* | *Sum DDT* | *Sum PCB* | *Total Mercury* |
|---|---|---|---|---|
| Chlordane | 1 | | | |
| Sum DDT | 0.87 | 1 | | |
| Sum PCB | 0.96 | 0.97 | 1 | |
| Total Mercury | 0.70 | 0.27 | 0.50 | 1 |

## A10.6 Summary and options to support model development

The compilation of local and literature soil/sediment and stormwater organochlorine pesticide concentrations provides a starting point for identifying possible land use and/or source area contributions to pollutant loading. The soil/sediment data provide more classes of land use than the stormwater data. Additionally, these data (maximum concentrations) also span many orders of magnitude between the land uses (chlordane =4; DDT and dieldrin = 3) which provides a range of pollutant contributions from high to low. However, much of the soil/sediment data are more than 10 years old and therefore may not be representative of current conditions. In contrast, the stormwater data span about 2 orders of magnitude but do have some empirical data on source areas (Superfund site, nurseries, agriculture). There were no identified organochlorine pesticide soil/sediment source area data sets.

Since there is limited specific legacy pesticide source area information, our current GIS land-use designations would be the most relevant spatial data set for attempting to model loading estimates. The newly revised old industrial land use data layer (old industrial areas pre-1968) will aid in identifying those areas that were polluted during the period of max organochlorine usage (1960s). Industrial areas showed the highest soil/sediment concentrations for DDTs and chlordanes. There would be some

benefit to incorporating stormwater source area data as well since this information could provide a finer spatial scale of pollutant sources in the landscape. However, using the source area stormwater data would require a hybrid model (a combination of the base sediment and the base hydrology spreadsheet models) or converting the stormwater concentrations to particulate concentrations (if feasible). As noted above, the soil/sediment database is more extensive and provides information on the land-use basis. Below is a summary of recommendations:

What is the proposed model architecture for integrating OP pesticides into the RWSM?

- Given there is more sediment data available, more variability in sediment data between land uses, sediment appear to be the optimal basis for modeling regional scale loads of OP pesticides (This assumes the successful development of a calibrated sediment model which is still in development)
- Could explore the hybrid model architecture that capitalizes on available soil/sediment as well as stormwater data
- Could consider development of a co-transport model based on the relationship between local empirical legacy pesticide and PCB data

What GIS layers are proposed for modeling OC pesticides using the suggested modeling architecture? What is the availability and quality of those GIS layers?

- Primary GIS layers include current land use (industrial, commercial, residential, agriculture, open space) data including the updated pre-1968 industrial data layer. Other GIS data layers already in existence to support source area resolution in the model include rail transport, and recycling for drums and metals more generally. These data layers are already developed and are of good quality but could be optimized to be a little more specific to OC pesticides; for example, splitting out warehousing or light industrial from “old industrial”.
- Consider development of GIS source area data layers for nurseries and wholesale/ retail agricultural and garden supply centers and wholesale for commercial pesticide applicators.

What are the proposed data to support the concentration inputs and calibration/validation for the suggested model?

- Local and world literature soil/sediment/stormwater empirical data have been collated to be used as input coefficients for each of the proposed model parameters. Additional exploration of other potential legacy pesticide source areas could provide more spatially resolute information on pollutant contributions.
- Calibration/verification data at the watershed scale are presently sparse.

What data could be developed to support the model, and what is the relative importance of each dataset suggested (e.g. how high of a priority and how much would it help the model outcome or reduction in uncertainty)?

- Consider selectively adding legacy pesticides to the pollutant list for influent data at monitoring sites associated with the BASMAA EPA grant funded "Clean Water for a Clean Bay project". Stormwater data are being collected at a number of sites and would provide information at finer spatial scales in industrial drainage areas.
- Consider adding legacy pesticides to existing stormwater monitoring projects at Bay Area LID sites being monitoring through grant projects especially in areas with high percent urban, industrial, or agricultural land use.
- Consider mining county records for legacy pesticide use and spatial application data during peak period of the 1960s in order to determine relative application of OC pesticides in the Bay Area.

What methods do we suggest for developing that data? – Back-calculation from existing data; monitoring specific sites?

- An option is to use the inverse optimization methodology (Lent, 2011) for estimating land use based input concentrations (EMCs) using local empirical sediment data.
- Could consider adding OC pesticides to the analytic list for source area monitoring (RMP funding) should it occur in relation to improving PCB and Hg information.

## A10.7 References

Bidleman, T. F., F. Wong, et al. (2004). "Chiral signatures of chlordanes indicate changing sources to the atmosphere over the past 30 years." Atmospheric Environment **38**(35): 5963-5970.

Dearth, M. A. and R. A. Hites (1991). "Complete analysis of technical chlordane using negative ionization mass spectrometry." Environmental Science & Technology **25**(2): 245-254.

Eye, J. D. (1968). "Aqueous Transport of Dieldrin Residues in Soils." Journal (Water Pollution Control Federation) **40**(8): R316-R332.

Foster, G. D., E. C. Roberts Jr, et al. (2000). "Hydrogeochemistry and transport of organic contaminants in an urban watershed of Chesapeake Bay (USA)." Applied Geochemistry **15**(7): 901-915.

Guenzi, W. D. and W. E. Beard (1976). "The effects of temperature and soil water on conversion of DDT to DDE and soil." Journal of Environmental Quality **5**(3): 243-246.

Hitch, R. and H. Day (1992). "Unusual persistence of DDT in some Western USA soils." Bulletin of Environmental Contamination and Toxicology **48**(2): 259-264.

Hunt, J., G. DC, et al. (2012). Pollutant Monitoring in the North Richmond Pump Station: A Pilot Study for Potential Dry Flow and Seasonal First Flush Diversion for Wastewater Treatment, SFEI. **684**.

KLI and O. Eisenberg, & Associates (2002). "Joint Stormwater Agency Project To Study Urban Sources of Mercury, PCBs, and Organochlorine Pesticides."

Kratzer, C. R. (1999). "TRANSPORT OF SEDIMENT-BOUND ORGANOCHLORINE PESTICIDES TO THE SAN JOAQUIN RWER, CALIFORNIA1." JAWRA Journal of the American Water Resources Association **35**(4): 957-981.

Lent, M.A., 2011. Regional Spreadsheet Model: Contaminants. Presentation to the Sources pathways and Loadings Workgroup of the Regional Monitoring Program for Water Quality in San Francisco

Bay. October 25th, 2011. San Francisco Estuary Institute, Richmond, CA. http://www.sfei.org/node/4048

Mangiafico, S. S., J. Gan, et al. (2008). "Detention and Recycling Basins for Managing Nutrient and Pesticide Runoff from Nurseries." HortScience **43**(2): 393-398.

Mangiafico, S. S., J. Newman, et al. (2009). "Nutrients and Pesticides in Stormwater Runoff and Soil Water in Production Nurseries and Citrus and Avocado Groves in California." HortTechnology **19**(2): 360-367.

McKee, L., E. R, et al. (2004). The concentration and load of PCBs, OC pesticides, and mercury associated with suspended sediments in the lower Guadalupe River, San Jose, California. A Technical Report of the Regional Watershed Program, SFEI. **86**.

Medina, V. F., A. B. Waisner, et al. (2009). Legacy chlordane in soils from housing areas treated with organochlorine pesticides, United States Army Corps of Engineers.

Meharg, A. A., J. Wright, et al. (2000). "Spatial and temporal regulation of the pesticide dieldrin within industrial catchments." Science of the Total Environment **251–252**(0): 255-263.

Mischke, T., K. Brunetti, et al. (1985). "Agricultural Studies Of DDT Residues In California's Environment."

Network, E. T. from http://pmep.cce.cornell.edu/profiles/extoxnet/carbaryl-dicrotophos/ddt-ext.html.

Nowell, L. H., P. D. Capel, et al. (1999). Pesticides in stream sediment and aquatic biota – distribution, trends, and governing factors, CRC Press.

Rinella, J. F., P. A. Hamilton, et al. (1993). "Persistence of the DDT Pesticide in the Yakima River Basin Washington."

Salop, P., K. Abu-Saba, et al. (2002). "2000-01 Alameda County Watershed Sediment Sampling Program: Two-Year Summary and Analysis."

Scholtz, M. T. and T. F. Bidleman (2007). "Modelling of the long-term fate of pesticide residues in agricultural soils and their surface exchange with the atmosphere: Part II. Projected long-term fate of pesticide residues." Science of the Total Environment **377**(1): 61-80.

Services, E. T. (2013). Operations Maintenance Plan 2011-2012. Richmond, California, Prepared for: Levine Richmond Terminal.

SFBRWQCB (2009). California Regional Water Quality Control Board San Francisco Bay Region Municipal Regional Stormwater NPDES Permit, San Francisco Bay Regional Water Quality Control Board. Order R2-2009-0074; NPDES Permit No. CAS612008.

Smit, M. J., T. Grotenhuis, et al. (2008). "Desorption of Dieldrin from field aged sediments: Simulating flood events." Journal of Soils and Sediments **8**(2): 80-85.

Werner and Hitzfeld (2012). "50 years of eco-toxicology since Silent Spring-A review" GAIA **21**(3): 217-224.